The Conservation of Suppressor of Cytokine Signalling 3 in Mediating Intestinal Homeostasis

Emily Smith, MSc

This thesis is submitted in fulfilment of the requirements for the Degree of Doctor of Philosophy

Submitted June 2016

Faculty of Health and Medicine, Lancaster University

Abstract

A key function of the gastrointestinal tract is to break down ingested food and absorb the contained nutrients and water. Within the intestinal tract are a number of specialised epithelial cells that aid in this process as well as maintaining immune homeostasis through their functioning as a physical barrier, and secretion of antimicrobial peptides. The intestinal tract has one of the highest turnover rates within organisms, so because of this, and the variety of functions these cells can carry out, it is essential that the balance of proliferation and cell death is regulated to maintain homeostasis. There are several conserved signalling pathways that are responsible for the proliferation of intestinal cells. Suppressor of cytokine signalling 3 (SOCS3) is produced upon activation of the Janus kinase/Signal transducer and activator of transcription (Jak/Stat) pathway and this is an inducer of negative feedback inhibition and is implicated in regulation of intestinal homeostasis, with SOCS3 dysregulation reported in intestinal pathologies, such as cancer and inflammatory bowel disease. Intestinal epithelial cells are also in close proximity to the commensal gut microbiota and they too are known to regulate intestinal turnover. In the work presented here, we assessed the role of SOCS3 in normal intestinal homeostasis and how microbe-mediated proliferation impacts upon this. These experiments were performed in three different biological models, allowing us to assess the impact of SOCS3-regulated homeostasis at the molecular level, the tissue level, and at an organismal level, and also determine whether the function of SOCS proteins is conserved across different biological systems.

Using *in vitro* human intestinal epithelial cells, mice and *Drosophila melanogaster*, we observed consistent negative effects upon reduction of SOCS3, which affected proliferation and cytokine profiles, tumour tolerance and, survival and the gut-brain axis, in our respective models. In both *in vivo* models, we were able to discover functional outcomes due to reduced SOCS3 expression, in the form of facilitation of helminth expulsion and increased stress resistance in mice and *Drosophila*, respectively, thus suggesting potential benefits of reduced SOCS3 in young animals whose ability to adapt to homeostatic changes is higher. Overall, we were able to deduce that SOCS3 is responsible for maintaining normal intestinal homeostasis, and ultimately host health, at a number of levels within multiple biological systems. However, our results also indicated that SOCS3 is a complex, multi-functional protein, with much investigation still needed to determine its complete role.

For R.J.H

There isn't a day that goes by where I don't miss you,

and through your absence, you have kept me going

in life in the hope that I can do you proud.

Acknowledgements

First, I cannot thank my supervisors, Dr. Rachael Rigby and Dr. Sue Broughton, enough for all they have done during my time at Lancaster. Your support, feedback and patience were invaluable and I am incredibly grateful you took me back for another postgraduate degree. My gratitude is also extended to the Faculty of Health and Medicine for helping to fund my PhD, as without the studentship, I definitely would not have been able to continue my studies at Lancaster University.

Secondly, I would like to extend a big thank you to Dr. Elisabeth Shaw, not only for your contribution and execution of the *in vivo* mouse experiments, but for all of your help and support during my PhD, and always being there to answer my seemingly obvious science questions. I've enjoyed working with you, and we definitely don't know what we would have done without you in the Rigby lab. Additional thanks also go to the University of Manchester for the use of their animal facility, allowing the rearing of animals and collection of tissue used in experiments shown here.

I would like to thank Dr. Jane Andre and Dr. Imtiyaz Thagia for teaching me how to use the confocal microscope, and various molecular laboratory techniques respectively, that have proved to be incredibly important and useful for my research. I would also like to give thanks to Dr. Matt Hodges who generated the transduced HIEC cell lines that were extensively used for the *in vitro* experiments, and Jack Sloan and Idira Obasse whose work contributed to this thesis.

Thanks go to Dr. Karen Wright and all past and present members of the "Gut group"- I've enjoyed getting to know you all and working alongside you, and greatly appreciate all the help and feedback, both in the lab and during our lab meetings.

To all past and current members of the BLS department and my office buddies- thank you for your friendship and support over the years- having people around you who are in the same boat definitely makes the ride smoother! I'd also like to acknowledge my ever-expanding bar sports family who are not only talented, incredible people but who also unknowingly gave me a haven away from research.

To Taylor, Christie, Tara, Claire, Charlotte, John and Gemma- I am so grateful for you all being there with me along this journey. There was no way I could have made it this far without your support, kindness and humour to keep me going.

Finally, to my parents- there are not enough words for me to express how grateful I am to you both and how indebted I am for all the love and support you've given me. All my life, you've supported me in the pursuit of my dreams and interests, and I would not be writing this now if it wasn't for you. I am eternally thankful, and I love you both.

Declaration

I declare that this thesis is my own work and has not been submitted in part, or as a whole, for the award of a higher degree or qualification elsewhere. Sections of this thesis which have been published have been clearly identified in the figure legends.

Emily Smith, MSc

Contents

Lists of Figures

List of Tables

Abbreviations

1-MT	1-Methyl Tryptophan
AMPs	Antimicrobial Peptides
AOM	Azoxymethane
APC	Adenomatous Polyposis Coli
CAC	Colitis-Associated Carcinogenesis
CIS	Cytokine-Inducible SH2-protein
CD	Crohn's Disease
CNS	Central Nervous System
CR	Conventionally-Raised
CRC	Colorectal Cancer
DCs	Dendritic Cells
Dilps	*Drosophila* insulin-like peptides
Dlg	Discs large
dMyD88	*Drosophila* Myeloid Differentiation Primary Response Gene 88
Dro	Drosomycin-like
DSS	Dextran Sodium Sulphate
Duox	Dual Oxidase
EB	Enteroblast
EC	Enterocyte
Ecc15	*Erwinia carotovora carotovora 15*
EEC	Enteroendocrine Cell
EGFR	Epidermal Growth Factor Receptor

Esg	Escargot
ESS	N-extended SH2 domain
FLA	Flagellin
GF	Germ Free
G.I tract	Gastrointestinal tract
HIEC	Human Intestinal Epithelial Cell
IBD	Inflammatory Bowel Disease
IBS	Irritable Bowel Syndrome
IDO	Indoleamine 2,3-Dioxygenase
IEC	Intestinal Epithelial Cell
IFN	Interferon
IIS	Insulin/IGF
IL-(6)	Interleukin-(6)
Imd	Immune deficiency
IPCs	Insulin-Producing Cells
ISC	Intestinal Stem Cell
Jak	Janus kinase
JNK	Jun N-terminal Kinase
KIR	Kinase Inhibitory Region
Lgr5	Leucine-rich-repeat containing G protein-coupled Receptor 5
LPS	Lipopolysaccharide
LTA	Lipoteichoic Acid
MAPK	Mitogen-Activated Protein Kinase
MyD88	Myeloid Differentiation Primary Response Gene 88

NF-κB	Nuclear Factor Kappa-Light-Chain-Enhancer of Activated B Cells
NK cells	Natural Killer cells
PAMPs	Pathogen-Associated Molecular Patterns
PEST motif	Proline-, Glutamic acid-, Serine- and Threonine-rich motif
PGRP	Peptidoglycan Recognition Protein
PH3	Phosphorylated Histone H3
P.I	Performance Index
PIAS	Protein Inhibitor of Activated Stat
Poly I:C	Polyinosinic:Polycytidylic Acid
PRR	Pattern Recognition Receptor
RNAi	RNA interference
ROS	Reactive Oxygen Species
RPLPO	Large Ribosomal Protein
SCFAs	Short-Chain Fatty Acids
SCID	Severe Combined Immune Deficiency
SOCS	Suppressor of Cytokine Signalling
Sod	Superoxide dismutase
Stat	Signal transducer and activation of transcription
SH2	Src-Homology 2 domain
siRNA	Small interfering RNA, or silencing RNA
T.A cell	Transit Amplifying cell
TDO	Tryptophan 2,3-Dioxygenase
TLR	Toll-Like Receptor
TNF	Tumour Necrosis Factor

TNFR2	TNF Receptor 2
Tregs	Regulatory T-lymphocytes
UAS	Upstream Activation Sequence
UC	Ulcerative Colitis
Upd	Unpaired

Chapter 1:

Literature Review

1.1 Introduction

Biomedical research has proven invaluable in determining factors that contribute to human health, and also the development and manifestation of diseases. However, dependent on the area of research and experimental design, it is not always possible to actually conduct the research in human subjects. For instance, there are much higher ethical considerations using human samples or participants compared with other species. Additionally, compared with *in vitro* and *in vivo* models, it is much harder to control genetic and environmental conditions in humans, so therefore it is not surprising that inconsistent results are obtained. Furthermore, some studies may require long-term sampling and follow ups, such as those investigating chronic conditions, ageing or drug testing, which may be difficult due to changes in the participants' circumstances (health, job, living location for instance). Therefore, a multitude of biological models have been developed and utilised in the hope of expanding the depth of research that can be carried out. For instance, *in vitro* models (which translates to "within the glass") only uses certain parts of organisms which are capable of division (such as intestinal stem cells, or those derived from tumours) within petri dishes and culture flasks. Although there are numerous cells that can be cultured and studied *in vitro*, there is a much larger range of *in vivo* models that exist, and these can be divided into prokaryotic or eukaryotic organisms. Eukaryotes can then be further subdivided into vertebrates and invertebrates, with both of these also able to be subdivided into classes (e.g. insects can be found within invertebrates, mammals and fish are found within vertebrates). In short, this project will be investigating the role of the Suppressor of Cytokine Signalling 3 (SOCS3) in intestinal homeostasis and using models to determine whether the functions of this protein are conserved. Our experiments will be performed using *in vitro* models (human intestinal cell lines), and two *in vivo* models (mice, and fruit flies- *Drosophila melanogaster*).

To consider *in vitro* models first, they have many advantages for their use in scientific research as they are much cheaper, have a higher throughput and have reduced ethical considerations when compared to *in vivo* models. *In vitro* models are also considered to be much "simpler" than *in vivo* systems and this can allow easier dissection and manipulation of signalling processes (Fritz et al. 2013), due to focussing on a single cell line, for example. Furthermore, there are a large number of normal and transformed cell lines that are commercially available, and this allows research into both healthy and disease states. However, when using cultured cells, it is difficult to replicate all conditions found within *in vivo* organisms, and with regards to the gut, these can include: presence of luminal contents/ microbiota, oxygen levels (cells are typically cultured in 21% O_2, whereas physiological

levels are between 1 and 10%), pH, the gut-specific immune system, the constant flow of luminal contents, and also the proximity of other cells, nerves and, blood and lymphatic vessels, to name a few (Fritz et al. 2013).

Although mice are more expensive to maintain compared to *Drosophila*, and are associated with higher ethical considerations and limitations in relation to both *Drosophila* and cultured cells, one large advantage of their use in biomedical research is that the mouse genome has been fully sequenced and they have been found to share 99% of their genes with humans (Mouse Genome Sequencing Consortium 2002, Fritz et al. 2013, Kostic et al. 2013). In relation to our focus on the gastrointestinal (G.I) tract, mice also exhibit similarities in their anatomy, cell signalling pathways and the composition and function of their microbiota (Kostic et al. 2013). Mice are small in size so are therefore relatively easy to handle and can be housed with several mice in a single cage (depending on the experiment). The gestational time for the generation of mice is also substantially shorter than that of humans and other higher mammals, which results in quicker turnover of animals. Compared with humans, mice also have much shorter lifespans (approximately 2-3 years in the laboratory), and this makes lifespan and longitudinal studies more feasible (Fritz et al. 2013). However, one limitation that is particularly important when studying the G.I tract, is that environmental conditions, such as diet and housing, differ considerably between mice and humans (Fritz et al. 2013), and extrinsic, non-genetic factors are known to influence microbiota composition and can also impact on G.I disease susceptibility and severity (Hanauer 2006).

Finally, *Drosophila* have been used as model organisms for several decades and particular contributions to research include genetics, development and ageing. Like mice, *Drosophila* have very short generation times (approximately 10 days from egg to adult fly, at 25°C), and females are able to lay at least 1 egg every 2 hours, so this can result in the large number of progeny in a small period of time. Compared to both mice and humans, fruit flies have very short lifespans (approximately 60-80 days, although this is genotype dependent), also permitting ageing and longitudinal experiments to be carried out more easily, and potentially allowing multiple/repeated experiments to be performed in a relatively short period of time (Helfand and Rogina 2003). *Drosophila* are the easiest organism to genetically manipulate compared to humans and mice, and due to the vast number of commercially available fly lines, it is possible to target deletion or overexpression of target genes in particular cells or tissues. They have also proven to be useful models in intestinal research due to similarities in intestinal cell composition and conservation of cell renewal signalling pathways (such as

Janus kinase/Signal transducer and activator of transcription- Jak/Stat), although a disadvantage compared to vertebrate *in vivo* models is that they do not possess an adaptive immune system, thus limiting the study of immune homeostasis and immunological disorders (Apidianakis and Rahme 2011, Kostic et al. 2013). Additionally, female are able to reproduce with multiple male flies, so when generating experimental flies, it is essential that virgin females are used, and are bred with the appropriate male genotype.

To conclude, when conducting scientific research into health and disease, it is important to investigate the pathway/ molecule/ tissue etc. of interest in multiple models in order to achieve translatable results. Even where components are conserved, (such as those of the Jak/Stat pathway), and manipulated in the same way within each model (e.g. increased signalling activity), the responses may not be identical due to the clear differences between models. For instance, research animals will induce different and additional responses to those obtained *in vitro* due to crosstalk with other pathways/tissues etc. and also the involvement of the brain for instance, in regulation of certain behaviours. Therefore, *in vivo* responses may be different to those obtained *in vitro* so results should not always be generalised. It is also incredibly important for drug development to use a multitude of models, starting "low" with *in vitro* models as they can be used to ascertain molecule and pathway interactions, toxicity and permeability for example. Thus, *in vitro* studies allow valuable information to be obtained before investigating the effects in animals.

1.2 The Gastrointestinal Tract

1.2.1 Intestinal Structure

In the three organisms that are the focus of this literature review and overall project- humans, mice and *Drosophila*- the intestines are the site of food digestion. Concentrating on humans and mice first due the high level of similarity in their anatomy, their G.I tracts can be divided into two parts; the upper G.I tract, and lower G.I tract. The upper G.I tract consists of the oesophagus, stomach and duodenum, with the lower G.I tract comprising of the small intestine, cecum, large intestine, and anus. The major functions of the small and large intestines are to absorb macronutrients (i.e carbohydrates, fats and proteins), and water and minerals from ingested food, respectively. Although the function and general tissue structure of the intestines are alike in both mice and humans (reviewed by Nguyen et al. 2015), there are some differences between these two species (as demonstrated in figure 1.1). For instance, whilst the human cecum is relatively small in size with no distinct function, the murine cecum is considered to be large in relation to the size of the whole G.I tract and is responsible for production of certain vitamins and, digestion and fermentation of plant matter (Treuting and Dintzis 2011). Additionally, the human colon is comprised of different sections, consisting of the ascending colon, the transverse colon, the descending colon and finally the sigmoid colon before reaching the rectum (cited by Kararli 1995), with these sections so named based on their orientation and direction of the flow of luminal contents. However, the murine colon exists as more of a smooth continuous tract, rather than compartmentalised like the human colon, and this may explain the differences in colon microbiota (reviewed by Nguyen et al. 2015). Despite these differences, the small intestine in humans and mice is similar, consisting of the duodenum, the jejunum and the ileum (Treuting and Dintzis 2011).

The entire G.I tract is made up of 4 layers, and these consist of: the mucosa, the submucosa, the muscularis and, the serosa and adventitia, with both mice and humans displaying the same type and arrangement of these muscle layers (Nguyen et al. 2015). Regarding the intestinal tract, the mucosa is further divided into the epithelium, which is the closest layer to the lumen, the underlying lamina propria which consists of immune cells and connective tissue, and the muscularis mucosae; a thin layer of smooth muscle. The submucosa however, consists of one layer and is made up of connective tissue, along with blood vessels, nerves and lymphatic vessels that serve the adjacent mucosa and muscularis layers. The muscularis comprises of two smooth muscle layers, with the muscular circular layer situated closest to the submucosa, and below this is the muscular longitudinal layer, with these two layers differing in the orientation of their muscle fibres. Contraction of the muscular sublayers leads to decreased

luminal diameter and decreased luminal length, respectively, and these contractions are coordinated to propel contents within the lumen down the G.I tract in a process referred to as peristalsis. The final layer is the serosa and adventita, and like the submucosa, comprises of connective tissue and blood vessels (Kierszenbaum and Tres 2015).
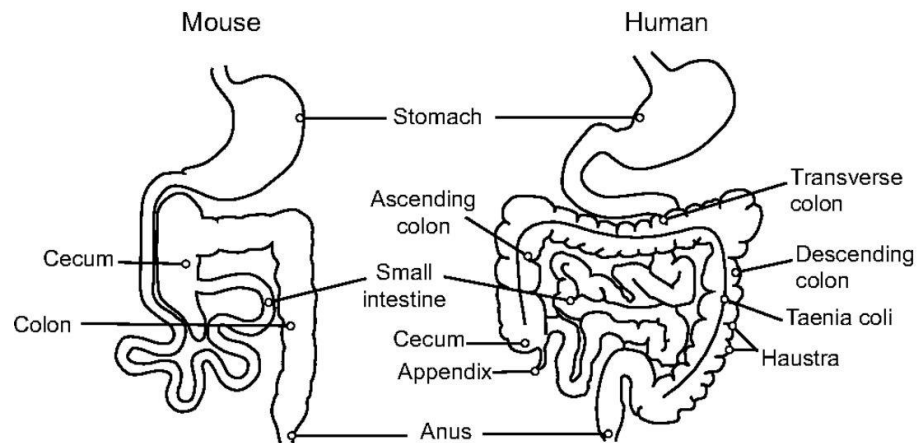
Figure 1.1: Comparison of gastrointestinal tracts between mice and humans, demonstrating similarities in organs present, as well as differences in organ size. The primary function of the gastrointestinal tract is to digest food, and extract nutrients and water. Any indigestible contents are then excreted as waste through the anus. (Image from Nguyen et al. 2015).

The lumen passes through the entirety of the intestinal tract and it is essentially a tube through which food for digestion, and pathogens pass. The lumen is also where a mucin layer and commensal bacteria reside, on top of the epithelial layer, and this layer acts as a physical barrier, separating the luminal contents from the adjacent lamina propria. The mucin layer can be further divided into an inner layer and an outer layer. The outer layer is thinner than the inner layer and contains an abundance of microorganisms. The inner layer however, is situated above the epithelial layer and under normal circumstances, is devoid of bacteria. This is due to the secretion of the antibody, IgA, by plasma B-lymphocytes in the lamina propria, and also antimicrobial peptides (AMPs) by intestinal epithelial cells (IECs), and this aims to inhibit microorganisms from associating and adhering to the epithelial layer and potentially penetrating the IECs to reach the underlying tissue (Hooper and Macpherson 2010).

Therefore, mucins have a vital role in maintaining immune homeostasis and the health of the host, and this is evident from studies using Muc2-deficient mice. Muc2 is a major constituent of the intestinal mucin layer, and these mice did not possess an inner layer devoid of bacteria, and thus, developed spontaneous inflammation in their intestinal tract (Van der Sluis et al. 2006, Johansson et al. 2008).
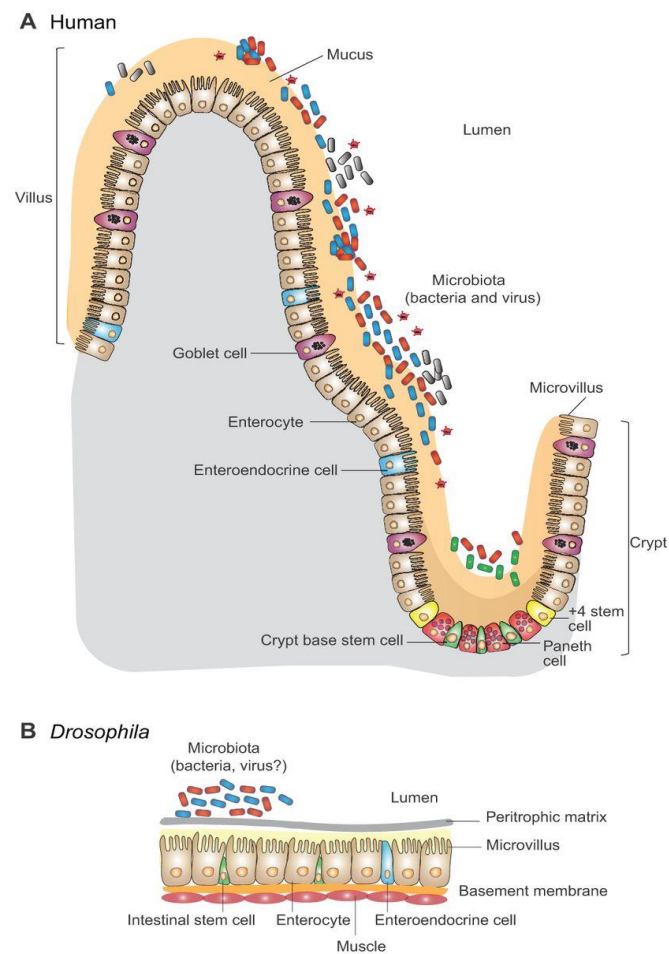
Figure 1.2: Comparison of structure and cell types of the intestinal epithelium in (A) humans, and (B) *Drosophila*. Both organisms possess an intestinal epithelial layer consisting of intestinal stem cells and, absorptive and secretory epithelial cells, with the epithelium acting as a barrier between underlying tissue and the luminal contents, which consists of commensal microbiota, as well as digested food. However, in humans, the epithelium consists of crypts, with cells migrating into the villi following differentiation. In *Drosophila*, the epithelial cells are situated on a basement membrane. There is an overlying peritrophic matrix, which is the equivalent of the mammalian mucin layer. (Note: The mouse epithelium also resembles that of humans). (Image from Wong et al. 2016).

The epithelial barrier consists of invaginations, called the crypts of Lieberkühn, and protrusions, called villi, although these villi are exclusive to the small intestine (Kirkwood 2004) (shown above in figure 1.2), and are in fact taller in mice than in humans (reviewed by Nguyen et al. 2015). Despite the size differences, mice and humans do exhibit similarities in villus shape, which may be expected, although the villi in rats are reported to be more "tongue-shaped" compared to the typically assumed "finger-shaped" villi normally described (Kararli 1995). Both organisms however, do possess microvilli on the surface of their IECs, which greatly increases the surface area of the small intestine. The intestinal epithelium is made up of four main cell types, all of which are derived from intestinal stem cells (ISCs), located just above the base of the crypts of Lieberkühn (reviewed by Wright 2000), with there being approximately 6-10 crypts for every villus (Potten 1991). Each ISC is capable of undergoing mitosis, and as each ISC divides, the cells migrate up the crypt and become more differentiated the further they move up the crypt (Schmidt et al. 1988, Marshman et al. 2002). Once differentiated cells reach the villi at the top of the epithelium, they are sloughed off into the lumen, with the whole renewal process taking 5-7 days. Each ISC typically divides asymmetrically to produce another ISC and a transit-amplifying (T.A) cell. T.A cells are only capable of dividing 4-5 times before differentiating into one of the four main cell types. There are three types of secretory cells; Paneth cells, goblet cells, enteroendocrine cells (EECs), and enterocytes (ECs), which have absorptive functions (reviewed by van der Flier and Clevers 2009). In addition to the secretory and absorptive functions of the IECs stated here (which will be discussed further in sections 1.2.3-1.2.6), all cells of the intestinal epithelium possess a range of cell junctions located on their lateral sides, and their overall aim is control transport of various small molecules (such as ions, nutrients and water) and uphold the barrier function, preventing (paracellular) translocation of luminal contents. Intestinal integrity is maintained through the presence of tight junctions, gap junctions, adherens junctions and desmosomes. Although adherens junctions and desmosomes help maintain adherence of neighbouring IECs, it is the tight junctions that play a more crucial role in intestinal permeability, as these are located nearest the lumen, at the apical end of lateral membranes, so therefore are one of the first physical barriers in the intestinal tract microorganisms will encounter that does not comprise of mucin or the microbiota. Increased permeability as a result of impaired function of tight junctions is detrimental to biological systems as it leads to increased translocation of both commensal and non-commensal microorganisms, thus inducing immune and inflammatory responses. If sustained, this can cause tissue damage, and potentially inflammatory and/or autoimmune disorders, such as inflammatory bowel disease (IBD) (Suzuki 2013). Furthermore, gap junctions are the most basal of the 4 lateral cell junctions and these are implicated in "horizontal" rather than "vertical" transport of molecules, permitting

the passage of ions and electrical impulses for example, between two neighbouring cells (Kleinzeller et al. 1999, Barreau and Hugot 2014).

1.2.2 Intestinal Stem Cells

ISCs are defined as proliferating, undifferentiated cells capable of producing progeny that continue to proliferate or differentiate into IECs, so are therefore classed as multipotent (Potten 1998, Wright 2000). These cells have an important role in the intestines as they are not only responsible for their own maintenance but also formation of the multi-functional IECs (discussed in more detail later) (shown in figure 1.3), and because of this, ISCs must be able to detect changes in cell populations within the intestine and respond appropriately. It is thought that in extreme situations, the differentiated IECs may de-differentiate in order to replenish ISC populations (Booth and Potten 2000). ISCs are found at the base of the crypts of Lieberkühn in both the small and large intestine, although their distribution differs between these two tissues. Crypt cell position 1 is in the centre of the very base of the crypt, and in the small intestine, ISCs can be found anywhere between position 2 and 7 amongst the Paneth cells, although on average, they are found at position 4. In the large intestine however, ISCs are also located at the base of the crypts but they originate from position 1 (Potten 1998). It is often described that the ISCs exist in their own intestinal niche, based on differences in the expression of receptors, growth factors and extracellular matrix proteins, and this is also reflected by the contrast in location, morphology, function and behaviour of the ISCs and the 4 main differentiated epithelial cell types (Booth and Potten 2000), thus creating a crypt-villus axis. Additionally, the basement membrane on which these cells lie is permeable, allowing secretion of various molecules, and also interaction between the ISCs and the cells underlying this membrane, which include fibroblasts, innate and adaptive immune cells and smooth muscle cells (Potten et al. 2009). Cell markers also differ between the proliferating and differentiated intestinal cells. For instance, expression of Leucine-rich-repeat containing G protein-coupled receptor 5 (Lgr5) is exclusively found at the base of intestinal crypts, in the ISCs (Barker et al. 2007), with the marker Ki67 associated with all proliferating crypt cells.

In the intestines, there are thought to be 4-6 "ultimate/true" stem cells and these make up the lowest level of proliferating crypt cells. These cells are the most sensitive to damage (particularly radiation, which was often used in the early intestinal studies, as cited in Potten and Loeffler 1990, and Potten 1998) and following cell death, the next layer of proliferative cells up the crypt assume the role of stem cells, in order to maintain intestinal homeostasis.

These cells are also known as clonogenic stem cells, and there are multiple layers of these in the crypts, with approximately 36 clonogenic stem cells in total. These cells are able to take over stem cell functions following loss of the underlying layer, with resistance to damage and radiation increasing with increasing position of the clonogenic stem cells too (Potten 1998). The T.A cells are situated above the clonogenic stem cells, and although they are also able to proliferate, they do not possess any stem cell attributes (Marshman et al. 2002).
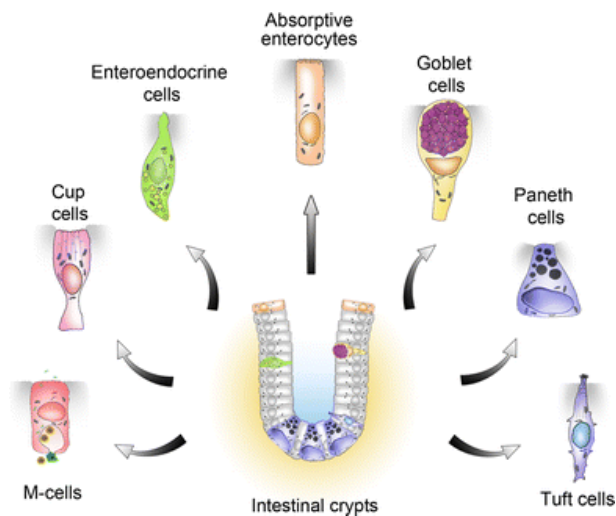
Figure 1.3: The differentiated cells of the intestinal epithelium. All differentiated intestinal epithelial cells originate from Lgr5+ stem cells located at the base of the crypts. Following proliferation, cells differentiate into one of the seven cell types shown and are found dispersed throughout the epithelium, with the predominant cell type being enterocytes. (Image from Gerbe et al. 2012).

1.2.3 Paneth Cells

Paneth cells are exclusive to the small intestine (as well as the cecum and occasionally the proximal colon in humans, Nguyen et al. 2015), and are located at the very base of the crypts with the first non-Paneth cell (i.e. ISC) situated, on average, at position 4, although this can range from 2 to 7 (Potten 1998). There are approximately 30 Paneth cells per intestinal crypt

(Potten 1998), and these are the only type of IEC that migrate downwards, rather than up the crypts during differentiation. Also unlike the three other main IECs, Paneth cells have the longest lifespan, with a duration of at least three weeks (Bjerknes and Cheng 1981). The role of Paneth cells in the intestines is to aid in innate immunity due to their phagocytic properties and the possession of large secretory granules that can release proteins such as lysozyme and tumour necrosis factor (TNF), which elicit antimicrobial effects (Wright 2000, van der Flier and Clevers 2009).

1.2.4 Goblet Cells

Goblet cells, unlike Paneth cells, are located in both the small and large intestine in both organisms, although there are differences in distribution. In mice, the largest population of goblet cells is located in the proximal colon, with lower numbers found in the distal colon and rectum. In humans however, there are fewer goblet cells in the proximal small intestine compared with the distal, although they are abundant from the cecum, throughout the large intestine to the rectum (Treuting and Dintzis 2011, Nguyen et al. 2015). The proportion of goblet cells within the whole IEC population increases from approximately 4% at the start of the small intestine, the duodenum, to around 16% in the descending colon (van der Flier and Clevers 2009). Similarly, moving along the large intestine, from proximal to distal, the ratio of goblet cells to ECs, the most abundant intestinal epithelium cell type, also increases (Treuting and Dintzer 2011). Goblet cells are so named due to their shape, and are responsible for secreting mucins and trefoil proteins, and these provide protection and lubrication to the mucosa surrounding the intestinal lumen, aid in the passage and expulsion of contents in the gut, and help to maintain epithelial integrity and contribute to repair processes (Wright 2000, Taupin and Podolsky 2003, van der Flier and Clevers 2009). There are approximately 20 identified mucins, with 9 of these expressed by both humans and mice. They can also either be secreted or remain bound to cell membranes (Natividad and Verdu 2013).

1.2.5 Enteroendocrine Cells

EECs are the final secretory cell type of the four main types of IEC and there are 15 different types, despite only making up 1% of the cells lining the lumen (Cheng and Leblond 1974). Each EEC type can be defined by its morphology, its location, the hormones/peptides they secrete and/or their expression of genetic markers (Cheng and Leblond 1974, van der Flier and Clevers 2009). For instance, N cells are found in the small and large intestine and they secrete neurotensin which inhibits intestinal contractions, whereas I cells are located in the

proximal small intestine and they secrete serotonin, which stimulates release of enzymes from the pancreas (Furness et al. 2013). Following recognition of environmental changes through communication with the central nervous system (CNS) and/or the intestinal lumen, EECs may then bind with and/or produce and secrete peptides to instigate further responses, such changes in appetite and food intake, and release of digestive enzymes (Wright 2000, Furness et al. 2013).

1.2.6 Enterocytes

ECs are the final cell type of the main four that make up the intestinal epithelium and are the only absorptive cells. They are polarised, columnar cells and they make up more than 80% of the cells lining the epithelium (Wright 2000, van der Flier and Clevers 2009). These cells are crucial to the epithelium as they have a brush border consisting of microvilli, which greatly increase the surface area, and are the site of digestion and absorption, due to the secretion of hydrolytic enzymes (Wright 2000, Radtke and Clevers 2005). This brush border also consists of glycoproteins similar to mucins (also termed the glycocalyx) that aid to protect the epithelium from contact with pathogens (Neutra 1998).

1.2.7 Additional Cells of the Intestinal Epithelium

In addition to these cells, there are also three other cell types that make up a small proportion of the intestinal epithelium. First, there are microfold, or M cells, that exhibit immune functions through transcytosis (transcellular transport) of pathogens from the apical surface to the underlying tissues, where immune cells such as dendritic cells, macrophages and T lymphocytes reside. Where M cells possess a brush border, the number of microvilli is lower than that of ECs, with a more irregular arrangement. If cells also have a glycocalyx, this is also not as thick as that found on the apical surface of ECs, along with the cell membrane, in order to allow close proximity to luminal contents (Neutra 1998). Next are cup cells, which are so named due to a depression in the apical cell surface causing the resulting chalice-like shape (Madara 1982). These cells are actually more numerous than EECs, and can comprise up to 6% of cells in the ileal epithelium (Gerbe et al. 2012). Like M cells, cup cells also exhibit a smaller brush border than ECs, as well as reduced activity of the enzyme, alkaline phosphatase- a hydrolytic enzyme involved in the removal of phosphate groups. However, despite these findings, the explicit functions of these cells are not currently known (Madara 1982, Gerbe et al. 2012). The final type of epithelial cells is tuft cells and these make up a smaller proportion of IECs than EECs, at 0.4%. These cells are named from the group of

microtubules that are attached to long, thick microvilli on the apical side of the cell protruding into the lumen, which resembles a "tuft." Similar to cup cells though, the functions of these cells have yet to be fully elucidated (Gerbe et al. 2012).

1.2.8 Structure of the *Drosophila* Midgut
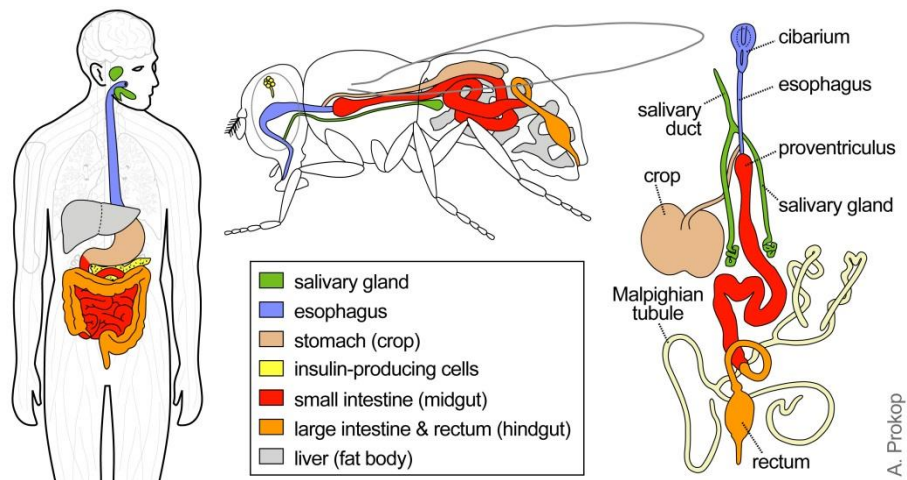
Figure 1.4: The gastrointestinal tracts of humans and *Drosophila*. (Colour coding depicts equivalent, homologous tissues between the two organisms). (WWW, Manchester University Fly Facility).

Considering *Drosophila* now, the anatomy of the GI tract shows some similarities to those in mammalian systems (shown in figure 1.4)- following the ingestion of food, this then travels down the foregut (oesophagus equivalent) where it may be stored in the crop momentarily (stomach equivalent) (Apidianakis and Rahme 2011). From the crop, it then passes through the midgut, which is similar to the mammalian small intestine (Ohlstein and Spradling 2006) and the main site of digestion ((Shanbhag and Tripathi 2009), and this is divided into the anterior, middle and posterior midgut. Finally, the digested food reaches the hindgut, the fruit fly equivalent of the large intestine (Ohlstein and Spradling 2006), and as in mammals, this is also the site of water, ion and electrolyte exchanges. Any indigestible food that remains in the tract will then be excreted from the anus. Also, located at the junction between the midgut and the hindgut are the Malpighian tubules, and these are the equivalent of the mammalian

kidneys (cited by Buchon et al. 2013a). As stated, the *Drosophila* midgut is the primary site of food digestion in *Drosophila*, and is a major defensive barrier against pathogens after the exoskeleton. It is also the first barrier against ingested pathogens. This is a particularly important function due to the main constituent of the *Drosophila* diet being microbe-containing rotting fruit and other food, so therefore an array of pathogens will be consumed on a frequent basis (Apidianakis and Rahme 2011). In mice and humans, the pH of the entire G.I tract is variable, with different pHs reported for each organ. Starting with the stomach, it is very acidic, ranging between pH 1-4, although this increases to 4-5 in the duodenum. By the end of the small intestine, at the ileum, the pH is higher still at 6.5-7.5. There is a decrease to approximately 5.7 in the cecum, although this increases to around 6.7 at the end of the G.I tract, in the rectum (Fallingborg 1999). The region-specific differences in pH can also be seen in the midgut of *Drosophila*, with the anterior midgut being fairly neutral. The middle midgut is very acidic due to the presence and functioning of iron and copper cells. The posterior midgut then becomes more alkaline due to secretion of bases into the lumen (Royet 2011).

Next, exploring the structure of the midgut, fruit flies do possess an epithelial barrier that also separates the luminal contents from the underlying tissue, along with a peritrophic matrix (shown in figure 1.2). This matrix consists of glycoproteins and chitin, and is situated above the IECs. It has similar functions to the mucin layer that lines the mammalian intestinal epithelium, protecting the lining from damage and pathogens, and lubricating food for passage through the tract, as well as having selective, semi-permeable properties (Lehane 1997). Despite the similarities, the actual arrangement of the *Drosophila* midgut epithelium differs from that in mice and humans. First, there are ISCs in the *Drosophila* midgut, although these are situated on a basement membrane, as there are no crypt structures (Micchelli and Perrimon 2006). ISCs are abundant, with approximately 800-1000 in the posterior midgut amongst a total of approximately 10,000 cells, although they are often located in certain areas of the midgut, due to different demands between niches (Ohlstein and Spradling 2006). As in mammals, *Drosophila* ISCs are the only proliferating cells found in the midgut, and these are also multipotent, capable of differentiating into multiple cell types. In mammalian systems, following proliferation of ISCs and, differentiation and migration of cells up the intestinal crypts to the tip of villi, cells undergo cell death and are shed from the tips of villi into the intestinal lumen. Drosophila ISCs also typically divide asymmetrically, producing another ISC and an additional midgut progenitor cell, known as an enteroblast (EB), although unlike T.A cells in mammals, EBs do not go on to proliferate themselves. However, it has been suggested that during the first few days following eclosion, all ISC divisions are symmetrical in order to generate sufficient numbers of ISCs to be maintained during the flies' lifespan

(Lucchetta and Ohlstein 2012). Depending on the level of Notch signalling, EBs will then differentiate into either one of the two IEC types, an EC or an EEC (Ohlstein and Spradling 2006), as there are no goblet cells or Paneth cells in *Drosophila*. Both of these cell types exhibit similar functions to their mammalian counterparts- ECs make up approximately 90% of the cells in the midgut epithelium (Ohlstein and Spradling 2007), with their primary function also consisting of digestion and absorption of food, aided by the presence of microvilli (Morgan et al. 1995). However, unlike EECs, and also ECs found in mice and humans, *Drosophila* ECs are able to endoreplicate, increasing their genome to 2-3 times its original size, and this also increases the size of these cells too, and may aid their absorptive function through increased surface area (Jiang and Edgar 2011). Similar to mammalian ECs though, those found in *Drosophila* are also capable of exhibiting apical-basal polarity (Micchelli and Perrimon 2006). *Drosophila* EECs maintain their secretory functions, releasing an array of response-inducing peptides dependent on the stimulus/environmental change in the CNS or the midgut, thus facilitating communication within and between the different tissues. However, whereas EECs can be found in both the small and large intestines in mammalian systems, they are exclusive to the *Drosophila* midgut (Veenstra et al. 2008). The type of peptide each EEC produces also dictates their specific location in the midgut. For instance, Marianes and Spradling (2013) found that short neuropeptide F (sNPF)-expressing EECs were located in the anterior midgut, with ion transfer peptide (Itp)-expressing cells confined to the middle midgut. (sNPF is a peptide involved in sugar metabolism, feeding behaviours and circadian rhythms, whereas Itp is implicated in locomotion, sleeping behaviours, in addition to circadian rhythms, cited on WWW, Flybase). The variabilities in EEC location are thought to either stem from differences in differentiation between region-specific ISCs, or from region specific signals and requirements influencing ISCs (Marianes and Spradling 2013).

The midgut renewal process in *Drosophila* is similar to that in mammalian systems, with *Drosophila* IECs also capable of undergoing apoptosis following differentiation and eventually being shed into the lumen. Under homeostatic conditions, the whole process from ISC proliferation to cell death takes approximately one week, similar to rates reported in mice and humans (Ohlstein and Spradling 2006). As seen in mammals, the structure and integrity of the midgut relies upon the presence and correct functioning of ISCs, and this was shown by Jiang et al. (2009), who found that ablation of ISCs led to the loss of all ISCs, EBs, EECs and several ECs, subsequently causing a decrease in midgut size. However, loss of ECs had less of a negative effect and midguts had regained their original size after 60 hours through proliferation of ISCs, verifying that IECs emanate from ISCs.

1.3 Intestinal Cell Renewal Pathways

The intestinal epithelium is one of the most rapidly proliferating tissues within biological systems, with the midgut being one of the few tissues in *Drosophila* that is renewed, as fruit flies are primarily post-mitotic organisms following eclosion (cited by Rudolph 2010). As with any tissue though, it is important that cell numbers are maintained, and this is achieved through a balance of cell proliferation and cell loss, either through apoptosis or anoikis. If cellular proliferation increases (perhaps along with decreases in cell death), this can lead to hyperplasia, and in terms of the gut, an increase in crypt and villus size. If intestinal proliferation continues to increase and regulation of one or more of the signalling pathways involved in renewal is impaired, this may ultimately result in carcinogenesis. Conversely, a decrease in proliferation (particularly if accompanied by an increase in cell death) can lead to loss of crypt integrity and increased intestinal damage, and may ultimately lead to inflammatory bowel disease. Reduced intestinal proliferation rates, and consequently crypt and mucosal depths, are also a common finding amongst germ free (GF) animals, when compared with conventionally raised (CR) animals (Abrams et al. 1962).

In terms of research concerning mammalian intestinal proliferation, a lot of our understanding has been obtained from the considerable number of studies that have been performed on mice, due to the difficulties in carrying out such invasive, tracking experiments in humans, and also the vast differences in lifespans when investigating proliferation changes with ageing as well, for instance. From said studies, we have learnt about the intestine by numbers, which may give us some indications about the human intestines. Starting with the murine small intestine, each crypt contains approximately 250 cells, with 150-160 of these being proliferative cells. These proliferative cells are typically found from the 4th crypt position (with Paneth cells occupying the lower positions), with about 16 cells per crypt ring/layer and approximately 10 rings per crypt (Potten 1991). The bottom ring of the 10 is where the ISCs reside. Each proliferative cell is capable of dividing 1-2 times per day, with cell cycle durations estimated to be between 12 and 32 hours, although this is depends on the requirements of each crypt, or regions within each crypt. This results in the generation of approximately 300 new intestinal crypt cells per day, and therefore, around 12 per hour. In the migration process from crypt to villus following differentiation of T.A cells, cells are reported to move 1-2 cell positions per hour, with each villus consisting of ≈3500 cells. Up to 1400 cells are lost from each villus per day, with an approximated 2×10^8 thought to be shed from the small intestine each day (Potten 1998). In humans, it is thought this number could be as high as 10^{11} cells, with the number of cells per crypt found to be higher too, with ≈450 (Potten 1991). When investigating

the murine large intestine, Potten (1998) found higher numbers, with approximately 300-450 cells per crypt. However, each crypt was found to have a circumference of 18 cells, which is only 2 more than in the small intestine. Cell cycle durations fall within the range of small intestinal cells too, with each proliferating colon cell dividing roughly every 20 hours (Potten 1998). In the *Drosophila* midgut, there are fewer cells in total, with approximately 10,000 and 800-1000 of these being ISCs (Ohlstein and Spradling 2006). However, this decrease is expected due to the substantial differences in organism size between flies, and both mice and humans. Additionally, the *Drosophila* midgut cells are situated on a basement membrane, rather than in crypts as found in mammalian systems (Micchelli and Perrimon 2006), and this could reduce the surface area of the midgut, and thus reduce the potential number of cells. Regarding mitotic rates of *Drosophila* ISCs, it is to be assumed that the cell cycle durations may be comparable to those in mice and humans due to their similarities in time taken for complete epithelium renewal. Typically, ISCs divide asymmetrically, producing another ISC and a maturing cell which will go onto differentiate into one of the intestinal epithelial cell types. However, 5% of ISC divisions are symmetrical, resulting in the production of either two ISCs, or two maturing cells (Loeffler and Potten 1997), so therefore the balance must be maintained in order to ensure there are not inappropriate increases or decreases in ISCs. It is important that the ISC population is constantly renewed as ISCs are sustained through the lifetime of many organisms (Booth and Potten 2000), including mammals and fruit flies, so therefore they must be protected from damage, or exhaustion from over-proliferation (Quante and Wang 2008). The loss of just one ISC from one crypt would result in a considerable decrease in the overall number of cells (Marshman et al. 2002), although ISCs are capable of detecting the death of one of their own cells and initiating a response accordingly (Potten 1991). Furthermore, ISCs are the only proliferating cells in the intestines, so each ISC has the potential of giving rise to carcinomas (Booth and Potten 2000), so therefore must be well-maintained. Despite this, ISCs are capable of switching between processes of differentiation, and, self-maintenance, depending on the needs of the crypt. Partially differentiated cells are also capable of de-differentiating back into stem cells if necessary (Booth and Potten 2000).

In both mammals and *Drosophila*, there are many signalling pathways involved in initiation and regulation of intestinal cell renewal. Examples found in all three systems include the Notch/Delta, Wnt, Jun N-terminal Kinase (JNK), Hippo, Epidermal Growth Factor Receptor/ Extracellular Signal-Regulated Kinases (EGFR/Erk), insulin and Jak/Stat signalling pathways. In addition to its roles in IEC differentiation, the Wnt pathway is also one of the predominant pathways implicated in intestinal cell turnover. Wnt is also the name of the protein ligand responsible for pathway activity, and in the absence of this ligand in mammals, β-catenin (a

protein involved in cell adhesion and gene transcription) is phosphorylated and targeted for proteasomal degradation by a complex of several proteins, including the tumour suppressor, adenomatous polyposis coli (APC). Upon Wnt binding to the Frizzled receptors and lipoprotein receptor-related protein coreceptors, the proteasomal complex is inactivated, so β-catenin accumulates in the cytoplasm and forms a transcriptional complex with other proteins, resulting in the transcription of Wnt target genes in the nucleus associated with cell proliferation. A gradient of Wnt signalling occurs within the intestine, with the highest amount of Wnt activity found at the base of the crypts, thus reinforcing the presence of the crypt-villus axis (cited by van der Flier and Clevers 2009).

As stated previously, there are several other signalling pathways responsible for intestinal renewal, although our main focus in this project is Jak/Stat, due to the ability of SOCS3 to inhibit signalling in this pathway. The Jak/Stat pathway is involved in cell growth and differentiation, as well as apoptosis (reviewed by Krebs and Hilton 2001). In mammals, signalling is activated upon binding of a cytokine (for example, interleukins such as interleukin-6 (IL-6), and interferon-γ, IFN-γ) to cytokine receptors, which induces receptor dimerisation and conformational changes in the receptor structure (as shown in figure 1.5). Jak proteins are also recruited to the receptors and Jak activation occurs through cross- or auto-phosphorylation of tyrosine residues located within the protein. The activated Jak proteins then phosphorylate tyrosine residues on the cytosolic domain of the receptors, causing Src-homology 2 (SH2) domains of Stat proteins to bind to these residues. The Stat proteins are activated through phosphorylation of their tyrosine residues by Jaks, which is followed by homo- or hetero-dimerisation- dimerisation of the same or different type of Stat protein, respectively. The Stat dimer enters the nucleus and transcription of genes associated with cell proliferation, differentiation or apoptosis occurs, as well as transcription of SOCS genes. SOCS are negative regulators of Jak/Stat signalling, and as their activation is based upon activation of the Jak/Stat pathway, this produces a negative feedback loop (reviewed by Greenhalgh et al. 2002). There are other negative regulators in the pathway, and these are protein inhibitors of activated Stats (PIAS) and SH2-containing protein tyrosine phosphatases (SHPs). PIAS is capable of preventing transcription that results from Stat binding to DNA, either directly, or indirectly by inhibiting the dimerization of Stat proteins. SHPs operate by binding to and desphosphorylating tyrosine residues on Jaks, thus reducing their catalytic activity (reviewed by Larsen and Röpke 2002).
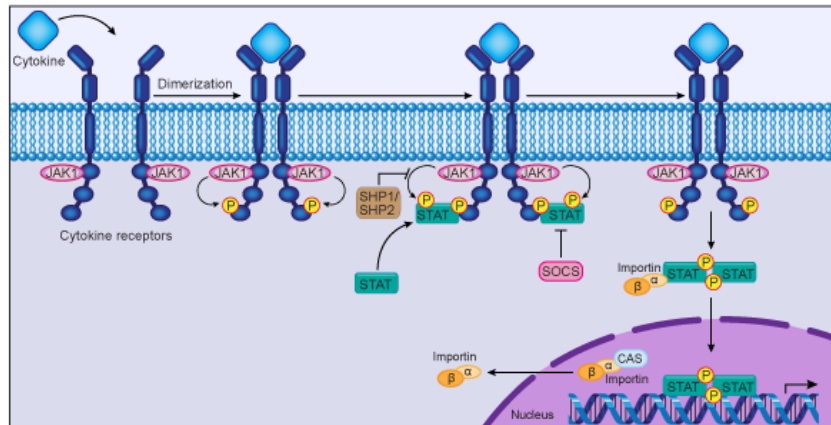
Figure 1.5: The mammalian Jak/Stat pathway. Ligand binding induces receptor activation and dimerisation, leading to recruitment and phosphorylation of Jak proteins. Jaks phosphorylate tyrosine residues on the receptor, recruiting Stat proteins. Stat proteins are activated once phosphorylated by Jak proteins, and subsequently dimerise and translocate to the nucleus in order carry out gene transcription. Upon activation of Jak/Stat signalling, the genes for SOCS are transcribed, leading to the production of SOCS proteins and suppression of Jak/Stat signalling (WWW, Mutagenetix, South Western Medical Centre).

Each component of the mammalian Jak/Stat pathway has several different types. For instance, there are 4 types of Jak: Jaks 1, 2 and 3, and tyrosine kinase (TYK) 2, along with 7 types of Stat protein: Stat1, Stat2, Stat3, Stat4, Stat5a, Stat5b and Stat6 (reviewed by Krebs and Hilton 2001). There are also 8 different SOCS: SOCS 1-7 and cytokine-inducible SH2-protein (CIS). Each SOCS protein can be paired with another SOCS, in relation to the homology between N-terminal regions (reviewed by Greenhalgh et al. 2002): CIS and SOCS2, SOCS1 and SOCS3, SOCS4 and SOCS5, SOCS6 and SOCS7. The SOCS proteins also inhibit Jak/Stat signalling at different points within the pathway. SOCS 1 and 3 contain a kinase inhibitory region (KIR) at the N terminus and this allows them to bind to Jaks and inhibit their activity, whereas CIS prevents Stat proteins from binding to the cytosolic domains of the cytokine receptors. SOCS proteins possess an N-terminal that can comprise of 50-380 amino acids, with the length and amino acid composition differing between each protein (Krebs and Hilton 2001). As stated, the KIR domain is located within the N-terminal and this consists of 12 amino acid residues, and is essential for inhibition of the Jak kinase activity, particularly in SOCS3, as mutations

not only affected the ability to interact with the Jak proteins, but the downstream inhibitory effect on Stat activity was prevented as well (Sasaki et al. 1999). Adjacent to the N-terminal and KIR domain lies an SH2 domain, and this is able to bind to activated, tyrosine-phosphorylated signalling molecules, such as Jaks within the Jak/Stat pathway specifically, and this also blocks binding sites for recruited Stat proteins (cited by Babon et al. 2006). At the N-terminal of the SH2 reside domains known as the N-extended SH2 domain (ESS in figure 1.6), and this also aids in the binding of the SH2 domain to phosphotyrosine residues as mutations in these domains affect the interaction that normally takes place between Jak and SOCS proteins (Sasaki et al. 1999). Additionally, the SH2 domain of SOCS3 specifically also contains an "unstructured motif insertion," which is Proline-, Glutamic-acid-, Serine- and Threonine-rich, so is therefore referred to as the PEST motif (Babon et al. 2006), and is conserved in several mammalian species (Babon et al. 2005). Although removal of this motif does not affect the function of the SH2 domain or the inhibitory effects of SOCS3, its role is to regulate the stability of the protein, so in doing so, this decreases its turnover and increases the half-life of SOCS3. Furthermore, it is thought that PEST may mediate degradation of SOCS3 (perhaps following cessation of signalling), as phosphorylation of residues within the PEST motif has been reported to affect degradation, and expression of SOCS3 was higher following removal of PEST; both with and without the addition of a proteasomal inhibitor (Babon et al. 2006). Finally, within the C-terminal of all SOCS proteins (in addition to other non-Jak/Stat proteins) is a conserved region 40 amino acids in length known as the SOCS box (Krebs and Hilton 2001, Piessevaux et al. 2008). Unlike the other domains within the SOCS proteins, the SOCS box is not implicated in direct inhibition of the Jak/Stat pathway, but is involved in proteasomal degradation of SOCS3 and other proteins (Zhang et al. 1999). The role of the SOCS box in the degradation of SOCS (and in this case, SOCS3) was shown through continual increases in IL-6-induced SOCS3 proteins levels following incubation of cells with a proteasomal inhibitor (compared to cells that were not treated with the inhibitor) (Zhang et al. 1999). The degradation process involves the binding of elongins B and C to form a dimer which is then able to interact with the SOCS box and link the protein targeted for degradation to a scaffold protein known as Cullin (Piessevaux et al. 2008). A protein known as RING-box protein 2 interacts with Cullin and recruits the ubiquitin complex to the SOCS box, and this consists of: an E1 ubiquitin-activating enzyme, an E2 ubiqutin-conjugating/transferase enzyme and an E3 ubiqutin ligase, and collectively, these all function to polyubiquitinate proteins (such as Jaks and SOCS) and target them for proteasomal degradation (Yoshimura et al. 2007, Croker et al. 2008).
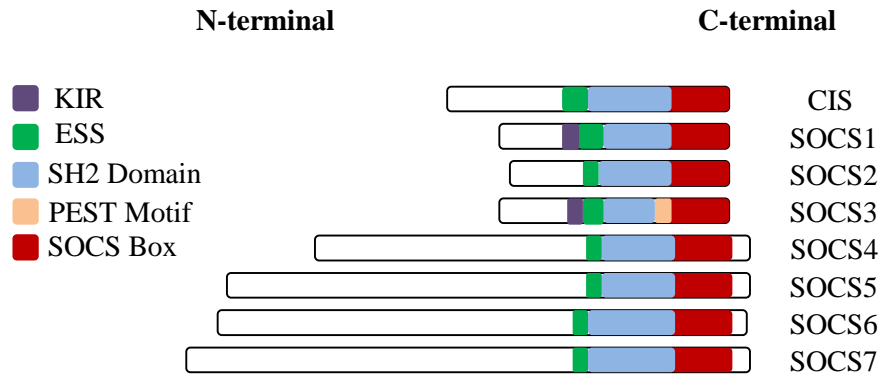
Figure 1.6: The structure and domains of the mammalian SOCS proteins. Each protein contains an ESS and an SH2 domain, along with a conserved SOCS box at the C-terminal. SOCS1 and SOCS3 contain an additional domain, the KIR domain, responsible for inhibiting Jaks, and SOCS3 also has a PEST motif within its SH2 domain, which is implicated in protein stability and degradation. (KIR= Kinase Inhibitory Region, ESS= N-terminal Extended SH2 domain) (Adapted from Piessevaux et al. 2008).

Focusing on SOCS3 in particular, its main, well-publicised role is the inhibition of cytokine-induced signalling (along with the other SOCS proteins), and in addition to Jak protein degradation, this is achieved through inhibition of Jak1, Jak2 and TYK2 proteins. SOCS3 is able to inhibit these proteins and not the remaining Jak- Jak3- as those 3 proteins contain a conserved motif consisting of glycine, glutamine and methionine residues that is not present in Jak3 (Babon and Nicola 2012). This process is required for limiting proliferation and inflammation, and often forms a negative feedback loop during this process. For instance, deletion of SOCS3 in multiple mouse studies has proven to not only affect cell signalling but also be detrimental to the health of the host. Generating mice with conditional knockout of SOCS3 in their haematopoietic and endothelial cells resulted in premature death due to the development of inflammatory lesions (cited by Croker et al. 2008). Additionally, deletion of SOCS3 in macrophages led to hyper-responsiveness following treatment with IL-6 and alterations to the usual IL-6 induced responses, in that inflammatory genes normally induced by IFNs and Stat1 were activated (cited by Babon and Nicola 2012). Conversely, many studies report elevation of SOCS3 in IBD due to increases in IL-6 and Stat3 (Suzuki et al. 2001, Li et al. 2010). These studies therefore demonstrate the importance of appropriately regulated SOCS3 levels, as both reduced and increased expression can affect inflammatory

processes. These findings also demonstrate the significant role of SOCS3 in particular subsets of cells and tissues, whereas the generation of SOCS3$^{-/-}$ mice (as a whole) results in embryonic lethality due to abnormalities in the placenta and development of vessels within the embryo. The accumulation of these defects must lead to rapid deterioration of mice embryos as they appear to develop normally by day 10 in utero, although by day 12, 50% of the embryos had died, and by day 13.5, SOCS3$^{-/-}$ mouse survival was at 0% (Roberts et al. 2001). In order to overcome this obstacle, Croker et al. (2003) were able to utilise Cre-lox recombinase technology to target deletion of SOCS3 following removal of SOCS3 DNA by the Cre recombinase enzyme at sites either side of the target gene where loxP has associated (Orban et al. 1992).

The Jak/Stat pathway is also conserved in *Drosophila*, and is required for the renewal of germ cells, as well as ISCs (Kiger et al. 2001). This pathway is actually simplified compared with the mammalian Jak/Stat pathway, and there are *Drosophila* homologues corresponding to components found in the mammalian pathway. The activator of Jak/Stat in *Drosophila* is related to mammalian IL-6 and known as Unpaired, or Upd, of which there are three: Upd1, Upd2 and Upd3 (Agaisse et al. 2003, Jiang et al. 2009), and this binds to the receptor, Domeless (Brown et al. 2001) (shown in figure 1.7). There is only one Jak protein, which is known as Hop, and this shows the most homology to Jak2 (Binari and Perrimon 1994). There is also only one Stat protein, Stat92E, which is homologous to mammalian Stat5 (Yan et al. 1996). However, there are three SOCS proteins found in *Drosophila*, and these are SOCS16D, SOCS44A and SOCS36E (Hou et al. 2002) (shown in figure 1.8). SOCS36E is the most documented SOCS protein in *Drosophila*, and is the homologue of human and murine SOCS5. It acts by preventing the phosphorylation of Stat92E, and therefore Stat dimerisation. Despite being homologous to human SOCS5, the fact that SOCS36E can inhibit Jak/Stat signalling means it is functionally similar to CIS and SOCS1-3 (Callus and Mathey-Prevot 2002). SOCS16D and SOCS44A are the homologues of human SOCS6 and 7 (Rawlings et al. 2004), although less has been published on the functions of these inhibitors.
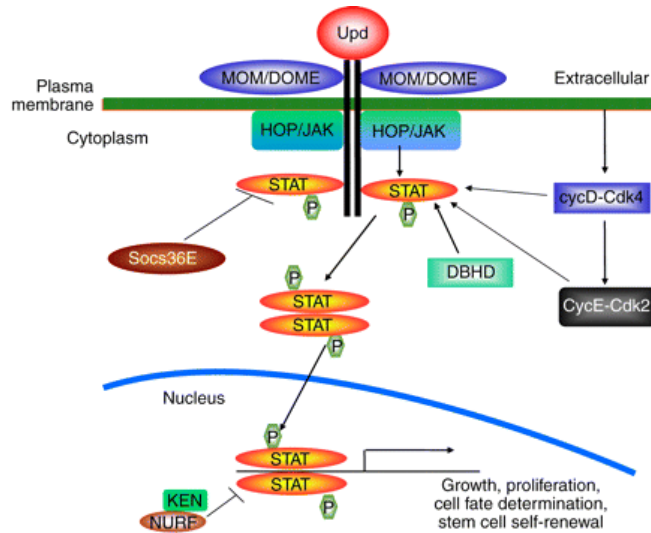
Drosophila	Mammals
Upd1, 2 and 3 ligands	IL-6
Domeless Receptor	IL-6 Receptor/ gp130
Hop	Jak (more specifically Jak2)
Stat92E	Stat (more specifically Stat5)
SOCS (SOCS36E, SOCS16D, SOCS44A)	SOCS (SOCS5, and SOCS6 and SOCS7)

Figure 1.7: The *Drosophila* Jak/Stat pathway. This pathway is conserved in fruit flies with homologues of the main components shown in the table above, and is activated through binding of the Upd ligand to the Domeless receptor. Receptor dimerisation occurs and Hop proteins are recruited. Once Stat92E is recruited to Domeless and phosphorylated by Hop, dimerisation occurs, followed by translocation of Stat92E dimers to the nucleus where gene transcription occurs. Among the genes transcribed are negative regulators of the pathway, including genes encoding SOCS proteins (Image reproduced with permission from The Journal of Experimental Biology, Singh and Hou 2009).

SOCS36E was first identified by Nicholson et al. (1999) due to the sequence homology in both the SH2 domain and in the 20 amino acids that precede it when compared with SOCS5. More specifically, Callus and Mathey-Prevot (2002) reported 68% identical homology between the SH2 domains and the SOCS box of SOCS36E and human SOCS5. However, no

homology was reported between N-termini, although this is not surprising as there is variability between N-termini even within the family of human SOCS proteins (Krebs and Hilton 2001). Interestingly, compared with *Drosophila* SOCS proteins, human SOCS1-3 have found to be at least 100 amino acid residues shorter, suggesting these differences may be evolutionary and arose following divergence of mammals and insects (Stec and Zeidler 2011). Within the SOCS36E protein, the SH2 domain is essential for the interaction of SOCS36E with its target molecules, such as Domeless and Hop (Rawlings et al. 2004, Stec et al. 2013), with maximal activity of the overall protein enhanced through the presence and appropriate functioning of the SOCS box (Callus and Mathey-Prevot 2002). Additionally, SOCS36E is able to inhibit Jak/Stat signalling not only through prevention of Stat92E activation and phosphorylation (and subsequent downstream signalling), but through destabilisation of the Domeless receptor facilitated by elongins B and C and the Cullin protein due to the conserved SOCS box domain (Stec et al. 2013). As in mammalian systems, expression of SOCS36E is initiated following activation of the Jak/Stat pathway, as larval studies revealed identical overlapping expression patterns for SOCS36E and the pathway ligand, Upd. Additionally, increases in mRNA expression of SOCS36E were observed in larvae exhibiting gain of function Jak/Stat mutations (Callus and Mathey-Prevot 2002). In contrast to findings of Roberts et al. (2001), Callus and Mathey-Prevot (2002) found that deletion of SOCS36E in embryos (achieved through RNA interference- RNAi- injection) did not result in embryonic lethality, nor were any defects observed either when compared with controls, potentially suggesting different roles of SOCS proteins during embryonic development between mammals and *Drosophila*. Conversely, Callus and Mathey-Prevot (2002) also expressed SOCS36E ubiquitously in adult flies, and this was found to lead to a shortening of lifespan although again, no other strong phenotypes were detected. However, despite these observations, one of SOCS36E's primary roles within *Drosophila* is the regulation of eye and wing development, as defects in both have been detected following both directed expression and RNAi depletion of SOCS36E, along with outgrowths (Callus and Mathey-Prevot 2002, Herranz et al. 2012). Results suggested that these effects were mediated by the SOCS box as its deletion resulted in decreases in outgrowth number.
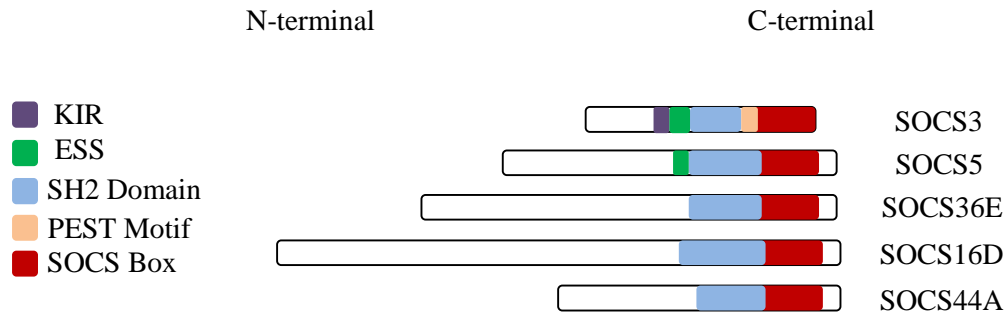
Figure 1.8: Comparison of the structure of *Drosophila* SOCS proteins, along with SOCS36E and its structural and functional mammalian homologues, SOCS5 and SOCS3, respectively. All *Drosophila* SOCS proteins lack KIR and ESS domains, but contain SH2 domains and a SOCS box, demonstrating the evolutionary conservation and important functions of these components. (Adapted from Arbouzova and Zeidler 2006, and Piessevaux et al. 2008).

Although the Jak/Stat pathway is present in mammalian intestinal cells and is implicated in proliferation and renewal, as indicated by its dysregulation in cancers of the G.I tract (discussed in further detail later in the chapter), the activity of the *Drosophila* pathway appears to play a more central role in gut turnover. Jak/Stat signalling is required for initiation and regulation of basal levels of proliferation, and it is also induced through either infection or injury, as damaged cells release Upd3 (Agaisse et al. 2003, Buchon et al. 2009a, Jiang et al. 2009). Buchon et al. (2009b) conducted several experiments investigating the role of the midgut Jak/Stat pathway, and did so by using the Gram-negative phytopathogen, *Erwinia carotovora carotovora 15* (*Ecc15*). *Ecc15* naturally infects *Drosophila* in the wild, but under normal circumstances, this infection will not lead to mortality; instead, immune and proliferative responses are initiated (Basset et al. 2000, Buchon et al. 2009a). However, flies whose Jak/Stat pathway is inhibited, or who are deficient in Upd3, succumb to *Ecc15* infection within a week of oral ingestion. Surprisingly, flies deficient in their immune pathway (Imd) did not exhibit *Ecc15*-induced mortality, indicating that proliferative, repair processes are more crucial to the health of *Drosophila* than immune responses (Buchon et al. 2009b). This increased susceptibility to infection was also continued in Stat RNAi flies infected with *Pseudomonas entomophila* (Jiang et al. 2009).

In the *Drosophila* midgut, there appears to be more crosstalk between Jak/Stat and other signalling pathways, than in mammals. For example, the *Drosophila* Jak/Stat pathway can be activated by JNK signalling, (which is similar in function to Jak/Stat), with the JNK pathway activated in the event of stresses, such as DNA damage, reactive oxygen species (ROS), inflammatory cytokines and infection. Initiation of JNK signalling can result in apoptosis, and tissue regeneration and repair through cell proliferation; both of which are essential for long-term tissue homeostasis (Biteau et al. 2011). Upon activation of the JNK pathway, the Jak/Stat ligands, Upd1-3 are induced, thus further promoting proliferation of ISCs (Jiang et al. 2009). Additionally, crosstalk also exists between the *Drosophila* Jak/Stat and Hippo signalling pathways. In this pathway, the activity of a growth-promoting transcriptional co-activator known as Yorkie is normally limited in order to prevent excess proliferation of ISCs. Inhibition of Yorkie activity is brought about through phosphorylation by a kinase known as Warts (Shaw et al. 2010). Decreased levels of Warts lift this inhibition on Yorkie and when active in ECs, promotes ISC proliferation through secretion of Upds (Upd3 in particular) (Irvine and Staley 2010). Activation of the JNK pathway also promotes Yorkie activity, so therefore JNK acts upstream of the Hippo pathway, which in turn is upstream of the Jak/Stat pathway (Irvine and Staley 2010). Furthermore, Jak/Stat is able to coordinate with the Wnt and Epidermal Growth Factor Receptor (EGFR) pathways, as their activation is increased following dysregulation and diminishing activity in one of the other pathways, to ensure efficient regulation of ISCs (Xu et al. 2011). Collectively, the numerous pathways involved in ISC proliferation and midgut renewal, along with the amount of signalling pathway crosstalk that has been reported, stress the importance of regulated homeostasis within *Drosophila* and also of the midgut as a whole.

1.4 Implications of Dysregulated Intestinal Homeostasis

Dysregulation and/or mutations within any cell signalling pathway in biological systems can be detrimental to the health of the host, with increases in pathways whose activation results in proliferation increasing the risk of developing hyperplasia, or if sustained, cancer. Cancer is a group of diseases characterised by the uncontrolled replication of cells, and this occurs due to the accumulation of genetic mutations. The accumulation of cells with uncontrolled proliferation also increases the chances of a mutation escaping cell checkpoint mechanisms. The process of carcinogenesis comprises of three steps: initiation, promotion and progression. Initiation consists of genetic alterations within a cell and if they are not rectified, or if they accumulate, then these changes could become irreversible. Promotion involves the survival

and replication of these cells, thereby increasing the number of cancerous cells. Finally, progression is the increase in growth of the tumour, and metastasis that may ensue (Rakoff-Nahoum 2006). With respect to colorectal cancer (CRC) specifically, one of the most commonly mutated genes is the APC gene. APC mutations are found in approximately 80% of sporadic CRC cases, with heterozygous mutations inherited in 100% of familial adenomatous polyposis coli (FAP) cases, with the severity and onset of FAP dependent on the location of the mutation (Bach et al. 2000). Along with other proteins, APC normally inhibits transcriptional activity of β-catenin, although mutations or induced deletion (i.e in mouse knockout studies) of APC results in increased accumulation of β-catenin and consequently increased transcription-induced proliferation (van der Flier and Clevers 2009). As stated previously, there is a crypt-villus axis that exists within the intestines, and this is particularly true for Wnt signalling, with higher activity levels found at the base of the crypts of Lieberkühn. Therefore, it is not particularly surprising that deletion of APC in the Lgr5+ stem cells results in their transformation within a matter of days (cited by Potten et al. 2009).

With respect to Jak/Stat signalling, one of the outcomes that results from activation of this pathway is also proliferation, so therefore dysregulated pathway activity (whether it is increased or decreased) would alter cell growth and possibly overall tissue homeostasis and host wellbeing. An increase in JAK/STAT signalling and/or a loss of regulation (through decreased SOCS for example) would lead to increased proliferation, and if sustained, could also lead to hyperplasia or tumourigenesis. Reductions or lack of SOCS proteins have been reported in a multitude of different cancer types (particularly SOCS3) as the expression levels are not sufficient enough to fulfil their role as tumour suppressors (He et al. 2003, Weber et al. 2005, Ogata et al. 2006, Croker et al. 2008). Due to the release of SOCS' inhibition on Jak/Stat signalling (with the pathway component differing depending on the SOCS protein affected), phosphorylation, dimerisation and translocation of Stat proteins is able to take place, although consequently gene transcription is increased. As a result, tumours with diminished SOCS levels also often exhibit increased levels of Stat, and phosphorylated Stat proteins (Croker et al. 2008, Li et al. 2010).

Many studies have been conducted into the role of Jak/Stat signalling in cancer, particularly with respect to CRC within the G.I tract, as the colon is more susceptible to tumours than the ileum (Potten 1998). For instance, increased activation of Jak/Stat signalling (and Stat3 in particular) has been reported in multiple *in vitro* intestinal cancer cell lines and colon carcinomas, with the addition of Jak or Stat inhibitors leading to cell cycle arrest and

apoptosis (Lin et al. 2005, Xiong et al. 2008 Grivennikov et al. 2009). In a murine model of colitis-associated carcinogenesis (CAC), Rigby et al. (2007) reported an increase in hyperproliferation following IEC-specific deletion of SOCS3. This led to tumourigenesis, and these mice also exhibited increases in both number and size of tumours, when compared to SOCS3-sufficient mice. Although experiments by He et al. (2003) were not performed in intestinal cells, they also found silencing of SOCS3 (caused by promoter hypermethylation) occurred in multiple cancer cell lines (e.g. lung, breast and mesothelioma), and restoration of SOCS3 in lung cancer cells specifically, led to decreased activation of Stat3, subsequently suppressing tumour growth and inducing cell death by apoptosis. These results were able to demonstrate the potential use of SOCS3 in cancer therapy. However, a slight limitation of these studies is that experiments investigating effects of SOCS3 and Jak/Stat on intestinal homeostasis were carried out using *in vitro* cancer cell lines and primary samples. In these, carcinogenesis has already been established and it may be possible that one or more mutations were present anywhere within the cells. There has been very little research into the role of SOCS3 in normal homeostasis. Along with tumour biopsies, Corvinus et al. (2005) did discover increased Jak/Stat signalling as a result of increased Stat3 activity in adjacent, non-neoplastic tissues. They suggested this event may precede the histological changes that arise during tumourigenesis, but it may have been the case that Stat3 increased due to the release of tumour-derived factors that promote Jak/Stat signalling so may not be entirely reflective of homeostatic changes in non-cancerous cells.

Conversely, SOCS3's role in cell turnover has also been demonstrated in overexpression studies. Rigby et al. (2007) overexpressed SOCS3 in two *in vitro* intestinal cell lines (IEC-6 and Caco-2- rat, and human cancer cell lines respectively), and this reduced proliferation. In an *in vivo* setting, it is to be assumed that limiting Jak/Stat signalling would increase sensitivity to injury and infection due to a reduced ability to repair and renew cells. This was demonstrated by Thagia et al. (2015) who showed that wound healing was compromised following stimulation with the microbial component, lipopolysaccharide (LPS). This process of increased sensitivity and decreased cellular repair is also thought to be the mechanism behind increased SOCS3 levels in IBD (Suzuki et al. 2001, Li et al. 2010), and will be discussed further in section 1.6.

As in mammals, dysregulation of midgut renewals pathways in *Drosophila* can also lead to increased or decreased signalling which in turn, results in excess proliferative and hyperplasia, or even increased mortality due to an inability to repair damaged or infected cells,

respectively. However, even in uninfected flies, overexpression of Upds in midgut cells induced hyperplasia, although this was able to be reversed within 2 weeks, following the silencing of Upd (Jiang et al. 2009, Lucchetta and Ohlstein 2012). Additionally, flies with constitutively active Hop kinases (e.g. as a result of gain of function mutations) display overproliferation and premature differentiation of haemocytes (a type of blood cell in *Drosophila*), and ultimately develop haematopoietic tumours (Arbouzova and Zeidler 2006, Stec and Zeidler 2011. This demonstrates a conserved outcome/function between Hop and Jak proteins, and strengthens the link between increased JAK/STAT signalling and uncontrolled cellular proliferation and tumourigenesis that has been observed in mammals. The role of SOCS proteins as tumour suppressors is also conserved. This was demonstrated by reductions in the size and number of haematopoietic tumours following overexpression of SOCS36E in haemocyte precursors of Hop mutant flies, and the reverse effect when SOCS36E was reduced using RNAi (Stec and Zeidler 2011). Herranz et al. (2012) also found microRNA responsible for cell proliferation regulation known as bantam, to downregulate SOCS36E, which resulted in tissue growth (in imaginal discs- epithelia found in larvae responsible for the formation of structures found in adult flies). However, the effects of reduced SOCS36E were not confined to proliferation as the authors also reported loss of apico-basal polarity in the disc cells, as well as altered cellular architecture, and these arose from a loss of cell junction proteins. As expected, decreased Jak/Stat signalling (due to loss of Hop) had the opposite effect and resulted in reduced and insufficient proliferation of the imaginal disc cells, thus producing discs that were smaller in size (Arbouzova and Zeidler 2006). Collectively, these summarised results from mammalian and *Drosophila* studies indicate a conserved role of Jak/Stat signalling and SOCS3 in the regulation of cell turnover in multiple tissues and the negative effects dysregulation can produce.

1.5 The Roles of the Commensal Intestinal Microbiota

Microbiota is the term used for the microbes that colonise organisms from birth (Hooper and Gordon 2001), and form a symbiotic relationship with their host. These microbes are located on the surface of the skin, and within the GI, respiratory and genitourinary tracts, with the number of microbes exceeding those of both somatic and germ cells combined at least 10-fold (Tancrède 1992). There are approximately 10^{14} microbial cells in total in the human body, with the total genomic content comprising of 100 times more genes (DuPont and DuPont 2011). The microbiota is acquired from birth, although the microbes that colonise will differ depending on whether the method of birth was natural or by Caesarean section, and also

whether infants are breastfed or bottle-fed (Guarner and Malagelada 2003). However, the maternal commensals do heavily influence the colonisation of offspring, as siblings, in addition to twins, have been reported to have similar microbiota (Sekirov et al. 2010). From birth until approximately 1 year of age, the diversity and numbers of microbes increase, although in healthy individuals, these numbers will then remain relatively stable until death, demonstrating how important early colonisation events are in establishing the permanent microbiota. The intestines are the richest microbiota site in terms of both number and diversity (Hooper ad Gordon 2001), although the numbers do increase moving along the G.I tract, starting with approximately 10^3 microbial cells per gram of luminal contents in the duodenum, and reaching 10^{12} cells per gram in the colon (Hooper and Gordon 2001). The colon is the most densely populated site, containing over 70% of the total microbes found within the human body (Sekirov et al. 2010). Within the gut reside bacteria, as well as some fungi and viruses, with approximately 500-1000 different species coexisting there (Tancrède 1992). The majority of the bacteria in the gut are strict anaerobes, dominating over facultative anaerobes and aerobes, with the whole of the gut microbiota consisting of four major phyla: Bacteroidetes, Firmicutes, Proteobacteria and Actinobacteria (Sekirov et al. 2010, Yurist-Doutsch et al. 2014). Mice and humans display similar proportions of these phyla, although differences in diversity within each phylum have been reported (Kostic et al. 2013). Firmicutes and Bacteroidetes are the two most dominant phyla, making up approximately 90% of the gut bacteria, in both humans and mice (DuPont and DuPont 2011). However, there will be variation at the species level, not only between individuals, as a result of differences in diet, hygiene and possible antibiotic use (Guarner and Malagelada 2003), but also within the gut of an individual, due to differences in oxygen levels and pH between the small and large intestines (Hooper and Gordon 2001). Interestingly, the type of bacteria found within the gut lumen differs too from those found within the mucus layer lining the intestinal epithelium (Sekirov et al. 2010).

The microbiota plays several roles within the gut, one of which includes aiding in the digestion and absorption of food, particularly in the colon. Here, bacteria break down and ferment previously indigestible dietary fibre into short-chain fatty acids (SCFAs), such as butyrate, propionate and acetate (Nguyen et al. 2015). From *in vitro* studies, SCFAs have shown to be beneficial in an intestinal setting, in that butyrate has reported to inhibit proliferation of neoplastic intestinal cells, in addition to promoting cell reversion from a neoplastic state to a non-neoplastic state (cited by Guarner and Malagelada 2003), which if in an *in vivo* setting, would ultimately benefit the overall health of the host too. Furthermore, the gut microbiota also helps in the production of vitamins K and B, and in the absorption of

minerals such as calcium and iron. Collectively, this aims to increase levels of nutrients, substrates and energy for both the host and the commensal populations (Nguyen et al. 2015). The gut microbiota can also contribute towards protection and immunity in that their colonisation means they can compete with pathogens for space and nutrients. Some commensals can produce antimicrobials too which will defend against harmful microorganisms (Yurist-Doutsch et al. 2014). Additionally, from studies performed on GF mice, the presence of commensals has proven to be essential for proper gut functioning. For instance, GF mice have impaired/slower intestinal renewal (Abrams et al. 1962), and this can increase their sensitivity to damaging, and infectious agents, particularly as GF mice also possess reduced numbers of goblet cells compared to CR, colonised mice, and this can lead to a thinner, less stable mucus layer between the lumen and epithelium, which could be easier for pathogens to penetrate (Natividad and Verdu 2013, Yurist-Doutsch et al. 2014). This is further exacerbated by the observation that the numbers of several types of immune cell and immune cell by-products, such as cytokines (Rakoff-Nahoum et al. 2004), are affected in GF mice also. The decreased epithelium renewal results in fewer crypt cells compared with CR mice, ultimately resulting in reduced villus thickness, a smaller surface area in the gut and impaired metabolism and digestion. As such, a substantially higher calorie intake is required for GF animals to obtain the same body weight as CR animals (Sekirov et al. 2010). However, intestinal homeostasis can be altered even in CR animals if the cell signalling pathways responsible for recognising microbial ligands are impaired/non-functional. For instance, Toll-Like Receptor (TLR) signalling (which will be discussed in more depth later on in this chapter) consists of multiple receptors; each able to recognise a different microbial component, and following ligand-receptor binding, several responses are induced, including cytokine production and cell proliferation, and therefore renewal. Rakoff-Nahoum et al. (2004) discovered that mice deficient in an adapter protein of the TLR signalling protein (Myeloid differentiation primary response gene 88- MyD88) had dysregulated proliferation and differentiation of IECs compared with controls, and this was in the absence of microbial stimulation.

Despite the differences between mammals and *Drosophila* (some of which have been mentioned here), fruit flies also possess gut microbiota, although they house a lower number of species compared to humans (5-20, and 500-1000 respectively, Royet 2011), and the total number of microbial cells is lower too (approximately 3.5×10^5 cells in the midgut, compared to 10^{12} cells in each gram of luminal contents) (Ryu et al. 2010, DuPont and DuPont 2011). There are some similarities in the species found in *Drosophila* and humans, but very few anaerobic species reside in the *Drosophila* midgut (Royet 2011), and they also lack any

species within the Bacteroidetes phylum, which is one of the two dominant phyla in humans (Charroux and Royet 2012). As seen in mammals, environmental factors are a major source of variation in microbiota composition between flies; not only between wild and laboratory populations, but also between the same strains in different laboratories (Chandler et al. 2011). Although natural *Drosophila* populations tend to have a more diverse microbiota than laboratory strains, Enterobacteriaceae, Acetobacteraceae and Lactobacillales make up the majority of the gut bacteria, with either one or all three of these capable of dominating. Chandler et al. (2011) also found there were 5 bacterial species that could frequently be found in both wild and laboratory flies: *Acetobacter pomorum*, *Acetobacter tropicalis*, *Lactobacillus brevis*, *Lactobacillus fructivorans* and *Lactobacillus plantarum*.

Although diet can influence the microbiota composition of mammalian systems, it is a major contributor in *Drosophila*, particularly as the natural diet for fruit flies is rotting microbe-containing fruit (amongst other foods) (Apidianakis and Rahme 2011). Laboratory studies have revealed a directly proportional relationship between bacterial counts and the number of days between food transfers, between bacterial counts and the amount of food present in the *Drosophila* gut, and also the starting bacterial density on the food and the bacterial density found in the fly (Blum et al. 2013, Broderick et al. 2014). Furthermore, no bacteria were detected in GF flies until their food was supplemented with *L. plantarum*, and the gut microbiota of CR flies could only be maintained if they were reared on food with a rich source of exogenous bacteria (Blum et al. 2013). These results indicate that the commensal gut microbiota is not stable, and is transient and must be frequently replenished through ingestion of microbe-containing food. It has been suggested that the constant expulsion and replenishment of microbes may be a mechanism carried out to reduce infection by pathogenic bacteria (Blum et al. 2013), especially as wild, natural populations of fruit flies harboured higher levels of *Serratia* and *Pseudomonas* (Chandler et al. 2011), which have shown to induce IEC damage and reduce lifespan in laboratory studies (Liehl et al. 2006, Nehme et al. 2007, Buchon et al. 2009b).

The *Drosophila* microbiota has shown to have similar functions to those in mammalian systems, in particular, regarding infection and immunity, and IEC homeostasis. For instance, Blum et al. (2013) found flies were more resistant to infection with either *Serratia marcescens* or *Pseudomonas aeruginosa*, and this was further improved following supplementation with *L. plantarum* (a species that is used as a probiotic, as well as a natural constituent of the *Drosophila* microbiota). *L. plantarum* is also able to increase activity of proteolytic enzymes,

aiding digestion, with the microbiota as a whole also sustaining nutrition, as it has shown to promote larval growth in conditions where nutrients have been depleted (cited by Bonfini et al. 2016). Conversely, larvae devoid of gut bacteria displayed increased sensitivity to infection with the yeast, *Candida albicans* (Glittenberg et al. 2011). Furthermore, the presence of indigenous microbiota may help to maintain immune (and also midgut) homeostasis by inducing basal, low level inflammation which allows the innate immune system to determine whether ingested exogenous microbes are pathogenic or not (Bonfini et al. 2016). The occupation of the *Drosophila* midgut by commensal bacteria will also help to prevent colonisation by pathogenic species, by outcompeting them for space and nutrients, along with the production of antimicrobials. Larvae themselves can act as antimicrobials as their presence is able to restrict growth of pathogenic fungi and also reduce the diversity of yeasts in *Drosophila* medium (cited by Buchon et al. 2013b). Regarding midgut homeostasis, Buchon et al. (2009b) reported that the microbiota is involved in regulation of cell turnover, as both rates of renewal and number of mitotic ISCs were reduced in GF flies, compared with CR flies. This correlated with an absence of Upd3 (the activating ligand of the *Drosophila* Jak/Stat pathway, and initiator of midgut renewal, Agaisse et al. 2003, Buchon et al. 2009a, Jiang et al. 2009) in GF flies, with basal levels found in CR flies, also indicating that the gut microbiota help regulate Jak/Stat activity and Jak/Stat-induced proliferation. These findings were also supported by the observation that flies deficient in their immune deficiency (Imd) pathway harboured commensal bacterial counts that were 10-fold higher than those in wildtype flies, and displayed higher numbers of mitotic midgut cells too. Buchon et al. (2009b) also found that compared to their young 3 day old counterparts, both 30 day old wildtype and Imd mutant flies had higher bacterial counts and increased numbers of mitotic ISCs, although GF Imd mutant flies exhibited proliferation rates similar to those of young flies, along with preserved midgut integrity. This suggests that gut microbial populations increase in *Drosophila* with age, and that the age-associated increases in midgut proliferation and deterioration (as observed by Biteau et al. 2008) may be as a result (at least partially) of the microbiota. In addition to proliferation, gut commensals also influence differentiation of IECs, as GF flies have higher ratios of EECs to ECs than CR flies (Broderick et al. 2014). It remains unclear as to whether this affects nutrient absorption in the midgut, and ultimately body size (as observed in mice), particularly as Storelli et al. (2011) reported no significant differences in body weight between GF and *L. plantarum*-mono-associated flies maintained on either a rich yeast diet, or a poor yeast diet. However, only body weights of female flies were recorded, and these flies were very young (3 days old) so it is not known whether the same results would have been obtained using older flies (30 days old, for instance) when effects of increased ratios of EECs to ECs may be prominent. In addition to immunity and IEC homeostasis, the midgut microbiota is also implicated in mating preference in

Drosophila; a factor which has so far not been identified in mammalian systems. Sharon et al. (2010) found flies that were reared on either a starch-based diet, or a sucrose-based diet preferentially mated with flies that were also reared on the same diet. They were able to deduce that this finding was due to influences of commensal bacteria, as the mating preference trend was abolished following administration of antibiotics, in addition to this trend continuing when flies were fed bacteria that had been deposited onto the fly medium. This microbial-induced behaviour must be evolutionarily important as it emerged after one generation of flies, and could be observed for at least 37 generations.

1.6 Dysbiosis and Microbe-Mediated Diseases

In a healthy organism, a symbiotic relationship exists between the host and the gut microbiota, with each side gaining benefits from this relationship, such as facilitation in nutrient digestion, and a niche to exist and also obtain nutrients, respectively. Although mechanisms are in place to ensure the host-commensal homeostasis is maintained, dysregulation may take place, or external environmental factors may induce changes in the microbiota, and this shift is referred to as dysbiosis. Dysbiosis may either occur as a result of: a reduction or loss of beneficial microorganisms, increases in pathogenic/opportunistic microbes, or a reduction in the overall diversity of microorganisms. However, these events are not mutually exclusive and often occur together (DeGruttola et al. 2016). In mammals, organisms are first exposed to microorganisms at birth, and are colonised with maternal commensals. The proportions of microorganisms infants are colonised with however, are dependent on the method of birth used, due to differences in bacteria residing in the maternal reproductive tract and on the skin's surface. For instance, Dominguez-Bello et al. (2010) reported that infants born naturally harboured large amounts of lactic acid bacteria, such as *Lactobacillus*, whereas infants born by caesarean section showed increased amounts of *Staphylococcus*, with little to no *Bifidobacteria*. Diet is also known to shape microbiota composition, with geographical contrasts in the standard diet and also in typical food preparation methods reflected by variations in bacterial proportions in different countries (Prideaux et al. 2013). However, even a change within an individual's diet could alter gut commensal proportions; for instance, an increase/decrease in dietary fibre could result in increases/decreases in SCFA-producing bacteria, respectively. Ingestion of probiotic products however can have beneficial gut effects, such as reduction of pathogen colonisation, and this is achieved by increasing health-promoting bacteria, such as *Lactobacillus* or *Bifidobacterium*, although the genus and species can vary between products (DuPont and DuPont 2011). For certain ailments, the prescription

of antibiotics can be essential and prove to be valuable to the individual's health. However, inappropriate antibiotic use, such as prescription for a non-bacterial condition, prolonged use, or premature cessation of treatment, can be detrimental to the host's health, especially regarding the G.I tract. Antibiotics are not able to discriminate between commensal and pathogenic bacteria, so although the ailment-inducing microorganism may be eradicated, beneficial populations may also be reduced or removed. This results in the emergence of more resistant strains that are normally kept at minimal levels, due to reduced competition, and this is the basis of antibiotic-associated diarrhoea, often caused by overgrowth of *Clostridium difficile*. Treatment for this involves cessation of the antibiotics, and administration of probiotics or restoration of gut microbiota by faecal transplant from a healthy individual (Du Pont and DuPont 2011). However, in addition to emerging pathogenic strains during dysbiosis, general overgrowth can also be detrimental due to increased production of bacterial by-products and waste which can be toxic to the host (Sekirov et al. 2010).

One particular group of diseases that are microbe-mediated and associated with dysbiosis in the G.I tract is IBD. IBD affects approximately 0.1% of individuals in Western countries (Hooper and Gordon 2001) and comprises of Crohn's disease (CD) and ulcerative colitis (UC). Both of these diseases are characterised by excessive inflammation of the G.I tract, abdominal pain, and diarrhoea but there are differences between the two. UC affects the colon; either particular areas or the whole colon, and is associated with destruction of the IEC lining and also anaemia, due to loss of blood from the G.I tract (Abraham and Cho 2009). CD on the other hand, can affect any part of the G.I tract (from the mouth to the anus), although the most commonly affected areas are the ileum and colon. Unlike UC, CD is characterised by transmural inflammation, intestinal blockages and ulcers, which may lead to the formation of fistulas if they become too deep (Abraham and Cho 2009).

Although IBD involves a breakdown in tolerance mechanisms towards luminal contents, resulting in inappropriate activation of the immune system, and also dysregulated intestinal homeostasis from increased inflammation-induced IEC damage and bacterial translocation, the exact cause is still not currently known (Duchmann et al. 1995). However, contributing factors have been determined, such as:

- The adoption of a "Westernised" lifestyle, living in urban areas, being exposed to pollution and higher consumption of fat- and sugar-enriched foods (Hanauer 2006).
- Sanitation, as increased hygiene reduces exposure to microorganisms, including helminths (Hanauer 2006, Abraham and Cho 2009).
- Genetic predisposition; whether this is due to a first- or second-degree relative having IBD, or due to mutations in identified genes such as Nucleotide-Binding Oligomerization Domain 2 (NOD2). NOD2 is part of the NOD Pattern Recognition Receptor (PRR) family responsible for recognising bacterial peptidoglycan, and is able to exert antimicrobial effects, thus preventing pathogen invasion (Cario 2005, Hanauer 2006).

A large volume of microbial analysis studies have been conducted in order to determine the changes that occur within the G.I tract during IBD. Results commonly show a decrease in bacterial diversity, along with reductions in the Firmicute and Bacteroidete populations, and Lactobacillus and Bifidobacterium in particular (affecting SCFA production as a result) (DuPont and DuPont 2011, Walker et al. 2011). Although it is not known whether depletion of bacterial populations arises from the increased inflammation or vice versa, the diminution of dominant commensal bacteria can encourage the growth and dominance of previously minor (potentially opportunistic) bacterial strains (Sekirov et al. 2010). Examples of emerging bacteria include *C. difficile*, *Escherichia coli*, and often Proteobacteria and Enterobacteriaceae in general (Sekirov et al. 2003, Martinez-Medina et al. 2006, DuPont and DuPont 2011). Although certain bacterial populations or strains are diminished during IBD, patients with either CD or UC have been reported to harbour higher bacterial counts within the ileum when compared with healthy controls. Individuals with CD however, tend to exhibit more generalised dysbiosis than individuals with UC as there are often similar bacterial strains found in both inflamed and non-inflamed ileal mucosal tissue (Kaur et al. 2011). Despite these findings, IBD comprises of complex diseases, and therefore it is more likely that there will be shifts in the microbiota population as a whole, rather than a select few species (DeGruttola et al. 2016). Results from study to study also often vary, most simply due to environmental and genetic differences between individuals, and also due to analysis techniques and sampling methods used, so therefore no "bacterial signature" as a potential biomarker is associated with

these diseases (Kaur et al. 2011). Changes in the microbial content of faeces are often reported too, although faecal microbes are known to be different from those associated with the mucosa, and the latter population may be more relevant in an IBD setting due to their close association with the epithelial barrier (Sun et al. 2011).

There are several pieces of evidence indicating that the gut microbiota is also a contributing factor towards IBD. For instance, IL-10-deficient mice that normally develop spontaneous colitis are devoid of inflammation and immune system activation when raised under GF conditions (Sellon et al. 1998, Madsen et al. 1999). Additionally, different types of antibiotic treatment have shown to be effective in ameliorating inflammation in both humans and in animal models (Hooper and Gordon 2001, Sekirov et al. 2010). Diversion of luminal contents has also proven to be a successful treatment method, although symptoms do return upon restoration of intestinal flow. Further evidence is derived from the presence of systemic antibodies against antigens associated with the gut microbiota, with one study reporting higher immune and antibody activity in the serum of CD patients to be associated with increased disease severity (Mow et al. 2004, DuPont and DuPont 2011). However, despite these findings, Kitajima et al. (2001) found that the commensal microbiota was beneficial during dextran sodium sulphate (DSS)-induced colitis, as GF mice exhibited higher frequencies of intestinal bleeding and mortality, and one suggestion for this may have been due to having a more immature immune system (Guarner and Malagelada 2003).

Although the pathophysiology of IBD has been established, the cause and effects of these events are not known either. IBD is associated with increased inflammation that can result from immune responses elicited against luminal contents, with detection and translocation of these luminal antigens increased during dysbiosis (either through increased bacterial loads or increased levels of pathogenic bacteria) and when the intestinal epithelial barrier is compromised and more permeable (Abraham and Cho 2009). The chronology of these processes is not clear but they are known to perpetuate each other and exacerbate the symptoms if treatment is not introduced (Sekirov et al. 2010). Intestinal renewal pathways may be in place in order to replenish the IECs damaged as a result of the inflammation, but if the rates of renewal cannot equal or overcome the rates of cell death, this can promote the chronicity of these diseases.

The increased inflammation during IBD is associated with an increase in pro-inflammatory cytokines, including IFN-γ, TNF-α and IL-6. IFN-γ and IL-6 are both known activators of the Jak/Stat pathway. The anti-inflammatory cytokine, IL-10 can also initiate Jak/Stat activity and is reported to be increased in some cases of IBD, most likely in an attempt to inhibit inflammatory processes (Kucharzik et al. 1995, Autschbach et al. 1998, Murray 2006). Along with IL-10$^{-/-}$ mice, Stat3-knockout mice also develop spontaneous colitis and this is presumed to be due to an inability to mediate IL-10 signalling, resulting in enhanced Th1-mediated inflammatory responses (Takeda et al. 1999). Conversely, Suzuki et al. (2001) found that Stat3 was activated in various models of colitis and this was dependent on IL-6, as Stat3 activation was reduced in IL-6-deficient mice. The level of Stat3 phosphorylation also correlated with the severity of the disease. Consequently, this also induced increases in SOCS3 and it was suggested its activation may be beneficial during IBD, in an attempt to inhibit inflammation-mediated Stat3 signalling. Transgenic mice with SOCS3-reducing mutations (along with SOCS1) showed a higher level of colitis severity compared with wildtype mice, following treatment with DSS, and this was demonstrated by more pronounced decreases in weight loss and goblet cell number, in addition to increased intestinal hyperplasia (cited by Greenhalgh et al. 2002). These findings suggest a protective role of SOCS3 in IBD, although the findings of Li et al. (2009) and Thagia et al. (2015) demonstrate how SOCS3 may also be disadvantageous. Li et al. (2009) suggested that the increased sensitivity in mice to DSS-induced colitis following a reduction in IL-6-mediated Stat3 signalling, and constitutive expression of SOCS3 in IECs are related processes, and that the increase in SOCS3 in IBD may limit IL-6/Stat3-mediated renewal, thus sensitising IECs to any subsequent inflammation-induced damage. Thagia et al. (2015) showed that appropriate regulation of SOCS3 during inflammation is essential as overexpression enhanced flagellin-induced production of TNF-α in a dose-dependent manner, and impaired wound healing following microbial stimulation in an intestinal epithelial cell line.

As discussed, IBD can be considered a group of diseases associated with dysregulated intestinal homeostasis, due to an overactive immune system and shifts in bacterial populations, but also increased inflammation-induced cell death and compensatory increases in proliferation. Additionally, individuals with IBD are often susceptible to developing G.I-associated cancers, due to the increase in cellular proliferation to compensate for the increase in apoptosis caused by chronic inflammation and subsequent tissue damage. For instance, IBD patients often display increased pro-inflammatory cytokine production, and these can drive intestinal proliferation through activation of cell signalling pathways. For instance, IL-6 is able to initiate Jak/Stat signalling as well as promote nuclear factor kappa-light-chain-

enhancer of activated B cells (NF-κB) signalling through IL-1 and TNF-α, and cell survival through induction of anti-apoptotic proteins (e.g. Bcl-2) and reducing the function of the tumour suppressor, p53. TNF-α itself is able to promote a favourable environment for tumour growth, through tissue remodelling, which may aid invasion and metastasis too (Quante and Wang 2008). The inflammation and breakdown in commensal bacterial tolerance leads to activation of both innate and adaptive immune cells, and these can also produce pro-inflammatory cytokines, thus creating a positive feedback loop, and perpetuating the pathogenesis of IBD. Immune cells are also capable of producing ROS and reactive nitrogen species against microorganisms which can result in their clearance, but if produced chronically (as may be the case with IBD), they can induce host cell damage, in particular DNA damage. If this damage accumulates and is replicated (particularly if cell survival is promoted), this increases the likelihood of cells mutating and resulting in tumourigenesis (Quante and Wang 2008). In the presence of ROS, cancer cells are also more likely to lose cell contacts and become detached from the basal lamina, thus increasing the chance of metastasis (Hold and El-Omar 2008).

As well as being a contributing factor towards IBD, the gut microbiota is also able to promote carcinogenesis, and this can occur in a multitude of ways. When performing their various functions in the gut, the microbiota naturally produce metabolites and waste products, some of which may be damaging to cells, or even be carcinogenic. The likelihood may increase in IBD following the shift in bacterial populations from *Lactobacillus* and *Bifidobacterium* that can exert anti-inflammatory effects and prevent carcinogenesis (e.g. through the production of SCFA), to Bacteroides and Clostridium species that can be more harmful to the host (Guarner and Malagelada 2003). Further evidence is derived from mouse studies, with Rakoff-Nahoum and Medzhitov (2007) reporting that the microbial sensing adapter protein, MyD88, promoted tumour progression in both a chemically-induced intestinal model (using azoxymethane/ dextran sodium sulphate -AOM/DSS) and a spontaneous intestinal tumour model (using mice with mutated APC, referred to as APC$^{Min/+}$). MyD88-sufficient APC$^{Min/+}$ mice exhibited increased incidence and tumour size, as well as increased mortality when compared to MyD88-deficient APC$^{Min/+}$ mice. These mice also displayed higher expression of tumour-promoting molecules, such as TNF, IL-6, matrix metalloproteases and cyclooxygenase-2. However, this effect of MyD88 was not confined to intestinal tumours, as they have also been replicated in skin cancer and sarcoma animal models as well (Rakoff-Nahoum and Medzhitov 2009). Additionally, the transplantation of gut microbiota from tumour-bearing mice into GF mice resulted in an increase in both the number and size of tumours, when compared to GF mice transplanted with healthy gut microbiota (Zackular et al. 2013).

SOCS3 and the Jak/Stat pathway have shown to be implicated in both carcinogenesis and IBD, so therefore their involvement in CAC should not be unexpected. Following induction of CAC using AOM/DSS, IEC-specific deletion of SOCS3 resulted in an increase in the number and size of colonic tumours, when compared with SOCS3-sufficient mice (Rigby et al. 2007). Induction of colitis using DSS alone also resulted in increased proliferation of crypt cells and hyperplasia in IEC SOCS3-deleted mice, compared with wildtypes. Li et al. (2010) discovered that whilst SOCS3 was significantly increased in both patients with inactive, or active UC, and its expression was positively correlated with the severity of colitis (along with IL-6 and phosphorylated Stat3), progression from UC to CAC was associated with a decline in SOCS3 expression (similar to that found in tumours not associated with colitis- He et al. 2003, Weber et al. 2005, Ogata et al. 2006). This decline was linked to silencing methylation of epithelial genomic DNA in CAC intestinal cell samples. The progression of UC to CAC due to SOCS3 silencing was reversed following restoration of SOCS3, and this led to decreased activation of Stat3, decreased tumour growth, as well as induction of apoptosis.

Similarly, *Drosophila* are also able to display midgut dysbiosis, and as known in mammalian systems, one way in which this can be induced is through a change in diet, and administration of antibiotics (Sharon et al. 2010, Chandler et al. 2011). However, "naturally-occurring" midgut dysbiosis occurs simply with increasing age, with older (30 day old) flies harbouring higher bacterial counts than young, 3 day old flies (Buchon et al. 2009b) and this can lead to increased ROS production, which drives age-associated increased in proliferation, dysplasia,and altered midgut architecture (Biteau et al. 2008, Buchon et al. 2009b, Jiang et al. 2009). This was also true for flies with induced bacterial increases through a mutation in their Imd pathway. Guo et al. (2014) discovered that one mechanism behind this increase was due to an age-associated decrease in a particular subtype of peptidoglycan recognition protein (PGRP)- PGRP-SC2- and this led to decreased suppression of the Imd pathway, consequently leading to hyperproliferation due to dysregulated NF-kB signalling, along with increased gut bacterial counts. These effects were reversed following overexpression of PGRP-SC2.

The *Drosophila* microbiota are able to regulate basal levels of AMP production, and one way through which is the Imd pathway (which will be discussed in further detail in section 1.7) However, flies with mutations in this pathway exhibited decreased production of AMPs, and this resulted in higher midgut bacterial loads (Buchon et al. 2009b) and increased susceptibility to infection by food-borne pathogens (cited by Capo et al. 2016). Dysbiosis may also occur if pathways associated with AMP production are "under-regulated" and increased

(for instance, through gain of function mutations within the pathway or through loss of negative regulators, Paredes et al. 2011) and this can lead to a shift in microbiota dominance from a major commensal strain to a normally minor commensal strain, consequently negatively affecting the health of the flies, by inducing increases in both IEC death (e.g. through increased ROS, Lee et al. 2013) and mortality (Ryu et al. 2008, Capo et al. 2016). This shift also induced symptoms similar to those seen with IBD in mammals, although IBD cannot be fully replicated in *Drosophila* as they lack the array of inflammatory cytokines and immune cells that drive the disease processes. Conversely, the Imd pathway is also regulated through big bang (BBG)- a gene that encodes a gut protein found on the apical and lateral sides of midgut epithelial cells. BBG helps to maintain the integrity of septate junctions (lateral intercellular junctions also located between the epithelial barrier cells), and together they dampen down microbiota-induced Imd activation (Bonnay et al. 2013). However, when the midgut epithelium becomes compromised (as demonstrated in BBG mutant flies, for instance), activation of the Imd pathway is substantially increased, and this led to increases in commensal- and age-associated midgut proliferation, intercellular space, infection-induced bacterial loads, and also mortality, and this was irrespective of infection status. These effects are reminiscent to those seen during IBD in mammals, and similarly, antibiotic treatment was able to ameliorate the symptoms observed in flies (Bonnay et al. 2013).

On a slightly different note, (as stated) gut dysbiosis is capable of producing a number of symptoms and disorders within both mammals and fruit flies. However, dysbiosis-related phenotypes are not confined to the G.I tract. Much research has been carried out in recent years into the effects that changes in the gut, and in the gut microbiota, have on CNS function and behaviour, and vice versa- a bidirectional relationship named the gut-brain axis. With regards to evidence of the CNS influencing gut responses, psychological stress in mice induced through food, water or bedding deprivation resulted in microbiota changes, with stressed mice displaying a reduction in Lactobacilli compared with unstressed controls (cited by Collins and Bercik 2009). These bacterial changes were also observed in infant rhesus monkeys that had been separated from their mothers. Maternal separation in mice also resulted in increased intestinal permeability and this increased susceptibility to inflammation-inducing stimuli (Collins and Bercik 2009), for instance commensal and non-commensal populations, most likely due to increased translocation across the gut epithelium. Conversely, changes within the gut environment can induce CNS responses, with expression levels of various molecules (such as cytokines) and assessment of behaviour often measured to quantify these changes. Rats administered Bifidobacterium treatment for 14 days had increased (plasma) levels of tryptophan (Collins and Bercik 2009), with decreases in

tryptophan leading to decreased serotonin production- a common finding in mood disorders (Myint and Kim 2003). Additionally, changes in feeding behaviour in mice have been observed following infection with *Helicobacter pylori*, and this was found to continue even after the infection had been resolved (Bercik et al. 2002). Furthermore, gut disorders such as IBD and irritable bowel syndrome (IBS) are also bi-directional in that mood disorders can induce microbiota changes, possibly instigating or exacerbating these conditions. Also, due to the substantial amount of morbidity with IBD and IBS, and the chronicity of these disorders, it is common for affected individuals to suffer from depression (cited by Whitehead et al. 1980, and Bercik et al. 2010). Overall, these results show that regulation and changes to the gut microbiota are not just derived from within, and that elicited microbial responses are extended beyond the intestinal tissues.

1.7 Host Recognition of Microbes

As discussed earlier, the commensal gut microbiota has fundamental roles within humans, mice and *Drosophila*, and these functions can be affected if their levels are not appropriately balanced and/or if pathogens also infiltrate these organisms. Each of these three organisms (along with other biological living organisms) can elicit an array of mechanisms, as part of their immune systems, in order to maintain immune and gut homeostasis, and ultimately good health. Immunity can be subdivided into innate, and adaptive (or acquired) immunity, with innate immunity consisting of initial, quick responses that are elicited to prevent invasion and infection by pathogens that may occur whilst the adaptive immune system becomes fully activated and sufficiently expanded (and this can take at least 4-5 days) (Davies 2013). In short, the innate immune system comprises of physical epithelial barriers, coagulation processes, production of AMPs, immune cells (such as macrophages and dendritic cells – DCs)- and PRR pathways, for example, with receptors located on a multiple of host cells within mammalian systems (Todd 2010, Davies 2013, Yurist-Doutsch et al. 2014). One example of a pathway within the PRR family is the TLR signalling pathway, and it comprises of several cellular receptors, with each receptor able to recognise a variety of pathogen-associated molecular patterns (PAMPs) (shown in figure 1.9). These PAMPs are found on many types of microbes, such as viruses and bacteria, and are actually found on all microorganisms, regardless of their pathogenicity. Humans have 10 TLRs in total, with mice possessing 13, and these receptors are expressed on an array of immune cells, as well as IECs (Seya and Miyake 2009, Abreu 2010). TLR receptors contribute a significant part of gut immunity due to the proximity of the microbiota to the intestinal epithelium (Seya and

Miyake 2009), although the expression of TLRs on IECs is often lower, in order to maintain a state of hyporesponsiveness and appropriate immune tolerance towards commensal populations (Abreu et al. 2003).
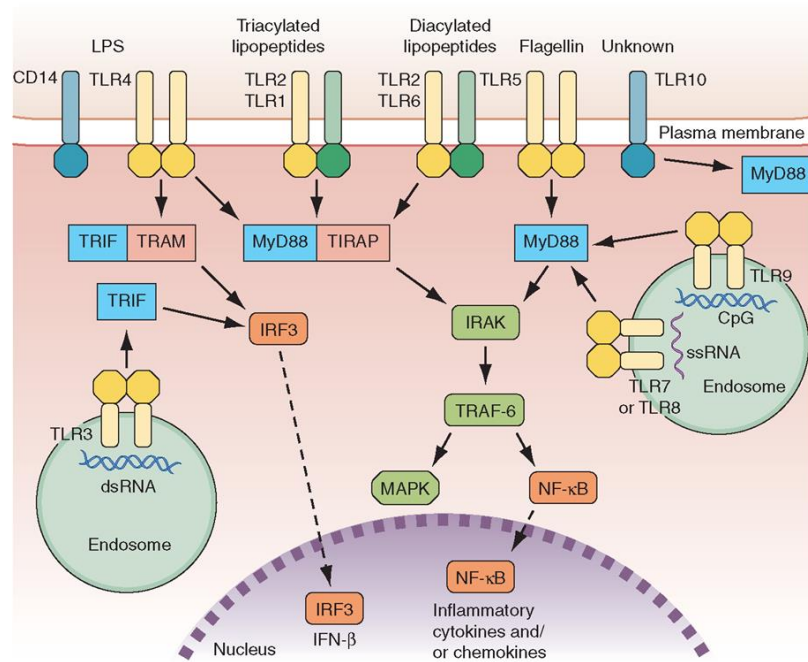
Figure 1.9: The mammalian Toll-Like Receptor signalling pathway. Upon binding of a microbial ligand to its respective receptor (with examples shown above), either located within the cell membrane, or intracellularly within endosomes, a MyD88-dependent or –independent signalling cascade is initiated. These cascades ultimately result in gene transcription in the nucleus, leading to production of inflammatory cytokines and chemokines, activation of immune cells, and proliferation. (Mice have additional receptors- TLRs11, 12 and 13). (CD14= Cluster of Differentiation 14, CpG DNA= Cytosine-phosphate-Guanine deoxyribonucleic acid , dsRNA= Double-stranded ribonucleic acid, IRAK= Interleukin-1 Receptor-Associated Kinase, IRF= Interferon Regulatory Factor, LPS= Lipopolysaccharide, MAPK= Mitogen-Activated Protein Kinase, MyD88= Myeloid Differentiation primary response gene 88, NF-κB= Nuclear Factor Kappa-light-chain-enhancer of activated B cells, ssRNA= Single-stranded ribonucleic acid, TLR= Toll-Like Receptor, TIRAP= Toll-Interleukin 1 Receptor domain containing Adaptor Protein, TRAF= TNF Receptor Associated Factor, TRAM= TRIF-Related Adaptor Molecule, TRIF= TIR-domain-containing adapter-inducing Interferon-β). (WWW, The Immune System in Health and Disease).

The Jak/Stat pathway is also reported to be implicated in the regulation of microbial-induced TLR signalling. Baetz et al. (2004) discovered that multiple members of the SOCS family (i.e SOCS1, SOCS3 and CIS) were induced by multiple TLR ligands in a MyD88-dependent manner (in murine DCs) and this was thought to lead to inhibition of crosstalk between

pathways, such as TLR signalling and, IFN and/or IL-6 signalling pathways, with SOCS3 also able to inhibit MyD88 directly (Frobøse et al. 2006). As demonstrated in figure 1.9, microbial binding initiates activation of TLRs which then signal through MyD88 and also MyD88-Adaptor-Like protein (MAL) to bring about Tumour-Necrosis Factor (TNF) Receptor-Associated Factor 6 (TRAF6), and Transforming Growth Factor-β (TGF-β)-Activated Kinase 1 (TAK1)-mediated activation of MAPK and NF-κB pathways downstream (Yoshimura et al. 2007). Initiation of both MAPK and NF-κB signalling can result in increased proliferation and production of pro-inflammatory cytokines. However, SOCS3 is able to inhibit IL-1-induced TRAF6- and TAK1-mediated activation of these pathways, with IL-1 capable of being produced as a result of TLR signalling (Frobøse et al. 2006). SOCS1 however, is capable of inhibiting TLR-mediated MAPK and NF-κB activation (also through TRAF6 and TAK1), thus suggesting shared roles of SOCS proteins in limiting microbe-mediated proliferation and inflammation (Yoshimura et al. 2007). In IECs specifically, Thagia et al. (2015) found that SOCS3 was responsible for regulating flagellin (TLR5)-induced production of TNF-α, as SOCS3 overexpression resulted in an increase in TNF-α, relative to SOCS3-sufficient cells, and this was found to be associated with downregulation of TNF Receptor 2 (TNFR2). Additionally, Abreu et al. (2003) reported a decrease in IFN-γ-mediated TLR4 co-receptor, MD-2, expression following an increase in SOCS3, thus providing further evidence of SOCS proteins limiting inflammatory signalling. However, despite the findings of Thagia et al. (2015) and Abreu et al. (2003), the majority of research into TLR signalling and the Jak/Stat pathway is conducted in immune cells, which are known to be more responsive than IECs so consideration must be taken when generalising findings. This demonstrates that further research is needed with regards to IECs specifically, particularly as both TLR and Jak/Stat signalling are implicated in IBD.

In the event that pathogens still persist following the induction of innate immune responses, the adaptive immune system becomes fully functional at least 4-5 days following pathogen exposure. There are large differences between the innate and adaptive immune systems, with the major distinctions being the constituents in that adaptive immunity consists exclusively of B- and T-lymphocytes. Their functions consist of: interaction with and recruitment of innate immune cells, production of antigen-specific antibodies (B-lymphocytes), and cytokine production by subsets of T-lymphocytes that are activated by particular pathogens (e.g. Th2-mediated responses can be induced during helminth infection) (Davies 2013, Yurist-Doutsch et al. 2014). Memory functions are also attributed to adaptive immunity in that immune responses are much more rapid and enhanced if antigens are ever re-encountered, so much so that no symptoms may be detected by the host (Davies 2013).

Regarding immune responses in *Drosophila* now, and as seen in other invertebrates, they rely completely on innate mechanisms, and have no adaptive immune system, unlike mammalian systems. However, similar to mammals, their innate immune system is multi-layered, and there is some overlap in immune responses and defences possessed by these organisms, such as phagocytic cells and physical barriers. Additionally, as a main constituent of the *Drosophila* diet is rotting microbe-containing fruit (and other food), often the first immune defence the microbes will encounter is the midgut. As in mammals, this also acts as a barrier between (exogenously sourced) luminal contents and peripheral tissues and can act as a hostile environment for pathogens, due to areas of varying pHs and the secretion of lysozymes and digestive enzymes (Lemaitre and Hoffmann 2007). Following ingestion of microbes, an oxidative burst of ROS is released by Dual oxidase (Duox) in order to kill any potential infectious microorganisms. This process is crucial to *Drosophila* immunity as Duox RNAi prevents the midgut production of ROS, allowing ingested microbes to proliferate and persist. This ultimately results in increased mortality of the fly, and this was discovered with both midgut specific- and systemic Duox RNAi (Ha et al. 2005). In order to reduce extensive damage to the midgut, the ROS are then removed (or "neutralised") by catalase. However, midgut cells are still damaged during the infection and oxidative burst events, and this leads to Upd3 release from damaged ECs, initiating ISC proliferation via the Jak/Stat pathway (Buchon et al. 2009a and b). Oxidative stress also activates the JNK pathway, causing further release of Upd3 (Hiang et al. 2009). The process of midgut epithelium renewal is also essential too, as flies with deficient Jak/Stat or JNK pathways, or silenced Upd3, succumb to infection with pathogens that are usually non-lethal under normal circumstances, whereas flies with deficiencies or mutations in their Imd pathway are able to survive (Buchon 2009b). These findings signify the importance of balancing ROS production with epithelial renewal in the maintenance of a healthy midgut and organism following infection. Furthermore, peristalsis induced by the midgut is also regarded as an immune defence mechanism as the contractions can help to propel pathogens into areas of the gut that are more acidic or have higher AMP levels, or help to eliminate them from the fly completely (Buchon et al. 2013).

In addition to the involvement of *Drosophila* Jak/Stat in infection-induced epithelial renewal, this pathway is also able to produce a specific AMP, Drosomycin-like 3 (Dro3), which shares homology with the *Drosophila* antifungal peptide, Drosomycin (Buchon et al. 2009a). Following infection with the Gram-negative phytopathogen, *Ecc15*, expression of this peptide (along with Dro2 and Dro4) was increased, and the involvement of Jak/Stat was discovered when Dro3 levels decreased upon Upd3 RNAi, Stat RNAi and a loss of function mutation in the Hop protein. Conversely, Dro3 became strongly expressed in flies with a Hop gain of

function mutation. Furthermore, in contrast to bacterial infection, Jak/Stat signalling is also implicated in viral immunity, and the *Drosophila* C virus (DCV) in particular. DCV is a pathogenic RNA virus that is a natural pathogen of *Drosophila* and usually causes mortality within days following infection. Dostert et al. (2005) discovered that infection with DCV induced a different set of genes than those produced following infection with bacteria or fungi, and that a substantial of these DCV-induced genes required Hop. Hop was found to be important for viral immunity as loss of function mutations resulted in both increased viral loads and mortality when compared to wildtype flies. Similar findings were also obtained when flies were infected with a different insect virus- Flock House Virus (Dostert et al. 2005), demonstrating another level in Jak/Stat's contribution to *Drosophila* immunity.

Drosophila also have their own subset of immune cells, known as haemocytes, and these are located in the circulating haemolymph (equivalent to the circulatory system in mammals). There are three different types of haemocyte and these are known as plasmatocytes, crystal cells and lamellocytes (Lemaitre and Hoffmann 2007). However, due to an innate immune system only being present, immune responses in *Drosophila* are often dependent on the production of AMPs. These are produced through the Imd or Toll pathways (depending on the pathogen being targeted) either systemically by the fat body (the equivalent of the mammalian liver), or locally, for instance within the midgut (Lemaitre and Hoffmann 2007), and are able to target fungi, and Gram-positive and Gram-negative bacteria. The Toll pathway (shown in figure 1.10) is similar to the TLR pathway in mammals, but is responsible for recognition of Gram-positive and fungi only, unlike the TLR pathway which is capable of recognising an array of PAMPs. Additionally, Toll signalling is activated following detection of secreted pathogens, often in the haemolymph, whereas the TLR pathway (and Imd pathway) recognises membrane bound pathogens, and these differences could reflect on the detection of different types of microbes by these pathways (Lemaitre and Hoffmann 2007). There are nine Tolls encoded by the *Drosophila* genome, although only one is involved in host immunity. Upon pathogen recognition, a series of *Drosophila* MyD88 (dMyD88)-mediated signalling cascade events occur, with dMyD88 being a homologue of the mammalian TLR adaptor protein, MyD88. The roles of these adaptor proteins appear to be conserved as dMyD88 mutant flies have increased sensitivity to fungal infections in particular (Takeda et al. 2003). Toll signalling activation ultimately results in Dorsal (a homologue of NF-κB) translocating into the nucleus and inducing transcription of genes, such as production of AMPs. Dorsal is also able to translocate with transcription factors, Dorsal-type Immune Factor (DIF) and Relish from the Imd pathway, indicating conserved functional outcomes between these two immune pathways (Takeda et al. 2003).
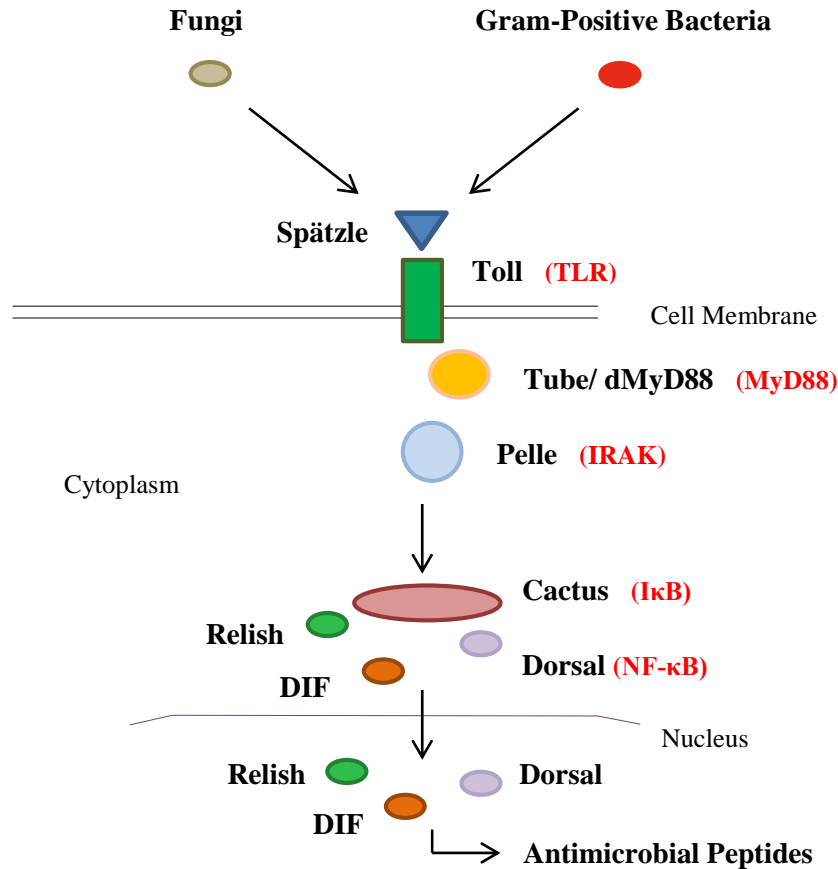
Figure 1.10: The *Drosophila* Toll pathway. Recognition of microbes by PGRPs initiates a series of proteolytic cleavages, leading to production of Spätzle. Spätzle binds to Toll, triggering a chain of dMyD88-mediated cascade events. Phosphorylation-induced degradation of Cactus results in dissociation of Dorsal (Lemaitre and Hoffmann 2007), which is then able to translocate into the nucleus with transcription factors, DIF and Relish, and induce transcription of genes, that lead to production of antimicrobial peptides, for instance (Takeda et al. 2003). (DIF= Dorsal-type Immune Factor, dMyD88= *Drosophila* Myeloid Differentiation primary response gene 88, IκB= Inhibitor of NF-κB, IRAK= Interleukin-1 Receptor-Associated Kinase, NF-κB= Nuclear Factor Kappa-light-chain-enhancer of activated B cells, TLR= Toll-Like Receptor) (Mammalian homologues in red). (Image adapted from Bowie and O'Neill 2000, and Khush et al. 2001)

Similar to mammals, pathogens that are recognised by the *Drosophila* innate immune system can also be the same type as microbes that reside in the gut. However, there are regulatory mechanisms in place that both prevent overactivation of immune responses towards

commensals, and also limit overpopulation of these populations. For instance, PGRPs are responsible for recognition of both Gram-positive and Gram-negative bacteria, although a different group of PGRPs known as amidase PGRPs are located in the gut and these proteins remove peptides from the glycan chains of peptidoglycan, reducing their biological and immunostimulatory activity as a result. Amidase PGRPs are not only able to target pathogenic microorganisms, reducing their immunogenicity following recognition by the appropriate signalling pathway, but also the commensal microbiota, preventing inappropriate activation of either the Imd or Toll pathway (Lemaitre and Hoffmann 2007). Tolerance towards commensal populations is also induced by a transcription factor known as Caudal, that is capable of regulating AMP production, as inhibition of Caudal through RNAi resulted in overexpression in AMPs and a shift in commensal populations (Ryu et al. 2008). This dysbiosis affected the flies' health, causing apoptosis of midgut cells and increased mortality, and could be rescued following either re-introduction of Caudal, or removal of commensal bacteria, inducing a GF state, thus demonstrating the importance of this gene in *Drosophila* gut and immune homeostasis, and also the importance of both gut and immune homeostasis in maintaining both gut health, and the health of the organism as a whole.

1.8 Research Aims

The intestinal tract is one of the most rapidly proliferating tissues within an organism and homeostasis is achieved through a balance of proliferation and cell death, with dysregulation of one or both of these processes impacting on health. The Jak/Stat pathway, and SOCS3 in particular, are known to be implicated in intestinal homeostasis, although the majority of findings are more relevant in a pathological state. The gut microbiota is also known to influence turnover of IECs so therefore it is important that intestinal homeostasis is efficiently regulated by the host.

In biomedical research, a multitude of models can be used, and in order to increase the translatability of findings to human health and disease, ideally, experiments should be carried out in more than one research model. Therefore, using three different models, we aimed to investigate:

- The role of SOCS3 in the regulation of normal, basal IEC turnover
- The impact of microbe-mediated proliferation on the regulation of IEC homeostasis by SOCS3

Using our three models- an *in vitro* human intestinal cell line, and two *in vivo* models using mice, and *Drosophila melanogaster*- this allowed us to investigate the impact of SOCS3-regulated homeostasis at the molecular level, the tissue level, and at an organismal level, respectively. Additionally, our experiments helped us to determine the conservation of SOCS3 proteins across different biological systems.

Chapter 2:

Materials and Methods

2.1 Materials

2.1.1 Reagents

Table 2.1 – List of Reagents

Reagent	Company
2-Mercaptoethanol	Sigma
5x M-MLV Reverse Transcriptase Buffer	Thermo Fisher Scientific
Anchored Oligo-dT	Thermo Fisher Scientific
Bradford Reagent	Sigma
Bovine Serum Albumin	Sigma
Clarity™ Western Enhanced Chemiluminescence (ECL) Substrate	Bio-Rad
CyQUANT® Cell Proliferation Assay Kit	Thermo Fisher Scientific
Deoxynucleotide Mix (dNTP, D7295)	Sigma
Dimethyl Sulphoxide (DMSO) Hybri-Max®	Sigma
Epidermal Growth Factor (EGF)	Thermo Fisher Scientific
Flagellin (from *Salmonella typhimurium*)	InvivoGen
Foetal Bovine Serum (FBS)	Thermo Fisher Scientific
Goat Serum	Sigma
Glycine	Sigma
HEPES Buffer	Sigma
Human Recombinant IFN-γ (#300-02)	Peprotech
Human Recombinant TNF-α (#300-01)	Peprotech
Hydrochloric Acid	Sigma

Hydrogen Peroxide solution (30% w/w, H_2O_2)	Sigma
IGEPAL® CA-630	Sigma
Lipopolysaccharide (LPS, from *Escherichia coli,* O111:B4 strain)	InvivoGen
Lipoteichoic Acid (LTA, from *Bacillus subtilis*)	InvivoGen
Luria Broth	Thermo Fisher Scientific
M-MLV Reverse Transcriptase	Thermo Fisher Scientific
Minimal Essential Medium (MEM)	Thermo Fisher Scientific
Minimal Essential Medium Non-Essential Amino Acids (MEM NEAA)	Thermo Fisher Scientific
Opti-MEM-1 + Glutamax Medium	Lonza
Paraformaldehyde	Sigma
Phosphate Buffered Saline (PBS)	Sigma
Phosphatase Inhibitor Cocktail	Sigma
Polyinosinic:Polycytidylic Acid (Poly I:C)	InvivoGen
Propidium Iodide	Thermo Fisher Scientific
Protease Inhibitor Cocktail	Sigma
Puromycin	Sigma
RevertAid 5x Reaction Buffer	Thermo Fisher Scientific
RevertAid Reverse Transcriptase	Thermo Fisher Scientific
Sodium Dodecyl Sulfate (SDS)	Sigma
Sodium Chloride	Sigma
Sodium Deoxycholate	Sigma
SYBR® Green JumpStart™ Taq ReadyMix™	Sigma

TMB Stabilized Chromagen	Thermo Fisher Scientific
TRI Reagent®	Sigma
Tri-Sodium Citrate (Dihydrate)	Sigma
Triton X-100	Sigma
Trizma® Base	Sigma
Trypan Blue Solution (0.4%)	Sigma
Trypsin with EDTA (0.25%)	Thermo Fisher Scientific
Tween-20	Sigma
Vectashield® Mounting Medium	Vector Laboratories Limited
Vectashield® Mounting Medium with DAPI	Vector Laboratories Limited
Xylene	Thermo Fisher Scientific

Table 2.2 – List of Antibodies

Primary Antibody	Company	Catalogue Number	Concentration	Block
Mouse β-Actin	Cell Signalling Technology	3700S	1:1000	5% BSA
Mouse α-Tubulin	Santa Cruz Biotechnology	sc-8035	1:1000	2% BSA
Rabbit SOCS3	Cell Signalling Technology	2923	1:1000	5% BSA
Rabbit Anti-Phospho-Histone H3	Millipore	06-570	1:1000	TNT + 4% FBS
Rat IDO	Santa Cruz Biotechnology	sc-53978	1:400	TBS + 1% BSA
Rat IDO (western blotting)	Santa Cruz Biotechnology	sc-53978	1:750	1% BSA

Secondary Antibody	Company	Catalogue Number	Concentration	Block
Goat Anti-Mouse IgG HRP	Santa Cruz Biotechnology	sc-2031	1:5000	TBST
Donkey Anti-Rabbit IgG AlexaFluor 488	Life Technologies	A21206	1:1000	TNT+2% FBS
Goat Anti-Rabbit IgG HRP	Santa Cruz Biotechnology	sc-2030	1:5000	TBST
Goat Anti-Rat IgG HRP	Santa Cruz Biotechnology	sc-2006	1:5000	TBST
Goat Anti-Rat IgG AlexaFluor 488	Life Technologies	A11006	1:500	TBS+1%BSA

2.1.2 Buffers and Solutions

<u>Freezing Medium (10ml per flask)</u>

4ml FBS (= 40%)

1ml DMSO (= 10%)

5ml Medium (= 50%. MEM or Opti-MEM for Caco-2 and HIEC cells, respectively)

<u>RIPA Buffer (per ml)</u>

100µl Tris 500mM

30µl Sodium Chloride 5M

100µl Sodium Deoxycholate

10µl SDS 10%

10µl IGEPAL® CA-630

10µl Phosphatase Inhibitor

5µl Protease Inhibitor

750µl Distilled Water

<u>Tris-Glycine Running Buffer (10X)</u>

30.3g Trizma® Base

144g Glycine

10g SDS

Make up to 1 litre with distilled water

<u>Stripping Buffer</u>

15g Glycine

1g SDS

10ml Tween-20

pH to 2.2 using Hydrochloric Acid

Make up to 1 litre with distilled water

2.2 Methods

2.2.1 Human Intestinal Epithelial Cells

2.2.1.1 Cell Lines and Culture

Human Intestinal Epithelial Cells (HIECs) are a human, foetal-derived cell line and were a gift from Jean-Francois Beaulieu (Université de Sherbrooke). The HIECs were maintained in Opti-MEM-1 + Glutamax medium, supplemented with 5% foetal bovine serum (FBS), 1% 0.01M HEPES and 10µl 0.1mg/ml epidermal growth factor (EGF). The Caco-2 human Caucasian colon adenocarcinoma cell line was purchased from European Collection of Authenticated Cell Cultures (ECACC, catalogue #09042001), and were maintained in minimum essential medium (MEM), supplemented with 10% FBS and 1% MEM non-essential amino acids (NEAA). Cells were grown in a humidified incubator at 37°C in 95% air: 5% CO_2, and were passaged once they reached 80-90% confluency, and more frequently in Caco-2 cells in order to avoid them differentiating. When passaging the cells, the media was first discarded before washing the cells twice gently in PBS. Trypsin was used to detach adhered cells from the bottom of cell culture flasks, before resuspending and reseeding in a new flask with fresh media.

2.2.1.2 Generation of SOCS3-Knockdown and Control HIEC Cell Lines (carried out by Dr. Matt Hodges)

SOCS3 and non-silencing shRNA GIPZ lentiviral constructs (Thermo Scientific) were used to generate SOCS3 knockdown and control HIEC cell lines, respectively, with each construct containing a resistance marker against the antibiotic, puromycin. Both cell lines were seeded at a concentration of 2×10^4 cells per well and were incubated with the respective lentivirus, according to manufacturer's instructions. Puromycin (puromycin dihydrochloride derived from *Streptomyces alboniger*) was used at varying concentrations to select for successfully transduced HIEC cells. Complete Opti-MEM media containing 1.35µg/ml of puromycin was then used to maintain transduced HIEC cells during culture. Cells containing the SOCS3 and non-silencing constructs will be further referred to as SOCS3^{Low} and SOCS3^{Ev} (Ev- Empty vector, as the construct used was non-silencing, rather than SOCS3 silencing), respectively.

2.2.1.3 Cell Freezing

All cells used were cultured for 20 passages from thawing, and to ensure there were ample cell stocks (stored in liquid nitrogen), cells were routinely frozen. First, media was removed from the flask(s) and cells were gently washed twice in PBS before incubation at 37°C in 1ml of trypsin. Once cells had detached, they were resuspended in freezing medium (5ml per T75 flask used, see section 2.1.2), with the cell suspension then centrifuged for 5 minutes at 500 RCF (using an Allegra™ X-22R centrifuge, Beckman Coulter). The supernatant was removed, with each cell pellet resuspended in 4ml of freezing medium. Each 4ml cell suspension was then divided between 4 (labelled) cryovials, with cryovials frozen overnight at -80°C in a Mr. Frosty freezing container (VWR) with isopropanol (Fisher Scientific), before being transferred to a liquid nitrogen container for long-term storage.

2.2.1.4 Cell Counting

When preparing plates for experiments, media was first removed and cells were washed twice using PBS, as previously stated. Following incubation in trypsin, cells were resuspended in complete medium (approximately 4-7ml with 1ml trypsin, depending on the confluency). A 1:2 suspension was prepared by suspending cells in an equal volume of 1:10 diluted trypan blue (10-20µl). This was then used to determine the approximate number of cells, counted using a haemocytometer. The number of viable cells in each of the 4 corner 4x4 squares was counted, with an average calculated. This was then multiplied by the dilution factor (2) and 10^4, to determine the number of cells per ml of suspension. The initial cell suspension was diluted with complete medium appropriately, according to the cell numbers desired (as stated below, per experiment) in a 2ml volume per well.

2.2.1.5 RNA Extractions, cDNA Synthesis and Quantitative PCR

Normal HIEC and Caco-2 cells were seeded into 6-well plates at 1 x 10^6 cells per well, and SOCS3^{Ev} and SOCS3^{Low} HIEC cells were seeded into either 6- or 12-well plates at concentrations ranging from 1 x 10^5 to 1 x 10^6 cells per well and were incubated at 37°C for approximately 24 hours to allow cells to adhere to the bottom of the wells. Media was removed, replaced with serum-free media, and plates were incubated at 37°C for a further 12-16 hours. For quantification of SOCS3 mRNA, cells were then released using serum-containing media from 0 to 6 hours. For quantification of IL-10, TNF-α and indoleamine 2,3-dioxygenase (IDO) mRNA, HIECs were treated with serum-containing media alone (no

treatment), or serum-containing media with 0.1µg/ml of either flagellin, LPS or Poly I:C for 2 hours. For additional quantification of IDO mRNA, HIECs were also treated with 10ng/ml of IFN and 0.1mg/ml *Trichuris muris* excretory/secretory protein (E/S, a gift from Professor Kathryn Else) for 2 hours. After stimulating cells with the stated treatments and durations, cells were lysed in TRI-Reagent® and RNA was extracted according to manufacturer's instructions.

The concentration and purity of RNA was measured using the Nanodrop 2000c (Thermo Scientific), and nuclease-free water was used to generate 1-2µg of RNA in a volume of 9µl in order to generate complimentary-DNA (cDNA). 1µl of oligo-dT was added to each sample, which were then incubated at 70°C for 5 minutes, using the Programmable Thermal Controller-100™ (MJ Research Incorporated). The following master mix was then made and added to each sample before incubation at 42°C for 1 hour then 70°C for 10 minutes, again using the Programmable Thermal Controller-100™.

RevertAid Reverse Transcriptase Master Mix:

Reagent	Volume (µl)
RevertAid 5x Reaction Buffer	4
10mM dNTP	2
RevertAid Reverse Transcriptase	1
Nuclease-Free Water	3

Table 2.3: The reagents and volumes used for the RevertAid Reverse Transcriptase master mix, in order to generate cDNA from RNA.

mRNA levels of SOCS3, IL-10, TNF-α and IDO were assessed using quantitative PCR (qPCR), using the SYBR® Green JumpStart™ Taq ReadyMix™ and the Bio-Rad CFX96™ Real-Time System and C1000™ Thermal Cycler. A 20μl reaction was used for each well of a 96-well plate, as shown below, and no template controls were included for each primer set to ensure that only the desired PCR product was amplified in the reaction.

qPCR Master Mix:

qPCR Master Mix	Volume (μl)
SYBR® Green JumpStart™ Taq ReadyMix™	10
Forward Primer (10μM)	1
Reverse Primer (10μM)	1
Nuclease-Free Water	7
cDNA Template	1

Table 2.4: The reagents and volumes used within the qPCR master mix, in order to quantify changes in mRNA transcription of various target genes.

The table below shows the different qPCR protocols for each of the primers used, including step duration and temperature:

Step	Number of Cycles	SOCS3	IL-10 and TNF-α	IDO
Initial Denaturation	1	94°C 2 minutes	94°C 2 minutes	95°C 2 minutes
Denaturation	40	94°C 1 minute	94°C 15 seconds	95°C 15 seconds
Annealing		62°C 30 seconds	60°C 1 minute	67°C 30 seconds
Extension		72°C 30 seconds		72°C 30 seconds
Melt Curve, with increases in temperature from 65°C to 95°C with 0.5°C increments, with each increment lasting 5 seconds				

Table 2.5: Cycle times and temperatures for each of the primers used for the *in vitro* qPCR experiments.

Data was analysed with Microsoft Excel, using the $2^{(-\Delta\Delta Ct)}$ method, where changes in Ct value for each gene were normalised to those of a housekeeping gene, RPLPO (Large Ribosomal Protein). Fold-change in mRNA levels was then calculated relative to no treatment controls.

2.2.1.6 Primer Design and Sequences

Primers used for qPCR were designed using the National Center for Biotechnology Information (NCBI) Primer-BLAST primer designing tool and ordered from Sigma Aldrich, UK.

	Forward Primer	**Reverse Primer**
RPLPO (142bp)	GCAATGTTGCCAGTGTCTG	GCCTTGACCTTTTCAGCAA
SOCS3 (95bp)	TCGATTCGGGACCAGCCCCC	GAGCCAGCGTGGATCTGCG
IL-10 (85bp)	AGGACTTTAAGGGTTACCTGGG	TTCTCAGCTTGGGGCATCAG
TNF-α (82bp)	AGGTTCTCTTCCTCTCACATAC	ATCATGCTTTCAGTGCTCATG
IDO (122bp)	CATGCTGCTCAGTTCCTCCA	CCAGCATCACCTTTTGAAAGGA

Table 2.6: The forward and reverse sequences and product sizes for each of the qPCR primers used.

2.2.1.7 Cell Lysis for Western Blotting

Normal HIEC and Caco-2 cells, and SOCS3^{Ev} and SOCS3^{Low} HIEC cells were seeded into 6-well plates at 1×10^6 cells per well, and were incubated at 37°C for approximately 24 hours to allow cells to adhere to the bottom of the wells. Media was then removed, replaced with serum-free media, and plates were incubated at 37°C for a further 12-16 hours. For quantification of SOCS3 protein, cells were then released using serum-containing media from 0 to 6 hours. After 6 hours, the media was removed and cells in each well were lysed in 200µl of RIPA buffer (see section 2.1.2). Using a cell scraper, cells were removed from the bottom of the plate and lysed, before lysates were transferred to eppendorfs and centrifuged at 13,000g for 10 minutes at 4°C. Supernatants were transferred to new eppendorfs and either used straight away in a Bradford assay, or stored at -20°C.

2.2.1.8 Bradford Assay

Bradford assays were carried out for protein quantification of generated cell lysate samples. Bovine Serum Albumin (BSA) was used to produce protein standards with a range of concentrations between 0 and 500µg/ml. 450µl of Bradford reagent was added to 50µl of each standard. Standards were thoroughly mixed, with 100µl of each transferred to a 96-well plate in duplicate. The plate was read on a microplate reader using Magellan 7.0 software and a Tecan infinite 200Pro plate reader, and a standard curve was generated from the results. This process was then repeated using 450µl of Bradford reagent with 50µl of each sample diluted 1:10 with distilled water. The standard curve was then used to determine the protein concentration of each sample and the equivalent sample volume for 30µg of protein.

2.2.1.9 Western Blotting

Samples were prepared using 4x Laemmli Sample Buffer (Bio-Rad) and 10% 2-Mercaptoethanol, and were then boiled at 95°C for 2 minutes. Samples were loaded into Mini-PROTEAN® TGX Precast Gels (10%, Bio-Rad) and ran at 200V for approximately 30 minutes, until the gel front was near the bottom of the gel. Gels were then transferred onto nitrocellulose membranes, using a Trans-Blot® Turbo™ Transfer System (Bio-Rad) and Trans-Blot® Turbo Transfer Buffer (Bio-Rad). Membranes were blocked using 5% BSA in Tris-Buffered Saline with 0.1% Tween (TBST) for 1 hour at room temperature. Membranes were then incubated in primary SOCS3 antibody overnight at 4°C (see table 2.2).

Membranes were washed with TBST before being incubated with secondary antibody for 1 hour at room temperature (see table 2.2). Membranes were washed with TBST and Clarity™ Western Enhanced Chemiluminescence (ECL) Substrate was used for development, before exposure using the ChemiDoc™ MP Imaging System (Bio-Rad). Densitometry analysis was carried out using Image Lab 5.2.1 software (Bio-Rad) and Microsoft Excel, to determine SOCS3 protein levels, normalised to those of β-actin.

2.2.1.10 CyQuant Cell Proliferation Assay

CyQuant assays were carried out to assess differences in basal and microbial-stimulated proliferation in normal and cancerous intestinal cell lines (HIECs and Caco-2 cells, respectively). Assays were also carried out to determine the role of SOCS3 in basal and

microbial-stimulated proliferation in SOCS3-knockdown and control HIECs. HIECs and Caco-2 cells were seeded into a 96-well plate at 2000 cells per well, and allowed to adhere to the bottom of the plate for 24 hours at 37°C. The media was then removed and replaced with serum-free media, and incubated at 37°C for 12 hours. Plates were treated as shown below (table 2.3), with 4 wells used per treatment. HIECs and Caco-2 cells were treated for 24, 48 and 72 hours, and HIEC clones were treated for 48 hours, with treatments removed at the end of incubation and plates frozen at -80°C. For the 48 and 72 hour plates, half of the media was removed from each well and treatments were replenished after every 24 hour period.

Cell proliferation was assessed according to manufacturer's instructions, with known numbers of untransfected HIECs, and Caco-2 cells used to generate a standard curve in order to determine cell number following treatments. Fluorescence was measured using Magellan 7.0 software and a Tecan infinite 200Pro plate reader.

Cells	Treatments and Concentrations		Treatment Durations
Untransfected HIECs and Caco-2 cells	0.1µg/ml Poly I:C 1µg/ml Poly I:C 0.01µg/ml LTA 0.05µg/ml LTA 0.1µg/ml LTA	0.1µg/ml FLA 1µg/ml FLA 0.1µg/ml LPS 1µg/ml LPS	24, 48 and 72 hours
SOCS3^{Low} and SOCS3^{Ev} HIEC clones	0.01µg/ml FLA 0.1µg/ml FLA 1µg/ml FLA 0.1µg/ml LPS 1µg/ml LPS 10µg/ml LPS	0.01µg/ml Poly I:C 0.1µg/ml Poly I:C 1µg/ml Poly I:C 0.02 µg/ml LTA 0.2µg/ml LTA	48 hours

Table 2.7: Concentrations and treatment durations of TLR ligands used to stimulate HIEC and Caco-2 cells for the cell proliferation assays.

2.2.1.11 Data Analysis

Microsoft Excel was used for all data analysis (unless otherwise stated) and generation of graphs. To determine statistical significance ($p < 0.05$), two-tailed t-tests and ANOVA were performed using JMP software (version 12, SAS Institute), with Control Dunnett's post hoc test used where appropriate.

2.2.2 Mice

2.2.2.1 Generation of Mice

As SOCS3 null mice (SOCS3$^{-/-}$) are embryonic lethal (Roberts et al. 2001), conditional knockout mice with SOCS3 knockout specifically in IECs were used, as described in Croker et al. (2003) and Rigby et al. (2007). Experimental mice were generated by Dr. Elisabeth Shaw and were bred and reared at the animal facility at the University of Manchester. To create the experimental mice, first, two sequences containing loxP sites are inserted around the second exon of the SOCS3 gene (Croker et al. 2003). Mice homozygous for this pLox-SOCS3 modification (HO) (on a C57/BL6 background) were mated either with C57/BL6 mice (WT) or C57/BL6 mice hemizygous for the Villin-Cre transgene (VC), to produce wildtype (HO-WT) and SOCS3 knockout (HO-VC) animals, respectively. The Cre protein is a DNA recombinase enzyme that recognises loxP sequences and excises the DNA (belonging to the target gene) between them (el Marjou et al. 2004), in this case, SOCS3. This recombinase activity was targeted to the IECs specifically through the use of a Villin promoter, with Villin being an actin-binding protein located in the brush border of IECs (cited by Wang et al. 2008). All experiments were conducted under Home Office licence in accordance with the Animals in Scientific Procedures Act (1986) and PPL 40/3217 and 40/3633. Genotyping was performed by Dr. Elisabeth Shaw as described in Rigby et al. (2007).

2.2.2.2 *Trichuris muris* Infection

The Edinburgh isolate of *T. muris* whipworm was maintained in Severe Combined Immune Deficiency (SCID) mice. HO-WT and HO-VC mice were infected by oral gavage, as described by Wakelin (1967), and performed by Dr. Elisabeth Shaw and Professor Kathryn Else. Mice were infected at 6-8 weeks of age, with 25-30 eggs (low dose).

2.2.2.3 Tissue Collection and Histology

At 35 days-post infection, all mice (regardless of infection status) were sacrificed, with cecal tips removed and fixed in 4% formaldehyde for 24 hours, before wax embedding and sectioning for immunofluorescence (Immunofluorescence, 2.3.5). Mucosal scrapes from ceca were also obtained using RIPA buffer (see section 2.1.2) and passed through a blunt 18-gauge needle (Becton Dickinson) before centrifugation at >10,000g for 10 minutes at 4°C. Supernatants were retained and stored at -20°C until quantification using the Bradford assay

(2.3.6). (Wax embedding, sectioning and retrieving of mucosal scrapes performed by Dr. Elisabeth Shaw).

2.2.2.4 EdU Proliferation Assay

The Click-iT® EdU assay (Invitrogen) was performed to establish differences in proliferating IEC between uninfected and *T. muris*-infected HO-WT and HO-VC. This method involves the incorporation of EdU (5-Ethynyl-2'-deoxyuridine, administered 90 minutes before sacrifice at 10mg/kg), a nucleoside analogue, into the DNA of actively dividing cells, which is detected after addition of an Alexa Fluor® dye that binds to the EdU. In addition to quantifying proliferating intestinal cells, a Hoechst nuclear stain was used in order to determine cell position (based on crypt regions derived from Potten 1998, and Cliffe et al. 2005). Images were analysed blind using Zeiss LSM Image Browser software, which was also used to measure crypt depth. (EdU assay performed by Dr. Elisabeth Shaw, according to manufacturer's instructions).

2.2.2.5 Assessment of IDO Expression using Immunofluorescence

Immunofluorescence was carried out on embedded sections of ceca from *T.muris*-infected HO-WT and HO-VC mice, and colons from AOM/DSS-treated HO-WT and HO-VC mice (a gift from P.K Lund, prepared as described in Rigby et al. 2007). First, deparaffinisation was carried out on tissue sections, which involved placing slides in xylene, then into a container each of 100%, 90% and 70% ethanol, each for 3 minutes, before being kept in distilled water until antigen retrieval.

Heat-Induced Epitope Retrieval (HIER) was performed as the method of antigen retrieval, which involved heating slides in pH 6.0 sodium citrate buffer in a pressure cooker (Morphy Richards, model 48815) for 3 minutes before cooling in distilled water for 10 minutes. Slides were then washed in TBS+0.025% Triton X-100. A PAP pen (Sigma) was used to draw around each tissue section, forming a hydrophobic barrier, and slides were then blocked in 10% normal goat serum in TBS+1% BSA for 2 hours at room temperature in a humidified container. Slides were then incubated in 1:400 IDO in TBS+1% BSA overnight at 4°C, in a humidified container. A control slide incubated in TBS+1% BSA only, and no primary antibody was also included.

Following primary antibody incubation, slides were washed in TBS+0.025% Triton X-100 before being incubated in 1:500 Goat Anti-Rat IgG AlexaFluor 488 in TBS+1% BSA for 1 hour at room temperature. Excess antibody was washed off using TBS, and slides were then incubated in a nuclear stain, using 1:3000 propidium iodide in PBS for 3 minutes. Slides were then briefly washed in PBS and mounted using Vectashield® Mounting Medium, and sealed with a coverslip before being viewed on a Zeiss LSM 510 confocal microscope.

2.2.2.6 Bradford Assay

Bradford assays were carried out for protein quantification of cecal protein samples. BSA was used to produce protein standards with a range of concentrations between 0 and 1mg/ml. 450µl of Bradford reagent was added to 50µl of each standard. Standards were thoroughly mixed, with 100µl of each transferred to a 96-well plate in duplicate. The plate was read on a microplate reader using Magellan 7.0 software and a Tecan infinite 200Pro plate reader, and a standard curve was generated from the results. This process was then repeated using 450µl of Bradford reagent with 50µl of each sample diluted 1:10 with distilled water. The standard curve was then used to determine the protein concentration of each sample and the equivalent sample volume for 30µg of protein.

2.2.2.7 Assessment of IDO Expression using Western Blotting

Samples were prepared using 4x Laemmli Sample Buffer (Bio-Rad) and 10% 2-Mercaptoethanol, and were then boiled at 95°C for 5 minutes. Samples were loaded into Mini-PROTEAN® TGX Precast Gels (10%, Bio-Rad) and ran at 160V for approximately 45 minutes, until the gel front was near the bottom of the gel. Gels were then transferred onto nitrocellulose membranes, using a Trans-Blot® Turbo™ Transfer System (Bio-Rad) and transfer buffer. Membranes were blocked using 1% BSA in TBST for 1 hour at room temperature. Membranes were then incubated in mouse IDO primary antibody overnight at 4°C (see table 2.2).

Membranes were washed with TBST before being incubated with secondary antibody for 1 hour at room temperature (see table 2.2). Membranes were washed with TBST, and ECL was used for development, before exposure using the ChemiDoc™ MP Imaging System. Densitometry analysis was carried out using Image Lab 5.2.1 software (Bio-Rad) and Microsoft Excel, to determine IDO protein levels, normalised to those of α-tubulin, or β-actin

(following stripping of secondary antibody using mild stripping buffer (see section 2.1.2), and re-blocking before antibody incubation).

2.2.2.8 Data Analysis

All data analysis (unless otherwise stated), two-tailed t-tests (to determine statistical significance- $p<0.05$) and generation of all graphs was performed using Microsoft Excel.

2.2.3.1 Fly Stocks and Maintenance

The white[Dahomey] stock was obtained through backcrossing w[1118] flies into the outbred wild-type Dahomey background (Broughton et al. 2005). Both EsgGAL4, GAL80[ts] and UAS-SOCS36E RNAi 1/ Cyo stocks were obtained from the Bloomington Stock Centre, and were backcrossed six times onto the white[Dahomey] background to produce w[Dah]; EsgGAL4, GAL80[ts] and w[Dah]; UAS-SOCS36E RNAi 1/ Cyo, to ensure 100% of the genetic background had been replaced with the genetic material of w[Dah] flies. Fly stocks were maintained at 25°C and constant humidity on standard sugar/yeast medium (see Appendix 9), on a 12-hour/12-hour light/dark cycle.

2.2.3.2 Fly Genetics and Generation of Experimental Flies

The GAL4/UAS system in *Drosophila* was used to produce an ISC-specific knockdown of SOCS36E. GAL4 is a gene that can target activation of gene transcription in specific cells or tissues, but this can only occur when a fly containing GAL4 is crossed to a fly containing the Upstream Activation Sequence (UAS). UAS is found next to the target gene and contains GAL4 binding sites (Brand and Perrimon 1993). In our case, we used flies with the escargot (Esg) ISC driver and crossed them with flies containing SOCS36E RNAi attached to UAS. However, knockdown of SOCS36E through RNAi is homozygous lethal, so therefore a curly-winged balancer (Cyo) was used to ensure fly survival and prevent loss of the RNAi from the population. The balancer also aids selection following crosses as flies that contain the RNAi will not possess the balancer, and therefore will have straight, not curly wings.

To generate an RNAi knockdown, double-stranded RNA is introduced into the organism and any mRNA that contains the same sequence will be degraded (Fire et al. 1998). Furthermore, the EsgGAL4 line that we used was also coupled with GAL80[ts]; a temperature sensitive GAL4 repressor (McGuire et al. 2003). GAL80[ts] is active at temperatures ≤18°C, thus repressing GAL4 and preventing gene transcription. However, at temperatures ≥28°C, GAL80[ts] function is restricted, therefore relieving inhibition of GAL4, resulting in transcription of the target gene downstream of UAS, i.e. SOCS36E RNAi (as shown in figure 2.1). Once the experimental crosses were set up, eggs were left to develop at 17°C so GAL80[ts] repressed GAL4. However, once the flies had eclosed, they were kept in a 28°C incubator.

This ensured that the knockdown was restricted to adult flies, and that any potential effects of SOCS36E knockdown on development were prevented.
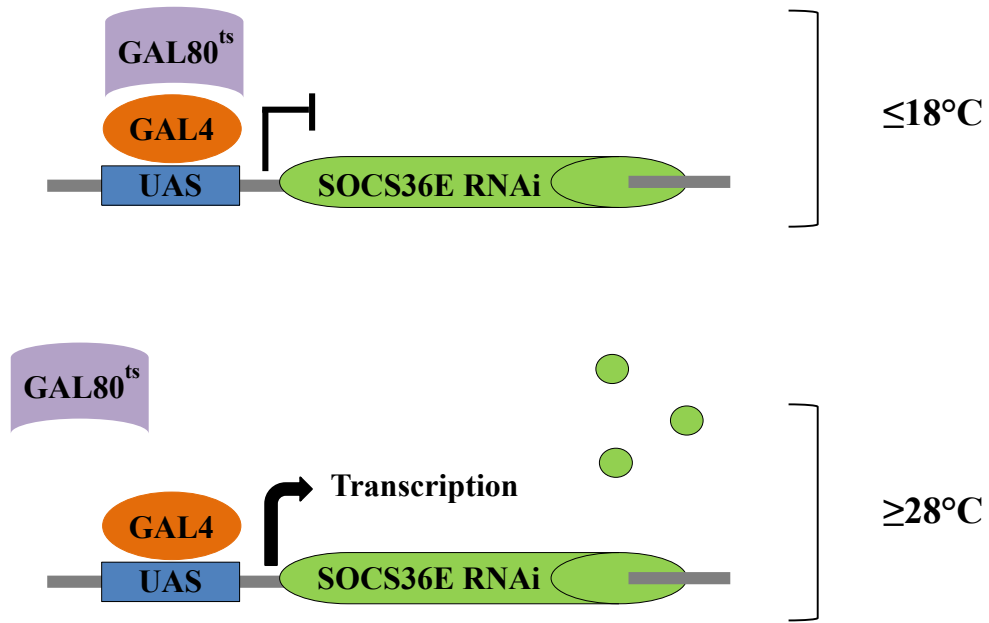
Figure 2.1: Functioning of the UAS-GAL4 GAL80ts system. At lower temperatures, such as 18°C, GAL80ts is bound to GAL4, preventing the transcription of target genes, i.e. SOCS36E RNAi. At higher temperatures, such as 28°C, GAL80ts is unable to repress GAL4, so both GAL4 and UAS are active, allowing transcription of SOCS36E RNAi and subsequent knockdown of SOCS36E to occur (Image adapted from WWW, Cold Springs Harbor Protocols).

Experimental flies were reared at standard larval density and in order to achieve this, male and female parent flies for each experimental genotype were placed in plastic cages, sealed with a petri dish containing agar (consisting of 15g agar, 30ml nipagen and 3ml of propionic acid per litre of grape juice used) and fresh yeast in order to stimulate egg laying. Grape plates were replaced every 24 hours, along with fresh yeast. Cages were kept at 25°C for one week, and every 24 hours, the grape plates were removed and any eggs that had been laid were rinsed off

into a falcon tube using PBS. Once the eggs had settled, they were pipetted into bottles of standard food in 130µl volumes until no eggs remained in the falcon tube. This was carried out to ensure that all bottles contained approximately the same number of eggs in each. Once completed, the eggs were left to develop, and ultimately eclose approximately three weeks later, at 17°C.

After eclosing, flies were sorted by gender and phenotype (as stated in table 2.4) under brief CO_2 anaesthesia. All experimental flies were maintained at 28°C, with 10 flies per vial, on standard sugar/yeast medium. Flies were transferred to vials of fresh food three times a week. This process was carried out for all experiments performed, as described in each following section.

	Female Parent	Male Parent	Experimental Offspring	
Genotype	w^{Dah}; Esg GAL4, GAL80^{ts}	w^{Dah}; UAS-SOCS36E RNAi 1/ Cyo	Esg GAL4, GAL80^{ts}/ UAS-SOCS36E RNAi 1	SOCS36E Knockdown flies
Phenotype	Red eyes, normal wings	Orange eyes, curly wings	Red eyes, normal wings	
Genotype	w^{Dah}; Esg GAL4, GAL80^{ts}	w^{Dah}	Esg GAL4, GAL80^{ts}/+	ISC Driver Control Flies
Phenotype	Red eyes, normal wings	White eyes, normal wings	Red eyes, normal wings	
Genotype	w^{Dah}	w^{Dah}; UAS-SOCS36E RNAi 1/ Cyo	UAS-SOCS36E RNAi 1/+	SOCS36E RNAi Control Flies
Phenotype	White eyes, normal wings	Orange eyes, curly wings	Orange eyes, normal wings	

Table 2.8: The genotypes and phenotypes of the flies used to produce the experimental flies for the subsequent lifespan and behavioural experiments.

2.2.3.3 Lifespan Analysis

Survival analysis was conducted and was composed of recording the number of live, dead and censored flies until no living flies remained. Censors accounted for flies that did not die naturally (for example, flies that were stuck in the food or vial, or escaped during transferral to a new vial), and therefore did not count towards the overall lifespan of the flies. The number of deaths was used to plot survival against time, with 1 indicating 100% survival, 0.5 representing 50% survival and the median lifespan, and 0 indicating there were no living flies for that particular genotype. Maximum survival was the time point at which 10% of a genotype remained.

2.2.3.4 RNA Extraction, Reverse Transcription and Quantitative PCR

Guts from 10 day old experimental flies were dissected in 1xPBS then transferred to an eppendorf containing 1ml of TRI-Reagent®. Once twenty guts had been dissected and transferred, the eppendorf was snap frozen in liquid nitrogen. This was repeated until sixty guts per gender, per genotype had been obtained. RNA was extracted according to manufacturer's instruction, and the concentration and purity was measured using the Nanodrop 2000c (Thermo Scientific).

1µg of RNA was used per sample in order to generate cDNA, using the M-MLV Reverse Transcriptase manufacturer's instructions, and the Programmable Thermal Controller-100™ (MJ Research Incorporated): 1µg of each RNA sample was diluted in nuclease-free water (Sigma) to give a final volume of 9µl. 1µl of 1:2 oligo-dT was added to each sample. Samples were incubated at 70°C for five minutes, using the Programmable Thermal Controller-100™. The following master mix was made and added to each sample before incubation at 37°C for 1 hour then at 80°C for 1 minute, again using the Programmable Thermal Controller-100™:

Reagent	Volume (µl)
5x M-MLV Reverse Transcriptase Buffer	4
M-MLV Reverse Transcriptase	1
dNTP (10mM)	1
Nuclease-Free Water	4

Table 2.9: The reagents and volumes used for the M-MLV Reverse Transcriptase master mix, in order to generate cDNA from RNA in *Drosophila*.

Levels of SOCS36E mRNA in the gut of experimental flies were assessed using qPCR, using SYBR® Green JumpStart™ *Taq* ReadyMix™, and the Bio-Rad CFX96™ Real-Time System and C1000™ Thermal Cycler. A 96-well plate was used to carry out qPCR, and each well consisted of a 20µl reaction, containing the following reagents:

qPCR Master Mix	Volume (µl)
SYBR® Green JumpStart™ Taq ReadyMix™	10
Forward Primer (10µM)	1
Reverse Primer (10µM)	1
Nuclease-Free Water	7
cDNA Template	1

Table 2.10: The reagents and volumes used within the qPCR master mix, in order to quantify changes in mRNA transcription of SOCS36E within *Drosophila* midguts

No template controls (wells containing an extra 1µl of nuclease-free water, instead of 1µl of cDNA) were also included to ensure that the required product was being amplified.

The protocol included an initial 2 minute denaturation step at 94°C, followed by 39 cycles of a 94°C denaturation step for 15 seconds and a 63°C annealing step for 1 minute. This was followed by a melt curve step, which consisted of an increase in temperature from 65°C to 95°C, with 0.5°C increments, with each 0.5°C increment lasting 5 seconds. Data was analysed using Microsoft Excel, and gene expression was calculated using the $R = 2^{(-\Delta\Delta Ct)}$, where the Ct values for SOCS36E were normalised to the Ct values of the housekeeping gene, Actin 5C.

2.2.3.5 Primer Design and Sequences

Forward and reverse primers for SOCS36E were designed using the National Center for Biotechnology Information (NCBI) Primer-BLAST primer designing tool and ordered from Sigma Aldrich, UK, and were reconstituted in nuclease-free water to a concentration of 100µM before use, according to the data sheet supplied by the manufacturer. Primers for Actin 5C, as use as a housekeeping gene, were derived from Broughton et al. (2005).

	Forward Primer	**Reverse Primer**
Actin 5C (83bp)	CACACCAAATCTTACAAAATGTGTGA	AATCCGGCCTTGCACATG
SOCS36E (127bp)	AGTTCAGCTTCGACTGCCAC	CTGTGCAGGGGTATCGTCAG

Table 2.11: The forward and reverse sequences, and product sizes for each of the qPCR primers used.

2.2.3.6 Midgut Infection

The gram-negative bacteria, *Erwinia carotovora carotovora 15* (*Ecc15*), were aseptically streaked onto a Luria Broth (LB) culture plate and incubated overnight at 29°C. A single colony was then removed to aseptically inoculate 10ml of LB media. This suspension was left in a shaking incubator overnight at 29°C, shaking at 150rpm. The bacterial suspension was then used to inoculate 1 litre of sterile LB media, which was also incubated overnight at 29°C, shaking at 150rpm. Cultures were centrifuged for 20 minutes at 4000rpm (using an Avanti® J-26 XP centrifuge, Beckman Coulter), and after removing the supernatants, pellets were re-suspended in 2ml of LB media and the OD_{600} was measured using a plate reader.

The suspension was then diluted with sterile 5% sucrose. Following 2 hours of starvation on agar medium, flies were briefly anaesthetised with CO_2 whilst a filter paper circle (approximately 2.5cm in diameter) was inserted into the vial and 200µl of the bacterial suspension was added. Flies were left to feed for two hours and were anaesthetised again

briefly with CO_2 for transfer into vials of fresh medium. Infection with *Ecc15* took place at approximately 1 and 2 weeks of age. In order to establish the effect of infection on health- and lifespan in the experimental flies, an uninfected cohort were used and during the infection process, these flies were on agar medium for 2 hours, before being transferred into new vials of standard medium.

2.2.3.7 Immunofluorescence

Instructions for *Ecc15* infection were carried out as described above on female flies from all three experimental genotypes. Each genotype was subdivided into four groups: an uninfected control group that were transferred back onto standard food following two hours of starvation, and three infected groups whose guts were dissected in 1xPBS, either 1, 3 or 7 days post-infection. Following dissection, guts were fixed in 4% paraformaldehyde before being washed in 1xPBS, TNT (0.1M Tris HCl /0.3M NaCl, 0.5% Triton X-100) and then blocked in TNT + 4% FBS for 90 minutes at room temperature, with gentle shaking. Guts were then incubated at 4°C overnight with rabbit anti-phospho-histone H3, diluted in TNT + 4% FBS. A control was included that remained in TNT+4% FBS, with no primary antibody.

After the overnight incubation, guts were washed in TNT then incubated with donkey anti-rabbit IgG AlexaFluor 488 conjugated secondary antibody diluted 1:750 in TNT + 2% goat serum, for 90 minutes at room temperature, with gentle shaking. Guts were then washed in TNT, and 1xPBS before being mounted onto microscope slides using Vectashield® Mounting Medium with DAPI and then sealed. Slides were visualised using a Zeiss LSM 510 confocal microscope.

2.2.3.8 Negative Geotaxis Assay

Negative geotaxis was carried out on a weekly basis, using a maximum of 15 flies and a minimum of 7 flies per tube, with a maximum of 5 tubes and a minimum of 3 tubes used per genotype, per gender each week. Flies were briefly anaesthetised with CO_2 and allowed to recover for one hour at 28°C. The assay was performed at 25°C and at constant humidity.

The assay involved physically striking the bottom of the tube, forcing the flies to the bottom, then recording the number of flies that reached the top, and the number of flies that remained at the bottom of the tube after 45 seconds. This was performed three times for each tube. The performance index (P.I), the measure of healthspan in this assay, was generated using the following calculation: ½ x (Total number of flies in the tube + Number of flies that reached the top of the tube – Number of flies remaining at the bottom of the tube) / Total number of flies in the tube. The average P.I for each genotype at each time point was then calculated.

2.2.3.9 Exploratory Walking Assay

The exploratory walking assay was carried out on a weekly basis, using a maximum of 15 flies per genotype, per gender each week. This assay was based on methods described by Martin (2004), and the apparatus used consisted of 4 chambers, with each chamber measuring 4cm in diameter, and 1cm in height. Each chamber contained one fly, and an aspirator was used for transferring flies from vials to each chamber. The flies' movements were recorded for 15 minutes, with four chambers able to be recorded per video. Video analysis was conducted using Ethovision XT software (Noldus). Microsoft Excel was used to analyse the decline in each walking parameter with increasing age and to calculate the total function.

2.2.3.10 Starvation Resistance (carried out by Jack Sloan as part of an Undergraduate research project)

Experimental flies were reared in vials of standard sugar/yeast food until 4 days of age, when they were transferred into vials containing 1.5% agar medium. Flies were transferred to new vials of agar medium twice weekly, with survival analysis carried out daily. Each vial contained 10 flies, with 10 vials used per gender, per genotype.

2.2.3.11 Oxidative Stress Resistance (carried out by Jack Sloan as part of an Undergraduate research project)

Experimental flies were reared in vials of standard sugar/yeast food until 4 days of age, when they were transferred into vials containing 1.5% agar medium with 5% sugar and 5% H_2O_2. Flies were transferred to new vials of agar medium twice weekly, with survival analysis carried out daily. Each vial contained 10 flies, with 6 vials used per gender, per genotype.

2.2.3.12 Cold Stress Tolerance (carried out by Jack Sloan as part of an Undergraduate research project)

Experimental flies, at 10 days of age, were placed in an ice bucket at 4°C for 4 hours, before being allowed to recover at 25°C. The time taken from the removal of vials from the ice bucket to each fly standing upright was recorded. Each vial contained 5 flies, with 10 vials used per gender, per genotype.

2.2.3.13 Fecundity

To measure fecundity, the number of eggs laid by experimental female flies per vial was counted and recorded once the females had been transferred to fresh vials of food. This was carried out once a week and was performed alongside lifespan analysis in order to determine the average number of eggs laid per female in each genotype, over a 24 hour period.

2.2.3.14 "Smurf" Intestinal Integrity Assay

This assay was performed to assess midgut integrity of experimental flies and was based on methods described by Rera et al. (2011). Flies were transferred into vials of standard food containing 2.5% w/v blue food dye (FD&C Blue #1, SPS Alfachem) for 9 hours, before transferral into vials of fresh standard food. Flies were briefly anaesthetised using CO_2 before imaging using a Nikon Coolpix 990 digital camera. The dye will be incorporated in the proboscis and crop of healthy flies with an intact midgut. Flies that experienced a loss in integrity were termed "Smurf" flies and demonstrated dye incorporation in all tissues. w^{Dah} were used initially to optimise this assay, followed by experimental flies, with both genders and flies of various ages used for all genotypes.

2.2.3.15 Data Analysis

To determine statistical significance, t-tests and ANOVA were performed using JMP software (version 12, SAS Institute), Tukey's post hoc test was used where appropriate. Microsoft Excel was used for all data analysis, and to generate all graphs and survival curves, with statistical differences in survival also determined using Microsoft Excel.

Chapter 3:

Investigating the role of SOCS3 on normal and microbe-mediated mucosal homeostasis using a novel, *in vitro* model of normal human intestinal epithelium

3.1 Rationale

For many decades, intestinal cell research has been carried out using various *in vitro* cancer cell lines (for example, Caco-2 and SW480) or primary animal-derived cell lines (such as IEC-6, which originates from rat). Although both of these have proven to be useful, neither is without their limitations, so caution must be taken when translating the results to normal, healthy (human) IECs *in vivo*. For instance Caco-2, a human epithelial colorectal adenocarcinoma cell line (Fogh and Trempe 1975), can be used as a model of proliferative and differentiated cells, resembling intestinal ECs (Pinto 1983) and, due to the polarisation and expression of various cell junctions and transporters, they are often used in barrier and drug absorption studies (Hidalgo et al. 1989, Artursson 1990). However, they have been reported to respond differently to various cytokines when compared to other transformed cell lines (Daig et al. 2000), and primary IECs from patients. This was also true for HT29 too, which is a human colon adenocarcinoma cell line (Fogh and Trempe 1975) also capable of differentiating (Pinto et al. 1982), as well as producing mucins (Rousset et al. 1978, Augeron and Laboisse 1984). IEC-6 is an untransformed small intestine rat cell line (Quaroni et al. 1979) that resembles intestinal crypt cells and has been found to express microvilli and various tight junctions. They have been used extensively in animal research, although it may be difficult to extrapolate results into humans (Souba and Wilmore 2001). A non-cancerous, human, foetal-derived small intestine *in vitro* cell line was developed by Perreault and Beaulieu (1996), named the HIEC cell line, and initial studies found that these cells most resemble the undifferentiated cells found in the small intestinal crypts and can be continuously cultured; a desirable feature of the widely-used Caco-2 cells. Additionally, although our interests are concerning intestinal homeostasis with regards to proliferation and turnover, like Caco-2 cells, HIEC cells can also be used and studied as both proliferating crypt cells (Perreault and Beaulieu 1996), and as differentiated cells following the overexpression of various differentiation transcription factors (Benoit et al. 2010). However, one has to weigh up the pro- and contra-indications of available *in vitro* cell models dependent upon the research questions, and we chose to use the HIEC cell line as they are thought to be more responsive to exogenous stimuli, and also more representative of intestinal cells found *in vivo* (i.e. more physiologically relevant), as cancer cells may be regarded as autonomous, and self-sufficient in growth, maintenance and proliferation (Hanahan and Weinberg 2000). Therefore, as our overall focus in the project is SOCS proteins (SOCS3 in particular in our mammalian models), it is not known whether manipulation of SOCS3 would have much of an effect on cytokine and microbial signalling pathways in Caco-2 cells.

Despite the development of the HIEC cell line approximately 20 years ago, very little has been published on their use, especially when compared with the more commonly used SW480 and Caco-2 cell lines. We aimed to use these cells as a model for investigating "normal" intestinal homeostasis, in particular looking at the role SOCS3 plays. It is well established the functions SOCS3 has involving regulation of proliferation, through its role as a tumour suppressor due to a decrease or silencing (due to hypermethylation) of SOCS3 associated with a multitude of cancer types (He et al. 2003, Weber et al. 2005, Ogata et al. 2006, Rigby et al. 2007, Li et al. 2009), to a perpetuator of IBD. This is due to reports of increased IL-6 in UC patients, thus resulting in increased Jak/Stat and SOCS3 signalling as a consequence (Suzuki et al. 2001, Li et al. 2009). Increased SOCS3 has also shown to lead to both the increased production of the pro-inflammatory cytokine, TNF-α, as well as decreased wound healing of IECs following microbial stimulation (Thagia et al. 2015), which when combined, could lead to insufficient repair of cells following damage. However, despite these findings, little is known about the role SOCS3 has in normal homeostasis, so we aimed to investigate whether SOCS3 is involved in IEC turnover, using a potentially more physiologically relevant line, initially determining baseline levels of SOCS3 and proliferation and comparing them with those of the widely used adenocarcinoma cell line, Caco-2.

3.2 Comparison of basal SOCS3 expression in a normal HIEC cell line, compared with Caco-2 cells

3.2.1 HIEC cells produce more SOCS3 mRNA than Caco-2 cells following serum recovery

In order to determine baseline SOCS3 levels, we quantified SOCS3 mRNA in both Caco-2 and HIEC cells following serum recovery. Figure 3.1 (a) shows SOCS3 levels in HIEC cells alone, and shows that there was a 3-fold increase of SOCS3 mRNA within an hour of addition of serum (p<0.0001). When compared with HIECs (figure 3.1b), Caco-2 cells expressed lower levels of SOCS3 mRNA (ranging from 1.3-fold lower at 180 minutes, to 4-fold lower at 60 minutes), both in the presence and absence of serum, and at all time points. Using a Student's t-test, significance between HIEC and Caco-2 cells' SOCS3 mRNA levels was also evident at all time points (p<0.05). Additionally, following addition of serum in HIEC cells (figure 3.1a), SOCS3 mRNA levels varied noticeably over the duration of the experiment, with the fold-change never falling below 1.1±0.3 (at 180 minutes). However, figure 3.1 (b) shows that there appeared to be very little fluctuation in SOCS3 mRNA in Caco-2 cells throughout the 6 hours, with fold-changes remaining between 0.55±0.03 (at t=0) and 0.9±0.06 (at 180 minutes, both relative to HIEC t=0). Therefore, in accordance with previous studies, we found that

Caco-2 cells were found to have low expression of SOCS3, at least in this case at the mRNA level.
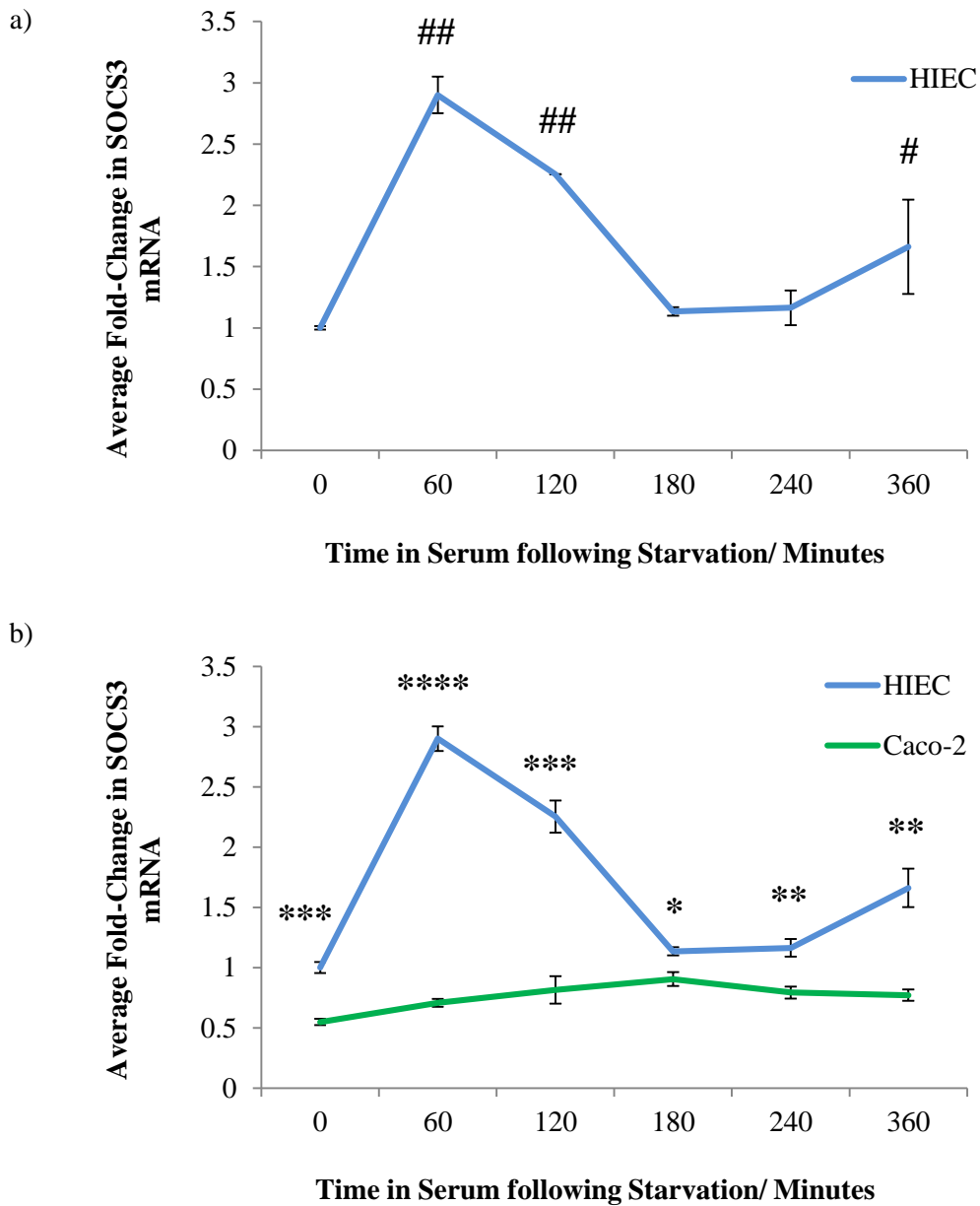
Figure 3.1: The change in SOCS3 mRNA expression levels following serum recovery (±SEM) in (a) the normal HIEC cell line (blue), and in (b) the transformed Caco-2 cell line (green). Cells were seeded at 1×10^6/well and allowed to adhere overnight, before serum starvation overnight. Cells were then treated with serum-containing media for the times stated before lysis with TRI-Reagent® for RNA extraction. Expression levels of SOCS3 mRNA were measured using qPCR, and calculated using the $2^{(-\Delta\Delta Ct)}$ method, with values relative to the HIEC t=0 average ratio. (# = p<0.01, ## = p<0.0001 using a one-way ANOVA with control Dunnett's post-hoc test vs. HIEC t=0. * = p<0.05, ** = p<0.01, *** = p<0.001, **** = p<0.0001 using a Student's t-test vs. Caco-2 within time points). (n= 4).

Following the observation of more regulated, varying levels of SOCS3 mRNA in HIEC cells compared with Caco-2 cells, we performed western blotting to establish whether these differences were continued to the protein level, thereby indicating a functional regulatory role. Figure 3.2 (a) shows that following addition of serum over the duration of the time course, expression of SOCS3 protein did not significantly increase in HIEC cells (relative to serum-starved HIEC cells), ranging between 0.5 ± 0.04 (at 360 minutes) to 1.6 ± 0.6 (at 240 minutes). Contrary to the mRNA results (figure 3.1a), serum-induced changes in SOCS3 were not seen to the same extent at the protein level. However, expression of SOCS3 protein (in addition to mRNA) was also found to fluctuate over time (figure 3.3).

When compared with Caco-2 cells, SOCS3 protein levels were significantly higher in serum-starved HIEC cells ($p=0.002$) (figure 3.2b). However, at 120 and 180 minutes following addition of serum, Caco-2 cells appeared to upregulate SOCS3 protein, although this was not a significance increase ($p=0.252$ and $p=0.0821$, respectively). Interestingly, at 240 and 360 minutes, SOCS3 protein expression in the two cell lines was similar, with approximate fold-changes of 1.6 and 0.6, respectively (relative to serum-starved cells).

In conclusion, from mRNA to protein, HIECs expressed more SOCS3 than Caco-2 cells during serum starvation. However, following re-introduction of serum, results were more variable- protein levels did not match those of mRNA in that Caco-2 cells appeared to express more protein at 120 and 180 minutes, with both cells lines displaying similar SOCS3 protein levels at 240 and 360 minutes in serum. The contrasts observed at both the mRNA and protein level could suggest that: SOCS3 mRNA is more efficiently regulated in HIEC cells, different translational mechanisms are active in HIECs and Caco-2 cells, and/or that SOCS3 degradation processes are differentially regulated in these two cell lines.

a)

b)
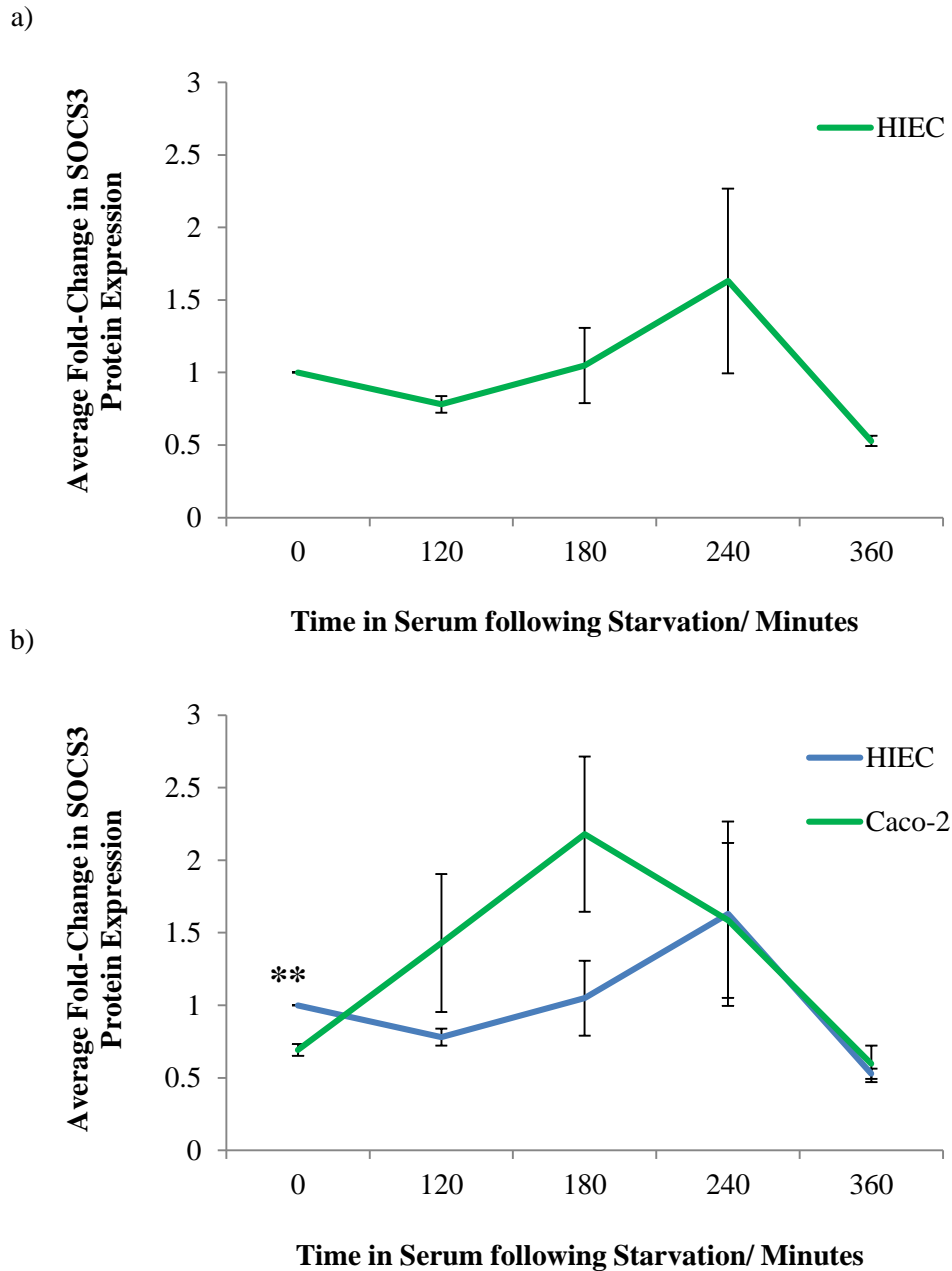
Figure 3.2: SOCS3 protein expression following serum recovery (±SEM) in (a) HIEC cells (blue) and compared with (b) Caco-2 cells (green). Cells were seeded at 1×10^6/well and allowed to adhere before serum starvation overnight. Cells were treated with serum-containing media for the times stated before lysis with RIPA buffer. Samples were run on 10% SDS-PAGE gels before transfer onto nitrocellulose membranes and incubation in SOCS3 primary antibody at 1:1000 overnight. Membranes were then incubated in secondary antibody for 1 hour at room temperature. Membrane imaging and densitometry was carried out using a ChemiDoc™ MP Imaging System and Image lab software, with values relative to HIEC t=0. (** = $p < 0.001$, using a two-tailed t-test, vs Caco-2 cells, within time points). (n= 3).
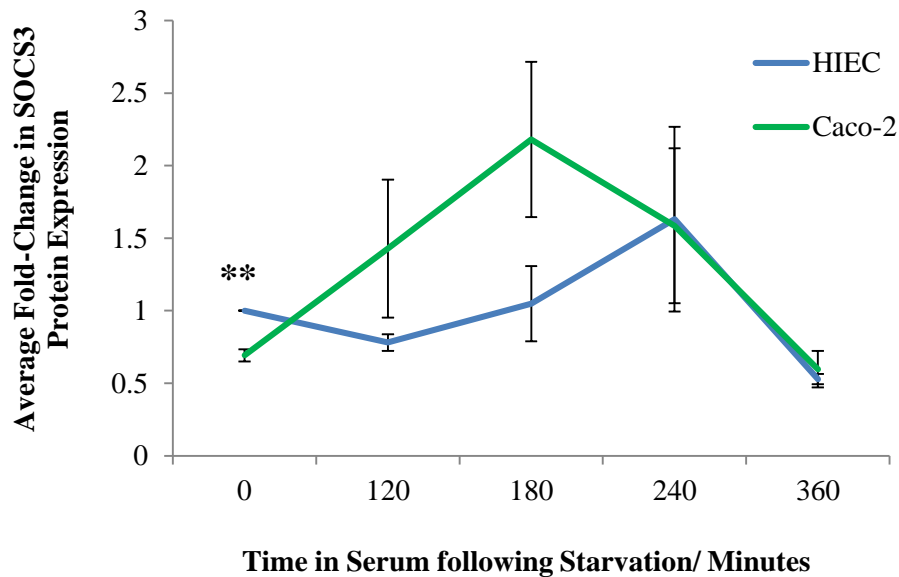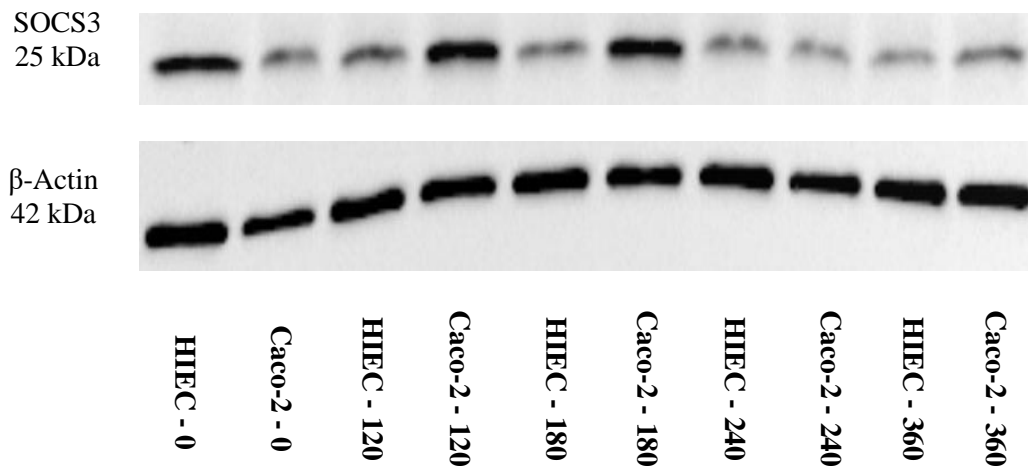
Figure 3.3: Cycling of SOCS3 protein expression following serum recovery (±SEM) in HIEC (blue) and Caco-2 cells (green). Following serum recovery, cells were lysed, ran on 10% SDS-PAGE gels, and transferred onto nitrocellulose membranes before incubation overnight in 1:1000 SOCS3 primary antibody. Membranes were then incubated in secondary antibody for 1 hour at room temperature, and re-blotted for β-actin as a loading control. Membrane imaging and densitometry was carried out using a ChemiDoc™ MP Imaging System and Image lab software, with values relative to HIEC t=0. (** = $p<0.001$, using a two-tailed t-test, vs. Caco-2 cells, within time points). (n= 3).

3.3 Successful generation of a HIEC line with SOCS3 knockdown

3.3.1 HIEC cells were successfully transduced using both SOCS3 knockdown and control constructs

After establishing that Caco-2 cells produced lower amounts of SOCS3 mRNA in the basal state than untransformed HIECs, in accordance with previous studies demonstrating lower levels of SOCS3 in various tumours, we generated a SOCS3 knockdown HIEC cell line (SOCS3^{Low}, alongside a control, SOCS3^{Ev}, transduced with a non-silencing construct) to investigate how reduction of SOCS3 impacts upon normal intestinal cell responses to a variety of physiological stimuli, using a small interfering, or silencing RNA lentiviral construct (siRNA). We confirmed the efficacy of the knockdown using a variety of methods. First, images were taken of the transduced cells on a Zeiss Axiovert 35 microscope, along with untransduced HIECs to confirm uptake of the lentiviral construct. Both constructs contained GFP regions, so therefore both transduced lines should fluoresce when imaged, whereas untransduced HIEC should not. Figure 3.4 shows fluorescence corresponding to GFP in both (a) SOCS3^{Ev} and (b) SOCS3^{Low} transduced HIEC cells. Untransduced HIECs however, did not display any fluorescence (figure 3.4c, left panel), corresponding to the absence of transduction using a GFP-containing lentiviral construct. Therefore, this suggests that the transduction process was successful for both SOCS3^{Ev} and SOCS3^{Low} cells.

a)

SOCS3^{Ev}
HIEC
cells

b)

SOCS3^{Low}
HIEC
cells

c)

Untransduced
HIEC
cells
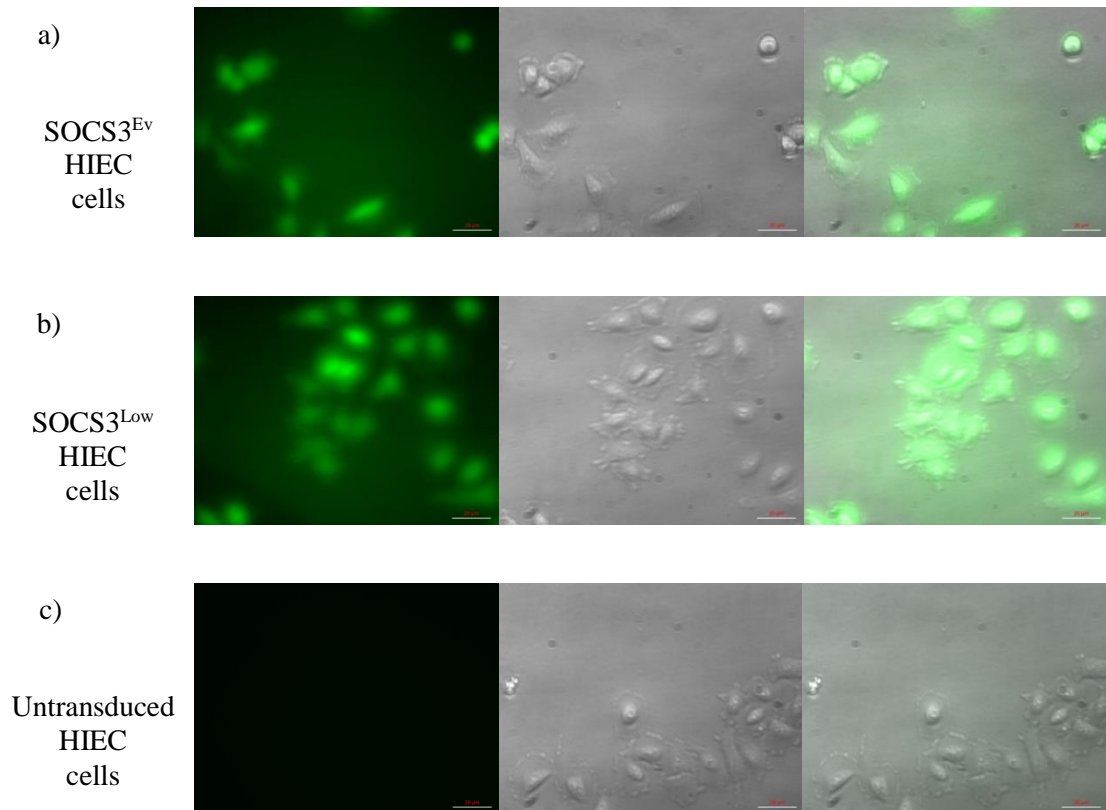
Figure 3.4: Fluorescent microscopy images of transduced (a) SOCS3^{Ev} and (b) SOCS3^{Low} HIEC cell lines, along with (c) untransduced HIECs. Images displaying the GFP fluorescence (green) of HIEC cells (left panels) were taken along with bright-field images (centre panels), and then merged to demonstrate the localisation of the GFP fluorescence (where present) within the HIEC cells (right panels). Images of live cells were taken on a Zeiss Axiovert 35 microscope, at 20x magnification. (Scale bar = 20µm).

3.3.2 SOCS3 mRNA was significantly reduced both in the presence and absence of serum in the SOCS3^{Low} cell line

After demonstrating that both SOCS3^{Ev} and SOCS3^{Low} HIEC lines were successfully transduced with their respective lentivirus constructs, we needed to confirm that baseline SOCS3 mRNA levels were indeed lower in SOCS3^{Low} cells than in SOCS3^{Ev} cells. To do this, we used qPCR to quantify SOCS3 mRNA produced in both transfected HIEC lines following serum recovery. Figure 3.5 (a) shows that in the SOCS3^{Ev} cell line, addition of serum led to an

increase in SOCS3 mRNA at all 5 time points, compared with t=0, although only the increases at 90 and 120 minutes were found to be statistically significant ($p < 0.05$).

Figure 3.5 (b) compares SOCS3 mRNA in SOCS3^{Low} cells with SOCS3^{Ev} cells, and shows that at five of the six time points, there was significantly less SOCS3 mRNA produced in SOCS3^{Low} cells ($p < 0.05$), confirming that the transfection and knockdown of SOCS3 in these cells was successful. When both cell lines were synchronised at t=0 in the absence of serum, SOCS3^{Low} cells showed a 0.4 average fold-change in SOCS3 mRNA, compared with 1 in SOCS3^{Ev}, indicating that a 60% knockdown of SOCS3 had been achieved in (serum-starved) SOCS3^{Low} cells. However, when analysed using a two-tailed t-test, the difference in SOCS3 mRNA in SOCS3^{Ev} and SOCS3^{Low} (serum-starved) cells did not quite reach significance ($p = 0.07$). The percentage knockdown of SOCS3 was also calculated for the remaining time points, and overall, there was approximately a 53±4% reduction in SOCS3 mRNA in SOCS3^{Low} cells when compared to SOCS3^{Ev}.

In conclusion, both figures 3.4 and 3.5 show that we were able to successfully transfect HIEC cells in order to produce a normal HIEC cell line with reduced SOCS3, along with a suitable transfected control HIEC cell line. We also found that there were still fluctuations in SOCS3 mRNA levels over the duration of the time course following transduction.

a)

b)
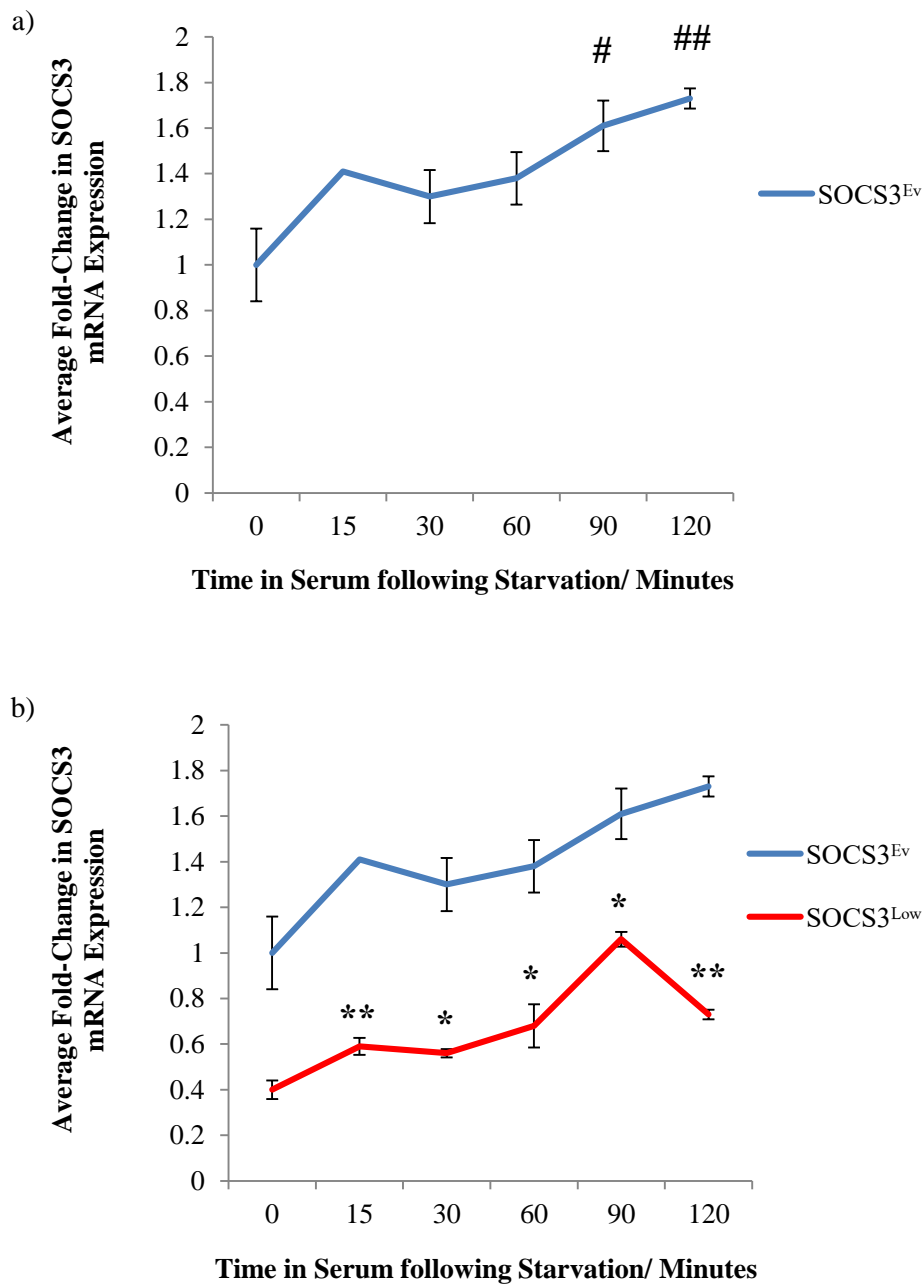
Figure 3.5: SOCS3 mRNA expression levels following serum recovery (±SEM) in (a) SOCS3^{Ev} control HIEC cells, and in (b) both SOCS3^{Ev} control cells and SOCS3^{Low} knockdown HIEC cells. Cells were seeded at 1 x 10^6/well and allowed to adhere, before serum starvation overnight. Cells were treated with serum-containing media for the times stated before lysis with TRI-Reagent® for RNA extraction. Expression levels of SOCS3 mRNA were measured using qPCR, and calculated using the 2$^{(-\Delta\Delta Ct)}$ method, with values relative to the SOCS3^{Ev} t=0 average ratio. (# = p<0.05, ## = p<0.01 using a one-way ANOVA with control Dunnett's post-hoc test vs. SOCS3^{Ev} t=0. * = p<0.05, ** = p<0.01, using a Student's t-test vs. SOCS3^{Low} at each time point) (n= 4).

3.3.3 SOCS3 protein expression was consistently reduced following serum recovery in the SOCS3^{Low} knockdown cells

Following confirmation of the SOCS3 knockdown in HIEC cells using qPCR, we analysed protein levels of SOCS3. The time course was extended to 4 hours, rather than 2, as protein translation takes longer than mRNA transcription. As observed previously, serum recovery did not result in increases in SOCS3 protein in SOCS3^{Ev} cells (figure 3.6a), indicating that translation was not affected following lentiviral transduction. However, as seen in untransduced HIEC cells (figure 3.2a) and also in SOCS3^{Ev} cells at the mRNA level (figure 3.5a), SOCS3 continued to fluctuate at the protein level in SOCS3^{Ev} HIECs (figure 3.6a).

As seen with mRNA, figure 3.6 (b) shows that in the absence and presence of serum, SOCS3^{Low} cells produced lower amounts of SOCS3 protein at all time points, compared to SOCS3^{Ev}. The lower levels of SOCS3 protein in SOCS3^{Low} cells were found to be statistically significant at t=0 and 180 minutes (p=0.001 and p=0.007, respectively). As seen in figure 3.5 (b), both cell lines had fluctuating levels of SOCS3 protein, although they exhibited different patterns of oscillation (figure 3.7), due to the increase in SOCS3 protein in SOCS3^{Low} at t=60 minutes, compared with a decrease in SOCS3^{Ev}. As with SOCS3 mRNA expression in the transduced HIECs, the percentage reduction in SOCS3 protein was calculated for each time point of the serum recovery time course, and overall, there was approximately a 52±10% reduction in SOCS3 protein in SOCS3^{Low} HIECs, relative to SOCS3^{Ev}. Despite the slight increase in variability calculated for SOCS3 protein levels, the reduction does fall within the range of percentage of reduced mRNA, which indicates that overall, the transduction-induced knockdown in SOCS3 mRNA also translated to protein as well.

In conclusion, we found that SOCS3^{Low} cells produced lower amounts of SOCS3 protein when compared to SOCS3^{Ev} cells, thus confirming knockdown of SOCS3 in SOCS3^{Low} at both the mRNA and protein levels. We also calculated that the percentage reductions in SOCS3 mRNA and protein expression in SOCS3^{Low} cells were very similar, with 53±4% and 52±10%, respectively. Therefore, as these cells were confirmed as physiologically responsive and we were able to knockdown our protein of interest, SOCS3, we deemed these transduced cells were suitable for use in further experiments.
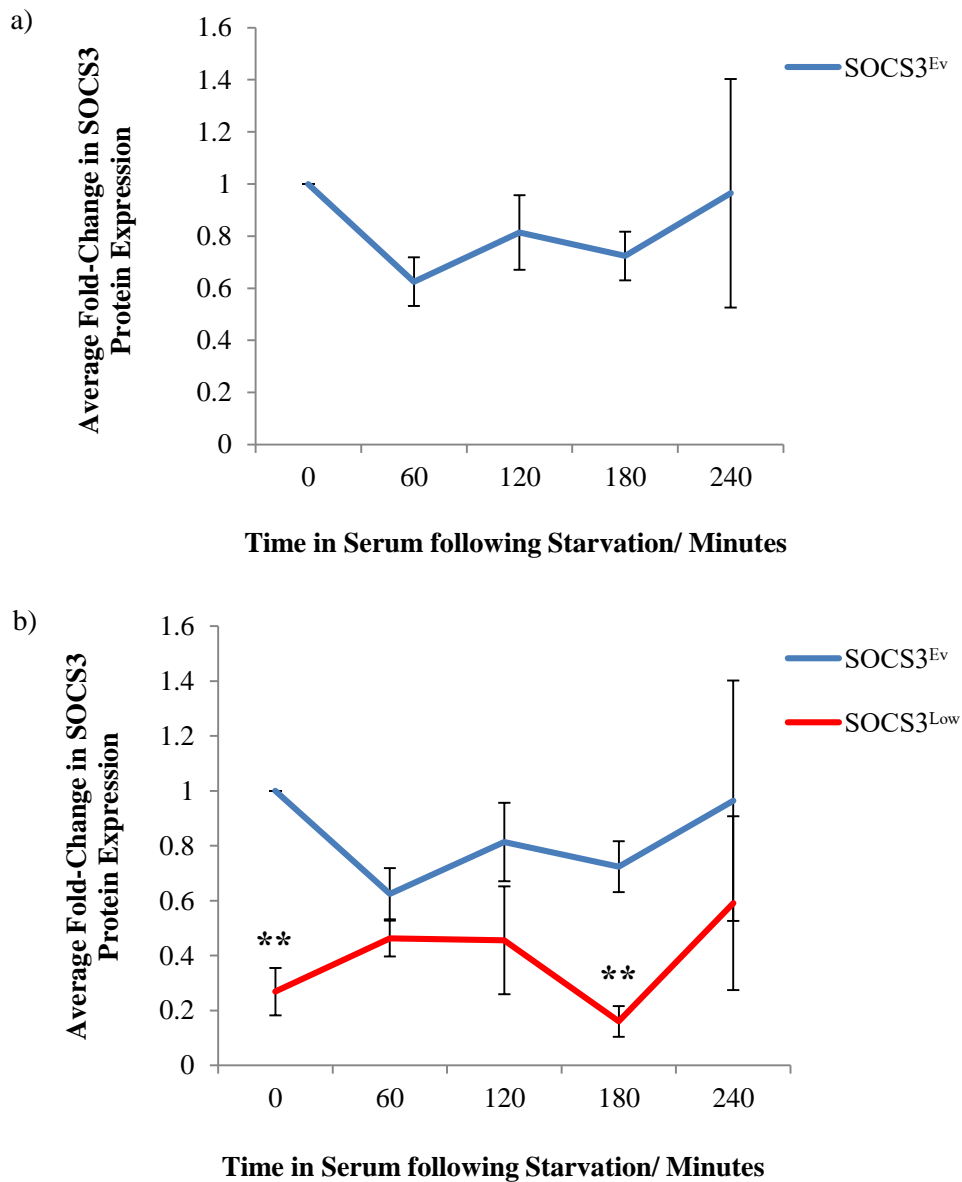
Figure 3.6: SOCS3 protein expression following serum recovery (±SEM) in (a) SOCS3^Ev control cells and (b) compared with SOCS3^Low knockdown HIEC cells. Cells were seeded at 2.5×10^5/well and allowed to adhere before serum starvation overnight. Cells were treated with serum-containing media for the times stated before lysis with RIPA buffer. Samples were run on 10% SDS-PAGE gels before transfer onto nitrocellulose membranes and incubated in a SOCS3 primary antibody at 1:1000 overnight. Membranes were then incubated in secondary antibody for 1 hour at room temperature. Membrane imaging and densitometry was carried out using a ChemiDoc™ MP Imaging System and Image lab software, with values relative to SOCS3^Ev t=0. (** = $p<0.01$ vs. SOCS3^Low using a two-tailed t-test) (n= 3).
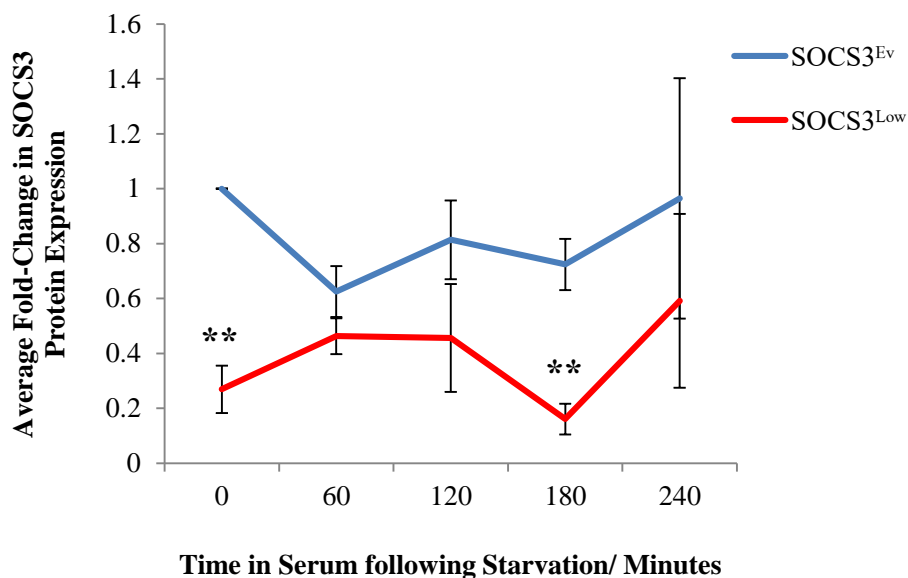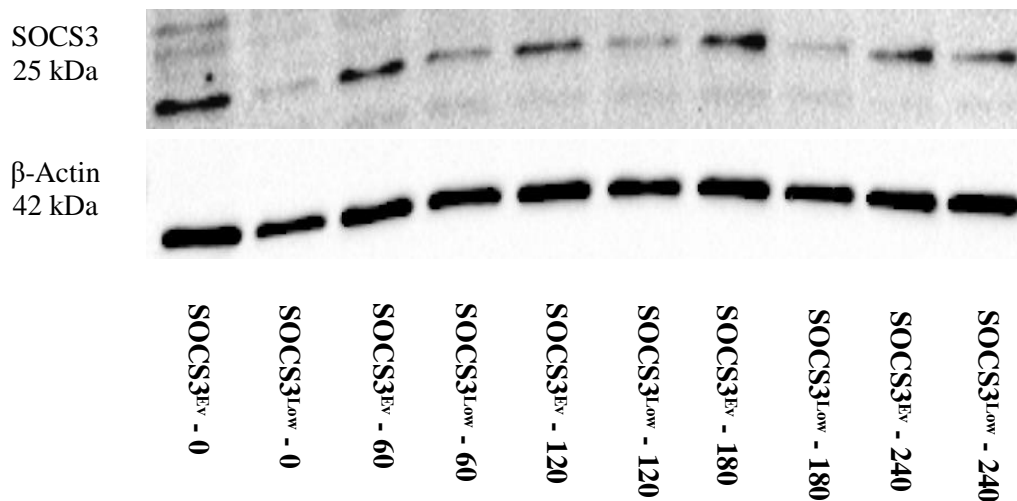
Figure 3.7: Cycling of SOCS3 protein following serum recovery (±SEM) in SOCS3^{Ev} control cells and SOCS3^{Low} knockdown HIEC cells. Following serum recovery, cells were lysed, ran on 10% SDS-PAGE gels, and transferred onto nitrocellulose membranes before incubation overnight in 1:1000 SOCS3 primary antibody. Membranes were then incubated in secondary antibody for 1 hour at room temperature, and re-blotted for β-actin as a loading control. Membrane imaging and densitometry was carried out using a ChemiDoc™ MP Imaging System and Image lab software, with values relative to SOCS3^{Ev} t=0. (** = $p < 0.01$ vs. SOCS3^{Ev} using a two-tailed t-test) (n= 3).

3.4 Proliferation of HIEC vs. Caco-2 cells in response to microbial stimulation

As discussed previously, the Caco-2 cell line has been widely used, and is useful for many aspects of biomedical research. However, characterisation of the cell cycle, renewal and homeostasis cannot be completely translated to those of normal/untransformed systems, due to the cell line being transformed and originally derived from a colon adenocarcinoma, with cancer being a disease associated with increased cellular proliferation due to gain of mutations, or loss of regulation at cell cycle checkpoints. As well as cellular renewal and homeostasis being controlled from within the cell, for example through gene transcription and nuclear mitosis, intestinal homeostasis specifically is also controlled through the close proximity of commensal microbiota in the intestinal lumen. Interaction of different microbial components with cellular receptors, such as TLRs on IECs, is essential for intestinal homeostasis. For example, mice deficient in MyD88 (an adapter molecule within the TLR signalling pathway, Medzhitov et al. 1998) have dysregulated proliferation and differentiation of IECs compared with controls, as well as increased colonic bleeding and mortality following intestinal injury using DSS (along with $TLR2^{-/-}$ and $TLR4^{-/-}$, to a lesser extent). Additionally, wildtype mice depleted of their commensal microflora, failed to produce protective cytokines (such as IL-6 and TNF-α) following DSS administration. However, mice that were also given water containing either LPS or LTA were protected from the DSS-induced mortality seen in other animals (Rakoff-Nahoum et al. 2004). These are in addition to early findings that GF mice had lower intestinal proliferation rates as well as reduced crypt and mucosal depths, compared to CR animals (Abrams et al. 1962). Therefore, we aimed to assess the suitability of using the normal HIEC cell line as a model for intestinal proliferation, and to determine baseline and microbial-induced proliferation levels in comparison with those of Caco-2 cells. This was performed by treating both cell lines either with media only, or with media containing different TLR ligands at varying concentrations, for 24, 48 and 72 hours. Changes in proliferation were measured using the CyQuant cell proliferation assay. We hypothesised that the Caco-2 cells may have higher unstimulated, basal proliferation rates, but may be less responsive to TLR ligands as in an *in vivo* setting, it would be assumed this would involve activation of the immune system, which would be disadvantageous as cancer cells would want to remain undetected by the host.

Figure 3.8 shows the changes in (a) unstimulated and (b)-(j) microbially-stimulated proliferation rates of both HIEC and Caco-2 cells, after 24, 48 and 72 hours. With the exception of 0.1µg/ml LTA (figure 3.8j), fold-changes in proliferation between HIECs and Caco-2 cells were very similar 24 hours after either no treatment or treatment with TLR ligands. At 48 hours, both cell lines either exhibited no considerable changes in cell number, or decreases in cell number, indicative of a decrease in proliferation (with the exception of 0.1µg/ml FLA in Caco-2s, where there was a 1.4±0.1 fold increase, p=0.0002 vs. HIECs, figure 3.8b). Greater decreases were seen in HIEC cells, with significance found vs Caco-2 cells with 1µg/ml FLA (p=0.013), 0.01µg/ml LTA (p=0.024) and 0.1µg/ml LTA (p=0.026).

There were increases in cell number observed with all treatments at 72 hours signifying increases in proliferation, and these were seen in both HIECs and Caco-2 cells. However, the differences in proliferation from 48 to 72 hours were much greater in Caco-2 cells, with statistical significance found between both cell lines in all conditions at 72 hours (p<0.05). Collectively, these results suggest that cells could become susceptible by 48 hours due to decreases in cell number seen, corresponding to cell death. Any surviving cells would be more resilient and therefore keep proliferating, with the possibility of more space and nutrients being available due to a reduction in competing cells. This theory applies to both cell lines, but overall, Caco-2 cells were found to proliferate more than HIECs, not only following no treatment, but also following treatment with all concentrations of TLR ligands used, with their decreased SOCS3 (mRNA) expression levels a possible cause of this.

a)

No Tx

b)

FLA 0.1μg/ml

c)

FLA 1μg/ml

d)

LPS 0.1μg/ml

e)

LPS 1μg/ml
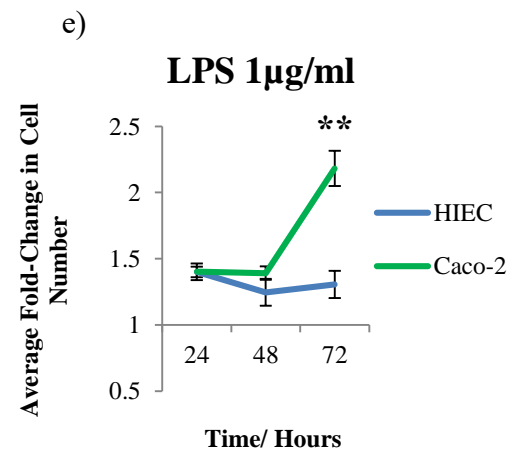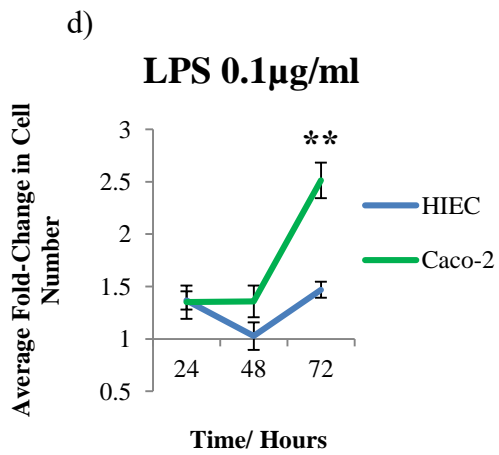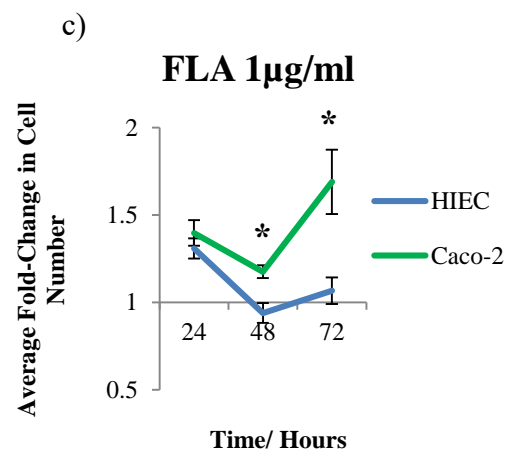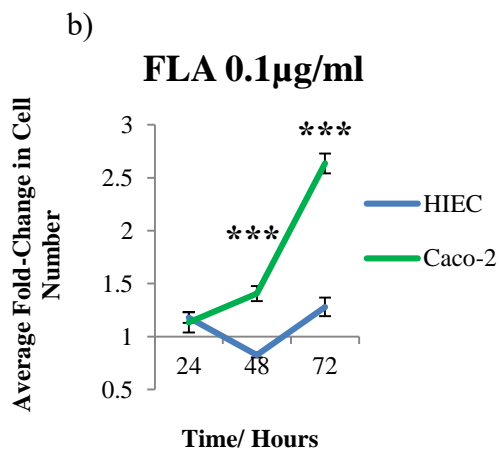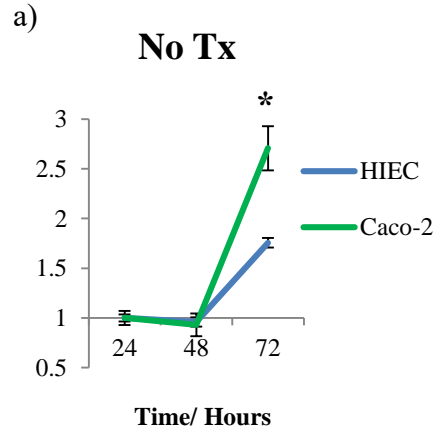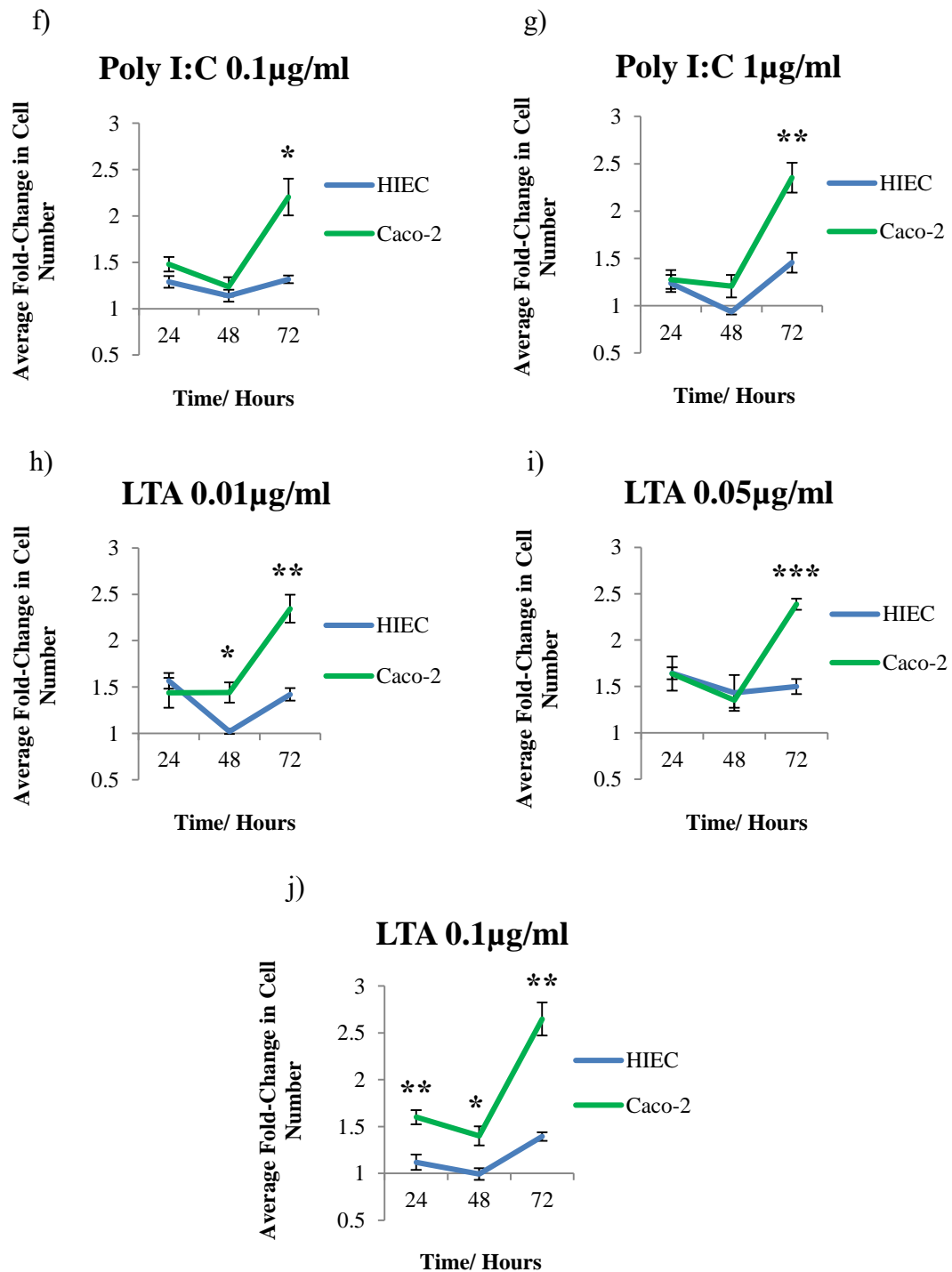
Figure 3.8: Differences in proliferation between a normal (HIEC, blue) and a transformed (Caco-2, green) intestinal epithelial cell line, both following no treatment (a-No Tx) and addition of TLR ligands (b-j) (±SEM). Cells were seeded at 2000/well in a 96-well plate and allowed to adhere, before serum starvation for 12 hours. Cells were treated with the stated TLR ligands for 24, 48 and 72 hours. Cell proliferation was measured using the CyQuant cell proliferation assay, with cell number changes relative to the No Tx 24 hour average within each cell line. (* = p<0.05, ** = p<0.01, *** = p<0.001, using a two-tailed t-test vs. HIEC cells at each time point) (n= 4).

3.4.2 SOCS3 limited microbe-mediated proliferation in HIEC cells

It has been previously shown that SOCS3 can be induced by TLR ligands along with various cytokines (although this was in peritoneal macrophages, Baetz et al. 2004), as well as by IL-10 (Ito et al. 1999), which is known to have anti-inflammatory effects and suppress gene transcription following signalling through TLRs (cited by Yoshimura et al. 2007). Frobøse et al. (2006) also found that SOCS3 is able to inhibit MAPK and NF-κB responses downstream of the TLRs, and this was through preventing the interaction between TNF-Receptor-Associated Factor 6 (TRAF6) and Transforming Growth Factor-β (TGF-β)-Activated Kinase (TAK1)- normally activated by MyD88 (Yoshimura et al. 2007) (although this was discovered in a human pancreatic β cell line and a human embryonic kidney cell line). Following *in vivo* experiments where SOCS3 was also found to limit IEC proliferation (Rigby et al. 2007), we aimed to further investigate how SOCS3 impacts on unstimulated and microbial-induced proliferation, using SOCS3^{Ev} and SOCS3^{Low} HIEC cells. As we showed that Caco-2 cells had lower SOCS3 expression levels and higher proliferation rates than the normal HIEC cell line, we aimed to determine whether knockdown of SOCS3 in the non-transformed cells would produce a cancer cell like-proliferative phenotype, thus replicating that seen in Caco-2 cells.

Figure 3.9 (a) shows the fold-change in cell number in SOCS3^{Ev} control HIECs, following treatment with different TLR ligands, with respect to no treatment (No Tx). Fold-increases in cell number were observed in all conditions, with the greatest increase seen with 0.02µg/ml LTA, although this was only 1.7±0.3 fold-higher than No Tx. There was also some variability, which can be seen by the large error bars. A one-way ANOVA (with control Dunnett's post-hoc test) revealed there were no significant differences between any of the treatment conditions and no treatment alone (p>0.05).

Figure 3.9 (b) shows the fold-changes in cell number in SOCS3^{Low} cells following stimulation with various TLR ligands, with fold-changes in cell number observed upon addition of each concentration of all 4 TLR ligands used, ranging between 1.3 (0.01µg/ml FLA) and 2.1 (0.2µg/ml LTA). When compared to SOCS3^{Low} No Tx, fold-changes in cell number were significantly higher with 7 out of the 11 treatments (p<0.05-p<0.0001), in particular, at the 2 highest concentrations of LPS, and all concentrations used of Poly I:C and LTA.

Figure 3.9 (c) shows the fold-changes in cell number in both SOCS3^{Ev} and SOCS3^{Low} cells following stimulation with various TLR ligands. Following No Tx, there were increases in cell number in SOCS3^{Low} compared with SOCS3^{Ev} (data not shown), although unfortunately, this was not quite significant (p=0.06, using a Student's t-test). Upon addition of all 4 TLR ligands used, there were higher increases in cell number in SOCS3^{Low} than those seen in SOCS3^{Ev}- fold-increases in cell number ranged from approximately 1.3-2.1 and 1.2-1.7% respectively, although the highest and lowest fold-changes were obtained with the same ligands in both cell lines (LTA and FLA, respectively). Despite these observations, no statistical significance was found between SOCS3^{Ev} and SOCS3^{Low} at each treatment (using a two-tailed t-test). In summary, these results suggest that following knockdown of SOCS3, cells become more responsive in terms of proliferation following microbial challenge. More specifically, SOCS3 appears to be responsible for regulating TLR2, 3 and 4-mediated proliferative responses.

It appears that knockdown of SOCS3 induced a microbe-mediated proliferation profile similar to that of Caco-2 cells, so to verify this, we compared the fold-changes in cell number of Caco-2 and SOCS3^{Low} cells, following stimulation with multiple TLR ligands for 48 hours. Although there are small, visible differences in cell number between cell lines for each ligand, only addition of 1µg/ml Poly I:C led to significant differences, with increased cell numbers found in SOCS3^{Low} cells compared with Caco-2 cells (p=0.029, figure 3.9d). These results confirmed that knockdown of SOCS3 in untransformed HIEC cells altered the microbial-induced proliferative responses and induced a proliferative phenotype comparable to that of Caco-2 adenocarcinoma cells. Subsequently, we then determined the percentage reduction of both SOCS3 mRNA and protein in Caco-2 and SOCS3^{Low} cells to ascertain if the similarities in proliferation profiles were associated with comparable SOCS3 expression levels. On average, SOCS3 mRNA levels were reduced by similar amounts in SOCS3^{Low} cells compared with Caco-2s (as shown in figure 3.10a), with percentage reductions calculated as 68±5% and 62±9%, respectively (shown in figure 3.10c), and as expected, any variances between the two cell lines were not statistically significant (p>0.05, using a two-tailed Student's t-test). However, as figures 3.2 (b) and 3.10 (b) demonstrate, the low expression levels of SOCS3 mRNA in Caco-2 cells were not observed at the protein level, although SOCS3^{Low} cells continued to exhibit low SOCS3 expression, compared to both Caco-2 and SOCS3-sufficient HIEC cells. Relative to SOCS3-sufficient HIECs, SOCS3^{Low} cells exhibited an overall reduction in SOCS3 protein of approximately 71±12%, unlike Caco-2 cells who displayed an overall reduction of approximately 28±9% (shown in figure 3.10c). This time however, the differences observed between these two cell lines did reach statistical significance, with a p-

value of p=0.02 generated (using a Student's two-tailed t-test). Therefore, although results for SOCS3 protein in Caco-2 cells were unexpected, possibly reflecting differentially regulated protein translation mechanisms, SOCS3 mRNA levels and microbial-mediated changes in cell number were very similar between Caco-2 and SOCS3^{Low} cells, providing a link between the two cell lines.

a)

b)

c)

d)
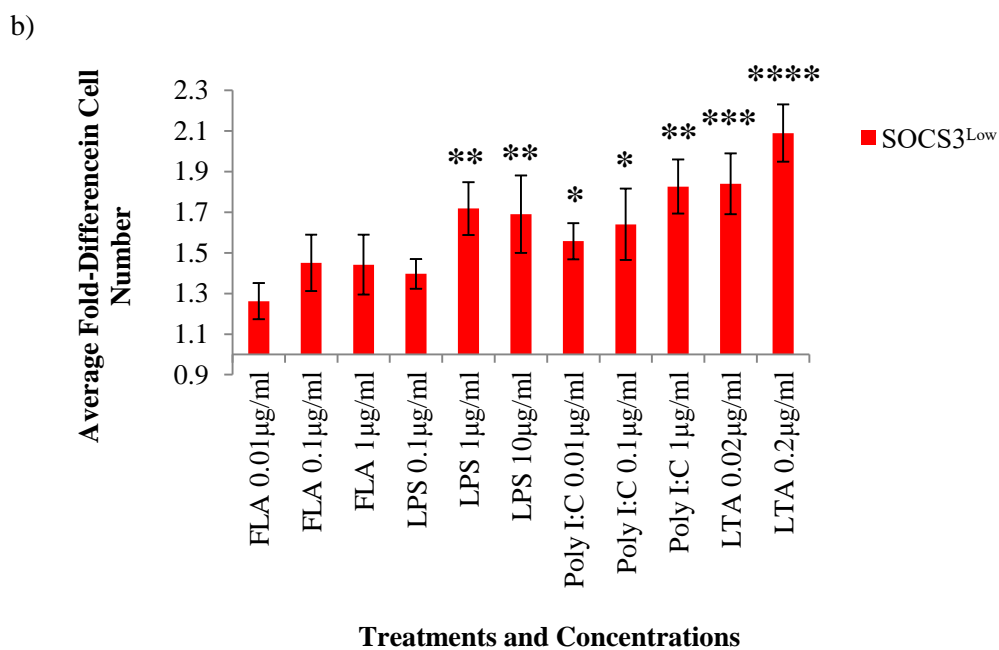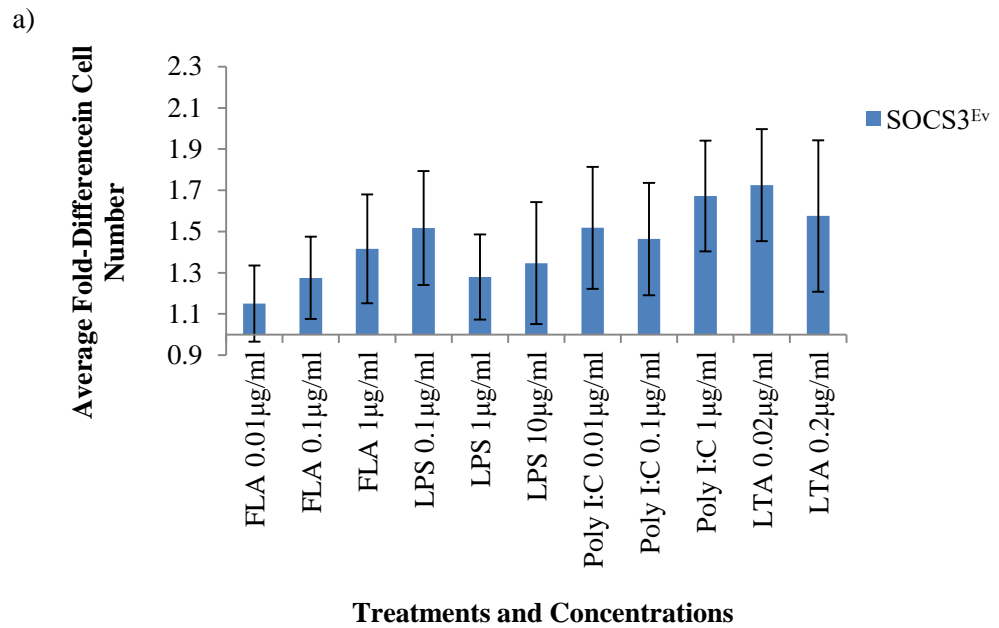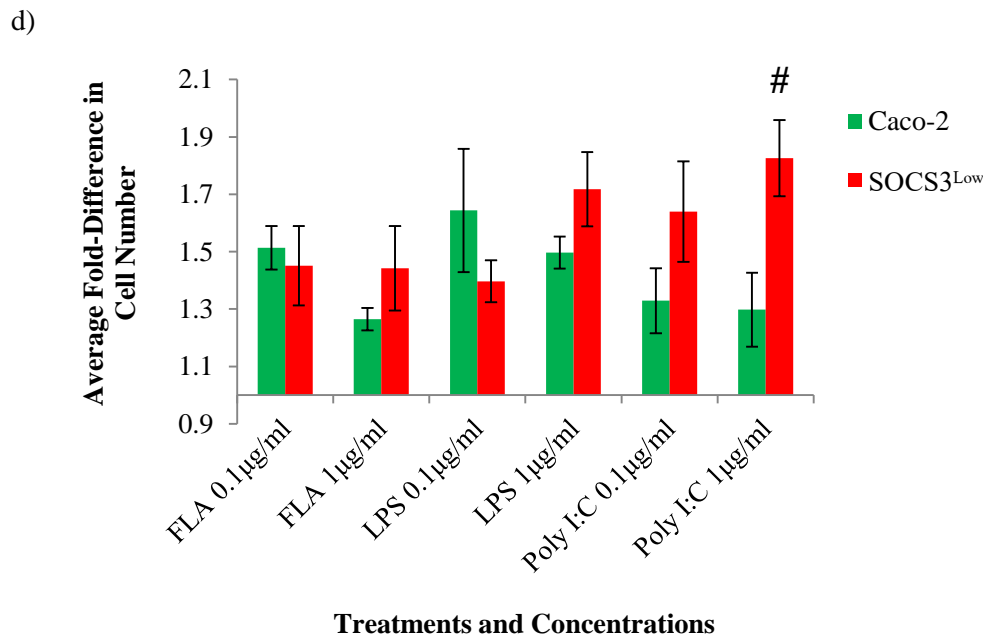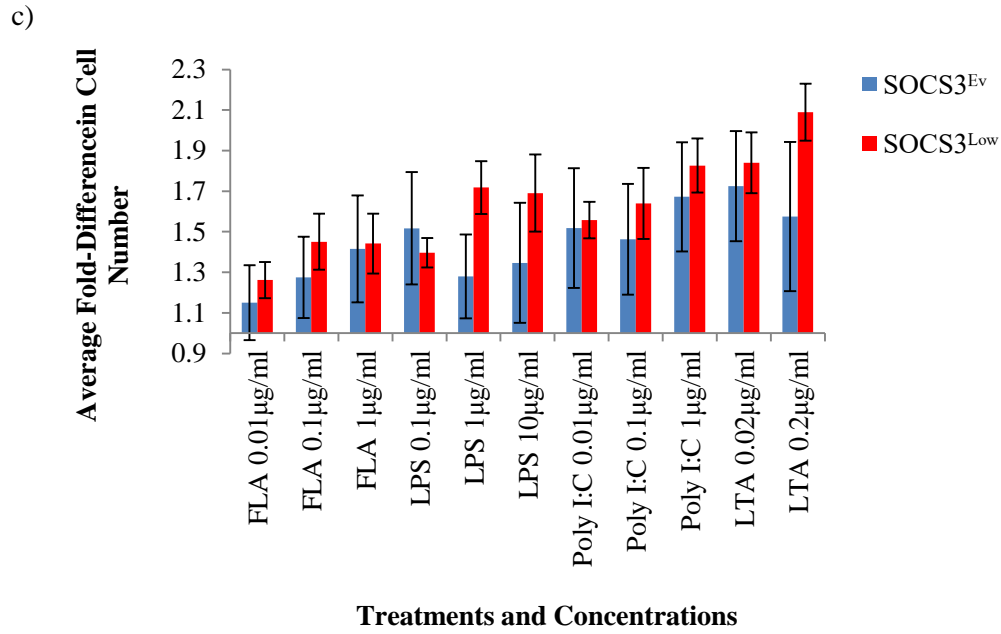
Figure 3.9: The effects of TLR ligands on proliferation (±SEM) in (a) SOCS3^Ev control cells, (b) SOCS3^Low knockdown HIEC cells, (c) both SOCS3^Ev and SOCS3^Low HIEC cell lines, and (d) Caco-2 and SOCS3^Low HIEC cells. Cells were seeded at 2000/well in a 96-well plate and allowed to adhere for 24 hours, before serum starvation for 12 hours. Cells were treated with the stated TLR ligands at varying concentrations for 48 hours. Cell proliferation was measured using the CyQuant cell proliferation assay, with fold changes relative to the No Tx average within each cell line. (* = $p<0.05$, ** = $p<0.01$, *** = $p<0.001$, **** = $p<0.0001$, using a one-way ANOVA with control Dunnett's post-hoc test vs. SOCS3^Low No Tx. # = $p<0.05$, using a Student's t-test vs. Caco-2). (n= 4).

a)

b)

—— HIEC ——Caco-2 ——SOCS3^{Low}

c)
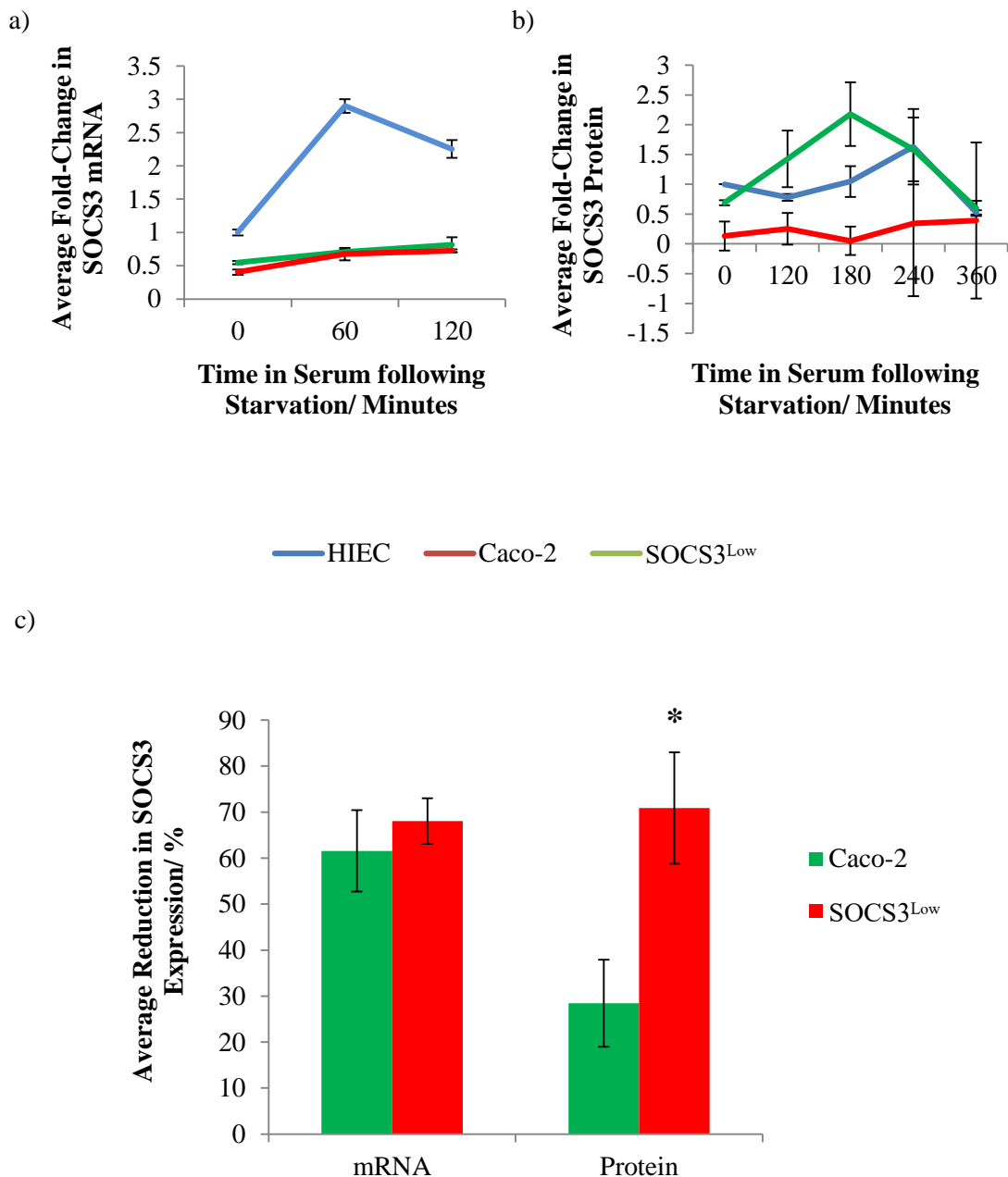
Figure 3.10: Differences in expression of (a) SOCS3 mRNA and (b) SOCS3 protein over time, and (c) overall percentage reduction in SOCS3, in normal, untransduced HIEC cells (blue), Caco-2 cells (green) and SOCS3^{Low} HIEC cells (red) (±SEM). (a) SOCS3 mRNA levels were measured using qPCR and calculated using the $2^{(-\Delta\Delta Ct)}$ method. (n= 4). (b) For assessment of SOCS3 protein, cell lysates were run on an SDS-PAGE gel and incubated in a SOCS3 primary antibody overnight. Membrane imaging and densitometry was carried out using a ChemiDoc™ MP Imaging System and Image lab software. (n=3). (c) * = p<0.05, using a two-tailed Student's t-test vs. Caco-2.

3.5 The impact of SOCS3 on IEC microbial-induced cytokine responses

Jak/Stat signalling can be activated by a range of stimuli (such as IFNs, IL-6, TNF-α, LPS), which if not regulated efficiently by SOCS proteins (for instance, as well as other Jak/Stat inhibitors, such as PIAS), could lead to excess inflammation (reviewed by Akhtar and Benveniste 2011). Activation of TLR signalling (in some cases by the same ligand, e.g. LPS) results in the transcription of various pro- and anti-inflammatory genes by the transcription factor, NF-κB, with the genes transcribed often dependent on the TLR involved, and also the site of the TLR expression (reviewed by Zhang and Schluesener 2006). Pro-inflammatory cytokines, such as TNF-α in particular, are produced to induce inflammation in order to elicit an effective immune response against a particular challenge (through TLR signalling for instance) within the body. In addition to immune responses, production of pro-inflammatory cytokines, such as TNF-α and IL-6, can initiate cell proliferation, alterations in the extracellular matrix and angiogenesis (reviewed by Zhang and Schluesener 2006); all processes also exhibited by cancer cells. Therefore, sustained/dysregulated increases in these cytokines may promote carcinogenesis, especially in already mutated cells. For instance, with respect to Jak/Stat, IL-6 is able to induce proliferation through activation of Jak/Stat signalling, both *in vitro* and *in vivo* (Starr et al. 1997). However, many cancers are associated with decreased SOCS3, and therefore increased Stat3 activity, so IL-6 is able to drive Stat3-mediated proliferation in cells with diminished negative feedback. This is also supported by findings that addition of hyper-IL-6 in IECs led to increases in both tumour size and number, respectively. Based on findings of IEC IL-6$^{-/-}$ vs. wildtype mice, IL-6 was also found to promote intestinal cell survival, through decreased numbers of apoptotic cells, increased expression of anti-apoptotic proteins and enhanced proliferation through increased expression proliferating cell nuclear antigen (PCNA) as well (Grivennikov et al. 2009).

Anti-inflammatory cytokines, such as IL-10 for instance, are capable of preventing the production and activity of both pro-inflammatory cytokines and chemokines, and nitric oxide. IL-10 in particular, can also inhibit antigen presentation which can prevent T-cell-induced responses, in addition to promotion of immune cells that can exert anti-tumour effects (reviewed by Meager and Wadhwa 2013). However, it is important that production of both classes of cytokines are efficiently regulated as insufficient expression of pro-inflammatory cytokines and/or overexpression of anti-inflammatory cytokines may result in pathogens evading the immune system and causing damage and disease. Additionally, increases in IL-10 have been found in many tumours, with expression levels positively correlated with disease severity and poor prognosis (Mocellin et al. 2005, Itakura et al. 2011, Wang et al. 2011, Oft

2014). High levels of IL-10 during cancer will prevent inflammatory responses but in turn, induce tumour tolerance, along with possible enhanced cellular proliferation, as examples of downstream targets of IL-10 are Stat1 and Stat3 (Mocellin et al. 2005, Oft 2014). On the other hand, over-production of pro-inflammatory cytokines and/or insufficient production of anti-inflammatory cytokines, can eventually lead to autoimmune diseases, such as rheumatoid arthritis and IBD. For example, CR, IL-10 knockout mice spontaneously develop colitis (which has resulted in these mice being used a model to further investigate IBD *in vivo*) (Kühn et al. 1993). However GF, IL-10 knockout mice do not go on to develop colitis (Sellon et al. 1998), demonstrating the crucial function of IL-10 and how sufficient levels are needed in order to prevent immune activation against commensal bacteria. CR IL-10$^{-/-}$ mice are also susceptible to developing G.I tumours (Berg et al. 1996), with one presumed mechanism being the inability to limit inflammation-mediated proliferation.

As previous experiments, cited by Yoshimura et al. (2007) and those shown here, have found that SOCS3 is able to inhibit NF-κB signalling, and limit proliferation induced upon interaction of microbial ligands with multiple TLRs, respectively, we used HIEC cells to first characterise their anti-inflammatory response (through production of the cytokine, IL-10) both in untreated, and TLR ligand-treated conditions, and also in SOCS3^{Low} cells to investigate how SOCS3 mediates this response. Using donor neutrophils, Cassatella et al. (1999) demonstrated that IL-10 is capable of inducing expression of SOCS3, independent of both Stat1 and Stat3 activity. As IL-10 can be produced following activation of TLR pathways, and SOCS3 can inhibit microbe-mediated Jak/Stat- and NF-κB-induced proliferation, it may be assumed that knockdown of SOCS3 may lead to increased IL-10, due to a reduction in negative feedback mechanisms.

Recent findings showed that SOCS3 is essential for regulation of microbial induced-TNF-α as overexpression in Caco-2 cells led to an increase following stimulation with FLA in a dose-dependent manner, and this was due to downregulation of TNFR2 (Thagia et al. 2015), which has more implications in IBD, as increases of TNF-α and SOCS3 separately are well publicised (reviewed by Rogler and Andus 1998, Suzuki et al. 2001). Therefore, we used HIEC cells to characterise TNF-α responses in normal intestinal cells and also to investigate whether SOCS3 is implicated in microbial-induced pro-inflammatory cytokine production, and whether there would be a dampened response, with knockdown of SOCS3 leading to decreased TNF-α- the converse of findings published by Thagia et al. (2015).

3.5.1 Knockdown of SOCS3 led to a decrease in the expression of the anti-inflammatory cytokine, IL-10, at the basal level and following TLR ligand stimulation

Figure 3.11 (a) shows the quantification of IL-10 mRNA levels in SOCS3^{Ev} cells following either no treatment, or stimulation with FLA, LPS or Poly I:C, and shows that when normalised to no treatment, there was little difference in IL-10 mRNA expression following addition of LPS. After treatment with Poly I:C and FLA, there were 1.5±0.2 - and 1.7±0.4 - fold increases, respectively, although neither of these were found to be statistically significant when analysed using a one-way ANOVA ($p > 0.05$).

Figure 3.11 (b) displays IL-10 mRNA levels of SOCS3^{Low} cells compared with SOCS3^{Ev}, and shows that following both no treatment and stimulation with TLR ligands, IL-10 mRNA expression was significantly reduced, with approximately 0.4-0.6 –fold increases compared to SOCS3^{Ev} no treatment. A Student's t-test produced p-values of $p < 0.05$ and $p < 0.001$ when SOCS3^{Low} FLA, and SOCS3^{Low} No Tx, LPS and Poly I:C respectively, were compared to the equivalent treatments in SOCS3^{Ev}. Additionally, although IL-10 mRNA levels were all relatively similar in SOCS3^{Low} cells, stimulation with FLA did lead to a significant increase in IL-10 mRNA ($p = 0.0239$) when compared to No Tx, and this mirrors the results observed in figure 3.11 (a).

In conclusion, knockdown of SOCS3 was found to lead to decreased IL-10 mRNA expression, both in unstimulated cells and following treatment with multiple TLR ligands, suggesting a possible regulatory role of SOCS3 regarding the production/release of IL-10.

a)

b)

Figure 3.11: Quantification of IL-10 mRNA levels (±SEM) in (a) SOCS3^{Ev} control HIEC cells, and in (b) both SOCS3^{Ev} control cells and SOCS3^{Low} knockdown HIEC cells, at the basal level and following treatment with various TLR ligands. Cells were seeded at 5 x 10^5/well in a 12-well plate, and allowed to adhere, before serum starvation overnight. Cells were treated as stated for 2 hours, before lysis with TRI-Reagent® for RNA extraction. IL-10 mRNA levels were measured using qPCR, and calculated using the 2$^{(-\Delta\Delta Ct)}$ method, with values relative to the SOCS3^{Ev} No Tx average ratio. (* = p<0.05, ** = p<0.01, *** = p<0.001 using a two-tailed t-test vs. SOCS3^{Ev}. # = p<0.05 using a one-way ANOVA with control Dunnett's post-hoc test vs. SOCS3^{Low} No Tx) (n=6).

Following stimulation with multiple ligands of the TLR pathway, the amount of TNF-α mRNA produced in response increased in SOCS3^{Ev} cells, when compared to no treatment (figure 3.12a). LPS and Poly I:C led to 2.7±0.3- and 1.4±0.3-fold increases respectively, although these were not found to be statistically significant when data was analysed using a one-way ANOVA (p>0.05). Treatment with FLA however, substantially increased TNF-α mRNA 21.1±6.8-fold, resulting in a p-value of p=0.002. These findings indicate that multiple activators of the TLR pathway are capable of inducing TNF-α in HIEC cells, with FLA being the most potent inducer.

Figure 3.12 (b) demonstrates the effect knockdown of SOCS3 had on unstimulated and microbial-induced TNF-α by comparing SOCS3^{Low} to SOCS3^{Ev} cells, and shows that even following no treatment, SOCS3^{Low} cells had higher TNF-α mRNA expression levels (p=0.009). As seen in figure 3.12 (a), addition of LPS, and Poly I:C in SOCS3^{Low} cells, also increased TNF-α mRNA (compared to No Tx), although in these cells, there was only a significant increase when Poly I:C was compared to its SOCS3^{Ev} counterpart (p=0.006). Conversely, after treating with FLA, there was an increase in TNF-α expression when compared to both SOCS3^{Ev} and SOCS3^{Low} No Tx (p=0.0034 vs. SOCS3^{Low} No Tx), but when compared to SOCS3^{Ev} FLA, it had reduced from 21.1±6.8- to a 9.8±2.9-fold increase. Due to the variability within each cell line, no statistical significance was found when using a Student's t-test (p>0.05). Collectively, the results in figure 3.12 indicate that out of the three TLR ligands used in HIEC cells, the most prevalent inducer of TNF-α was FLA, activating the TLR pathway through interaction with TLR5. Figure 3.12 (b) suggests that in the absence of stimulation, and upon recognition of Poly I:C, SOCS3 is responsible for limiting TNF-α. Therefore, it appears from both the proliferative and cytokine profiles that reduction of SOCS3 in HIEC cells is more representative of SOCS3 levels seen in Caco-2 cells, thereby potentially promoting a cancer-like phenotype in HIECs.
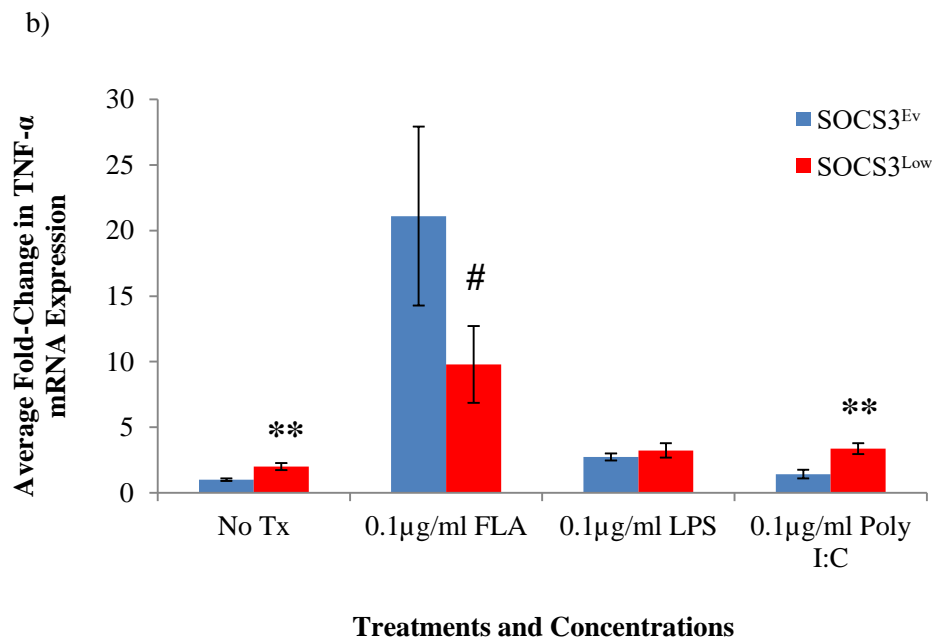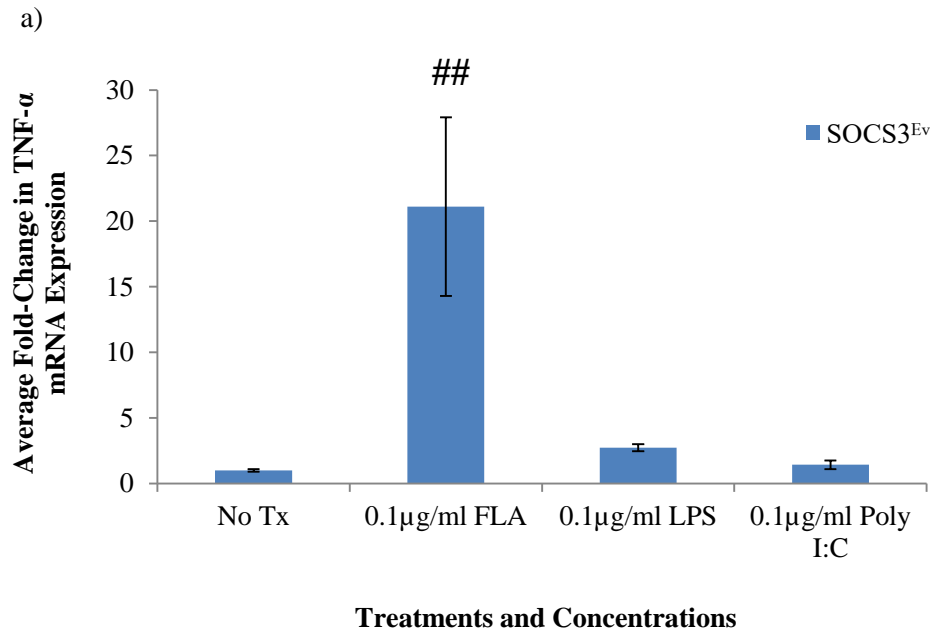
Figure 3.12: Quantification of TNF-α mRNA levels (±SEM) in (a) SOCS3^{Ev} control HIEC cells, and in (b) both SOCS3^{Ev} control cells and SOCS3^{Low} knockdown HIEC cells, at the basal level and following treatment with various TLR ligands. Cells were seeded at 5 x 10^5/well, and allowed to adhere for 24 hours, before serum starvation overnight. Cells were treated as stated for 2 hours, before lysis with TRI-Reagent® for RNA extraction. TNF-α mRNA levels were measured using qPCR, and calculated using the 2$^{(-\Delta\Delta Ct)}$ method, with values relative to the SOCS3^{Ev} No Tx average ratio. (** = p<0.01, using a two-tailed t-test vs. SOCS3^{Ev}. # = p<0.05, ## = p<0.01 using a one-way ANOVA with control Dunnett's post-hoc test vs. a) SOCS3^{Ev} No Tx, and b) SOCS3^{Low} No Tx). (n=6).

3.6 Potential relevance of SOCS3 in mediating cancer and tolerance mechanisms

Our findings, as well as in the literature (Hamilton et al. 2011, Thagia et al. 2015), demonstrate a role for SOCS3 in the regulation of cytokine expression. SOCS3 and regulation of TNF-α may be implicated in cancer and IBD- SOCS3 is found to be increased in IBD, and this is linked with increased TNF-α and, decreased TNFR2 expression and wound healing in response to microbial challenge (Thagia et al. 2015). Conversely, SOCS3 is decreased in several cancer types, resulting in an inability to limit proliferation as well as increases in Stat3-mediated expression of TNFR2 (Hamilton et al. 2011). TNF-α is also known to promote angiogenesis, and proliferation in both untransformed and tumour cells (Balkwill et al. 2002, Zhang and Schluesener 2006), suggesting that TNF-α promotes a pro-tumourigenic environment. Moore et al. (1999) found that mice that were deficient in TNF-α become resistant to skin carcinogenesis. Cancer and IBD are both diseases associated with immune tolerance. In cancer, mutated cells exhibit increased, uncontrolled proliferation, and tolerance of the host towards the tumour cells allows evasion of the immune system. Conversely in IBD, there appears to be a breakdown in tolerance mechanisms, with the immune system eliciting inappropriate responses against commensal microflora, coupled with dysregulated intestinal homeostasis due to an inability to repair damaged IECs sufficiently. In addition to SOCS3 and TNF-α, another protein implicated in immune tolerance, including cancer and IBD, is indoleamine 2,3-dioxygenase (IDO). IDO is an enzyme involved in the catabolism of the essential amino acid, tryptophan (Higuchi and Hayaishi 1967), and has found to be crucial in tolerance, indeed IDO inhibition leads to foetal rejection in mice (Munn et al. 1998). Increased IDO is also a common feature in IBD (Wolf et al. 2004), and in many cancers, including those in the GI tract (Uyttenhove et al. 2003), with IDO able to exert anti-proliferative effects on nearby T-cells through tryptophan depletion and the increase in tryptophan catabolites that ensues (Fallarino et al. 2002, Frumento et al. 2002), thereby dampening down the immune system towards tumour cells.

Many cancer types are associated with increases in IDO and concomitant decreases in SOCS3, so it could be hypothesised that the two processes may be connected. We used our HIEC model to investigate whether a relationship exists between SOCS3 and IDO, and determine whether this is a potential mechanism in promoting tumourigenesis. IDO mRNA expression was investigated using qPCR in both SOCS3[Ev] and SOCS3[Low] cells in response to microbial ligands. IFN-γ and excretory/secretory (E/S) antigens were used (along with FLA), as IDO has been shown to be induced by IFN in both mice (Yoshida et al. 1981) and humans (Yasui et al. 1986, Ozaki et al. 1987) and also by *T. muris* infection (Bell and Else 2011). *T. muris* is

the murine equivalent of *Trichuris trichiura* whipworm infection in humans, with E/S being one of the antigens of the *T. muris* whipworm, which induces an immune response in mice (Else and Wakelin 1989).

3.6.1 Knockdown of SOCS3 enhanced IFN-γ -induced IDO mRNA expression

Figure 3.13 (a) shows differences in IDO mRNA levels following treatment with FLA, IFN-γ and E/S in SOCS3^{Ev} cells (relative to SOCS3^{Ev} No Tx). There were slight fold-increases in IDO mRNA following addition of FLA and E/S (1.5±0.6 and 2.9±1.5, respectively), although they were minimal compared with No Tx, and due to variability and overlapping error bars, these increases were not statistically significant (p>0.05). Upon treatment with IFN-γ however, there was a 10.8±3.2-fold increase of IDO, supporting previous findings that IFN-γ is a potent inducer of IDO, and showing that IDO can be induced by IFN-γ in an untransformed HIEC cell line. Relative to SOCS3^{Ev} No Tx, this IFN-γ -induced IDO expression was found to be statistically significant (p=0.0054).

Figure 3.13 (b) shows that in SOCS3^{Low} cells, there were 2.5±0.4- and 4.4±0.7-fold increases in IDO following No Tx and addition of FLA, respectively, and these increases were also significantly higher when compared to their SOCS3^{Ev} counterparts (p=0.03 and p=0.01, respectively). As in SOCS3^{Ev} cells, treatment with IFN-γ led to production of IDO in SOCS3^{Low} cells, although when compared with SOCS3^{Ev} No Tx, there was a 65.7±19.8-fold increase. Compared with SOCS3^{Ev} IFN-γ, knockdown of SOCS3 enhanced IDO mRNA expression by 6-fold (p=0.02), suggesting SOCS3 is involved in limiting IFN-γ -induced IDO. Finally, treatment with the *T. muris* antigen, E/S did lead to an 8±4.3 fold-increase in IDO in SOCS3^{Low}, which is higher than the fold-changes seen in SOCS3^{Low} No Tx and SOCS3^{Ev} E/S, although significance was not found when compared with either of these. This is possibly due to the variability of IDO expression exhibited by SOCS3^{Low} following E/S treatment, as indicated by the large error bar.

To summarise, IFN-γ was capable of inducing IDO in HIEC cells, both in control cells and following knockdown of SOCS3, in line with induction of IDO by IFN-γ in other tissues and systems. The increases in IDO in SOCS3^{Low} cells indicates that SOCS3 may play a role in limiting production of IDO, at least in the intestine, both at an unstimulated, "healthy/normal" state, and following interaction with various microbial ligands, in particular IFN-γ.

Additionally, the higher IDO mRNA levels in the cancer-like SOCS3^{Low} cells (compared with SOCS3^{Ev}) also supports previous findings of increased IDO in a multitude of cancer types, which contributes to tolerance of the host's immune system towards the cancerous cells.
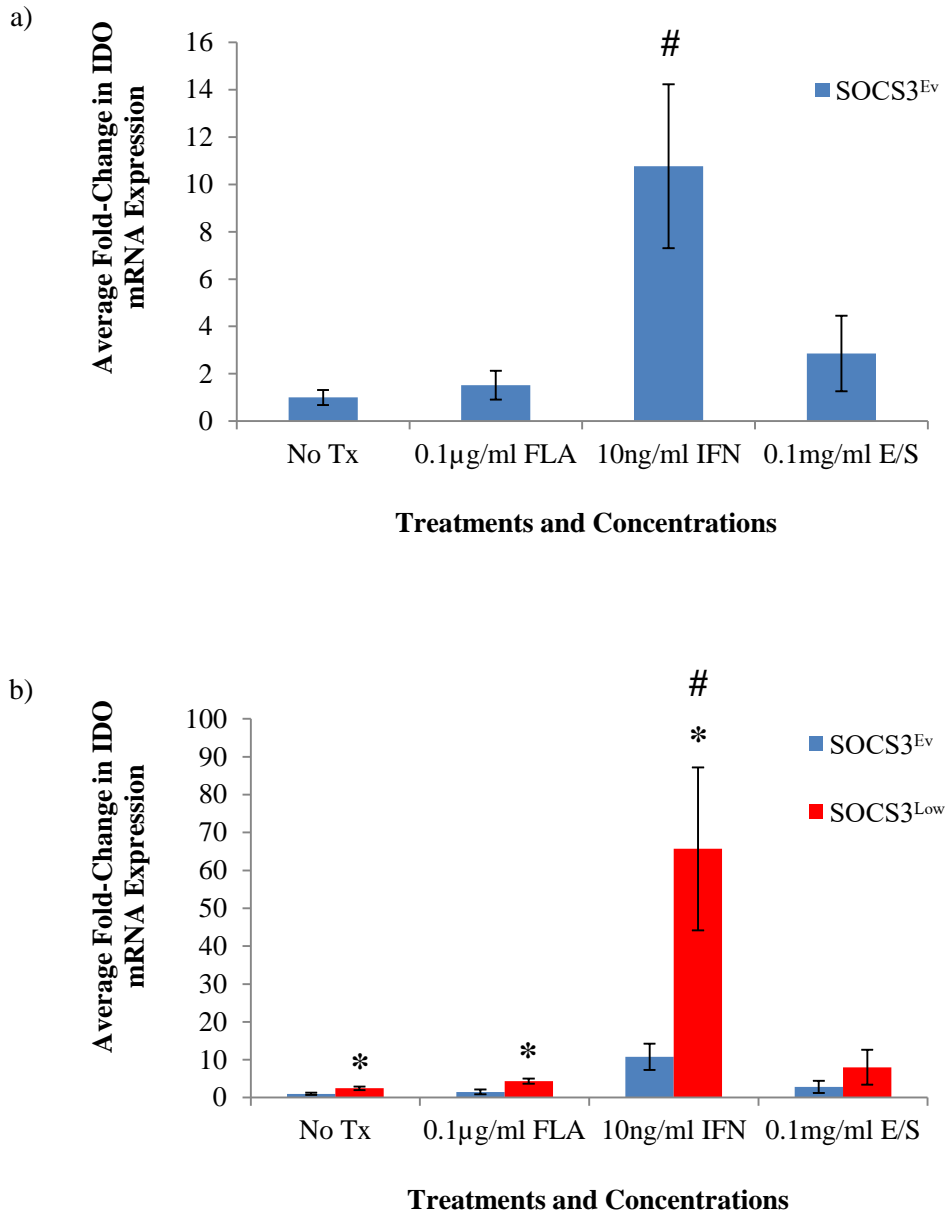
Figure 3.13: Quantification of IDO mRNA levels (±SEM) in (a) SOCS3[Ev] control HIEC cells, and in (b) both SOCS3[Ev] control cells and SOCS3[Low] knockdown HIEC cells, at the basal level and following various treatments. Cells were seeded at 1 x 10^5/well in a 12-well plate, and allowed to adhere for 24 hours, before serum starvation overnight. Cells were treated as stated for 2 hours, before lysis with TRI-Reagent® for RNA extraction. IDO mRNA levels were measured using qPCR, and calculated using the $2^{(-\Delta\Delta Ct)}$ method, with values relative to the SOCS3[Ev] No Tx average ratio. (* = $p<0.05$, using a two-tailed t-test vs. SOCS3[Ev]. # = $p<0.001$, using a one-way ANOVA with control Dunnett's post-hoc test vs. a) SOCS3[Ev] No Tx, and b) SOCS3[Low] No Tx) (n=6). (Figure 3.13b modified from Shaw et al., under revision in Immunology and Cell Biology).

The previous experiment was repeated to further investigate the role of SOCS3 in production of IDO, and to see whether IDO is implicated in innate immunity and potential tolerance of intestinal commensals, mediated by interaction of microbial ligands through TLR receptors on the surface of IECs. Figure 3.14 (a) shows that following treatment with FLA in SOCS3^{Ev} cells, there was a visible decrease in IDO mRNA, compared to SOCS3^{Ev} No Tx (0.9±0.4 and 1±0.4, respectively), although due to the similarities in fold-differences, this was not found to be significant. There were 1.2±0.5- and 1.3±0.5-fold increases in IDO mRNA, relative to SOCS3^{Ev} No Tx, following treatment with LPS, and Poly I:C, respectively. Due to these small increases, and the variability in IDO mRNA as depicted by the large, overlapping error bars, no statistical significance was found within the SOCS3^{Ev} cell line. It can be concluded that in SOCS3-sufficient HIEC cells, signalling through TLRs 3, 4 and 5 did not lead to increases in IDO mRNA.

Similar to figure 3.13 (b), figure 3.14 (b) shows that in all four conditions, there was an increase in IDO mRNA following knockdown of SOCS3. Treatment with FLA and Poly I:C led to 4.7±1.9- and 4.6±2.3-fold increases in IDO, respectively, with No Tx and LPS leading to 5.2±3.2- and 7.2±3.6-fold increases, respectively (relative to SOCS3^{Ev} No Tx). Despite these increases, there was a substantial amount of variability in IDO levels within each condition in SOCS3^{Low} cells, unlike in figure 3.13 (b). Statistical significance was achieved however, when comparing SOCS3^{Ev} and SOCS3^{Low} cells following addition of LPS (p=0.03). Due to variability in the repeated experiment, significance was not reached upon treatment with FLA, Poly I:C and in unstimulated cells, although results consistently indicate IDO expression is increased in SOCS3^{Low} cells.

In conclusion, TLR ligands did not induce IDO in control cells, but knockdown of SOCS3 may lead to an increase in IDO, both in unstimulated cells and following microbial stimulations.

a)

b)

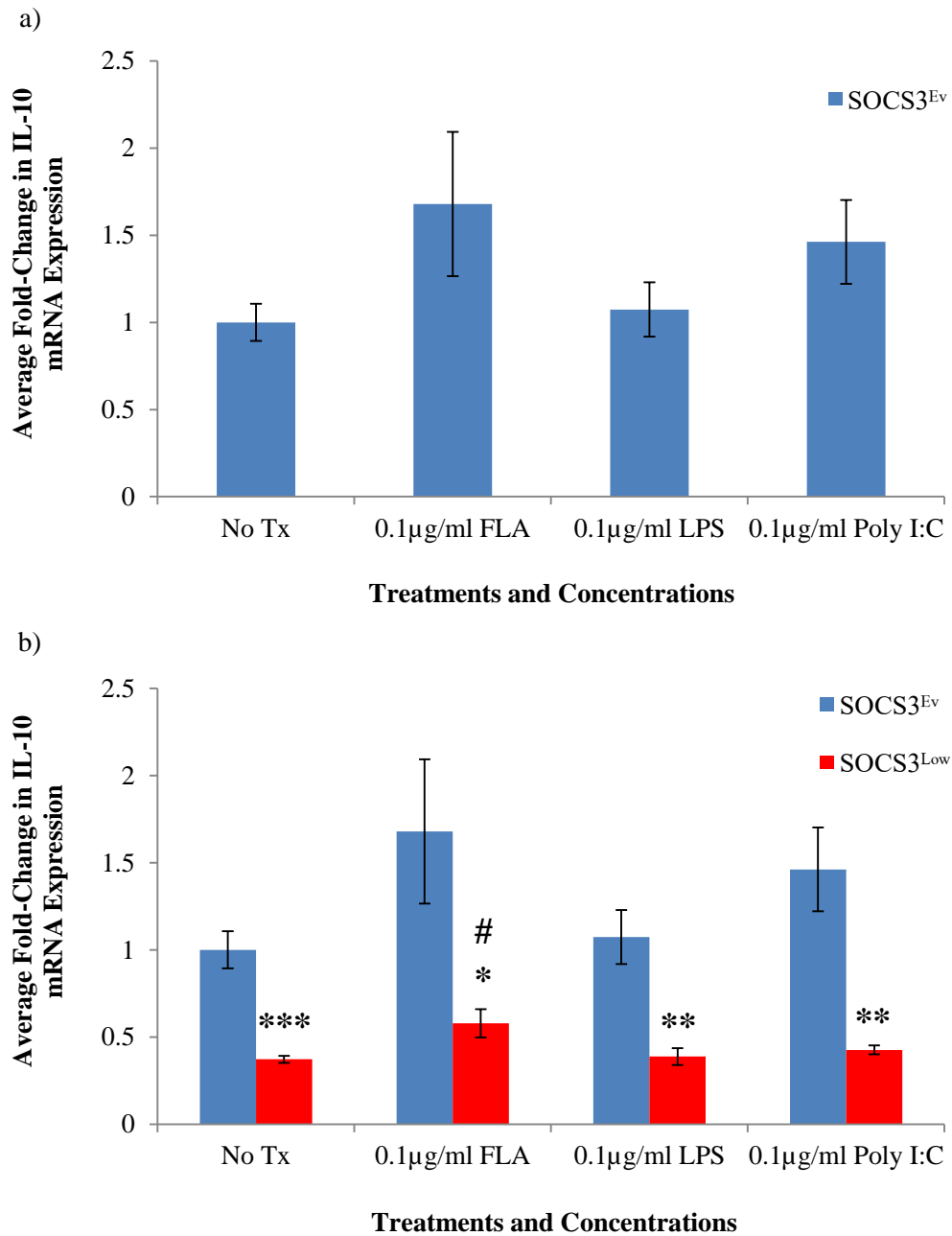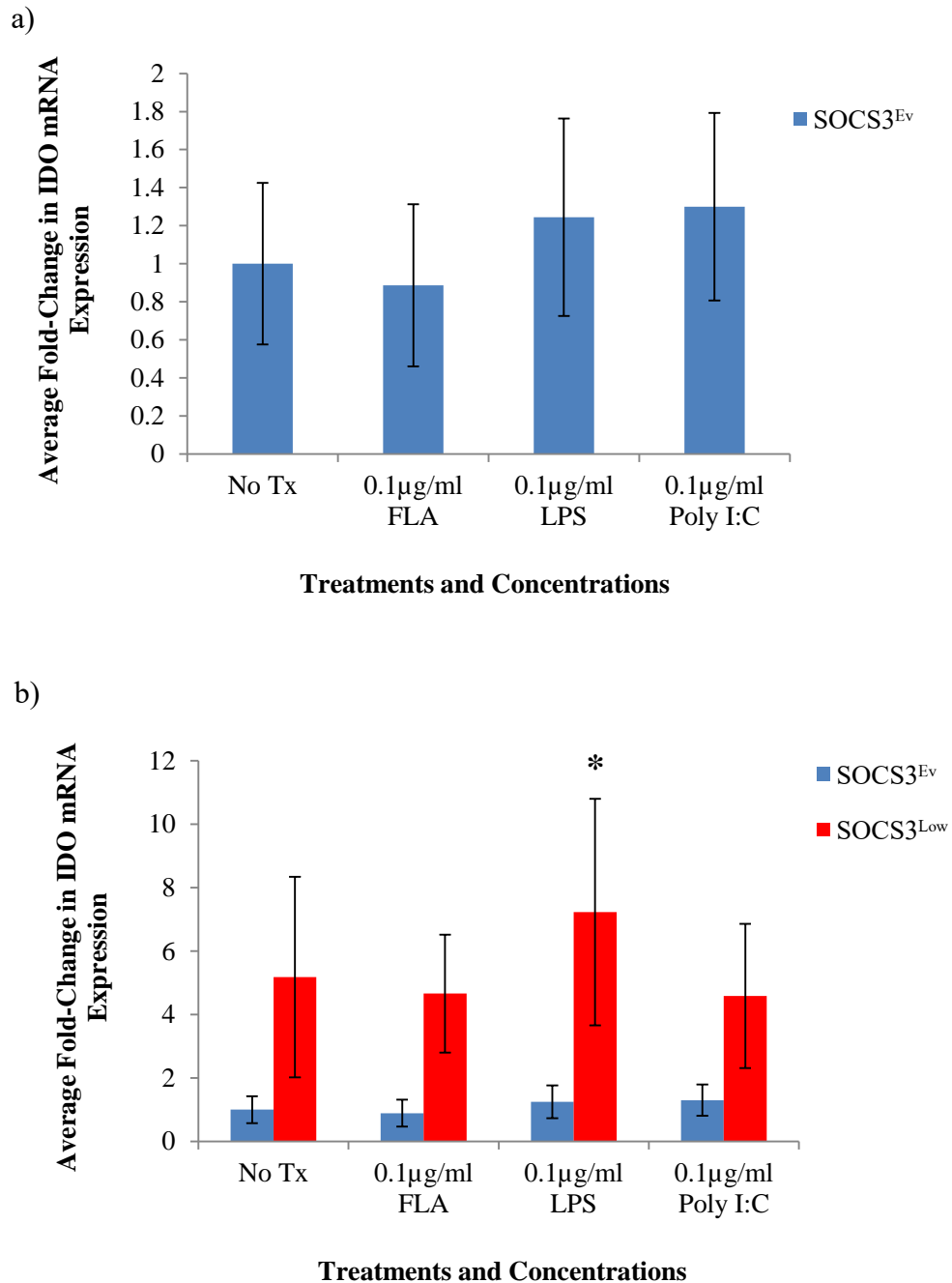**Figure 3.14: Quantification of IDO mRNA levels (±SEM) in (a) SOCS3[Ev] control HIEC cells, and in (b) both SOCS3[Ev] control cells and SOCS3[Low] knockdown HIEC cells, at the basal level and following treatment with TLR ligands.** Cells were seeded at 5×10^5/well in a 12-well plate, and allowed to adhere for 24 hours, before serum starvation overnight. Cells were treated as stated for 2 hours, before lysis with TRI-Reagent® for RNA extraction. IDO mRNA levels were measured using qPCR, and calculated using the $2^{(-\Delta\Delta Ct)}$ method, with values relative to the SOCS3[Ev] No Tx average ratio. (* = p<0.05, using a two-tailed t-test vs. SOCS3[Ev]) (n=5).

3.7 Discussion

A great deal of *in vitro* research into characteristics and processes of intestinal cells has been carried out using transformed cell lines (such as Caco-2 and HT29 cells), or cells obtained from primary cancerous tissue, and although they have advantageous features (such as the use of Caco-2 cells in drug absorption and barrier studies, due to expression of various transporters, Hidalgo et al. 1989, Artursson 1990) and have provided useful information regarding cells of the intestinal tract, the results cannot be completely translated to normal, *in vivo* settings. However, a human intestinal epithelial cell (HIEC) line has been developed more recently by Perreault and Beaulieu (1996), which is an untransformed line derived from normal, foetal, ileal tissue, with cells closely resembling the proliferating crypt cells of the small intestine. Although still relatively novel with regards to their use in intestinal studies (especially when compared to cell lines such as Caco-2), they have contributed to the field of intestinal homeostasis, particularly regarding processes involved in proliferation, differentiation and apoptosis (Pageot et al. 2000). Therefore, we aimed to characterise this recently developed HIEC cell line to compare against the commonly used Caco-2 cell line. Additionally, we wanted to use the HIEC cells as a model for investigating normal and microbial-mediated intestinal homeostasis and the involvement of SOCS3, as previous research has focused on the associations of reduced and increased expression of SOCS3 in diseases such as cancer and IBD, respectively (Rigby et al. 2007, Li et al. 2009).

Our initial experiments aimed to establish SOCS3 mRNA levels in HIEC cells and compare these against Caco-2 cells, and we found that during serum recovery, the expression of SOCS3 mRNA in HIEC cells fluctuated over the course of the experiment. The results obtained are similar to those of Yoshiura et al. (2007), who reported oscillations in SOCS3 mRNA following serum recovery in a mouse fibroblast cell line, so therefore our data extends their findings and shows SOCS3 mRNA also fluctuates in an untransformed human cell line in an ostensibly estimated state. These fluctuations are most likely due to the transcription of SOCS3 mRNA upon activation of Jak/Stat, which, once translated into protein, will then lead to inhibition of Jak/Stat signalling and reduced transcription of SOCS3 mRNA, thus producing a negative feedback loop. Once the inhibitory action of SOCS3 has receded, re-activation of the Jak/Stat pathway may then occur, leading to further transcription of SOCS3 mRNA, thus accounting for the variations in SOCS3 mRNA levels. However, it is also possible that decreases in SOCS3 mRNA as a result of reduced/inhibited Jak/Stat signalling may arise due to the activity of other negative regulators of the Jak/Stat pathway, such as

protein tyrosine phosphatases (PTPs) and protein inhibitors of Stats (PIAS), or in fact one of the other seven members of the SOCS family.

When compared against the colon adenocarcinoma cell line, Caco-2, we found higher levels of SOCS3 mRNA in serum-starved HIEC cells, and following serum recovery. This was reassuring and is supported by several studies that report low levels of SOCS3 in tumours, or tumour cell lines, both at the mRNA and protein level (He et al. 2003, Ogata et al. 2006). Using western blotting to determine whether our findings for mRNA also translated to protein, we found that SOCS3 protein levels also fluctuated over the course of the experiment, again similar to findings of Yoshiura et al. (2007), who showed SOCS3 is capable of oscillating at both the mRNA and protein level. However, our results suggested that following serum recovery, Caco-2 cells may express more SOCS3 protein than HIECs, which was not anticipated. Cancer is a disease associated with increased, unregulated cellular proliferation, with SOCS3 known to be reduced or silenced. Therefore, the lower protein levels observed in HIEC cells could be as a result of more active degradation processes. It may also be possible that there are less active translation mechanisms in HIEC cells or increased degradation of mRNA, and this could arise through the activity of microRNAs. MicroRNAs are considered as noncoding RNA, and are not completely complementary to the nucleotides of the mRNA, leading to mismatch base-pairing and ultimately prevention of protein translation (reviewed by Ambros 2004). MicroRNAs are capable of regulating considerable numbers of mRNA with this process, with each individual mRNA also possessing a large number of target sites for microRNAs (reviewed by Morris and Mattick 2014). SOCS3 has been reported to be regulated by microRNAs, with either silencing or overexpression of certain microRNAs (depending on the specific type, or cell type being studied) resulting in reduced SOCS3 expression, through promoter methylation-induced silencing, or through inhibition of Stat3 (Boosani and Agrawal 2015). Additionally, as one or more pathways responsible for cell proliferation may be dysregulated or non-functional in cancer, it may be that other regulatory pathways may not be efficiently regulated as well. With respect to our western blot findings, these pathways may be involved in the degradation of SOCS3 protein, perhaps either by autophagy, or through proteasomal degradation. Autophagy involves the formation of a lysosome with an autophagosome (a double-membraned structure that contains engulfed cellular contents), to become an autophagolysosome. Degradation of the consumed cellular components then occurs due to the activity of lysosomal enzymes (reviewed by Levine et al. 2011). It can be considered as a cellular defence mechanism as degradation of specific cellular components may prevent replication of damaged and mutated cells, which if allowed to accumulate, could lead to cancer. Additionally, autophagy can also result in engulfment and

subsequent degradation of intracellular pathogens (reviewed by Levine et al. 2011). Regarding the Jak/Stat pathway, Stat3 in particular is implicated in the autophagy pathway, with expression associated with decreased autophagy, and vice versa (reviewed by Zouein et al. 2013). Essentially, we found "normal" cells to have higher SOCS3 mRNA than transformed cells which initially could have resulted in more mRNA translated into protein. However, as this was not the case, signalling pathways are more likely to be efficiently regulated in the HIEC cells, compared with Caco-2, with Stat3 levels potentially decreasing due to the presence of SOCS3, causing an increase in autophagy, thus leading to the degradation of SOCS3. Cancer cells may have dysregulated autophagy pathways or reduced activity, thus promoting survival and replication of mutated cells (reviewed by Zouein et al. 2013), especially as normal-high Stat3 levels suppress autophagy and this can arise through lack of regulation due to diminished SOCS3 levels. However, to confirm this hypothesis, we would first have to establish differences in Stat3 levels between the two cell lines. One way in which we could test whether autophagy is increased in HIEC cells is to measure the conversion of microtubule-associated protein light chain 3 (LC3) from LC3-I to LC3-II which occurs during formation of the autophagosome (Kabeya et al. 2000). Furthermore, to determine if proteasomal degradation was responsible for decreased SOCS3 protein levels in HIECs, we would expect accumulation/increased levels of SOCS3, perhaps more similar to those of Caco-2 cells, following addition of a proteasomal inhibitor, such as epoxomicin and MG132 which have shown to prevent degradation of SOCS3 (in several human cell lines, Lee et al. 2008). SOCS3 proteins also contain a PEST motif (rich in Proline, Glutamic-acid, Serine and Threonine) which has shown to be involved in its stability and degradation as removal resulted in increased SOCS3 levels due to increases in its half-life; both with and without the additional of a proteasomal inhibitor (Babon et al. 2006). Therefore, it may be possible that the PEST motif is less abundant or perhaps not as functionally efficient in Caco-2 cells compared with HIEC cells.

SOCS proteins are also implicated in proteasomal degradation mediated through the SOCS box- a C-terminus domain that is conserved in all eight members of the SOCS family. The SOCS box binds with elongins B and C, and the scaffold protein, Cullin 2/5 to form a complex that is capable of ubiquitinylating substrates for degradation by the proteasome (Zhang et al. 1999). Regarding results obtained here, it may be that SOCS box activity is higher or more efficiently regulated in the HIEC cells, with other components of the Jak/Stat pathway targeted for degradation to cease signalling following sufficient activation. For instance, if the activated Jaks or Stats were degraded, transcription of target genes (such as SOCS3) would no longer take place, thus leading to decreased SOCS3 protein levels as a

result. Additionally, SOCS3 itself can be degraded- phosphorylation of SOCS3 on tyrosine residues (Tyr[204] and Tyr[221]) leads to protein destabilisation, resulting in dissociation from elongin C as a result, causing rapid proteasomal degradation to take place (Haan et al. 2003). In Caco-2 cells, it may be that SOCS3-mediated ubiquitinylation and subsequent degradation is taking place, but of proteins whose removal will promote survival and proliferation of the cell (for example, pro-apoptotic proteins). To test these hypotheses, as stated previously, cells could be treated with a proteasomal inhibitor, with the expectation that protein levels of SOCS3 would increase in cells that rely on SOCS box-mediated proteasomal degradation of SOCS3. We could also measure levels of pro-apoptotic proteins for example (such as caspases) to determine whether their degradation by Caco-2 cells is a mechanism for the survival of these cells. Furthermore, as the SOCS box mediates proteasomal degradation, antibodies against this domain could be used with the assumption HIEC cells may have higher abundance or perhaps an intact, and therefore functional SOCS box, compared with Caco-2 cells. If the lower SOCS3 protein levels in HIEC cells are as a result of SOCS box-mediated degradation, then we would also expect increased SOCS3 expression in these cells (relative to Caco-2 cells) if the SOCS box were to be deleted.

TLR signalling has shown to be essential for intestinal homeostasis, as MyD88^{-/-} mice exhibited dysregulated proliferation and differentiation of IECs, and succumbed to intestinal insult (using DSS) due to an inability to repair and replenish damaged cells (Rakoff-Nahoum et al. 2004). GF mice were found to have lower rates of proliferation as well as reduced crypt and mucosal depths when compared to CR mice (Abrams et al. 1962), also demonstrating the importance of the interaction with IECs and commensal microflora, which is mediated through TLRs. Furthermore, Cario et al. (2004) reported that induction of TLR signalling through TLR2 in human IEC lines, led to tightening of zona occludens-1 (ZO-1, a tight junction protein), thus demonstrating that TLR signalling helps to maintain intestinal epithelial integrity. As one of the major features of cancer is dysregulated proliferation, it was hypothesised that Caco-2 cells would proliferate more than HIECs in the absence of stimulation, but that HIECs may be more responsive to the TLR ligands, as in an *in vivo* setting, recognition of TLR ligands may lead to immune activation, which could be undesirable for cancer cells. In HIEC cells, fold-increases in cell number were observed after 24 hours, irrespective of the treatment and concentration, proving HIEC cells are able to respond to different TLR ligands. Caco-2 cells unexpectedly exhibited similar fold-increases with each respective treatment. At 48 hours, both cell lines either exhibited no considerable change in cell number, or decreases in cell number, indicative that microbial stimulation did not rapidly induce proliferation. Increases in cell number were observed in both cell lines at

72 hours, regardless of treatment and concentration of TLR ligands. However, when comparing fold-changes in cell number from 48 to 72 hours, the proportional increases in proliferation were much greater in Caco-2 cells, which was unexpected, as it was hypothesised that cancer cells are less responsive to exogenous stimuli.

In addition to greater decreases in cell number in HIECs 48 hours after treatment, compared with Caco-2 cells, more pronounced increases in cell number were observed in Caco-2 cells after 72 hours of TLR stimulations, and this may also be indicative of a reduction in apoptosis. Supporting findings of previous studies (He et al. 2003, Ogata et al. 2006), our initial experiments showed that HIECs consistently expressed higher levels of SOCS3 mRNA than the Caco-2 cancer cell line. Collectively, this could suggest that SOCS3 levels are connected with apoptosis, with lower SOCS3 levels (as observed in many cancers) resulting in reduced apoptosis, and higher SOCS3 levels (as demonstrated in HIECs, vs. Caco-2 cells) increasing the cells' susceptibility to apoptosis, or more likely to induce cell death pathways during damage and stress. Many studies have been published that support this hypothesis. For instance, deletion of SOCS3 in murine myocardial cells inhibited apoptosis following a myocardial infarction (Oba et al. 2009). Sitko et al. (2008) found that knockout of SOCS3 using *in vitro* fibroblasts, prevented cell cycle arrest at the G1 checkpoint following damage with ionising radiation, indicating a role for SOCS3 in DNA damage. The use of SOCS3 siRNA in preadipocytes was also found to inhibit apoptosis induced following treatment with TNF- α (Zhao et al. 2012). Conversely, overexpression of SOCS3 in adipocytes promoted TNF-α-induced apoptosis, through increased production of the pro-apoptotic proteins, Bax and Caspases 3 and 9, and downregulation of Bcl-2, which is anti-apoptotic (Liu et al. 2015). Additionally, overexpression of SOCS3 (as well as SOCS1) led to increased cell death of mouse embryonic stem cells (Duval et al. 2000). More specific to our interests, Wei et al. (2014) found that inhibition of Jak/Stat3 signalling in colorectal cancer cells, through overexpression of SOCS3, induced apoptosis and prevented tumour cell growth, both *in vitro* and *in vivo*. Comparison of expression of both pro- and anti-apoptotic proteins in these two cell lines could be tested to determine whether decreased apoptosis was a potential cause of increases in proliferation of Caco-2 cells, and this could potentially reveal an association between SOCS3 and apoptosis specifically in the two intestinal cell lines we studied.

Our hypothesis that differences in SOCS3 expression between Caco-2 and HIEC cells were responsible for the differences in proliferation are supported by our SOCS3 knockdown HIEC cells (referred to as SOCS3^{Low}, with controls named SOCS3^{Ev}) in order to investigate the

effects of reduced SOCS3 in a normal, untransformed intestinal cell line. We performed serum recovery experiments to confirm the knockdown, with SOCS3 reduced in SOCS3^{Low} cells compared to SOCS3^{Ev}, both at the mRNA and protein level. Similar to our initial serum recovery experiments, expression levels of SOCS3 were found to fluctuate over the course of the experiments, as reported by Yoshiura et al. (2007) using a mouse fibroblast cell line. Although the oscillation amplitudes and wavelengths observed here varied from those of Yoshiura et al. (2007), this may have been due to the use of different time points, and also using cells of a different origin and type so the culturing conditions would not have been the same. However, despite the slight dissimilarities, we were able to show that SOCS3 mRNA and protein expression continued to fluctuate even following transduction.

As with HIECs vs. Caco-2 cells, we then assessed the proliferative responses of both transduced HIEC cell lines. In the control, SOCS3-sufficient HIECs (SOCS3^{Ev}), no significant increases in cell number were observed following treatment with multiple TLR ligands. In the literature, it has been reported that normal IECs generally are hyporesponsive to the commensal bacteria and their products, located in the gut lumen, as being hyperresponsive and generating a pro-inflammatory response to these commensal populations would be disadvantageous and detrimental to the host. Studies revealed that this IEC unresponsiveness was due to low expression levels of TLR2, TLR4 and its co-receptor, MD-2, with regards to LTA and LPS, respectively (Abreu et al. 2003, Otte et al. 2004). Otte et al. (2004) found that the hyporesponsive state was present following prolonged exposure to TLR ligands and was detected just 6 hours post-treatment. Acute, short-term exposure however, was capable of inducing expression of pro-inflammatory cytokines from IECs. The HIECs in our experiments were treated for 48 hours so the phenotype displayed by SOCS3^{Ev} fits these findings. Abreu et al. (2003) also found that IFN-γ was able to increase expression of MD-2, although this was decreased following an increase in SOCS3, indicating that SOCS3 is implicated in TLR-mediated tolerance and that one mechanism through which SOCS3 inhibits TLR and subsequent NF-κB signalling may be through downregulation of the MD-2 coreceptor. This finding also supports results of SOCS3^{Low} cells, where there was a tendency of increased cell number, and thus proliferation and responsiveness compared with SOCS3^{Ev}, following addition of TLR ligands. This suggests that SOCS3 is capable of regulating and limiting microbial-induced proliferation mediated by signalling through multiple TLRs in HIEC cells. Additionally, as we observed enhanced proliferation following addition of multiple TLR ligands following knockdown of SOCS3- a phenotype also seen in Caco-2 cells- this could suggest that even a reduction in SOCS3 (not a complete knockout) could induce a more "cancer-like" phenotype in what are assumed to be otherwise normal IECs.

In SOCS3-sufficient HIECs, with the exception of flagellin (which is known to induce TNF-α, Ciacci-Woolwine et al. 1998, Thagia et al. 2015), microbe-mediated signalling through TLRs 3 and 4 did not induce significant increases in expression of TNF-α, and this is possible further evidence of normal IECs, and in this case HIEC cells, being hyporesponsive to components of the commensal microbiota, due to the undesirable effects increased pro-inflammatory cytokine production would have in a non-pathological setting. Following knockdown of SOCS3, we observed significant increases in TNF-α with LPS, Poly I:C and also in untreated cells, which may provide further evidence that SOCS3 is capable of limiting microbial-induced production of TNF-α. Interestingly, mice that were deficient in SOCS1 also exhibited increased TNF-α production following stimulation with LPS, and reduced tolerance to this TLR ligand (Nakagawa et al. 2002). Also, SOCS3 is required for IL-10-mediated inhibition of TNF-α, so therefore it is to be assumed that the reduction of SOCS3 in SOCS3^{Low} cells would hinder this inhibitory effect, thus resulting in increased TNF-α mRNA (Berlato et al. 2002). However (as soon to be discussed), when assessing mRNA expression of IL-10 in the same experiment, we found that knockdown of SOCS3 decreased IL-10 levels, regardless of treatment, so the fact that less SOCS3 is present to mediate IL-10 inhibition of TNF-α appears redundant, unless the two events are related. In previous *in vitro* research also using IECs, Thagia et al. (2015) found that overexpression of SOCS3 led to increases in FLA-induced TNF-α. The correct balance of SOCS3 is essential in intestinal homeostasis, as reduced expression can lead to hyperplasia and potentially carcinogenesis, with overexpression of SOCS3 implicated in inflammatory disorders, such as IBD. Although experiments carried out by Thagia et al. (2015) involved the use of the colon adenocarcinoma cell line, SW480, our combined findings may suggest that regulation of SOCS3 and TNF-α could be linked, as TNF-α has been found to drive both carcinogenesis and IBD.

Similar to our findings of TNF-α expression in SOCS3-sufficient HIECs, microbe-mediated production of the anti-inflammatory cytokine, IL-10, was also not significant following stimulation with ligands for TLRs 3, 4 and 5, and was not too dissimilar from levels observed in untreated SOCS3^{Ev} cells, possibly to maintain an appropriate level of tolerance towards microbes associated with the commensal gut flora. Additionally, substantial amounts of TNF-α mRNA were not expressed by these cells so transcription of IL-10 mRNA does not need to be upregulated in order to counteract this. Knockdown of SOCS3 however, led to significant decreases in IL-10 expression, regardless of treatment. Initially, this result was surprising as Niemand et al. (2003) discovered that SOCS3 can be strongly induced by IL-10, but is not capable of inhibiting IL-10-mediated signalling as SOCS3 is not able to bind to any phosphorylated tyrosine residues on the IL-10 receptor. However, their experiments were

performed in monocytes derived from human blood samples, so perhaps may not translate to our findings.

Evidence for a relationship between decreased IL-10 expression as a result of reduced SOCS3 implicates another protein of interest- indoleamine 2,3-dioxygenase (IDO). As described previously, IDO is an enzyme involved in catabolism of the essential amino acid, tryptophan (Higuchi and Hayaishi 1967). IDO activity results in tryptophan depletion and a subsequent increase in tryptophan metabolites, which in turn induces anti-proliferative effects, both towards an array of microbes (such as *Toxoplasma gondii* and, Streptococci and *Chlamydia* species, cited by Thomas and Stocker 1999), as well as host T-cells (Fallarino et al. 2002, Frumento et al. 2002). An important function of IDO is the induction of immune tolerance and this came to light when inhibition of IDO resulted in T-cell mediated foetal rejection in mice (Munn et al. 1998). Consequently, IDO is implicated in immune tolerance, and can be involved during disease processes, or as a result of disease, such as with cancer and IBD, respectively. With regards to cancer, tumour cells are capable of expressing their own IDO and due to its anti-proliferative effects on T-cells, the immune system is dampened down, promoting evasion of the tumour cells. This may be further exacerbated during inflammation-associated carcinogenesis as IFN-γ is a potent inducer of IDO (Yasui et al. 1986, Ozaki et al. 1987), and may be one of the inflammation-driving cytokines. Similarly, during IBD, IDO activity will be higher than in non-IBD sufferers, due to increases in pro-inflammatory cytokines; some of which are capable of activating IDO, such as TNF-α, along with IFN-γ. However, in this case, decreased proliferation (and potentially numbers) of T-cells is favoured in order to limit immune responses elicited against non-pathogenic, non-self entities, such as food and commensal microbiota in the gut lumen (Ferdinande et al. 2008). Metghalchi et al. (2015) discovered that deletion of IDO resulted in a more severe state in the IL-10$^{-/-}$ murine model of spontaneous colitis, compared with IDO-sufficient IL-10$^{-/-}$ mice. IL-10$^{-/-}$ mice were also found to exhibit higher IDO activity in their serum, spleens and mesenteric lymph nodes, when compared with IL-10$^{+/+}$ mice. Conversely, in a murine model of atherosclerosis (another disease characterised by inflammation), the authors found IDO$^{-/-}$ mice to have higher levels of circulating IL-10 (relative to IDO$^{+/+}$), in addition to increased IL-10 in the spleen and peritoneal macrophages. This increase was continued in both IDO$^{-/-}$ macrophages and dendritic cells as well, in unstimulated and LPS+ IFN-γ treated cells. These results suggest a conserved, indirectly proportional relationship between IL-10 and IDO across tissues and diseases, and this may act to ensure sufficient levels of anti-inflammatory and tolerance-related responses are induced. Our findings showed that IL-10 mRNA expression was consistently decreased regardless of treatment in SOCS3^{Low} cells, compared with SOCS3^{Ev}. In

addition to IL-10, we also investigated IDO mRNA responses following cytokine and microbial treatments (and how SOCS3 is implicated) in our HIEC model. We found that reduction of SOCS3 increased IDO mRNA compared to SOCS3^{Ev} cells, also irrespective of treatment. Although we observed both decreased IL-10 and increased IDO mRNA, this was only found in SOCS3^{Low} cells, which may stress the importance of regulated IL-10 and IDO responses in disease states with reduced SOCS3. This relationship may be of particular importance during cancer. For instance, many cancers, including those in the G.I tract, can be associated with decreased SOCS3, as this dysregulation of the Jak/Stat pathway can help drive proliferation of tumour cells. As demonstrated here, a reduction in SOCS3 may lead to increased IDO expression. IDO within tumours helps the cells evade detection (and possible damage or removal) by the host's immune system through suppression of T-cell proliferation. This could ultimately result in apoptosis of T-cells. Through IDO and/or SOCS, IL-10 expression is also decreased, reducing anti-inflammatory responses which could in turn, increase pro-inflammatory responses (i.e. through increased TNF-α, as shown here) and potentially drive inflammation-associated carcinogenesis. Activation of IL-10 can also lead to further immune responses, for example through increased B- and T-cell activity and production of antibodies. Therefore, downregulation of IL-10, as achieved here, would also aid evasion of the immune system by tumour cells.

Regarding IDO primarily, we used our HIEC model to determine whether a potential tumour-promoting mechanism existed between SOCS3 and IDO, following individual decreases and increases in these respective proteins in several cancer types, including those of the G.I tract (He et al. 2003, Uyttenhove et al. 2003, Weber et al. 2005, Ogata et al. 2006, Rigby et al. 2007, Li et al. 2009). In SOCS3^{Ev} cells, only treatment with IFN-γ significantly increased IDO mRNA expression, compared to no treatment. IFN-γ is known to be a strong inducer of IDO so therefore this result was not unexpected (Yasui et al. 1986, Ozaki et al. 1987). However, stimulation with multiple TLR ligands did not induce substantial fold-increases in IDO. Similar to the cytokine profile assessment in our HIEC model, large amounts of IDO may not be expressed following recognition of TLR ligands as this may result in increased tolerance towards pathogens that share microbial components with gut commensal populations, such as LPS- a component of the cell wall in Gram-negative bacteria. On the other hand, fold-changes in IDO lower than those of untreated cells could be detrimental and result in a breakdown in tolerance mechanisms in distinguishing "self" from "non-self." However, knockdown of SOCS3 resulted in significantly higher fold-changes in IDO regardless of treatment (relative to SOCS3^{Ev}), suggesting a role for SOCS3 in limiting IDO expression. In terms of carcinogenesis, SOCS3's role as a tumour suppressor appears to be divided into its ability to

suppress multiple signalling pathways and thereby regulating cell proliferation, and ensuring immune surveillance is maintained by limiting IDO expression.

Our findings in SOCS3^{Low} cells of increased IDO following knockdown of SOCS3 are similar to those of Orabona et al. (2004,) who found that in SOCS3-silenced cells, transcription and activation of IFN-induced genes (such as IDO) was increased following stimulation with IL-6. Although this study was performed using murine dendritic cells, the similarity in results of increased IDO following reduction of SOCS3 suggests the role of SOCS3 in limiting IDO may be conserved across cell types and perhaps organisms. Conversely, the same group also discovered that SOCS3 is responsible for ubiquitinylation of IDO, as kynurenine production increased following addition of a proteasomal inhibitor regardless of treatment with the SOCS3-inducer, IL-6 (Orabona et al. 2008), indicative of an increase in IDO activity. They also found that IDO contains two sites, known as immunoreceptor tyrosine-based inhibitory motifs (ITIMs), and these allow SOCS3 to bind and induce proteasomal degradation of IDO. These results support our findings in SOCS3^{Ev} cells, in that these cells are SOCS3-sufficient, so following translation of SOCS3 mRNA into protein, it is able to instigate IDO proteasomal degradation. Hence, this provides an explanation as to why small fold-increases were observed in TLR- and E/S-treated SOCS3^{Ev} cells, in relation to unstimulated cells.

Knockdown of SOCS3 led to increases in IDO mRNA in absence of microbial stimulation and following treatment with IFN and TLR ligands, but not E/S- contrasting results of Bell and Else (2011). Relative to unstimulated cells, they observed an approximate 10-fold increase in IDO, following stimulation with E/S, and at a lower concentration than that used here. However, although Bell and Else (2011) also used a human intestinal cell line (LS174T cells specifically), it is a goblet cell adenocarcinoma cell line so therefore it is to be expected that these cells would express more IDO than an untransformed cell line, especially when stimulated. For instance, following treatment with IFN-γ, we observed an approximate 11-fold increase in IDO, compared to a 100-fold increase in LS174T cells (Bell and Else 2011). Additionally, whilst our results here and those in other studies have shown IECs other than goblet cells are capable of expressing IDO (Ferdinande et al. 2008), it may be that goblet cells are more sensitive to E/S.

Collectively, findings from this chapter revealed how reduction of SOCS3 (through siRNA knockdown) in an otherwise ostensibly normal intestinal cell line, induced a more "cancer-

like" phenotype, as they exhibited similar SOCS3 expression levels and microbial-mediated rates of proliferation to the adenocarcinoma cell line, Caco-2. Our results demonstrated a multi-faceted role of SOCS3 in intestinal cells in processes implicated in inflammation, carcinogenesis and immune tolerance. Although the sequence of events are yet to be determined, it appears that reduction of SOCS3 promotes carcinogenesis not only as a result of increased proliferation and dysregulated Jak/Stat signalling, but also through increased sensitivity to TLR signalling demonstrated through increased microbial-mediated proliferation. Expression of pro-inflammatory cytokines, with respect to TNF-α specifically, were increased which may be due to lack of regulation by SOCS3 and/or as a result of increased TLR signalling. This in turn may potentiate proliferation and in an *in vivo* setting, could potentially drive inflammation-associated carcinogenesis. If sustained, this situation may be further exacerbated by the low expression of IL-10 we observed following SOCS3 knockdown. Furthermore, the enzyme, IDO was also increased in SOCS3^{Low} cells, regardless of stimulation conditions and this would be key to carcinogenesis in an *in vivo* setting through catabolism of tryptophan, leading to suppression of T-cells and thereby dampening down the immune system. Increased IDO could then facilitate microbial-mediated proliferation due to decreased immune responses elicited towards both commensal and non-commensal populations. Therefore, we have shown that the HIEC cell line is a suitable model, although many further experiments are needed to elucidate the full extent of the "cancer-like" phenotype induced in these cells following reduction of SOCS3.

Chapter 4:

The use of an *in vivo* model to investigate the role of SOCS3 on homeostatic IEC turnover

4.1 Rationale

For many decades, mice have been used as an *in vivo* model organism, proving very useful in biomedical research, particularly regarding human health and disease. Although associated ethical and monetary costs are higher with mice than using cultured cell lines *in vitro*, or lower organisms such as *Drosophila* or the invertebrate nematode, *Caenorhabditis elegans*, their benefits greatly outweigh these disadvantages. For instance, there is a high level of similarity between mice and humans, not only at an anatomical level, but also at a genomic level, as 99% of mouse genes have homologues in humans (Mouse Genome Sequencing Consortium 2002). Mice have short lifespans and gestational periods, allowing for longitudinal studies, with feasible turnover of offspring and litter sizes (cited by WWW, Transgenic Animal Web). Regarding the G.I tract specifically, it is possible to replicate and study many diseases similar to those seen in humans, such as IBD, cancers of the G.I tract and colitis-associated carcinogenesis (CAC) (Lin and Hackam 2011). The similarities in gut microbiota between humans and mice, and the facilities and techniques available allow the study of GF-, gnotobiotic- and human-derived flora associated mice, thus enabling insight into microbial-derived effects and host-microbe interactions (Sekirov et al. 2010). Furthermore, since the mouse genome was mapped in 2002 (Mouse Genome Sequencing Consortium 2002), researchers are able to utilise genetic tools to identify genetic similarities between mice and humans, including Cre-Lox recombinase technology (as described in section 2.2.2.1 in Chapter 2), allowing genetic manipulation (i.e. deletion or insertion) of target genes in specific tissues or cells (Orban et al. 1992).

Our *in vitro* experiments investigating the role of SOCS3 in normal IEC homeostasis found that SOCS3 was responsible for limiting proliferation following stimulation with multiple TLR ligands. SOCS3 also regulated expression of IL-10, TNF-α and IDO in response to various cytokine and microbial treatments. *In vivo* intestinal research using mouse models have proven useful and revealed SOCS3 is responsible for perpetuating inflammation through inhibition of Stat3 signalling (in a spontaneous intestinal inflammation model, Mitsuyama et al. 2006), as well as limiting proliferation and development of hyperplasia in an AOM/DSS model of colitis-associated colorectal cancer in mice (Rigby et al. 2007). However, there is currently little research into the role of SOCS3 in normal intestinal homeostasis, *in vivo*. Therefore, utilising the IEC-specfic Villin-driven-Cre recombinase system, we generated a mouse model of IEC-specific deletion of SOCS3 (as SOCS3$^{-/-}$ mice are embryonic lethal, Roberts et al. 2001), and aimed to investigate how SOCS3 impacts on cell proliferation in a physiologically relevant model. We selected the *Trichuris muris* model as *T. muris* is known

to increase proliferation of intestinal crypt cells (Artis et al. 1999), and naturally infects mice (cited by Cliffe and Grencis 2004), and so is a more physiologically relevant model of intestinal turnover, compared with chemically inducing proliferation.

Cliffe et al. (2005) found that when coupled with increased cell migration (determined through crypt cell position), increased proliferation led to higher IEC turnover and more efficient expulsion of *T. muris*- a mechanism which was termed the "epithelial escalator." Increases in proliferation without the increased cell migration led to chronic infection, as well as crypt hyperplasia. Our initial experiments were to see if SOCS3 is implicated in normal and *T. muris*-mediated homeostasis, and whether SOCS3 has a role in the "epithelial escalator" response. We chose to look at the cecum of these mice as this is the site *T. muris* larvae become associated with following hatching (Fahmy 1954). To establish differences in proliferation between control and IEC SOCS3-deficient mice, with and without infection, we quantified proliferating intestinal cells, determined the crypt position of these cells and measured crypt depth. The regions used for crypt position were based on parameters described by Potten (1998) and Cliffe et al. (2005), with positions 0-10 at the base of crypts defined as the stem cell region, and 11-20 being the transit amplifying (T.A) cell region (as shown in figure 4.1).
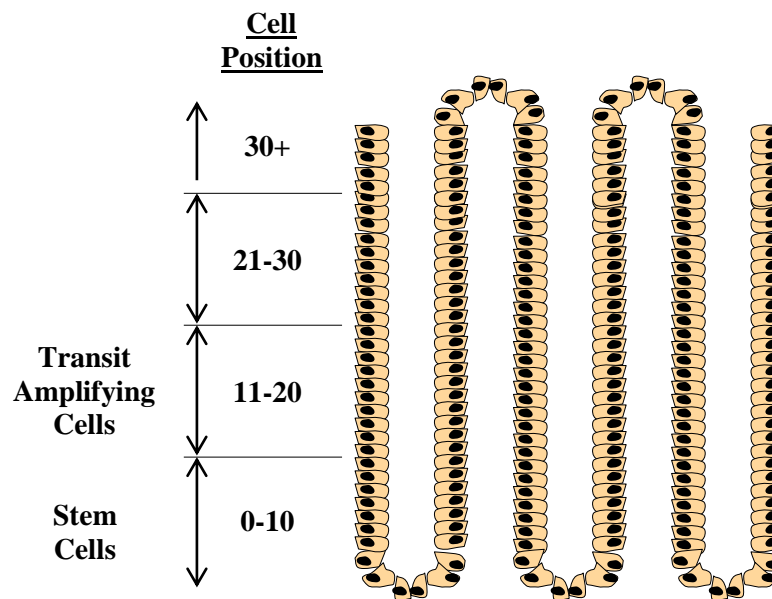
Figure 4.1: A representation of the structure of the epithelial crypts in the cecum, depicting the crypt positions and regions used to determine the proportion of proliferating cecal cells within each zone in wildtype (HO-WT) and conditional SOCS3 knockdown mice (HO-VC). (Adapted from Cliffe et al. 2005).

4.2 Assessment of IEC SOCS3 deficiency on IEC proliferation and cecal crypt morphology

4.2.1 IEC-specific deletion of SOCS3 had little effect on crypt properties in uninfected mice

Figure 4.2 shows the number of actively proliferating crypt cells (a), the position of the highest proliferating cell (b), the distribution of proliferating cells (c) and the depth of the crypts (d) in ceca from uninfected wildtype mice (HO-WT) and mice with IEC deletion of SOCS3 (HO-VC). Figure 4.2 (a) shows that on average, both HO-WT and HO-VC mice contained six proliferating cells within each cecal crypt, although taking the error bars into consideration, there appeared to be less variation in numbers of proliferating cells in HO-VC mice.

When determining whether IEC deletion of SOCS3 increased migration of cells in the crypt and led to higher cell turnover, there was also very little difference in the highest EdU-positive cell position between the two genotypes (figure 4.2b), with their highest EdU-positive cell situated, on average, at position 9 (HO-WT: 9.4±1.2, HO-VC: 9.5±1.5) As there are no Paneth cells in the ceca of mice, position 1 is located at the very base of the crypts (Treuting and Dintzis 2011).

Although no differences were observed in crypt position of the highest EdU-positive cell, this did not give us an indication of the distribution of proliferating cells within the crypts. Therefore, we then determined the percentage of EdU-positive cells in crypt regions as described previously (shown in figure 4.1). Figure 4.2 (c) shows that in both uninfected genotypes, the majority of proliferating cells were located within the stem cell region, with 92.0±2.2% and 88.5±3.4% calculated for HO-WT and HO-VC mice, respectively. Consequently, the remaining 8.0±2.2% and 11.5±3.4% of proliferating cells (in HO-WT and HO-VC, respectively) were then found in the T.A region. However, due to overlapping variability within both cell regions, and lack of statistical significance when the data were analysed (using a two-way Student's t-test), this indicates there were no differences in crypt cell migration between HO-WT and HO-VC mice.

IEC-specific deletion of SOCS3 had little effect on IEC homeostasis, using the parameters assessed in figure 4.2 (a)-(c), as neither number nor position of proliferating cells were significantly increased at the basal state. There was a tendency of HO-VC mice to have slightly larger crypt depths, although this could possibly be confirmed with larger sample sizes, or more equal group sizes. Figure 4.2 (d) may indicate that the average crypt depth in HO-VC mice may have been slightly larger than that in HO-WT mice, with approximate depths of 137±3μm and 129±6μm, respectively, but statistical significance was not reached, with a p-value of p=0.08 obtained. Together these results suggest that loss of SOCS3 had little effect on crypt dynamics in unchallenged mice.

a)

b)

c)

d)
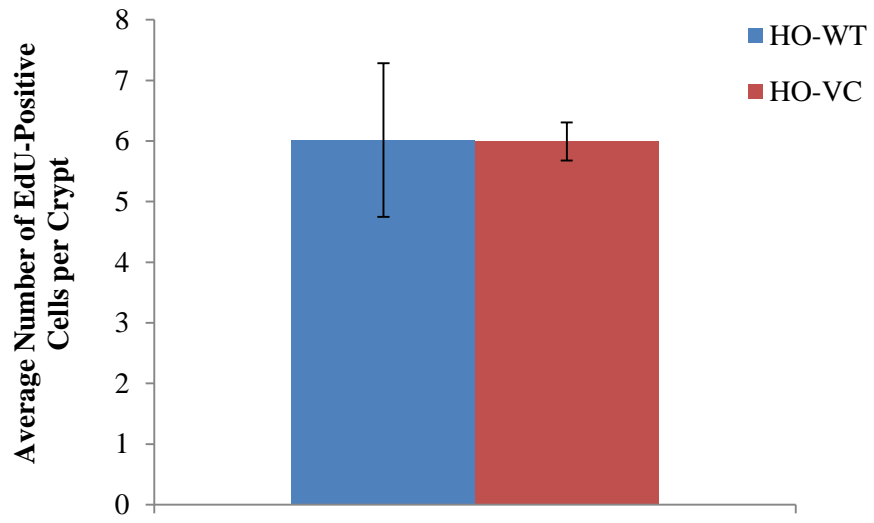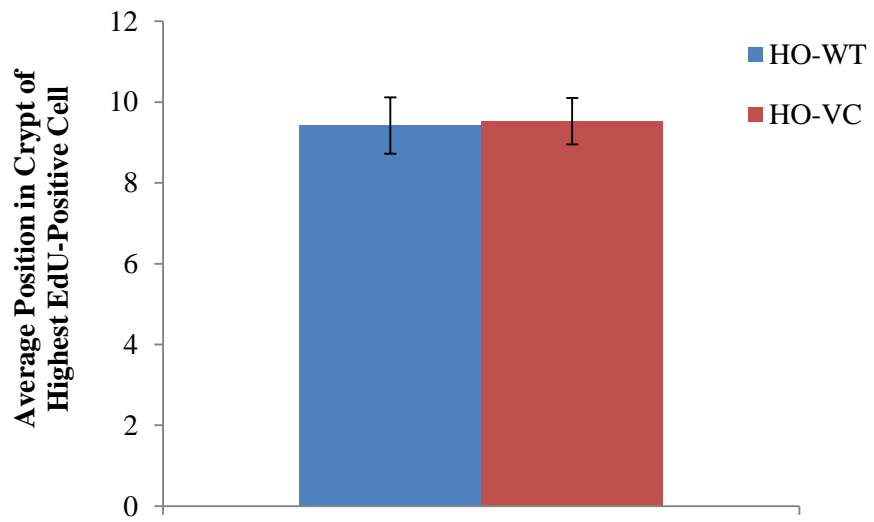
Figure 4.2: Differences in (a) the number of proliferating cells, (b) the position of the highest proliferating cell, (c) distribution of proliferating cells within cecal crypts and (d) crypt depth between uninfected wildtype (HO-WT) and conditional SOCS3 knockdown mice (HO-VC) (±SEM). At 6-8 weeks + 35 days, ceca were removed and following paraffin embedding and sectioning, the Click-iT® EdU assay was performed according to manufacturer's instructions for assessment of cecal crypt proliferation. Confocal images were analysed blind on a Zeiss confocal microscope, using multiple crypts per mouse (≥7), with averages taken for the whole genotype. (HO-WT- n=3, HO-VC- n=7).

4.2.2 Infection with T. muris increased cell proliferation, migration and crypt depth in ceca

Figure 4.3 shows the comparison of crypt properties in both uninfected and infected HO-WT and HO-VC mice, to demonstrate the effect of *T. muris* infection had on these mice. The infected mice were given a low dose of 25-30 *T. muris* eggs as mice generate inappropriate Th1 responses to low doses, (such as the production of IFN-γ and IL-2, Mosmann et al. 1986, Else and Grencis 1991), with a reduction of Th2 responses, resulting in failure to expel worms in mice strains either susceptible or resistance when administered higher doses of *T. muris* eggs (Bancroft et al. 1994, Wakelin 1973). Mice in our experiments were infected for 35 days following low dose egg administration as worms will still be present at this time point.

Upon infection, there were large increases in the number of proliferating cecal crypt cells in both groups of mice (figure 4.3 a), with approximately 2- and 3-fold increases in infected HO-WT and HO-VC mice, respectively (compared with their uninfected counterpart). This can also be seen in figure 4.4, showing representative confocal images from each genotype and infection group, with an increase in proliferating cells depicted by an increase in the number of green, EdU-positive cells. However, when a Student's t-test was performed, differences between the HO-WT cohorts did not reach statistical significance, although differences between HO-VC cohorts were very significant (p=0.002), and this may have been due to the dissimilarities in sample sizes between the two uninfected genotypes.

In addition to proliferation, *T. muris* infection led to a higher position within the cecal crypt of the highest EdU-positive cell (figure 4.3 b), with positions being approximately 1.5- and 2-fold higher in infected HO-WT and HO-VC mice, respectively, compared with their uninfected counterparts, and both of these were found to be statistically significant (p=0.05 and p=0.0003, respectively). Following this, we then analysed the effect of *T. muris* infection on distribution of EdU-positive cells within each region of cecal crypts. As expected, infection led to increased migration of cells up the crypt, with a lower percentage of proliferating cells recorded in the stem cell region, and higher percentages found in the T.A and 21-30 region, regardless of genotype (figure 4.3c). Table 4.1 shows p-values obtained during data analysis of average percentages obtained for each region and confirms that *T. muris* infection led to increased migration from the stem cell region to the T.A region in both genotypes (p<0.05). However, differences in percentages of EdU-positive cells in the T.A region within HO-VC were more substantially significant (p<0.0001, compared to p=0.0312 within HO-WT), and infection also led to significantly more proliferating cells in the 21-30 region (p=0.0167).

Together with figure 4.3 (a) and (b), these results reiterate that infection leads to increased proliferation of IECs as well as increased cell migration up crypts.

Figure 4.3 (d) shows the average cecal crypt depths of all four cohorts of mice, and shows *T. muris* infection induced an increase in crypt depth, and this can be clearly seen when comparing confocal images of HO-WT and HO-VC mice in figure 4.4 (a) and (c), and figure 4.4 (b) and (d), respectively. Both genotypes within each infection group exhibited similar crypt depths, with approximately 1.5-fold increases in length obtained for both infected HO-WT and HO-VC mice, both of which were found to be statistically significant (p=0.007 and p=0.0009, respectively). Although both genotypes within each infection group exhibited similar crypt depths, higher significance was found in HO-VC mice, and this may have been due to less variation within uninfected mice as demonstrated by the smaller error bars, when compared with uninfected HO-WT. Collectively, these results show that infection with *T. muris* led to increases in all four parameters measured; higher position and number of EdU-positive cells per cecal crypt, increased migration of proliferating cells up the crypt and also crypt depth. This could indicate that proliferation and crypt cell migration were increased as a host response to the worms, and that the increase in crypt depth resulted from higher numbers of proliferating cells.

Genotype Cell Position in Crypt	HO-WT	HO-VC
0-10	0.0316 (↓)	0.0001 (↓)
11-20	0.0312 (↑)	<0.0001 (↑)
21-30	0.4341	0.0167 (↑)
30+	0.6349	0.4608

Table 4.1: P-values calculated using a two-way Student's t-test to determine statistical significance for distribution of EdU-positive cells within cecal crypts, between uninfected and *T. muris*-infected mice within the same genotype. (Where statistical significance was found, the arrows denote the effect *T. muris* infection had within each zone: ↓ = Less cells were found in infected mices. ↑ = More cells were found in infected mice).

a)

b)

c)

d)
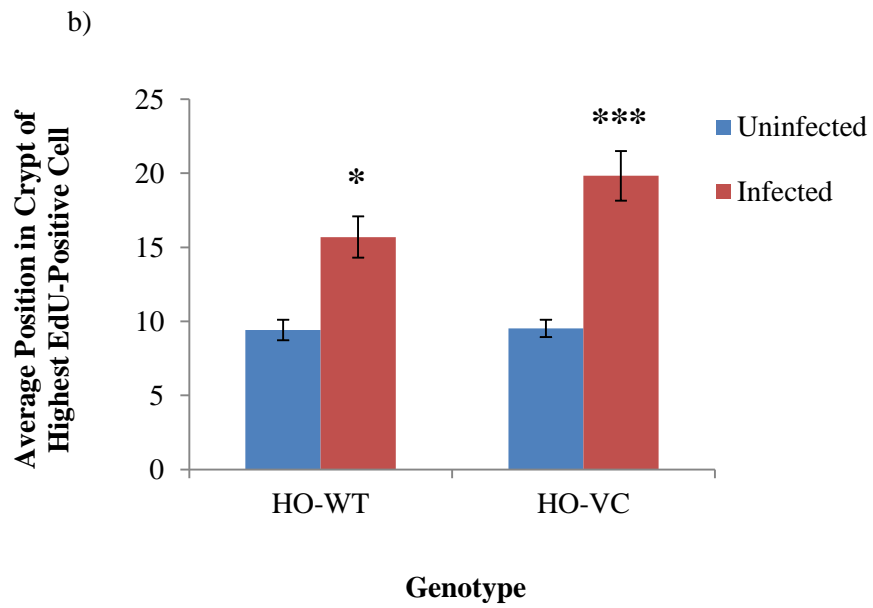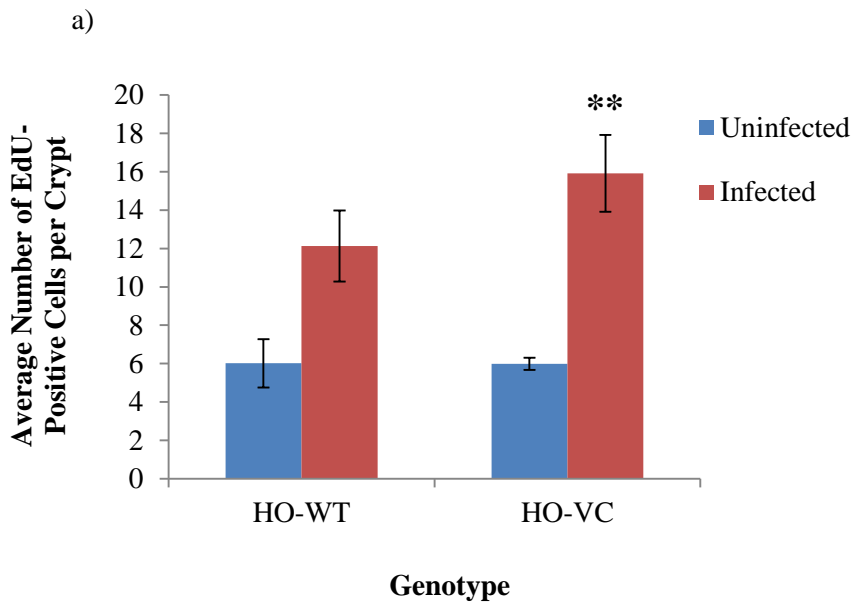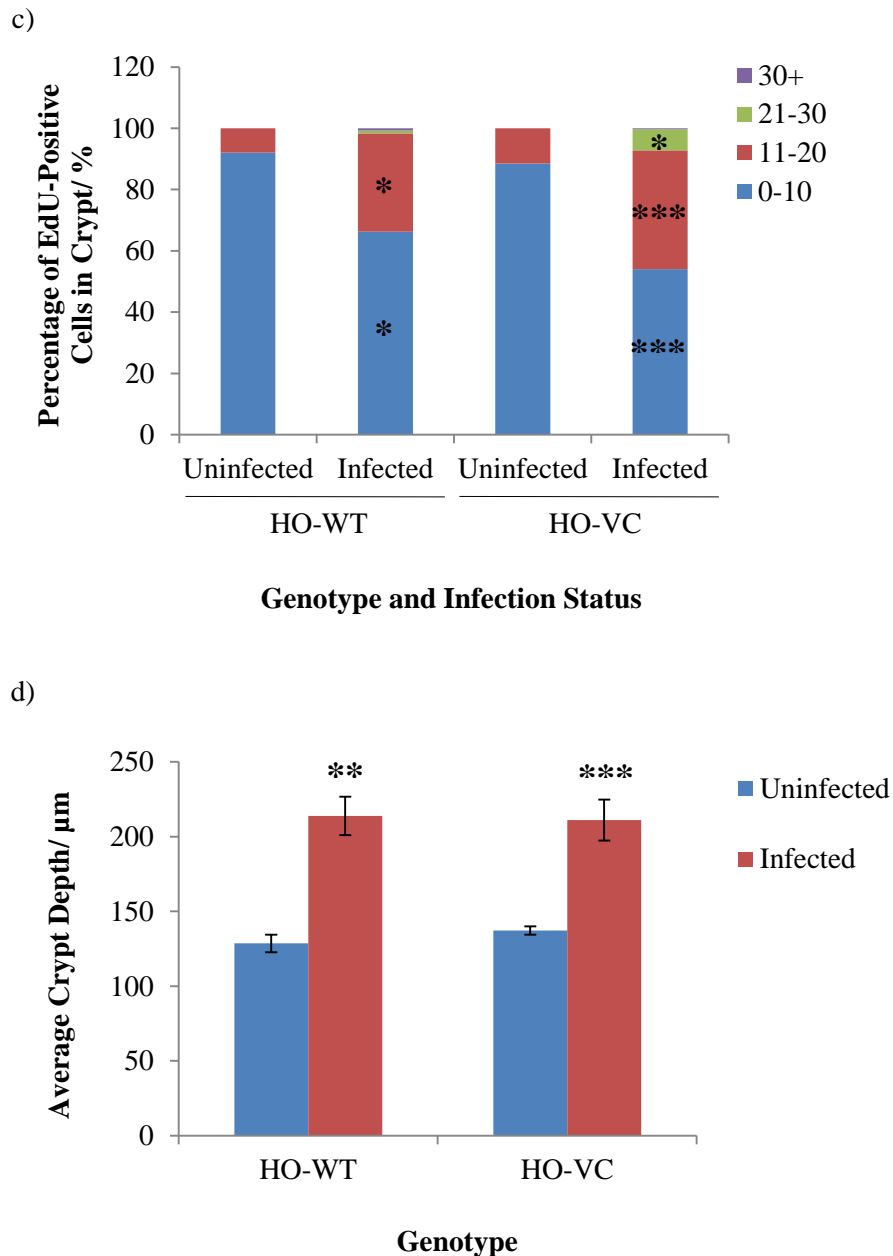
Figure 4.3: Differences in (a) proliferating cell numbers, (b) highest proliferating cell position, (c) distribution of proliferating cells within cecal crypts and (d) crypt depth between uninfected and *T. muris*-infected wildtype (HO-WT) and conditional SOCS3 knockdown mice (HO-VC) (±SEM). At 6-8 weeks + 35 days, ceca were removed from uninfected mice, and low dose *T. muris*-infected mice. Following paraffin embedding and sectioning, the Click-iT® EdU assay was performed for assessment of cecal crypt proliferation. Slides were imaged using a Zeiss confocal microscope. Confocal images were analysed blind, using multiple crypts per mouse (≥7), with averages taken for each genotype. (* = p<0.05, ** = p<0.01, *** = p<0.001, using a two-way Student's t-test, within genotypes) (Uninfected: HO-WT- n=3, HO-VC- n=7. Infected: HO-WT and HO-VC- n=12).
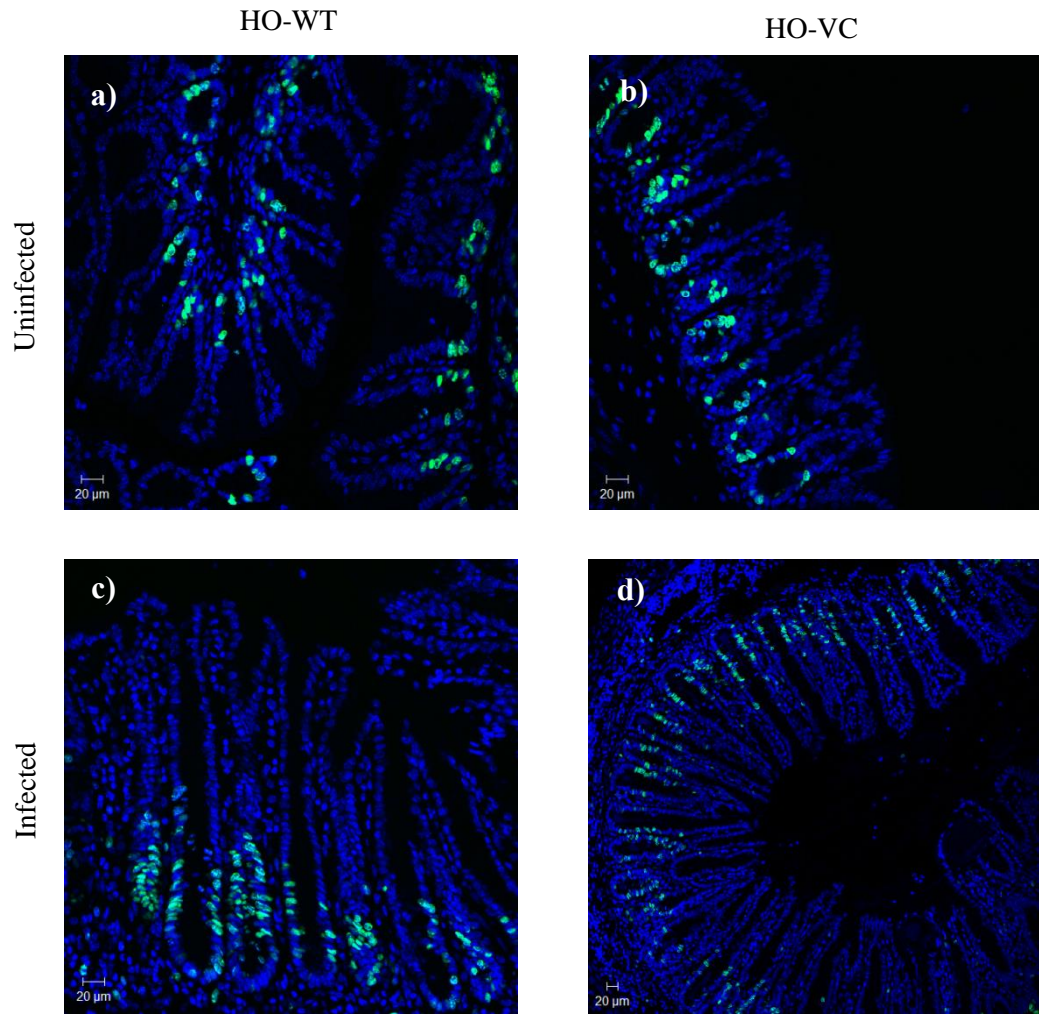
Figure 4.4: Visualisation of proliferating cells in the cecal crypts of uninfected HO-WT (a) and HO-VC mice (b), and HO-WT (c) and HO-VC (d) mice 35 days post- *T. muris* **infection.** At 6-8 weeks + 35 days, ceca were removed from uninfected mice, and low dose *T.muris*-infected mice. Following paraffin embedding and sectioning, the Click-iT® EdU assay was for assessment of cecal crypt proliferation. Slides were imaged using a Zeiss confocal microscope at 10x magnification, and confocal images were analysed blind. (Green= EdU+ proliferating cells. Blue= Hoechst nuclear stain). (Scale bar = 20µm).

4.2.3 Deletion of SOCS3 in IECs led to increased migration of cells up cecal crypts

Following analysis of crypt dynamics upon infection with *T. muris*, we then focused on analysing the infected data specifically and assessing differences within this cohort of mice to determine whether SOCS3 is implicated in infection-induced cell proliferation of IECs, and whether SOCS3 may play a role in the "epithelial escalator" mechanism that occurs during expulsion of worms. Figure 4.5 (a) differs from that of uninfected mice in figure 4.2 (a) in that there appeared to be more EdU-positive cells in HO-VC mice than HO-WT, with each genotype having on average, 16 ± 2 and 12 ± 2 EdU-positive cells per cecal crypt, respectively. However, there was overlapping variability within each genotype, in figure 4.5 (a), and when a Student's t-test was performed, this difference was not found to be statistically significant ($p=0.18$).

Figure 4.5 (b) also differs from figure 4.2 (b), as there was an observable difference in cell position between the two genotypes (a difference also similar to that seen in 4.5a). The position of the highest EdU-positive cell in HO-VC mice was higher at cell position 20 ± 2, compared to 16 ± 1 in HO-WT mice, although this was not quite significant ($p=0.07$). As described previously in uninfected mice (figure 4.2c), we then analysed the percentage of EdU-positive cells in each "cell region" within the crypt. However, as there was an increase in both crypt depth and proliferating cells upon infection, additional regions were included (21-30 and 30+). During analysis of effects of *T. muris* infection on proliferating cell distribution (figure 4.3c), we found that although there were fewer proliferating cells in the stem cell region, and a higher percentage of proliferating cells in the T.A region, regardless of genotype, differences between uninfected and infected mice were much more significant in HO-VC. Also, infection led to a significantly higher percentage of proliferating cells in the 21-30 region in HO-VC mice only, possibly indicating that IEC-deletion of SOCS3 further increases infection-induced crypt cell migration. This led us to then specifically compare proliferating cell distribution in infected mice. Figure 4.5 (c) shows there was a higher percentage of proliferating cells in the stem cell region, and fewer in the T.A region in HO-WT mice ($66\pm5\%$ and $32\pm5\%$, respectively), compared with HO-VC ($54\pm5\%$ and $39\pm3\%$, respectively). Despite differences in both of these crypt regions, no statistical significance was found. Only one mouse out of 12 was reported to have EdU-positive cells higher than crypt position 30, in both genotypes, so therefore differences in percentages in this region were negligible. In the 21-30 region however, HO-VC mice had a higher percentage of proliferating cells with $7\pm2\%$, compared $1\pm0.6\%$ in HO-WT, with a Student's t-test reaching statistical

significance (p=0.008), thus confirming our hypothesis suggested from results in figure 4.3 (c).

Finally, when measuring cecal crypt depths of infected mice, the results in figure 4.5 (d) contrasted those of uninfected mice in that there was less of a difference in depth between the two genotypes. Average crypt depths were 214±13µm and 211±14µm for HO-WT and HO-VC mice, respectively. In summary, although figure 4.5 (a) and (b) show that IEC-deletion of SOCS3 did not definitively lead to a higher number or position of proliferating cells within cecal crypts following *T. muris* infection, figure 4.5 (c) showed that this deletion did lead to an increase in the percentage of cells further up the crypt, suggesting increased cell migration in these mice. However, as the results obtained here were not associated with an increase in crypt depth, this indicates that even following *T. muris* infection (an intestinal challenge known to induce proliferation, Artis et al. 1999), IEC deletion of SOCS3 did not lead to hyperplasia. These findings also mirror those seen by Cliffe et al. (2005) when describing the "epithelial escalator" mechanism that occurs during worm expulsion in the resistant BALB/c mouse strain, suggesting SOCS3 may contribute to susceptibility of mice to *T. muris*, and possibly impede expulsion of these worms.
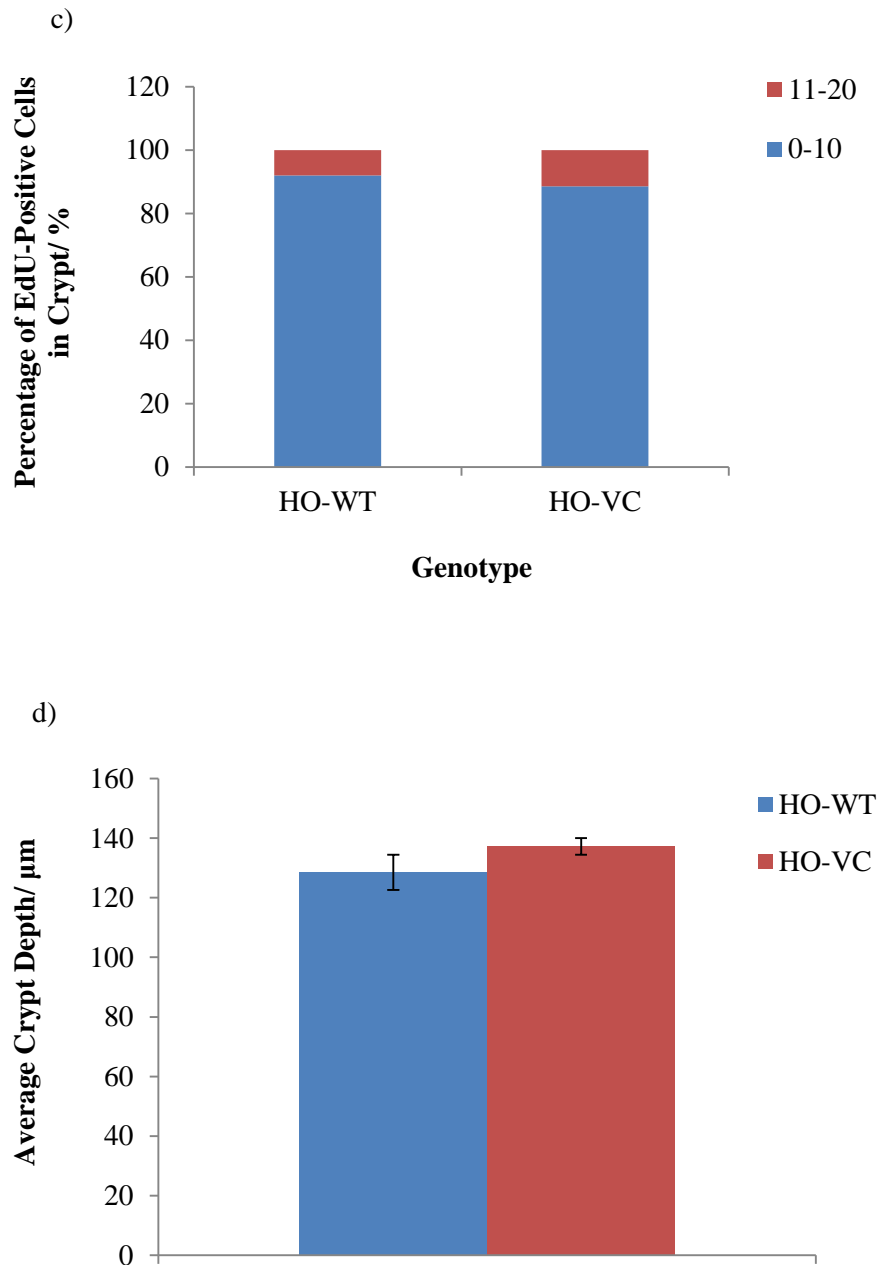
a)

b)

c)

d)
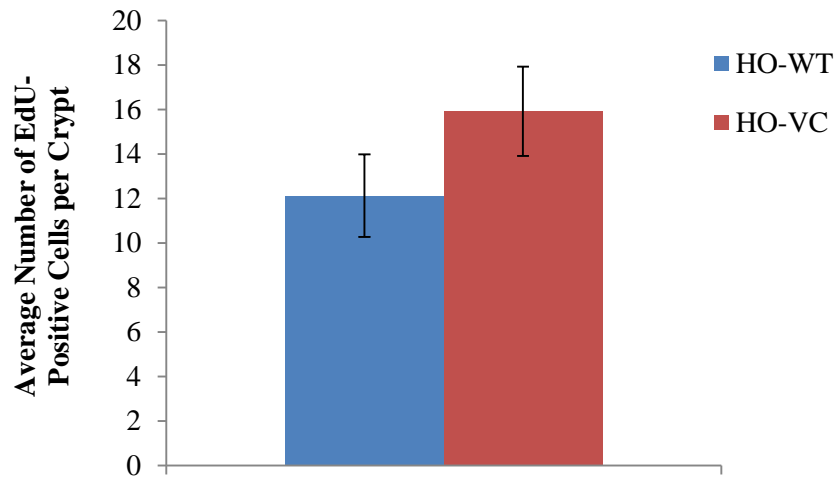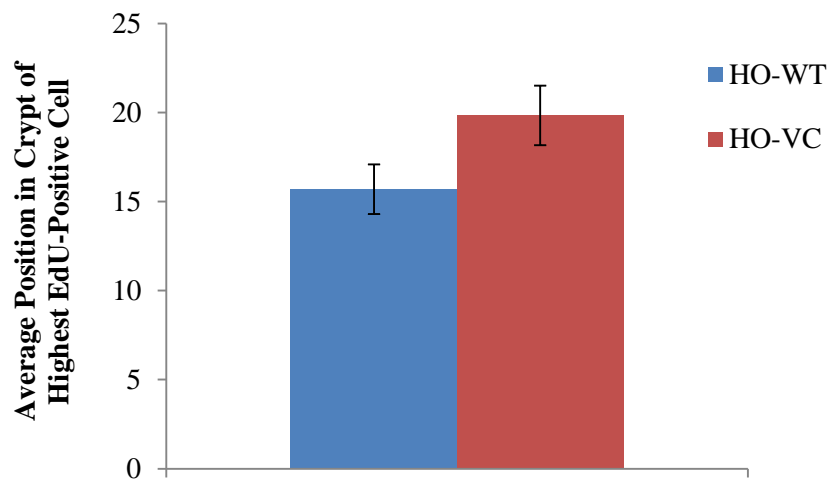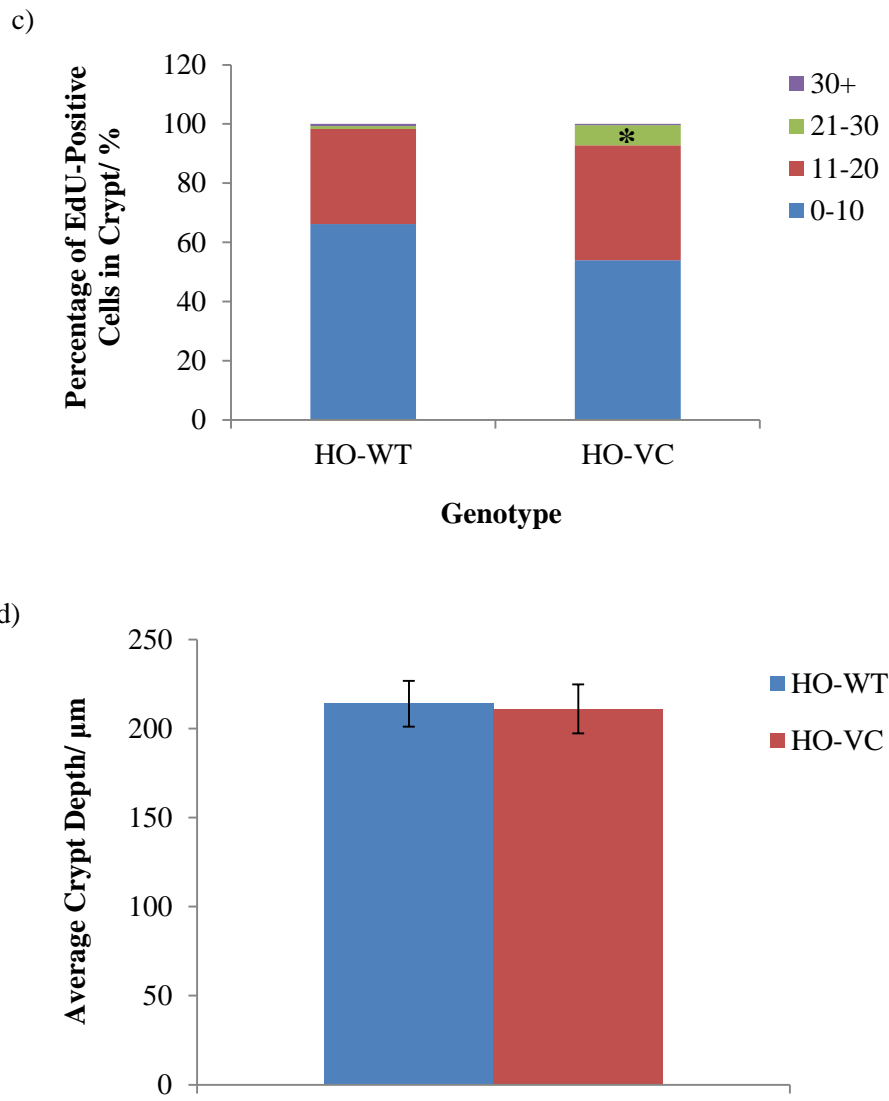
Figure 4.5: Differences in (a) the number of proliferating cells, (b) the position of the highest proliferating cell, (c) distribution of proliferating cells within cecal crypts and (d) crypt depth between wildtype (HO-WT) and conditional SOCS3 knockdown mice (HO-VC) infected with *T. muris* (±SEM). Mice were infected with a low dose of T. muris eggs (25-30 eggs) at 6-8 weeks of age, and ceca were removed 35 days post infection. Following paraffin embedding and microtome sectioning of the cecal tip, the Click-iT® EdU assay was performed according to manufacturer's instructions for assessment of cecal crypt proliferation. Confocal images were analysed blind using multiple crypts per mouse, with averages then taken for the whole genotype. (* = p<0.01, using a two-way Student's t-test) (HO-WT and HO-VC- n=12). (Figure 4.4c modified from Shaw et al., under revision in Immunology and Cell Biology).

4.3 Investigating the roles of SOCS3 and IDO in *Trichuris muris* infection

As shown above, SOCS3 is implemented in the proliferative response to *T. muris* infection and IEC-deletion of SOCS3 supported the "epithelial escalator" mechanism that was shown to aid worm expulsion (Cliffe et al. 2005). Work by Datta et al. (2005) found that IDO was one of several genes upregulated following *T. muris* infection and this protein has also been found to be implicated in the proliferative/expulsion response to this helminth (in addition to its role in tryptophan catabolism, cancer and immune tolerance, Higuchi and Hayaishi 1967, Munn et al. 1998, Uyttenhove et al. 2003). Bell and Else (2011) found that inhibition of IDO led to significant migration of cells up crypts and expulsion of worms without increasing crypt depth. As these mirror the results seen in our SOCS3-deleted mice, we investigated whether there was a relationship between SOCS3 and IDO. For this, we infected HO-WT and HO-VC mice with *T. muris* for 35 days and measured expression of IDO in the cecum using immunofluorescence and western blotting.

4.3.1 Infection with T. muris led to an IDO response in the cecum of wildtype and SOCS3-deleted mice

Figure 4.6 shows confocal microscope images of immunofluorescence staining for IDO in HO-WT and HO-VC *T. muris*- infected mice and shows there was regional expression levels of IDO within the ceca of both genotypes, as depicted by the images with low and high levels of fluorescence. Multiple images were taken per section from individual mice, and even within one section, regional differences in fluorescence were observed. Distribution of IDO was also changeable, ranging from local expression towards the bottom half of cecal crypts (HO-WT, second image), potentially from the goblet cells (as Bell and Else 2011, found), to widespread expression across the whole crypt (HO-VC, second image). This suggests that the *T. muris*-induced IDO response may be localised to the niche of the worm (i.e. the site of egg hatching and worm attachment).
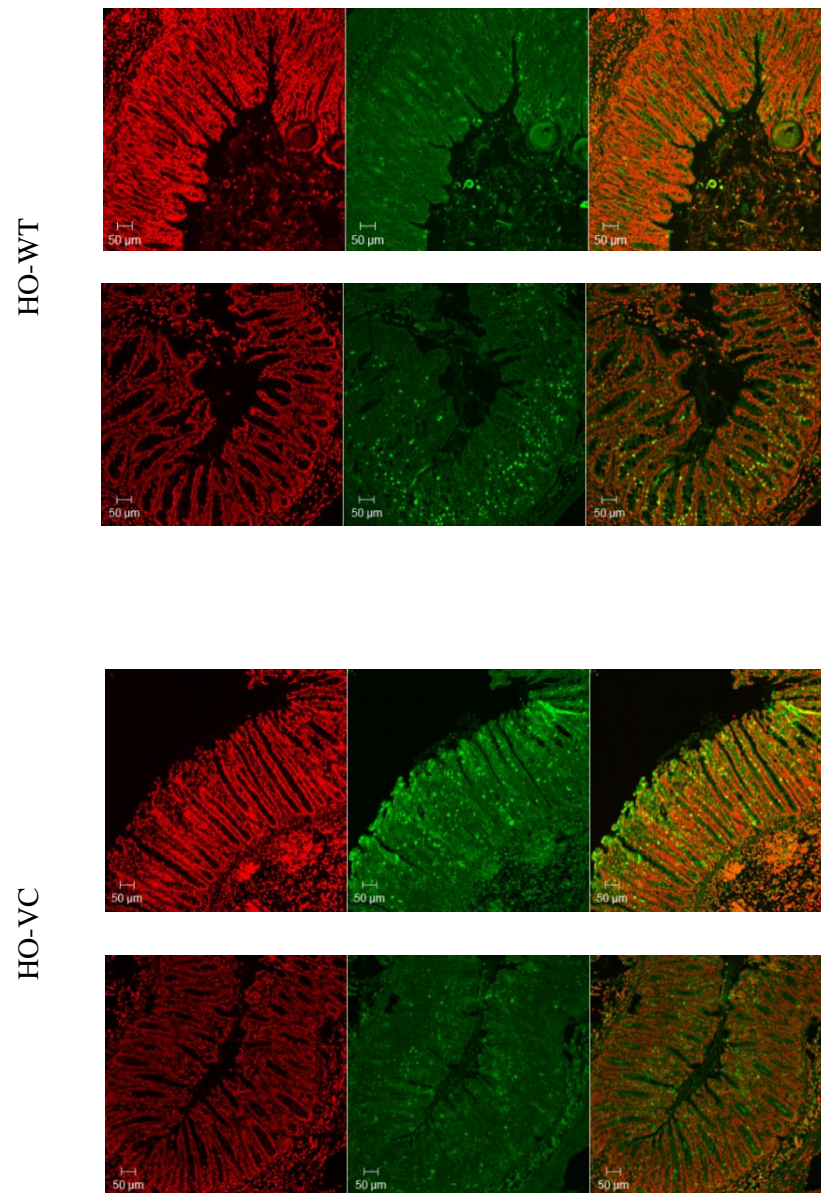
Figure 4.6: Expression of indoleamine 2,3-dioxygenase, using immunofluorescence, in the ceca of wildtype (HO-WT) and conditional SOCS3 knockdown (HO-VC) *T. muris*-infected mice. At 35 days post-infection, ceca were removed following administration of *T. muris* at a low dose, at 6-8 weeks of age. Following paraffin embedding and sectioning, deparaffinisation and rehydration of sections were performed before heat-induced epitope retrieval with sodium citrate buffer. Slides were incubated overnight at 4°C in 1:400 IDO primary antibody (green), with propidium iodide (red) used as a nuclear stain. Slides were imaged blind using a Zeiss confocal microscope, at 10x magnification. (Scale bar = 50µm, n=5). (Images modified from Shaw et al., under revision in Immunology and Cell Biology).

4.3.2 IDO protein expression was increased following T. muris infection

As we were unable to determine differences in IDO expression in cecal crypts of HO-WT and HO-VC mice using immunofluorescence, we obtained mucosal cecal scrapes and performed western blotting to investigate expression of IDO protein in these mice. As previously shown by Datta et al. (2005) and Bell and Else (2011), IDO expression was increased following *T. muris* infection, and this was irrespective of genotype (figure 4.7a and b). However, this increase was only found to be statistically significant in HO-WT mice (p=0.03). Within uninfected mice, IDO protein expression was 2.4-fold higher in absence of IEC SOCS3, although this was not quite significant (p=0.07). This trend was not observed in infected mice, with approximate IDO protein fold-changes of 5 obtained for both genotypes, although there was a large amount of variability within HO-VC mice (figure 4.7b), likely due to dissimilarities in sample sizes between genotypes. This may also contribute to the insignificant differences calculated between uninfected mice.

In conclusion, using western blotting, we confirmed *T. muris*-induced expression of IDO in our mice. As the "epithelial escalator" mechanism responsible for aiding expulsion of worms is associated with both reductions in IDO, and IEC SOCS3, it was perhaps to be assumed that infected HO-VC mice would express less IDO than infected HO-WT. However, due to differences in sample sizes between infection groups, as well as using heterogeneous mucosal samples, we were unable to confirm this. We did observe a tendency of increased IDO following loss of IEC SOCS3 in uninfected mice, and this supports our *in vitro* findings.

a)

IDO
42 kDa

α-Tubulin
55 kDa

| **HO-WT** | **HO-VC** | **HO-WT** | **HO-VC** |

Uninfected | **Infected**

b)
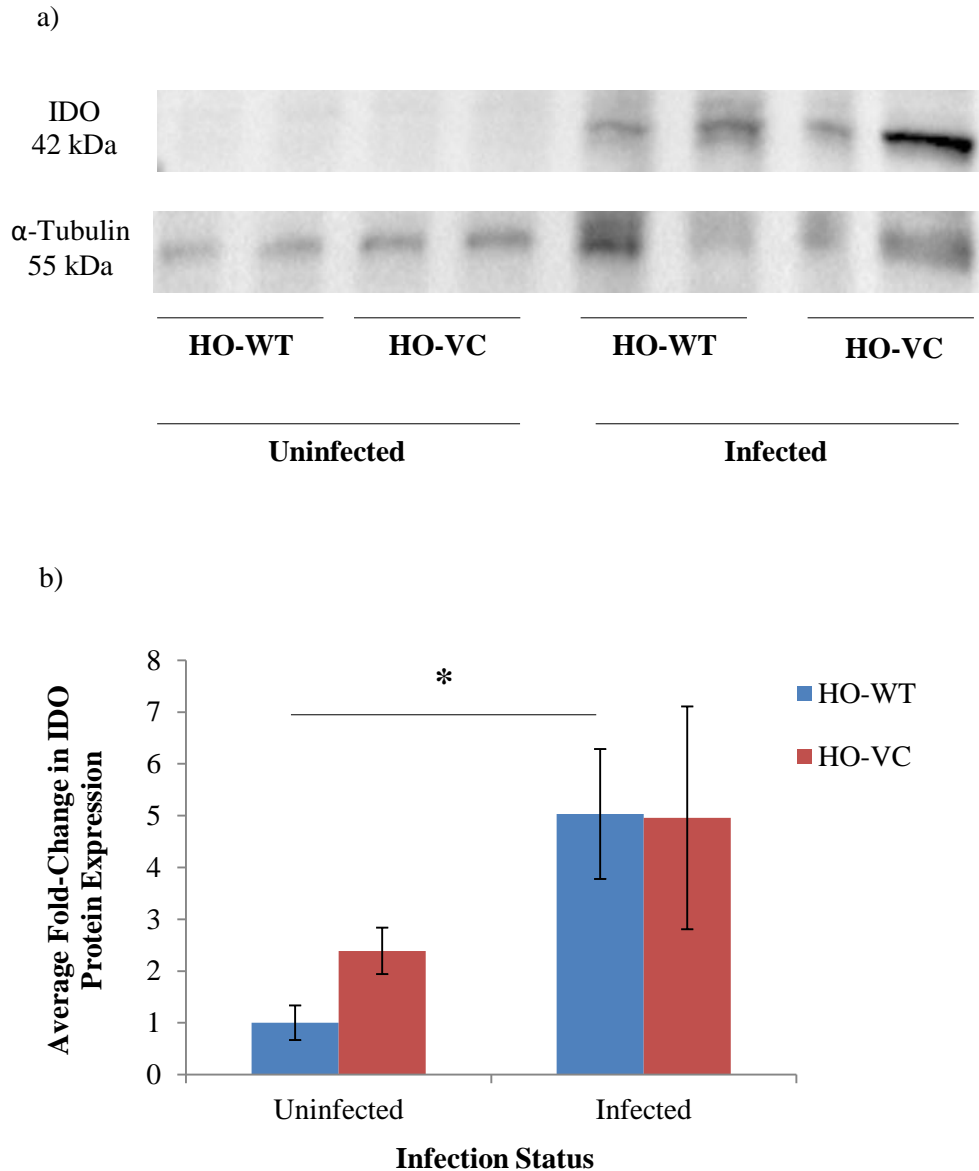
Figure 4.7: Mucosal indoleamine 2,3-dioxygenase in uninfected and *T. muris*-infected wildtype (HO-WT) and conditional SOCS3 knockdown (HO-VC) mice, using western blotting. At 35 days post-infection, ceca were removed following administration of *T. muris* at a low dose, at 6-8 weeks of age, with RIPA buffer used to obtain cecal mucosal scrapes. Samples were run on 10% SDS-PAGE gels before transfer onto nitrocellulose membranes and incubation in IDO primary antibody at 1:750 overnight. Membranes were then incubated in secondary antibody for 1 hour at room temperature. Membrane imaging and densitometry was carried out using a ChemiDoc™ MP Imaging System and Image lab software, with values relative to uninfected HO-WT. (* = $p<0.05$, using a two-tailed t-test, within genotypes). (HO-WT- n=5, HO-VC- n=2). (Figure 4.7b modified from Shaw et al., under revision in Immunology and Cell Biology).

4.4 IDO Immunofluorescence in an AOM/DSS mouse tumour model

The use of the tumour-inducing agent, AOM, with DSS as a tumour promoter, has become very common in the study of CAC. The use of both agents has shown to result in a higher incidence rate of colonic tumours, in a shorter period of time, compared to using either AOM or DSS alone (De Robertis et al. 2011). Following metabolic activation of AOM, macromolecules within the colon become alkylated, and methyl groups are added to guanine residues within DNA, forcing mutations to occur. Following inheritance and accumulation of these mutations, a multi-step process occurs, starting with the formation of aberrant crypt foci (ACF- early pre-neoplastic lesions). After proliferation of these foci, microadenomas form, before enlarging to polyps and ultimately, adenocarcinomas (De Robertis et al. 2011), which have been found to be similar in pathology to adenocarcinomas found in humans (Ward et al. 1973).

IDO has been found to be expressed in multiple cancer types in both humans and rodents (Yasui et al. 1986, Uyttenhove et al. 2003) and also by several antigen presenting cells (APCs) (Munn et al. 1999, Hwu et al. 2000). At tumour sites and tumour-draining lymph nodes, IDO exerts anti-proliferative effects on local T-cells due to depletion of the essential amino acid, tryptophan and increase in tryptophan catabolites (Fallarino et al. 2002, Frumento et al. 2002). This leads to suppression of the host immune system and induces a state of tolerance toward the tumour. Because of this, IDO expression (in particular high expression) can be associated with poor prognosis and metastasis in a multitude of tumours (Okamoto et al. 2005, Brandacher et al. 2006, Ino et al. 2006).

Previous research has found that IEC-deletion of SOCS3 in mice led to an increase in proliferation and crypt hyperplasia following treatment with AOM/DSS (Rigby et al. 2007), and in patient biopsy samples, reduced expression of SOCS3 correlated with progression to CAC (Li et al. 2010), so therefore we wanted to investigate whether there was a relationship between SOCS3 and IDO in colon cancer *in vivo*.

4.4.1 IEC-deletion of SOCS3 led to increased IDO in AOM/DSS colon tumours

AOM/DSS is known to induce tumours in the colon of mice, and as anticipated, multiple tumours were seen in the colons of both HO-WT and HO-VC mice, as depicted by the asterisks in the left panels of images in figure 4.8. IDO has been found to be expressed in

colonic tumours (Uyttenhove et al. 2003, Brandacher et al. 2006), so we expected to see fluorescence corresponding to IDO in both groups of mice (as shown in figure 4.8a and b). However, the fluorescence seen in HO-VC mice was brighter than that of HO-WT mice, indicating that expression of IDO within tumours was further increased following IEC-specific deletion of SOCS3, suggesting SOCS3 and IDO are implicated together in colon cancer. Given the previously known functions of IDO in cancer, this result could suggest a possible role for SOCS3 in IDO-mediated tolerance and suppression of the immune system in colon cancer.
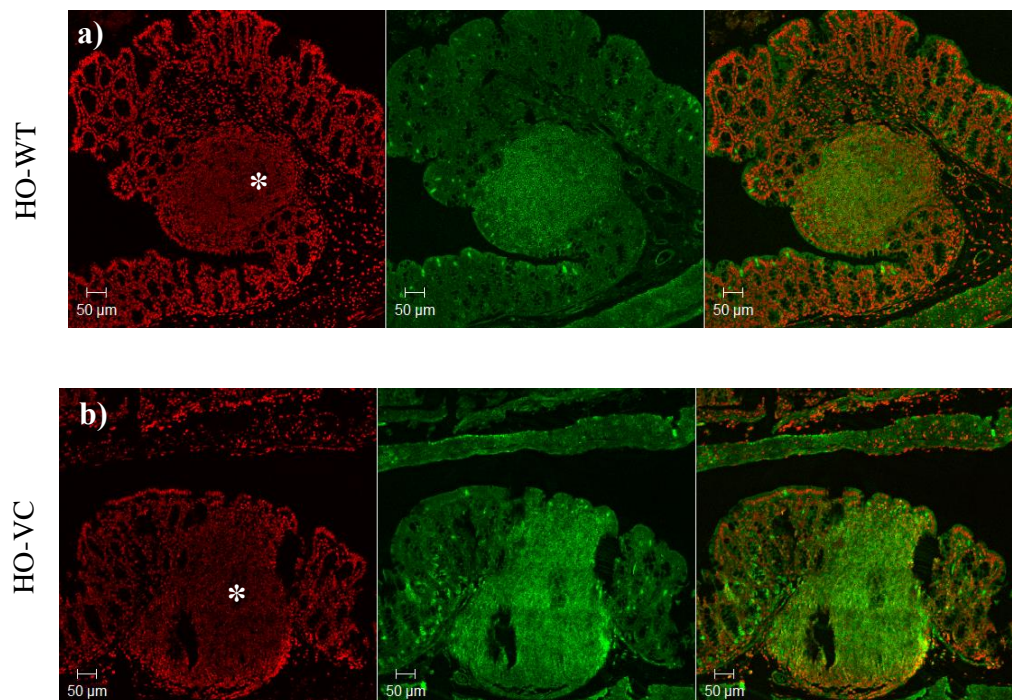
Figure 4.8: Expression of indoleamine 2,3-dioxygenase, using immunofluorescence, in the colon of wildtype (HO-WT) and conditional SOCS3 knockdown (HO-VC) mice in an AOM/DSS model. Embedded sections were received from P.K Lund, and AOM/DSS treatment was administered as described in Rigby et al. (2007). Deparaffinisation and rehydration of sections was performed before heat-induced epitope retrieval with sodium citrate buffer. Slides were incubated overnight at 4°C in 1:400 IDO primary antibody (green), with propidium iodide (red) used as a nuclear stain (right section = merged image). Slides were imaged blind using a Zeiss confocal microscope, at 10x magnification. (Scale bar = 50µm, n=3 for each genotype) (* depicts tumour location).

4.5 Discussion

Mice are often the model of choice in studies investigating intestinal structure and pathways involved in intestinal turnover (Potten and Loeffler 1990, Potten 1998). More specific to our research interests, mice have also been used for studying the functions of SOCS3, with IEC-conditional knockout mice able to be generated through the use of the Cre-LoxP system (as SOCS3$^{-/-}$ mice are embryonic lethal, Roberts et al. 2001, Croker et al. 2003). This allows for the investigation of SOCS3's associations with multiple cell signalling pathways and disease processes (such as cancer and IBD). However, very little research has been conducted into how SOCS3 is involved in normal homeostasis of the intestine. Therefore, we aimed to investigate SOCS3's role through assessment of proliferation in mice with SOCS3 deleted specifically in IECs, in comparison with wildtype mice. Additionally, also using these same genotypes, we investigated how SOCS3 is implicated upon dysregulation of intestinal homeostasis. This was achieved through assessment of proliferation following infection with the helminth, *T. muris*, which naturally infects mice (cited by Cliffe and Grencis 2004) and is known to increase intestinal cell proliferation (Artis et al. 1999). Therefore, this is a more physiologically relevant model of proliferation than other methods which often involve chemical-induction of proliferation.

We first investigated how intestinal SOCS3 affected basal proliferation in the unchallenged state, and found very little difference in the assessed cecal crypt properties between the two genotypes, an observation also seen by Rigby et al. (2007). This may indicate that at the basal level, intestinal SOCS3 levels must be reasonably low due to a lack of a different phenotype in its absence. Upon infection with *T. muris* however, both genotypes exhibited increases in the number of proliferating cells, increases in cell migration up cecal crypts, and also increases in crypt depth. This result has also been seen in other mice strains, such as susceptible AKR and SCID mice as well as resistant BALB/c mice (Artis et al. 1999, Cliffe et al. 2005). Increased intestinal cell turnover and migration has also been observed upon infection with several other intestinal parasites (cited by Artis et al. 1999), indicating this is a host response. This was confirmed by Artis et al. (1999), who also found that this response was IFN-γ-mediated, as depletion using an IFN-γ-neutralising antibody led to a decrease in proliferation.

The responses seen may also be due to the dose of *T. muris* administered during infection. Low doses consist of approximately 25-30 eggs, compared to a high dose, where

approximately 200 eggs are administered, and depending on genetic background, mice either expel worms or develop chronic infection following a high dose, due to the dominance of Th2 and Th1 immune responses, respectively. Th2 cytokines, such as interleukins-4, -5, -9, -10 and -13 aid worm expulsion due to the individual roles in recruiting and promoting growth of B and T cells, and exerting anti-inflammatory effects by inhibiting cytokines associated with the Th1 response (Else and Grencis 1991). However, due to the small quantity of eggs administered with a low dose, mice generate inappropriate immune responses, dominated by Th1 cytokines, such as IFN-γ, IL-18 and IL-12, which also promotes production of IFN-γ (Else and Grencis 1991, Bancroft et al. 1997, Helmby et al. 2001), and this results in insufficient expulsion of worms. Mice used here were infected with a low dose of *T. muris* eggs so therefore Th1 responses would have been prevalent. This would have led to higher increases in proliferation than if a high dose had been administered, as more susceptible mice exhibit higher levels of intestinal proliferation throughout infection in an attempt to aid expulsion (Cliffe et al. 2005), and C57BL/6 mice are resistant to *T. muris* at high doses (Richard et al. 2000).

Focusing on SOCS3's role in *T. muris*-induced proliferation, we found that infected HO-VC mice exhibited higher proportions of proliferating cells further up the cecal crypts and potentially higher average positions of proliferating cells and an increase in the number of proliferating crypt cells, indicating that following *T. muris* infection, deletion of SOCS3 increased IEC turnover. This was not accompanied by an increase in crypt depth, and would have been indicative of hyperplasia- a state of increased proliferation that is detrimental, presumably due to an increase in surface area, and therefore the niche in which worms can attach. Also, these are phenotypes found to be displayed by resistant BALB/c mice and are associated with the "epithelial escalator" phenomenon, presumably where worms are displaced through migration of IECs up crypts and then shedding from the tip of the villi, resulting in more effective worm expulsion (Cliffe et al. 2005). SOCS3 has been shown to limit proliferation following intestinal challenge with AOM/DSS (Rigby et al. 2007), so the presence of SOCS3 may play a role in susceptibility to *T. muris* infection in mice and an inability to expel worms sufficiently. Shaw et al. (under revision in Immunology and Cell Biology) found that 35 days following low dose *T. muris* infection, IEC deletion of SOCS3 led to a significantly higher proportion of mice with lower worm burdens (<10) compared with SOCS3 sufficient mice, demonstrating a positive, functional outcome of the increase in cell turnover.

Following the discovery that SOCS3 was implicated in the "epithelial escalator" process during *T. muris* infection, along with the results from Bell and Else (2011), who found that inhibition of IDO also aided worm expulsion, we aimed to investigate whether there was a relationship between SOCS3 and IDO during helminth infection in mice. There was a suggestion of differences in expression of IDO between infected HO-WT and HO-VC mice, as measured using immunofluorescence, although expression was variable within genotypes, and not just between. However, it can be difficult to draw conclusions from immunofluorescence experiments in some instances, as it is a semi-quantitative technique, and as we found, expression of proteins of interest (in our case, IDO) can be variable, even within one sample. In order to obtain a more definitive answer, a more quantitative experimental technique could be used, such as flow cytometry, for example. Goblet cells are a source of IDO within the gut (Bell and Else 2011), and using flow cytometry, goblet cells could be gated in the sample, by isolating trefoil factor 3-positive cells for example, as this protein is involved in protection of the intestinal epithelium and is a goblet cell marker (cited by Kim et al. 2014). Through inhibition of cell exportation and the use of an IDO antibody, we could compare IDO expression between the two genotypes, and also possibly pinpoint the cell source of potential differences.

IDO and SOCS3 have been found to have an inverse relationship, in that production of SOCS3 leads to a decrease in IDO, due to proteasomal degradation of IDO by SOCS3 (Orabona et al. 2008), and absence of SOCS3 (through siRNA) led to IDO production and subsequent tryptophan catabolism following activation of Stat3 by IL-6, both in dendritic cells (Orabona et al. 2005). Therefore, it was hypothesised that IEC deletion of SOCS3 (achieved here by using the Villin-driven Cre-LoxP system) would lead to an increase in IDO (as found *in vitro* in chapter 3). However, our results here, combined with previous findings, indicate that deletion of SOCS3 (in IECs), and inhibition of IDO (Bell and Else 2011), promotes increased IEC turnover and expulsion of *T. muris* worms. Collectively, this suggests that perhaps the role of IDO, and its relationship with SOCS3, could be context dependent. Additionally, for the immunofluorescence experiments, the cecal tip was removed and then embedded and sectioned before antigen retrieval and antibody staining for imaging. This is only a small part compared to the rest of the organ, and the variability in results suggests there may be a certain niche within the cecum where the *T. muris* worms occupy and that perhaps not all areas of the cecum are affected during infection. The results may also suggest that in addition to a specific cecal niche, IFN (which is increased during *T. muris* infection and is a potent inducer of IDO) may have a limited range of effect so it is possible that a more definitive answer of IEC deletion on *T. muris*-induced IDO expression could be obtained if

sections had been taken from the whole cecum (although in this case, the rest of the cecum was used for taking mucosal scrapes and determining worm burden, Shaw et al., under revision in Immunology and Cell Biology).

Western blotting was also performed to help determine the relationship between intestinal SOCS3 and IDO at the protein level. We found that regardless of genotype, *T. muris* infection increased protein expression of IDO up to 5-fold, and this is supported by the findings of Datta et al. (2005) and, Bell and Else (2011). We also observed there was a tendency of increased IDO in HO-VC mice in the absence of infection; significance was not quite reached (p=0.07) although this may have been due to the differences in sample sizes between the two genotypes. Had the sample size of uninfected HO-VC been equal to that of uninfected HO-WT (n=5), there may have been a larger (possibly significant) increase in IDO in HO-VC. This tendency however does help to confirm our *in vitro* findings that deletion of SOCS3 led to increased IDO expression in IECs, and is in agreement with findings of Orabona et al. (2008) that SOCS3 is responsible for proteasomal degradation of IDO in DCs. Additional experiments to further test this hypothesis would be to investigate whether overexpression of IEC SOCS3 resulted in reduced IDO compared to both HO-WT and HO-VC. The observation of increased IDO in uninfected HO-VC mice (compared to HO-WT) was not replicated in *T. muris*-infected mice, with both HO-WT and HO-VC expressing similar levels of IDO. This was due to the large amount of variability in IDO protein expression in infected HO-VC mice, most likely as a result of the small sample size. As the protein used in these experiments was from cecal mucosal scrapes, rather than the IECs specifically, there would have been a heterogeneous cell population (i.e. murine and bacterial) and this may have obscured proteins when assessed by western blotting. Also, immune cells are generally more responsive than IECs (otherwise IECs would be eliciting inappropriate immune responses when in contact with non-pathogenic microflora, resulting in increased inflammation, Otte et al. 2004), and are also known to induce IDO (Munn et al. 1999, Hwu et al. 2000), and this would have occurred in response to *T. muris* infection irrespective of genotype, so may have masked differences in IEC IDO.

In addition to inhibiting intestinal proliferation, thereby preventing expulsion of worms during *T. muris* infection, IDO may also hinder expulsion through promoting tolerance, through depletion of the essential amino acid, tryptophan and increased tryptophan catabolites as a result, which leads to suppression of T cell proliferation (Fallarino et al. 2002, Frumento et al. 2002), and also promotion of naive T cell differentiation into regulatory T cells (Tregs)

(Fallarino et al. 2006). Tregs also contribute to inducing tolerance through prevention of immune system activation (through secretion of anti-inflammatory cytokines, for example). IDO is implicated in cancer too for these same reasons- in addition to immune cells, tumour cells are also capable expressing IDO, in order to suppress the immune system and remain "undetected" so tumourigenesis (and potentially metastasis) can continue to occur. IDO has been found in a multitude of tumour types, with high levels of IDO associated with poor prognosis (Uyttenhove et al. 2003, Okamoto et al. 2005, Brandacher et al. 2006, Ino et al. 2006). Additionally, SOCS3 is associated with cancer as reductions or silencing through promoter hypermethylation have been found in many cancer types (He et al. 2003, Weber et al. 2005, Ogata et al. 2006, Rigby et al. 2007). We used immunofluorescence to determine whether loss of SOCS3 led to increased IDO expression in an AOM/DSS mouse model. As expected, administration of AOM/DSS induced colonic tumours in mice, irrespective of genotype, with fluorescence corresponding to IDO expression also seen with both genotypes (HO-WT and HO-VC), and was thus in conjunction with previous findings of IDO expression in tumours, and in particular colonic tumours (Uyttenhove et al. 2003, Brandacher et al. 2006, Ogawa et al. 2012). However, when comparing the two genotypes, there appeared to be more fluorescence within tumours in HO-VC mice, indicating that deletion of IEC SOCS3 led to increased tumoural expression of IDO. These findings help establish the inverse relationship between SOCS3 and IDO, as SOCS3 is capable of ubiquitinylating and degrading IDO (in DCs) (Orabona et al. 2008), but following IEC deletion of SOCS3, the increase in fluorescence corresponding to an increase in tumoural IDO was most likely due to a lack of proteasomal degradation. This suggests that the role of SOCS3 as a tumour suppressor is not limited to inhibiting cell proliferation but also extends to IDO degradation, which helps to uphold immune surveillance against tumours. Conversely, reduction/loss of SOCS3 that can ultimately result in tumourigenesis is a crucial event that can lead to a lack of IDO proteasomal degradation, thus promoting immune tolerance towards the tumour(s).

Several studies have demonstrated the tumour-promoter effects of IDO from the reduction in tumour size *in vitro* and *in vivo*, following either silencing of IDO through RNAi (Zheng et al. 2006), or through administration of an IDO inhibitor, known as 1-methyl tryptophan (1-MT) (Friberg et al. 2002, Muller et al. 2005). 1-MT prevents IDO activity through competition inhibition; binding to IDO and preventing binding and subsequent catabolism of tryptophan (Cady and Sono 1991). More specifically, increased tumour volume was reported in mice injected with IDO-positive mast cell tumours, compared to mice injected with control mast cell tumours (using a mouse mastocytoma cell line, P815B) (Uyttenhove et al. 2003). Similar to the studies mentioned, tumour volume decreased in mice that had been injected with IDO-

positive P815B cells and treated with 1-MT, relative to IDO-positive P815B cells alone. They determined that this reduction in tumour volume was T-cell-dependent, as there were no differences found (in tumour volume) between mice injected with IDO-positive P815B cells, and T-cell depleted mice who had been administered both IDO-positive P815B cells and 1-MT. To assess the effects of IDO within the tumours of the AOM/DSS-treated mice, IDO could be depleted, using either RNAi or 1-MT. It is to be presumed that reduction/inhibition of IDO would result in decreased tumour size in the AOM/DSS mice, regardless of genotype. However, as previous findings revealed an increase in colonic tumour number and size in AOM/DSS mice following IEC deletion of SOCS3 (Rigby et al. 2007), this observation may also be replicated following treatment with 1-MT.

From our *in vivo* experiments, we have been able to reveal further implications of SOCS3 following induction of intestinal proliferation, through infection with the helminth, *T. muris*, and in CAC, following treatment with AOM/DSS. SOCS3's role as a tumour suppressor was reiterated as results from our immunofluorescence experiments suggested that loss of IEC SOCS3 increased IDO expression, which is known to suppress anti-tumour immunity and potentially lead to increased tumour size. However, a functional outcome of IEC SOCS3 deletion was observed during *T. muris* infection, due to increased crypt cell migration, which was associated with more efficient worm expulsion (Shaw et al., under revision in Immunology and Cell Biology). Infection with *T. muris* is a more physiologically relevant and less harsh method of promoting intestinal proliferation than using AOM/DSS, which may explain the difference in phenotypes obtained. In contrast, it may be that the role of SOCS3 in regulating intestinal homeostasis (and subsequent outcomes) is context dependent, depending on the source of increased proliferation.

Chapter 5:

The use of the fruit fly, *Drosophila melanogaster*, in establishing an *in vivo* model for determining the role of SOCS36E-mediated homeostasis in ageing

5.1 Rationale

In vitro and *in vivo* experiments investigating the role of SOCS3 in normal IEC homeostasis found that SOCS3 is responsible for limiting proliferation following the addition of multiple TLR ligands, and following helminth infection, respectively. Despite previously published findings and results shown here concerning SOCS3, very little research has been conducted into the functional outcomes of SOCS3 on organisms as a whole, rather than at the cellular or tissue level. *Drosophila* have been used for many decades as a model organism for several aspects of human health; one in particular being ageing and behaviour. Reasons for this include: significantly shorter lifespans (especially when compared to mice and humans), genetic and physiological similarities to humans and the large number of commercially available fly lines (Helfand and Rogina 2003, Apidianakis and Rahme 2011). Collectively, this produces an organism where the effects of any genetic manipulations can be seen throughout the whole lifespan.

Our focus in this project has been on (intestinal) Jak/Stat, and more specifically SOCS proteins, with *Drosophila* possessing their own, simplified Jak/Stat pathway, in which 3 SOCS proteins are associated (SOCS16D, SOCS44A and SOCS36E, Hou et al. 2002), all of which possess mammalian homologues. The discovery that multiple SOCS proteins are evolutionarily conserved and show homology between flies and mammals signifies the importance of these proteins in organism functioning. We chose to investigate the role of SOCS36E in the *Drosophila* midgut, with this protein being a functional homologue of mammalian SOCS3 (as well as SOCS1, SOCS2 and CIS) (Callus and Mathey-Prevot 2002), and also the most documented out of the three SOCS proteins. Like SOCS3, SOCS36E has been found to limit cell proliferation in *Drosophila* through inhibition of the Jak/Stat pathway (Callus and Mathey-Prevot 2002, Bina et al. 2010, Buchon et al. 2010), and dysregulation of IEC regulation and repair, as well as damage to the midgut, have shown to be detrimental to the lifespan and survival of *Drosophila* (Amcheslavsky et al. 2009, Apidianakis and Rahme 2009, Apidianakis et al. 2009, Buchon et al. 2009b, Chatterjee and Ip 2009, Jiang et al. 2009 Biteau et al. 2010). However, little has been published on the effects of Jak/Stat, or more specifically, SOCS36E, on fruit fly survival. This led us to use a *Drosophila* model of ISC-specific knockdown of SOCS36E to determine how the impact of SOCS36E on cell proliferation affects ageing, through assessment of lifespan. We chose to use *Drosophila* as our model organism for survival and behavioural analysis rather than mice (in this chapter and the next chapter, respectively), with one reason being lower monetary and ethical costs for fruit flies studies, compared with using mice. Additionally, in order to obtain reliable

experimental findings for lifespan and behavioural analyses, it is preferable to use large sample sizes and also carry out experimental repeats. The average lifespan of a fruit fly is approximately 2-3 months, compared with an average lifespan of 1.5-2 years in a laboratory mouse (cited on WWW, Transgenic Animal Web). However, the longest lived laboratory mouse had a lifespan of 4 years (cited on WWW, Human Ageing Genomic Resources). Therefore, it is not feasible to perform these studies on mice, with respect to monetary and time costs.

5.2 Assessment of ISC SOCS36E deficiency on lifespan

5.2.1 ISC-specific knockdown of SOCS36E led to a shortening of both median and maximum lifespan.

With regards to the experiments performed on *Drosophila* within this and the next chapter, three experimental genotypes were used. In order to generate the knockdown flies, we used the GAL4/UAS system, with the GAL4 gene able to restrict activation of gene transcription to a specific tissue or cell type. This can only occur when a GAL4-containing fly is crossed with an Upstream Activation Sequence (UAS)-containing fly. UAS is located next to the gene of interest and contains GAL4 binding sites (Brand and Perrimon 1993). In our case, we used a UAS-SOCS36E RNAi fly line crossed with an EsgGAL4 line, in order to target knockdown of SOCS36E specifically in the Esg+ ISCs in the midgut (Micchelli and Perrimon 2006). In order to ensure our knockdown was specific to adult flies, our EsgGAL4 flies were also coupled with GAL80^{ts} which is temperature sensitive, so ensures that activation of gene transcription only occurs above the non-permissive temperature of 28°C when GAL4 is no longer repressed by GAL80^{ts} (McGuire et al. 2003). Therefore, flies were only maintained at this temperature following eclosion. For control genotypes, both of the fly lines used to generate the knockdown flies, EsgGAL4, GAL80^{ts}, and UAS-SOCS36E RNAi were individually crossed to wildtype, white^{Dahomey} (w^{Dah}) flies.

A pilot lifespan experiment was first conducted using EsgGAL/SOCS flies and both control genotypes to determine the cell drivers were functioning and to see whether there were any initial differences in lifespan amongst the three genotypes. Figure 5.1 shows that the lifespan of all genotypes was similar until approximately day 30, indicative of no early non-ageing related deaths. EsgGAL/SOCS flies had both the lowest median and maximum lifespans, with table 5.1a displaying the percentage differences between these and both control genotypes. Additionally, as shown in table 5.1a, the median and maximum lifespans of both EsgGAL/+

and SOCS/+ flies were not too dissimilar from each other, confirming their use as suitable controls in following experiments.

To confirm the observed lifespan effects in SOCS36E knockdown flies, a chi-squared p-value log-rank test was performed to determine whether the differences seen in survival between EsgGAL/SOCS and the two control genotypes were statistically significant, with p-values of $p < 0.0001$ generated, confirming that SOCS36E knockdown did negatively affect lifespan (shown in table 5.1b). Additionally, a p-value of $p > 0.05$ was calculated between EsgGAL/+ and SOCS/+, affirming that any small differences found between the two control genotypes were not statistically significant. In conclusion, knocking down SOCS36E in ISCs led to a reduction in both median and maximum lifespan, when compared with both control genotypes. Also, we hypothesised that knockdown of SOCS36E may result in increased midgut proliferation due to decreased regulation of the Jak/Stat pathway. The reductions in median and maximum lifespans in EsgGAL/SOCS flies may suggest that they are reasonably healthy at young ages, but become more susceptible at older ages and are less able to cope with a lack of midgut homeostasis.

Genotype	Median Lifespan/ Days	Maximum Lifespan/ Days
EsgGAL/SOCS	43.5	50.5
EsgGAL/+	47.5	60.0
SOCS/+	49.0	56.0

Percentage difference compared to EsgGAL/SOCS	Median Lifespan/ Days	Maximum Lifespan/ Days
EsgGAL/+	+8.4%	+15.8%
SOCS/+	+11.2%	+9.8%

b)

Chi-squared p-value for log-rank test on survivorship data	EsgGAL/SOCS	EsgGAL/+	SOCS/+
EsgGAL/SOCS	x	2.11E-10	1.70E-08
EsgGAL/+		x	0.43
SOCS/+			x

Table 5.1: (a) The median and maximum lifespans, and percentage differences in both lifespans between SOCS36E knockdown female flies and relevant controls. (b) P-values calculated using a chi-squared p-value log-rank test to determine statistical significances between lifespan differences in all three experimental genotypes.
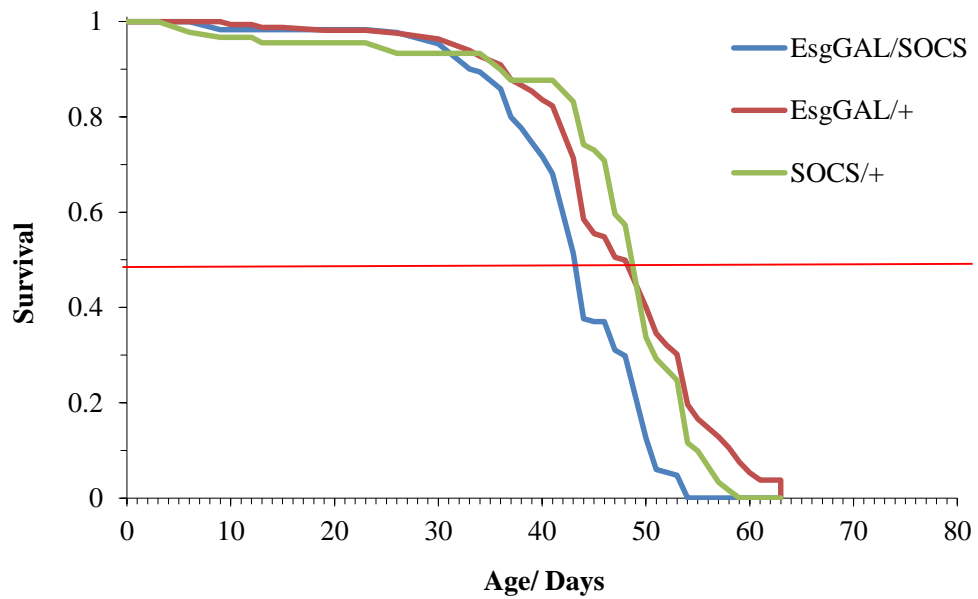
Figure 5.1: Lifespan analysis of SOCS36E knockdown female flies, compared with control genotypes, EsgGAL/+ and SOCS/+. Deaths were recorded three to five times over a period of five days each week, with median and maximum lifespans determined by the time points when 50% (depicted by the red line above) and 10% of each genotype remained, respectively. (EsgGAL/SOCS- red, n=190, EsgGAL/+ - blue, n=170, and SOCS/+ - green, n=90). Differences in lifespans between EsgGAL/SOCS, and EsgGAL/+ and SOCS/+ were calculated using a chi-squared p-value log-rank test- p<0.0001.

5.3 Measuring gut levels of SOCS36E using quantitative PCR

5.3.1 SOCS36E mRNA levels were not reduced in both male and female EsgGAL/SOCS flies

In order to be able to interpret the lifespan data, qPCR was carried out to confirm that the RNAi resulted in a knockdown of SOCS36E mRNA levels in male and female flies. Guts of 10 day old experimental flies were dissected, and following RNA extraction and cDNA synthesis, qPCR was performed, with SOCS36E mRNA levels normalised to those of Actin 5C, and results then compared to those of the EsgGAL/+ control genotype within each gender, in order to determine fold-changes. Figure 5.2 shows that there was no reduction in SOCS36E mRNA expression in both (a) female and (b) male EsgGAL/SOCS flies, compared with the two control genotypes. There was a 1.16-fold increase in SOCS36E mRNA in SOCS/+ relative to EsgGAL/+ females, which was a fairly small difference, thus further reiterating their use as comparative controls. However, figure 5.2 (a) shows there was actually an increase in SOCS36E mRNA levels in EsgGAL/SOCS females (58% and 35% higher than EsgGAL/+ and SOCS/+ females, respectively). Figure 5.2 (b) shows there was much less variability between all three experimental male genotypes, with EsgGAL/+ and SOCS/+ flies expressing almost identical amounts of SOCS36E mRNA, with a 1.01-fold increase found, similar to the result obtained in female flies. SOCS36E knockdown males were found to also have higher gut levels of SOCS36E, although the percentage differences were smaller than those calculated in females- 7% and 5% increases compared to EsgGAL/+ and SOCS/+, respectively. Despite the reported increases, statistical analysis using a one-way ANOVA revealed there were no significant differences between any of the three experimental genotypes, for both male and female flies ($p > 0.05$). Therefore, using this particular method, we cannot confirm that the EsgGAL/SOCS flies did in fact have reduced SOCS36E mRNA levels in their ISCs. Consequently, qPCR may not have been a sensitive enough technique for detecting knockdown of SOCS36E in ISCs, due to ISCs making up a small proportion of the total number of midgut cells (approximately 10%, Ohlstein and Spradling 2006), with whole midgut mRNA levels assessed here. Despite this, we were able to obtain a behavioural phenotype through a reduction in lifespan in female flies, and, increased stress resistance in both male and females (explored further in Chapter 6), which is an indication of phenotypic differences between EsgGAL/SOCS flies and the control genotypes. Also, the increased stress resistance in male flies (in addition to females), suggests that the lack of a phenotype regarding lifespan is genuine, and not due a lack of knockdown.

a)

b)
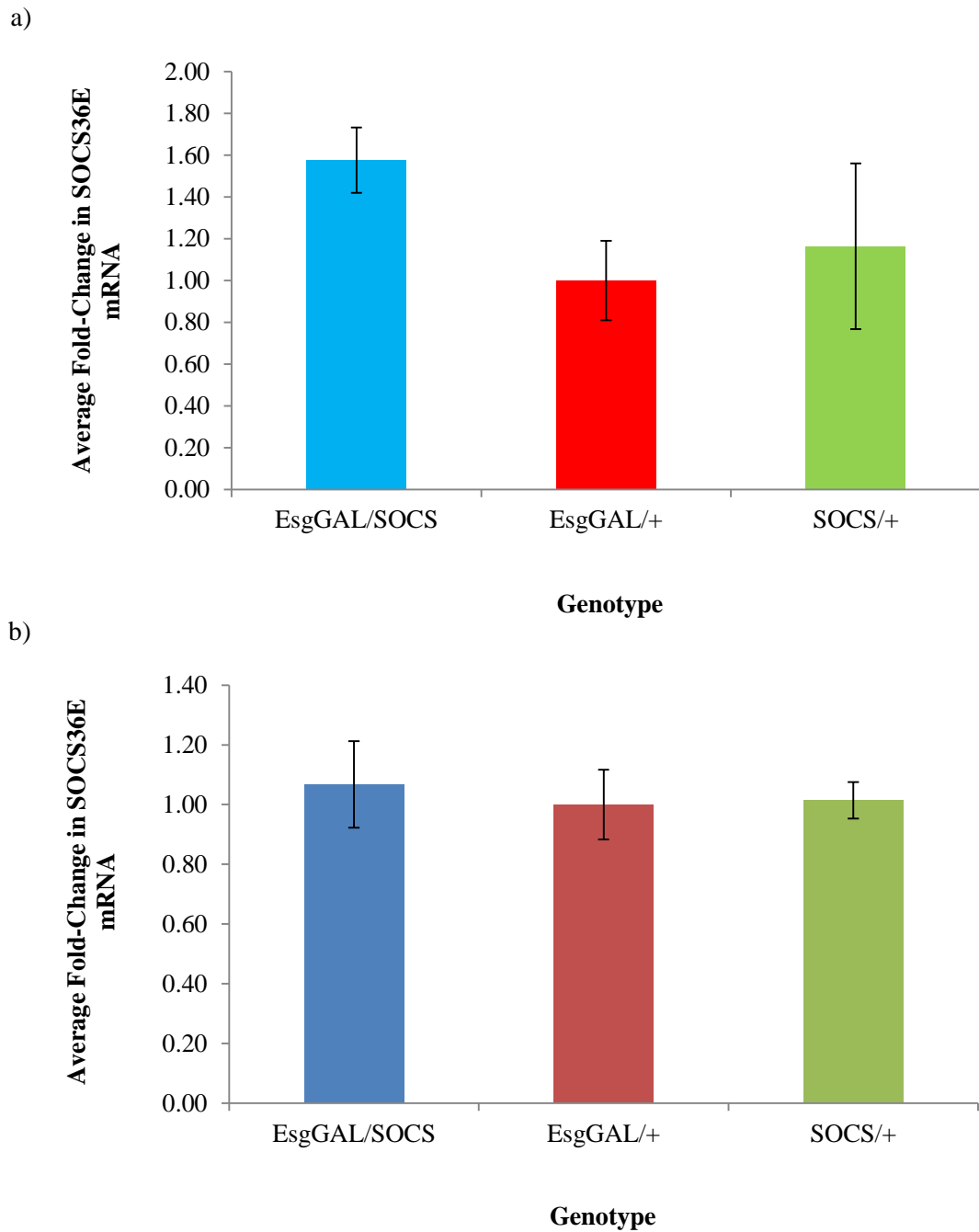
Figure 5.2: Quantification of SOCS36E mRNA levels (±SEM) in the guts of experimental male and female flies, as measured by quantitative PCR. mRNA was extracted from dissected guts of 10 day old (a) female and (b) male flies, with expression levels of SOCS36E mRNA measured using qPCR, and calculated using the $2^{(-\Delta\Delta Ct)}$ method, with values relative to the EsgGAL/+ average ratio within each gender. (n=60 per genotype, per gender).

Although we were unable to confirm the ISC-knockdown of SOCS36E at a molecular level in both male and female flies, previous work using immunofluorescence has revealed basal midgut proliferation to be increased in knockdown flies, compared with controls, as assessed using an anti-PH3 antibody which is a marker of mitosis (Buchon, personal communication). Oral infection with *Ecc15* is known to induce midgut proliferation (Buchon et al. 2009a), although upon infection in SOCS36E knockdown flies, this increase in proliferation was found to be enhanced (Buchon, personal communication, Obasse 2012). In infected knockdown flies, the increase in the number of mitotic cells was still sustained 2 days following infection, whereas in control flies, numbers started to decrease 16 hours post-infection (Buchon, personal communication). Confocal images demonstrated the microbial-induced increase in proliferation (as indicated by the increase in the number of nucleated midgut cells, top panels in figure 5.3) and also dysregulated organisation of the tight junction protein, discs large (Dlg) in SOCS36E knockdown flies (as depicted by the yellow arrowheads, white arrowheads= arranged Dlg arrangement). EsgGAL/SOCS flies also exhibited an increase in midgut diameter following *Ecc15* infection, compared with uninfected EsgGAL/SOCS flies, as well as uninfected and infected control genotypes. This may be as a result of increased midgut proliferation in these flies (due to infection and SOCS36E knockdown) and also irregular midgut cell arrangements, caused by dysregulated expression and organisation of Dlg. Overall, these images indicate that SOCS36E is implicated in regulation of *Drosophila* midgut homeostasis, in terms of both proliferation and renewal, and formation and organisation of midgut cells and the epithelial barrier.

EsgGAL/SOCS
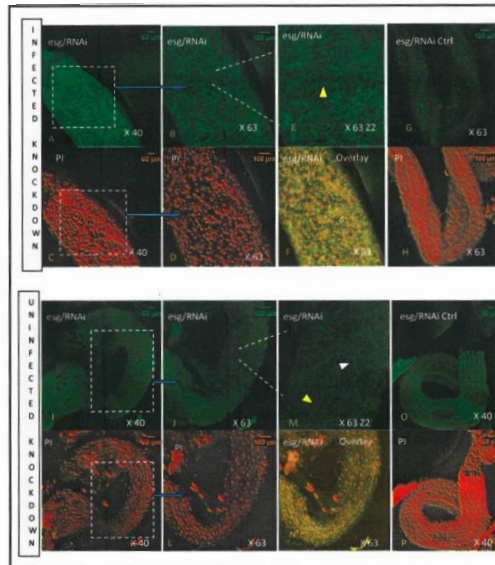
EsgGAL/+
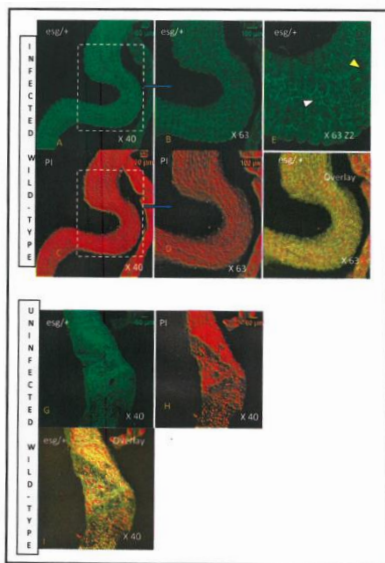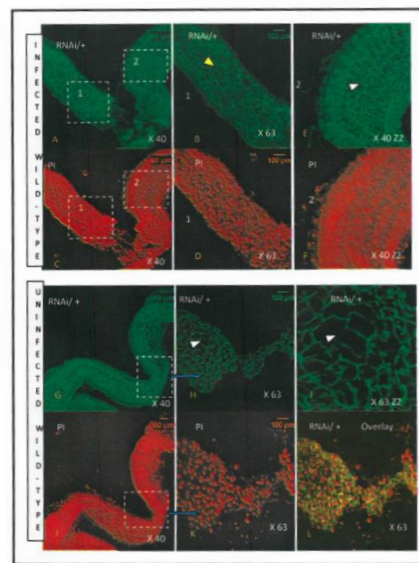
SOCS/+

Figure 5.3: Confocal images showing Dlg expression in the midgut of SOCS36E knockdown flies plus controls, both with (top panels) and without (bottom panels) *Ecc15* infection. One week old flies were dissected at 4 days post-*Ecc15* infection and were fixed in 4% paraformaldehyde before incubation overnight using an anti-Dlg primary antibody (at 1:100 at 4°C, green). Following washes and incubation in secondary antibody, guts were mounted onto slides using 2% n-propylgallate containing the propidium iodide nuclear stain (PI, red). Slides were visualised using a Leica DMIRE2 TCS-SP2 confocal microscope. (Scale bar and magnification: 60µm and 40x respectively, and 100µm and 63x respectively). (Obasse 2012).

5.4 Assessment of microbe-mediated midgut homeostasis on lifespan in SOCS36E knockdown and control flies

5.4.1 ISC-specific knockdown of SOCS36E led to a reduction in median lifespan in female flies, regardless of infection status

Research into *Drosophila* midgut homeostasis has previously revealed that Jak/Stat is required for activation and regulation of ISC proliferation (Buchon et al. 2009b), differentiation of ECs and EECs (in conjunction with the Delta/Notch pathway, Jiang et al. 2009, Lin et al. 2010), and is also activated upon damage or midgut infection (Buchon et al. 2009a, 2009b, Jiang et al. 2009). Infection with the Gram-negative phytopathogen, *Ecc15* in particular, is known to induce multiple components of the Jak/Stat pathway, which leads to proliferation and repair of midgut cells (Buchon et al. 2009a). Work carried out by Buchon (personal communication) also found that following ISC-specific knockdown of SOCS36E, basal and *Ecc15*-mediated midgut proliferation was increased, compared with control flies, with increased mitosis also sustained for up to 2 days following infection in knockdown flies. Therefore, we investigated whether *Ecc15*-induced proliferation, and ultimately, disruption to the microbiota would alter the reduction in lifespan induced by the knockdown of SOCS36E. Lifespan analysis was conducted using both male and female flies, larger population sizes, as well two cohorts of flies per genotype, per gender- an uninfected group, and an *Ecc15*-infected group of flies that were infected at approximately one and two weeks of age.

Figure 5.4 shows that in both uninfected (a) and infected (b) females, ISC knockdown of SOCS36E led to a shortening of lifespan. However, infection alone had no effect on the SOCS36E knockdown-induced lifespan reduction, as both cohorts of EsgGAL/SOCS females had the same median and maximum lifespan. Additionally, all uninfected genotypes had virtually the same median and maximum lifespans as their infected counterparts, showing that microbially-induced midgut proliferation through *Ecc15* infection had neither a positive, nor a negative effect on the lifespans of these particular genotypes.

As seen in figure 5.1, the survival curves of all genotypes were similar until approximately day 30, confirming that no early non-ageing deaths had occurred in these flies. Table 5.2a shows the median and maximum lifespans of the uninfected and infected SOCS36E knockdown and control flies, and both cohorts of SOCS36E knockdown females had lower median and maximum lifespans compared with all control flies. Using the chi-squared p-value log-rank test, differences in survival between the uninfected and infected EsgGAL/SOCS

flies, and both uninfected and infected cohorts of control flies were found to be statistically significant (p<0.001, shown in table 5.2b). However, in contrast to data presented in table 5.1a, EsgGAL/+ and SOCS/+ essentially had the same median and maximum lifespans.

a)

Genotype	Median Lifespan/ Days	Maximum Lifespan/ Days
Uninfected EsgGAL/SOCS	48	54.5
Uninfected EsgGAL/+	52.0	59.0
Uninfected SOCS/+	52.0	59.0
Infected EsgGAL/SOCS	48.0	54.5
Infected EsgGAL/+	52.0	59.0
Infected SOCS/+	52.0	61.5

Table 5.2: (a) The median and maximum lifespans of both uninfected and infected cohorts of SOCS36E knockdown female flies and relevant controls. (b) P-values calculated using a chi-squared p-value log-rank test to determine statistical significances between lifespan differences in the experimental flies (on the following page).

b)

Chi-squared p-value for log-rank test on survivorship data

	EsgGAL/SOCS Female Uninfected	EsgGAL/+ Female Uninfected	SOCS/+ Female Uninfected	EsgGAL/SOCS Female Infected	EsgGAL/+ Female Infected	SOCS/+ Female Infected
EsgGAL/SOCS Female Uninfected	x	1.70E-04	1.72E-06	7.39E-03	1.25E-04	1.44E-05
EsgGAL/+ Female Uninfected		x	0.21	7.04E-10	0.94	0.31
SOCS/+ Female Uninfected			x	1.60E-12	0.24	0.86
EsgGAL/SOCS Female Infected				x	1.72E-10	6.63E-11
EsgGAL/+ Female Infected					x	0.40
SOCS/+ Female Infected						x
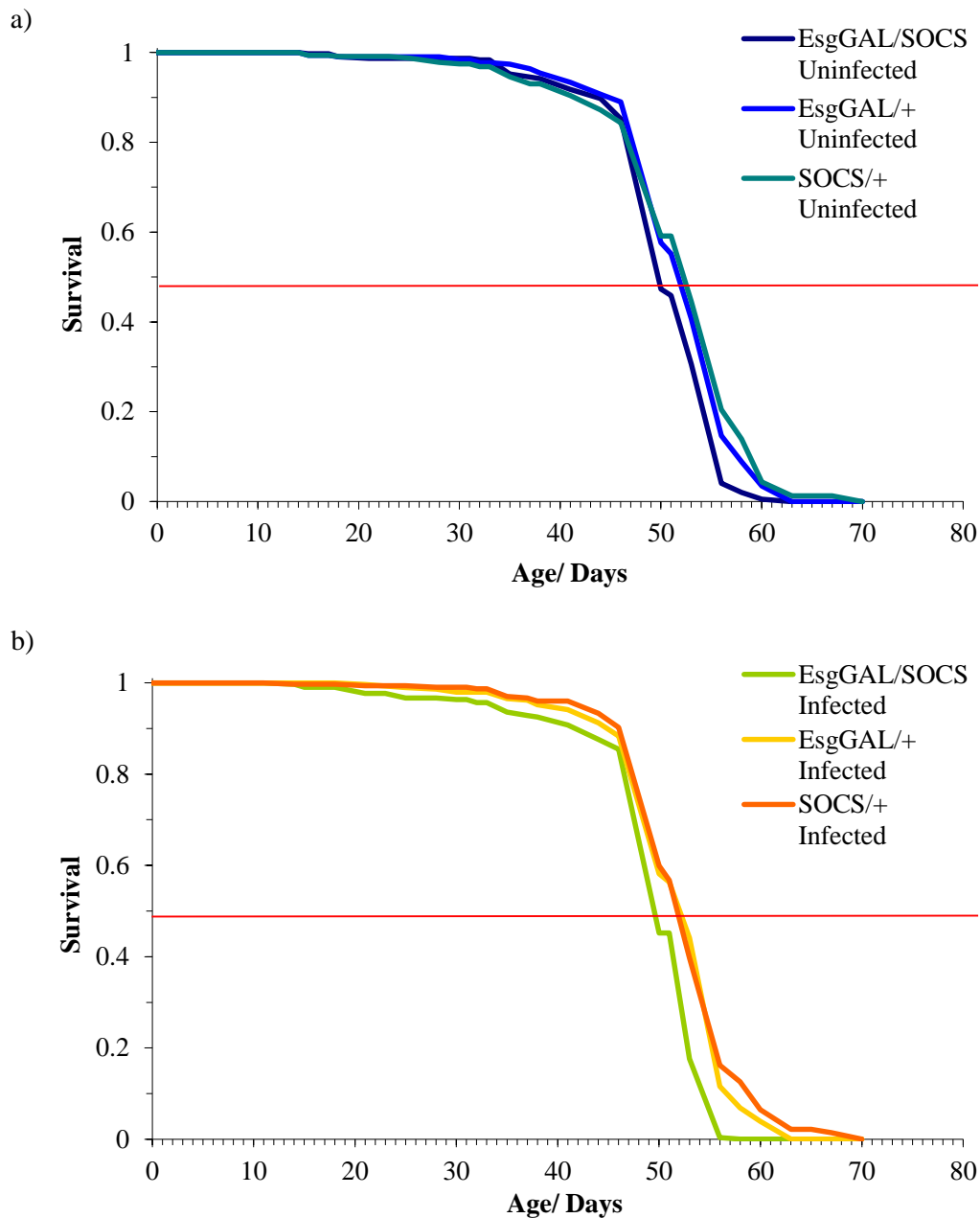
Figure 5.4: Lifespan analysis of (a) uninfected and (b) *Ecc15*-infected SOCS36E knockdown female flies, compared with control genotypes, EsgGAL/+ and SOCS/+. Deaths were recorded three to five times over a period of five days each week, with median and maximum lifespans determined by the time points when 50% (depicted by the red line above) and 10% of each genotype remained, respectively. (Uninfected: EsgGAL/SOCS- dark blue, EsgGAL/+ - blue, and SOCS/+ - turquoise. Infected: EsgGAL/SOCS- green, EsgGAL/+ - yellow, and SOCS/+ - orange. (n=350 for each genotype). Differences in lifespans between EsgGAL/SOCS, and EsgGAL/+ and SOCS/+ within and across infection groups were calculated using a chi-squared p-value log-rank test- p<0.001.

As seen in figure 5.5, the repeat of figure 5.4, the survival curves of all genotypes were similar until approximately day 30. Table 5.3a shows the median and maximum lifespans of the uninfected and infected SOCS36E knockdown and control flies. However, in this experiment, only median lifespan was lower in both cohorts of SOCS36E knockdown females when compared with all control flies, not median and maximum lifespans as in table 5.2a. Despite this finding, in concurrence with the previous experiment, differences in survival between uninfected and infected EsgGAL/SOCS flies and both cohorts of control flies were statistically significant ($p<0.001$, using a chi-squared p-value log-rank test, shown in table 5.3b). Furthermore, all three uninfected genotypes had almost identical median and maximum lifespans compared to their infected counterparts, thus confirming that microbial-induced proliferation through *Ecc15* infection did not affect the lifespans of these particular flies.

In conclusion, knocking down SOCS36E in the ISCs of female flies, thereby disrupting intestinal homeostasis, consistently led to a reduction in lifespan, although microbial-induced proliferation and microbiota perturbations through infection with the Gram-negative phytopathogen, *Ecc15*, had no effect. Our findings support the role of appropriately regulated gut homeostasis in the overall health of the organism.

a)

Genotype	Median Lifespan/ Days	Maximum Lifespan/ Days
Uninfected EsgGAL/SOCS	46.5	60.5
Uninfected EsgGAL/+	51.0	65.5
Uninfected SOCS/+	51.0	60.0
Infected EsgGAL/SOCS	48.0	60.5
Infected EsgGAL/+	51.0	65.5
Infected SOCS/+	51.0	60.5

Table 5.3: (a) The median and maximum lifespans of both uninfected and infected cohorts of SOCS36E knockdown female flies and relevant controls. (b) P-values calculated using a chi-squared p-value log-rank test to determine statistical significances between lifespan differences in the experimental flies (on the following page).

b)

Chi-squared p-value for log-rank test on survivorship data

	EsgGAL/SOCS Female Uninfected	EsgGAL/+ Female Uninfected	SOCS/+ Female Uninfected	EsgGAL/SOCS Female Infected	EsgGAL/+ Female Infected	SOCS/+ Female Infected
EsgGAL/SOCS Female Uninfected	x	1.98E-13	1.07E-10	0.39	2.14E-09	8.86E-11
EsgGAL/+ Female Uninfected		x	0.077	5.38E-10	0.32	0.25
SOCS/+ Female Uninfected			x	3.64E-07	0.71	0.62
EsgGAL/SOCS Female Infected				x	6.12E-07	1.37238E-07
EsgGAL/+ Female Infected					x	0.831277116
SOCS/+ Female Infected						x
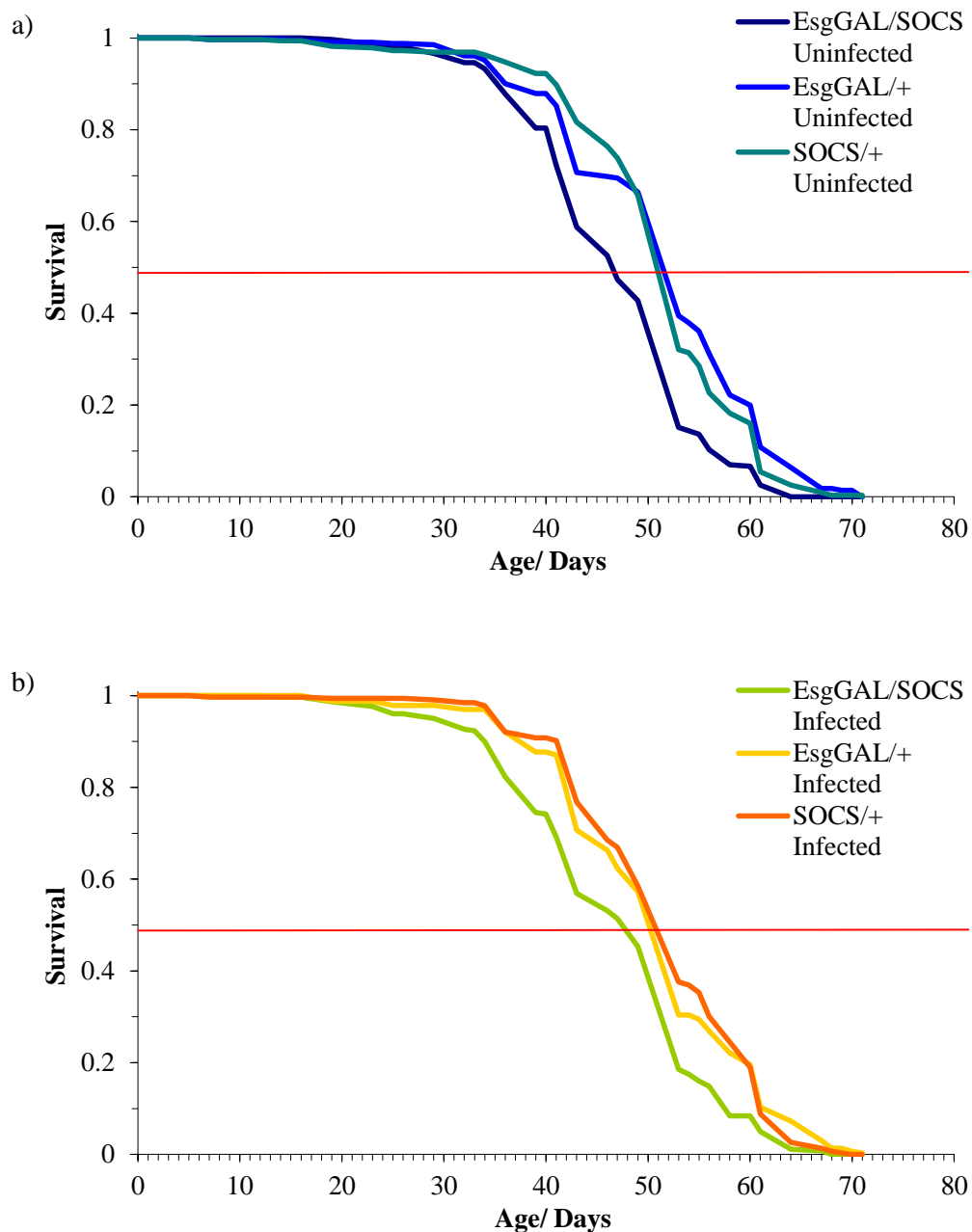
Figure 5.5: Lifespan analysis of (a) uninfected and (b) *Ecc15*-infected SOCS36E knockdown female flies, compared with control genotypes, EsgGAL/+ and SOCS/+. Deaths were recorded three to five times over a period of five days each week, with median and maximum lifespans determined by the time points when 50% (depicted by the red line above) and 10% of each genotype remained, respectively. (Uninfected: EsgGAL/SOCS- dark blue, EsgGAL/+ - blue, and SOCS/+ -turquoise. Infected: EsgGAL/SOCS- green, EsgGAL/+ - yellow, and SOCS/+ - orange). (n=350 for each genotype). Differences in lifespans between EsgGAL/SOCS, and EsgGAL/+ and SOCS/+ within and across infection groups were calculated using a chi-squared p-value log-rank test- p<0.001.

5.4.2 Neither SOCS36E knockdown, nor infection with Ecc15 in the midgut of male flies had an effect on lifespan.

Lifespan analysis was also carried out in male flies, and figure 5.6 shows that for both uninfected (a) and infected (b) males, all genotypes had similar survival curves, indicating that as found in female flies, microbial-induced midgut proliferation through *Ecc15* infection had no effect on lifespan, but also that the SOCS36E knockdown had gender specific effects, as in the male flies, uninfected EsgGAL/+ flies had the shortest median lifespan. Additionally, SOCS36E knockdown had no effect on maximum lifespan either as the maximum lifespans were approximately 48 days for all genotypes, with the exception of uninfected EsgGAL/SOCS and infected EsgGAL/+, which were 42.5 and 45.0 days, respectively (as shown in table 5.4a).

Using the chi-squared p-value log-rank test, there were significant differences (p<0.05) between EsgGAL/SOCS and control flies (shown in table 5.4b). However, as neither a shortening nor an extension of lifespan was observed in EsgGAL/SOCS males compared to both controls, the statistical differences observed cannot be attributed to the knockdown of SOCS36E, in addition to *Ecc15* infection.

In conclusion, no lifespan differences were observed between uninfected and infected male flies, indicating that increases in midgut proliferation as a result of *Ecc15* infection appeared to be neither beneficial nor harmful to survival of these flies; a finding also obtained in female flies. In contrast to the female flies though, EsgGAL/SOCS males did not exhibit a reduction in lifespan, suggesting the effects of ISC SOCS36E on survival may be gender specific.

Genotype	Median Lifespan/ Days	Maximum Lifespan/ Days
Uninfected EsgGAL/SOCS	36.0	42.5
Uninfected EsgGAL/+	34.0	48.5
Uninfected SOCS/+	37.5	48.0
Infected EsgGAL/SOCS	37.5	48.0
Infected EsgGAL/+	36.0	45.0
Infected SOCS/+	37.5	48.0

Table 5.4: (a) The median and maximum lifespans of both uninfected and infected cohorts of SOCS36E knockdown male flies and relevant controls. (b) P-values calculated using a chi-squared p-value log-rank test to determine statistical significances between lifespan differences in the experimental flies (on the following page).

b)

**Chi-squared p-value for log-rank test on
survivorship data**

	EsgGAL/SOCS Male Uninfected	EsgGAL/+ Male Uninfected	SOCS/+ Male Uninfected	EsgGAL/SOCS Male Infected	EsgGAL/+ Male Infected	SOCS/+ Male Infected
EsgGAL/SOCS Male Uninfected	x	9.78E-04	2.74E-04	0.35	0.68	0.024
EsgGAL/+ Male Uninfected		x	7.54E-12	9.24E-05	4.49E-03	6.89E-08
SOCS/+ Male Uninfected			x	0.017	8.61E-05	0.12
EsgGAL/SOCS Male Infected				x	0.22	0.31
EsgGAL/+ Male Infected					x	0.013
SOCS/+ Male Infected						x

a)

b)
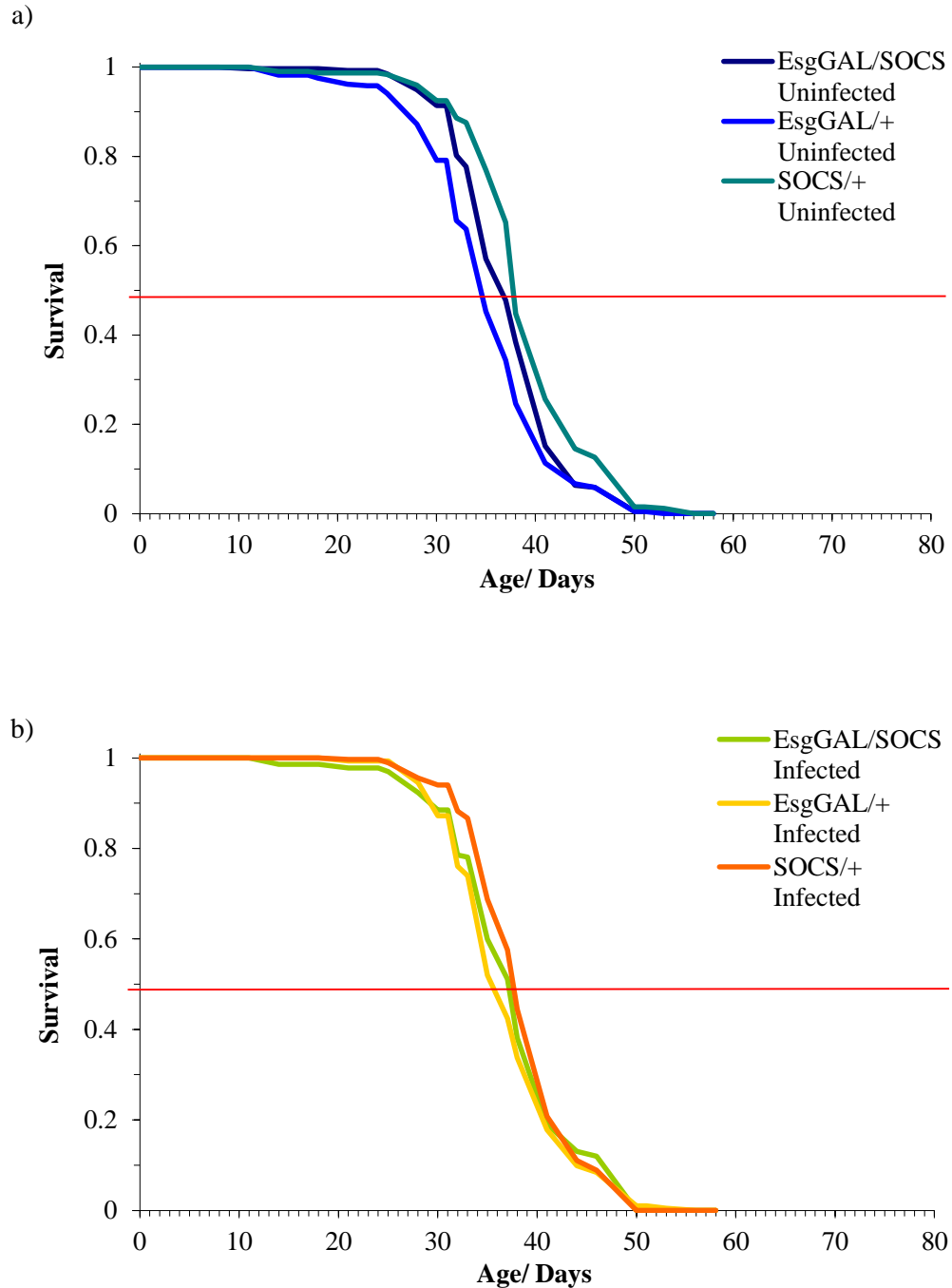
Figure 5.6: Lifespan analysis of (a) uninfected and (b) *Ecc15*-**infected SOCS36E knockdown male flies, compared with control genotypes, EsgGAL/+ and SOCS/+.** Deaths were recorded three to five times over a period of five days each week, with median and maximum lifespans determined by the time points when 50% (depicted by the red line above) and 10% of each genotype remained, respectively. (Uninfected: EsgGAL/SOCS- dark blue (n=310), EsgGAL/+ - blue (n=350), and SOCS/+ -turquoise (n=350). Infected: EsgGAL/SOCS- green (n=310), EsgGAL/+ - yellow (n=350), and SOCS/+ - orange (n=350)).

As in figure 5.6, figure 5.7 shows that for both uninfected (a) and infected (b) males, all genotypes had similar survival curves, confirming that neither SOCS36E knockdown, nor *Ecc15* infection had an effect on lifespan in these male flies. Similar to results in table 5.4a, EsgGAL/+ control flies had the lowest median lifespan, although in this case, the flies were infected (as shown in table 5.5a). Consistent with both cohorts of EsgGAL/+ having the two lowest median lifespans, these flies also had the lowest maximum lifespans (40.0 and 41.0 days for uninfected and infected EsgGAL/+ males, respectively). Surprisingly in this experiment, both sets of EsgGAL/SOCS were found to have the highest maximum lifespans (both at 50 days), contrasting results shown in table 5.4a where uninfected EsgGAL/SOCS had the lowest maximum lifespan, showing that maximum lifespan can be subject to more variation across experiments.

As found in the previous male lifespan experiment, significant differences were found between EsgGAL/SOCS and control flies ($p < 0.05$, using a chi-squared p-value log-rank test, shown in table 5.5b). Again however, neither cohort of EsgGAL/SOCS had consistent differences in lifespan compared with both control genotypes within the same infection group, so therefore the statistical differences observed could not be attributed to knockdown of ISC SOCS36E.

In conclusion, disrupting the microbiota and inducing proliferation through infection with *Ecc15* in male flies had no effect on survival, which is consistent with the findings in female flies. However, the negative effects that knocking down SOCS36E in ISCs had on lifespan was confined to female flies, as neither uninfected nor infected SOCS36E knockdown male flies had a reduced lifespan compared to control flies, suggesting that the impact of gut health on overall health may be sexually dimorphic.

a)

Genotype	Median Lifespan/ Days	Maximum Lifespan/ Days
Uninfected EsgGAL/SOCS	34.0	50.0
Uninfected EsgGAL/+	29.5	40.0
Uninfected SOCS/+	34.0	47.5
Infected EsgGAL/SOCS	32.5	50.0
Infected EsgGAL/+	26.5	41.0
Infected SOCS/+	34.0	47.5

Table 5.5: (a) The median and maximum lifespans of both uninfected and infected cohorts of SOCS36E knockdown male flies and relevant controls. (b) P-values calculated using a chi-squared p-value log-rank test to determine statistical significances between lifespan differences in the experimental flies (on the following page).

b)

Chi-squared p-value for log-rank test on survivorship data

|	EsgGAL/SOCS Male Uninfected	EsgGAL/+ Male Uninfected	SOCS/+ Male Uninfected	EsgGAL/SOCS Male Infected	EsgGAL/+ Male Infected	SOCS/+ Male Infected
EsgGAL/SOCS Male Uninfected	x	1.87E-11	0.73	0.37	3.93E-12	0.60
EsgGAL/+ Male Uninfected		x	1.36E-16	1.16E-08	0.50	1.77E-11
SOCS/+ Male Uninfected			x	0.19	6.92E-17	0.31
EsgGAL/SOCS Male Infected				x	3.01E-09	0.66
EsgGAL/+ Male Infected					x	1.55E-12
SOCS/+ Male Infected						x

a)

b)
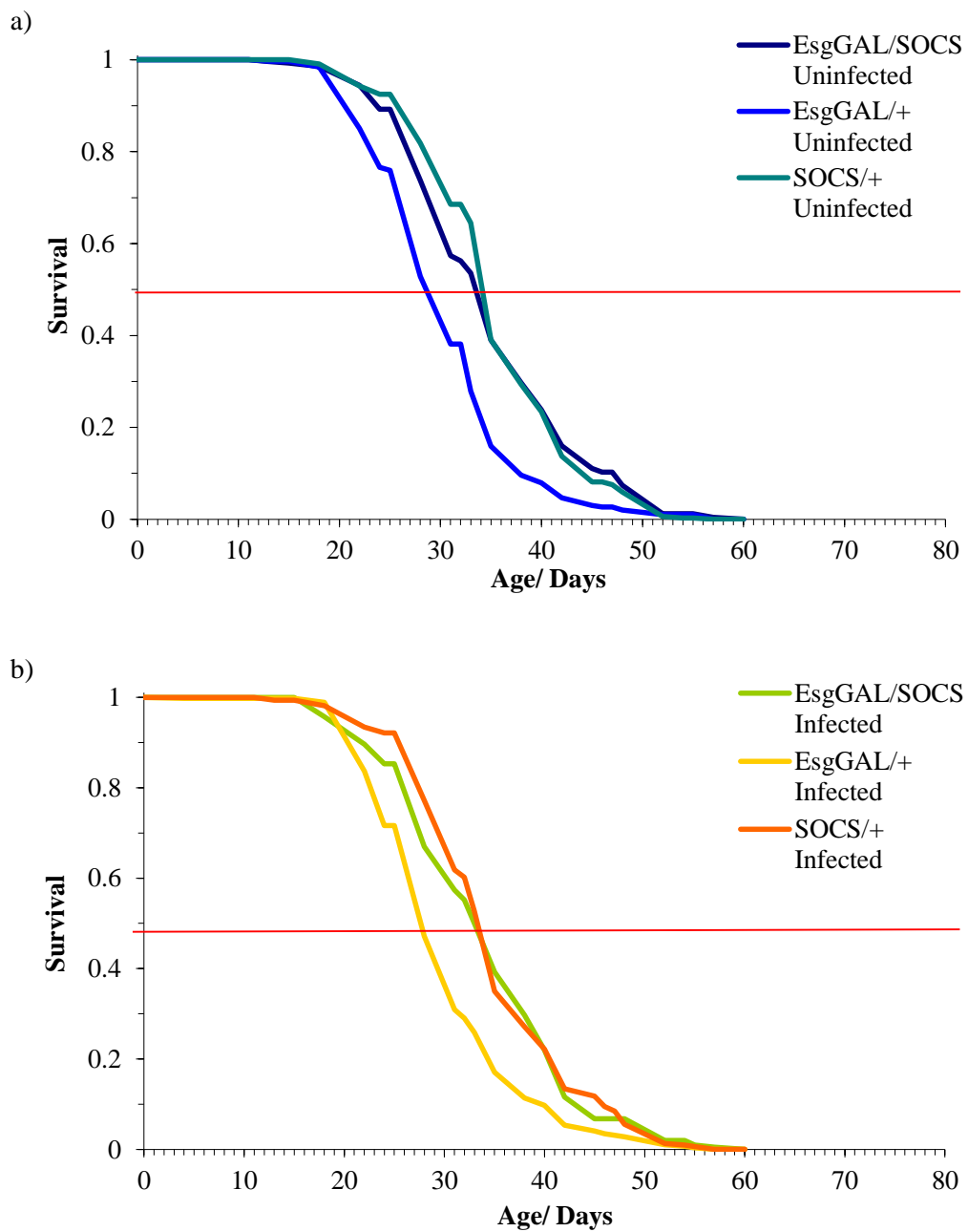
Figure 5.7: Lifespan analysis of (a) uninfected and (b) *Ecc15*-infected SOCS36E knockdown male flies, compared with control genotypes, EsgGAL/+ and SOCS/+. Deaths were recorded three to five times over a period of five days each week, with median and maximum lifespans determined by the time points when 50% (depicted by the red line above) and 10% of each genotype remained, respectively. (Uninfected: EsgGAL/SOCS- dark blue, EsgGAL/+ - blue, and SOCS/+ -turquoise. Infected: EsgGAL/SOCS- green, EsgGAL/+ - yellow, and SOCS/+ - orange). (n=350 for each genotype).

5.5 Assessment of *Ecc15*-induced midgut proliferation

As we were unable to confirm SOCS36E mRNA knockdown using qPCR, we assessed effects on midgut proliferation as previously performed by Buchon (personal communication). Although images by Obasse (2012) demonstrated microbe-mediated dysregulation of tight junction organisation and increased midgut diameter in SOCS36E knockdown flies relative to controls, thus disrupting midgut homeostasis, we wanted to confirm the persistence of midgut proliferation in SOCS36E knockdown flies, both at the basal level and following *Ecc15* infection in our lab.

Using four different groups of flies (uninfected, and flies dissected either 1, 3 or 7 days post-infection), we used immunofluorescence to determine differences in midgut proliferation between the three experimental genotypes, using an antibody recognising phosphorylated histone H3 (PH3); a marker of mitosis. Due to difficulties in accurately quantifying PH3+ cells, we chose to quantify those cells that were brightly fluorescing and therefore had pronounced levels of mitosis occurring. Consequently, there were very few prominent PH3+ cells observed, regardless of genotype, even using multiple fields of view per midgut. Figure 5.8 (a) shows examples of images taken, with (b) displaying the results from image quantification, confirming the low numbers of PH3+ cells, ranging from 0 to 4.5. Within EsgGAL/SOCS, there does appear to be a trend of a slight increase in PH3+ cells with increasing time following *Ecc15* infection. However, these increases are very small (with a difference of 1.5 cells between uninfected and 7 days post-infection), and overlapping error bars can be seen. A one-way ANOVA with Tukey-Kramer post-hoc test was performed and no significant differences were found between the four groups ($p>0.05$). The same statistical test was used within EsgGAL/+ and SOCS/+, as well as within each infection group, and no statistical differences were found either ($p>0.05$). In summary, this particular experimental method proved inconclusive in determining basal and infection-induced increases in midgut proliferation in SOCS36E knockdown flies. Although we were unable to confirm knockdown of SOCS36E using qPCR and immunofluorescence, our lifespan and stress resistance data (discussed further in Chapter 6), along with previous immunofluorescence performed in our lab (Obasse 2012), show that there are phenotypes attributed to both male and female EsgGAL/SOCS flies.

a)

EsgGAL/SOCS   EsgGAL/+   SOCS/+
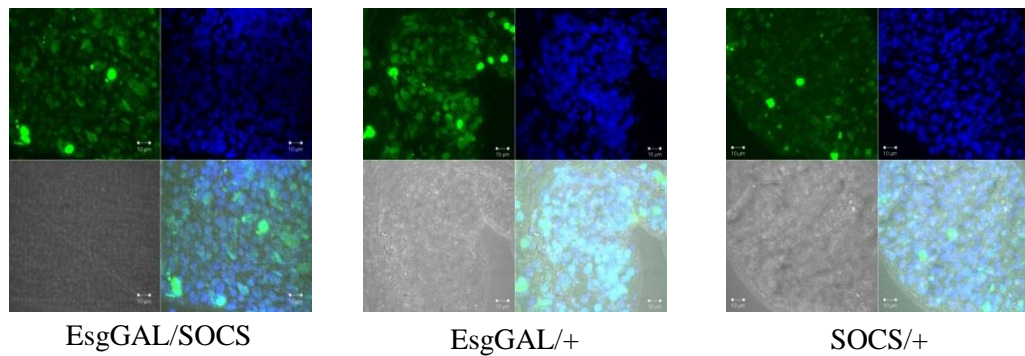
b)
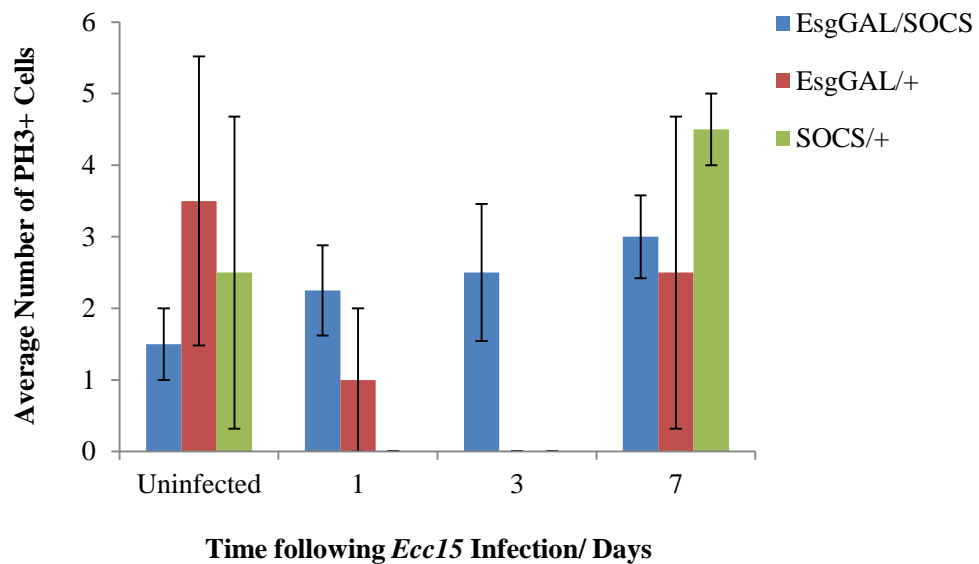
Figure 5.8: Confocal images (a) and quantification (±SEM) (b) of PH3+ mitotic midgut cells in EsgGAL/SOCS flies (left) and control genotypes, EsgGAL/+ (centre) and SOCS/+ (right). Flies were dissected at either 1, 3 or 7 days post-*Ecc15* infection (with uninfected flies dissected at 7 days) and were fixed in 4% paraformaldehyde before incubation overnight using a mitotic marker- an anti-phospho-histone H3 antibody (at 1:1000 at 4°C, green). Vectashield with DAPI (blue) was used as a nuclear stain. Slides were visualised using a Zeiss confocal microscope. (Scale bar= 10µm, n=4 per group, per genotype). (Images shown taken from 7 days post-infection, at 63x magnification).

5.6 Discussion

The use of *Drosophila melanogaster* as a model organism has proven to be beneficial to biomedical research, with reasons for their use including: relatively short lifespan (approximately 60-80 days) along with short generation times (especially when compared to humans where the gestation period is 9 months), fewer cost and ethical issues when compared to using organisms, such as mice or monkeys for scientific research, the evolutionary conservation of genes and their functions from *Drosophila* to mammals and also that flies can be easy to genetically manipulate, with gene expression able to be controlled through tissue-specific and temperature sensitive driver lines. Collectively, these allow the study of gene effects over the lifespan of the fly, with results translating to health and ageing in humans.

In recent years, *Drosophila* have also become a good model organism for studying health and disease of the G.I tract. This is due to similarities in gut structure, conservation of signalling pathways (such as Notch, Jak/Stat and JNK, for example) (Helfand and Rogina 2003, Apidianakis and Rahme 2011), and pathologies exhibited by mammals and *Drosophila*. For instance, both organisms possess ISCs, which following proliferation into a progenitor cell (enteroblasts in *Drosophila*, transit amplifying cells in mammals), differentiate into either absorptive or secretory intestinal cells, dependent on Delta/Notch and Jak/Stat signalling (Jiang et al. 2009, Lin et al. 2010). Also, tissues exist in *Drosophila* that are homologous to all sections of the mammalian G.I tract. For example, the crop is equivalent to the mammalian stomach, and specific to our research interests, the midgut and hindgut are similar to the small and large intestine, respectively (Apidianakis and Rahme 2011). With regards to pathologies, both mammals and flies possess equivalent signalling pathways for recognition of microbes and distinguishing between commensal and pathogenic microbes (the TLR pathway, and Toll pathway, respectively), and mutations in the respective pathways results in increased susceptibility and mortality following intestinal challenge (Rakoff-Nahoum et al. 2004, Dionne and Schneider 2008). Additionally, dysregulated intestinal homeostasis, either as a result of mutations or loss of cell junctions, or tumour suppressor genes (such as APC), or through increased activity in cell signalling pathways (such as JNK), can lead to hyperproliferation and cause irregular tissue architecture and multi-layering of cells (Hermiston and Gordon 1995, Licato et al. 1997, Biteau et al. 2008, Patel and Edgar 2014). It is well established that damage to the *Drosophila* midgut (for instance, through the use of DSS) as well as dysregulation of intestinal cell regulation and repair pathways have negative effects on lifespan and survival (Amcheslavsky et al. 2009, Apidianakis and Rahme 2009, Apidianakis et al. 2009, Buchon et al. 2009b, Chatterjee and Ip 2009, Jiang et al. 2009, Biteau

et al. 2010). Specific to this project, Buchon et al. (2009b) found that flies lacking the Jak/Stat activator, Upd3, and the transcription factor, Stat92E, in ECs and ISCs respectively, succumbed to infection with *Ecc15*, due to an inability to renew their midgut epithelium, thus demonstrating the importance of the Jak/Stat pathway in particular, in the *Drosophila* midgut. Although these studies demonstrate the important effects of dysregulated midgut signalling on survival, they do not give an indication as to how the ageing process is affected in these flies, as shortening of lifespan can either be due to specific functions limiting lifespan, or acceleration of the ageing process. As a result, decreased lifespan is often used as an indicator of organismal health, and these findings reveal that regulated intestinal homeostasis is essential for maintaining the wellbeing of flies, and this is also applicable to mammals (Rakoff-Nahoum et al. 2004)

The focus of this project has been on SOCS proteins, a group of negative regulators of Jak/Stat signalling. Previous studies have shown that a reduction or loss of SOCS has been implicated in dysregulated cell homeostasis, which could ultimately lead to disease. For example, in a murine model of inflammation-induced carcinogenesis, IEC-specific knockout of SOCS3 led to crypt hyperproliferation, as well as tumour development (Rigby et al. 2007). Although not entirely within the scope of this project, deletion of SOCS3 in hepatocytes promoted hepatitis-induced hepatocarcinogenesis (Ogata et al. 2006), enforcing the importance SOCS proteins have in preventing infection/inflammation-induced carcinogenesis. Additionally, an increase in villus height, crypt depth and cell proliferation in both the jejunum and colon were found in SOCS2 null mice, compared to wild-type litter mates (Michaylira et al. 2006). *Drosophila* have their own SOCS proteins- SOCS16D, SOCS44A and SOCS36E (Hou et al. 2002), all of which possess mammalian homologues. The fact that multiple SOCS proteins are evolutionarily conserved between flies and mammals is indicative that these proteins have crucial functions within these organisms. Our main focus was SOCS36E, which is the most-documented *Drosophila* SOCS protein. It is a homologue of both human and murine SOCS5, but through its role in preventing phosphorylation of Stat92E, it is actually a functional homologue of SOCS1-3 and CIS (Callus and Mathey-Prevot 2002). Like mammalian SOCS proteins, SOCS36E is activated by Jak/Stat and can inhibit Jak/Stat signalling *in vivo*, thereby producing a negative feedback loop. Additional roles include eye and wing development, and maintenance of germline stem cells (Stec and Zeidler 2011). As found with mammalian SOCS proteins, SOCS36E also functions as a tumour suppressor, due to its ability to inhibit EGFR signalling (Herranz et al. 2012). Additionally, knockdown of SOCS36E knockdown results in upregulated Jak/Stat signalling, and in haematopoietic tumours that develop in flies with constitutively active Hop (the

Drosophila homologue of Jak2, Binari and Perrimon 1994), deletion of SOCS36E led to an increase in the number and size of tumours (Stec and Zeidler 2011). Besides reports of SOCS36E increases upon Jak/Stat activation by Upds, particularly following infection (Buchon et al.2009a and b, Jiang et al. 2009), very little is known about SOCS36E in the *Drosophila* midgut, unlike SOCS proteins in the mammalian intestines. Consequently, dysregulation of mammalian SOCS3 is known to be implicated in diseases such as IBD and cancers of the G.I tract (Rigby et al. 2007, Li et al. 2009), which can lead to increased morbidity and mortality, so we made use of fruit flies' relatively short lifespan and used *Drosophila* as a model to first investigate the effect disrupting intestinal homeostasis (through knockdown of SOCS36E specifically in ISCs) had on lifespan, through survival analysis.

Survival analysis experiments showed a statistically significant decrease in both median and maximum lifespan in SOCS36E knockdown female flies, compared with controls. It has been previously shown that proliferation rates in the *Drosophila* midgut often increase with increasing age in flies (Biteau et al. 2008, Choi et al. 2008, Buchon et al. 2009b); an observation that is also conserved in the intestine of mammals (Holt and Yeh 1988, 1989, Ciccocioppo et al. 2002). Biteau et al. (2010) found that a moderate reduction in JNK and insulin/IGF (IIS) signalling in midgut progenitor cells, led to an extension in lifespan in *Drosophila*. They found that this lifespan extension correlated with a reduction in the age-associated dysplasia caused by overproliferation and midgut degeneration that can often lead to premature death in flies. In spite of this, altered activity in these pathways, such as decreased neural IIS and increased neural JNK signalling (Wang et al. 2003, Broughton et al. 2005, Ismail et al. 2015), has also led to increases in lifespan, so the extension reported by Biteau et al. (2010) could have been due to crosstalk between pathways, or even tissues. For instance, EECs in the midgut are capable of communicating with cells with the brain through recognition and production of neuropeptides (Veenstra 2008). If EECs are functioning efficiently as a result of adequate midgut homeostasis and health, signalling to the brain may result in healthy neuronal cells as well. Additionally, the effects of JNK activity appear to be tissue specific, as decreased midgut signalling was able to increase lifespan through limiting age-associated dysplasia, whereas increased JNK signalling in the brain can increase lifespan through increased stress resistance (Wang et al. 2003, Biteau et al. 2010). However, using this theory of increased midgut proliferation with increasing age, then an increase in Jak/Stat cell signalling (as theorised in the SOCS36E knockdown flies) leading to further proliferation of ISCs may have induced intestinal dysplasia sooner in the knockdown flies than in control flies, resulting in a reduction in median and maximum lifespans. Additionally, Jak/Stat signalling is known to function upstream of the Notch pathway (Jiang et al. 2009), and in

cooperation with the EGFR pathway (Buchon et al. 2010). Therefore, an increase in ISC proliferation, due to a knockdown of SOCS36E, could lead to increased proliferation through these pathways, thus further promoting dysplasia and potentially compromising the health and lifespan of the fly. Biteau et al. (2008) also found that older flies demonstrated higher levels of JNK signalling than younger flies, and one outcome of this pathway is the production of Upds (Jiang et al. 2009)- the activating ligand of the *Drosophila* Jak/Stat pathway- and this could potentially cause further Jak/Stat activation.

As stated earlier, intestinal proliferation rates have been reported to increase with increasing age in both mammals and flies, and if sustained, may be the result of genetic mutations or, may increase the chance of mutations not being detected by components of DNA damage repair pathways or then at cell cycle checkpoints. This could result in these mutations being passed on to daughter cells, which may result in mutation accumulation and irreversible cell changes, then ultimately tumorigenesis (Rakoff-Nahoum 2006). Therefore, it is has been proposed that increasing age predisposes organisms to cancer (Xiao et al. 2001). In a study by Salomon et al. (2008), they reported tumours in the midgut of two commonly used wildtype laboratory strains of fruit fly (Canton-S and w[1118]) at 4 and 5 weeks of age. Although only a small percentage of flies had midgut tumours by 5 weeks of age (1.29% of 154 flies), their results did show an increase in tumour development with age. However, they only studied flies up to 5 weeks of age, so it would be assumed that there may be further increases in the number of flies that developed midgut tumours older than 5 weeks. Images also showed a reduction or obstruction of the lumen in flies at 4 weeks of age. This leaves the possibility that the flies used here could have developed severe dysplasia, and possibly severe enough to completely obstruct the midgut lumen, which would have a negative impact on lifespan, especially as the median lifespan for male and female flies was 5 and 7 weeks respectively, and the maximum lifespan was 6-7 weeks and 9 weeks for male and female flies respectively. Although these findings were reported in wildtype flies, other studies have also reported dysplasia in the midgut of various knockdown flies (for example Notch, Jak/Stat, APC), and this led to multilayering of cells in the midgut (an increase from the single layer of cells that normally line the midgut) and distorting of the epithelium (Lee et al. 2009, Patel and Edgar 2014). Taking these findings into account, the SOCS36E knockdown female flies may have had a reduced lifespan caused by obstruction of the midgut lumen, although this is speculative. In order to test this hypothesis, we could replicate experiments performed by Salomon et al. (2008) in our flies, sectioning dissected midguts and then using microscopy to visualise them and measure lumen diameter, and possibly epithelium depth if multilayering had occurred. If obstruction of the gut lumen does occur, this could impact on feeding,

digestion and energy storage. To determine effects of ISC knockdown of SOCS36E on energy storage, various assays could be performed to determine content of nutrients, such as lipids, trehalose (one of the predominant sugar molecules in *Drosophila*) and glycogen with these and control flies.

Considering findings from other groups of reduced lifespan as a result of dysregulated midgut homeostasis, it was therefore not completely surprising to find this phenotype in our flies. What was unexpected however, was the gender-specific effects the SOCS36E knockdown had on lifespan, in that only females were affected. Sexual dimorphism is known to occur in many behaviours studied in *Drosophila*, for example, locomotor activity (Martin et al. 1999), desiccation resistance (Chippindale et al. 1998), sleep (Liu et al. 2015), responses to ethanol (Devineni and Heberlein 2012), as well as longevity (Spencer et al. 2003, Magwere et al. 2004). Specifically in intestinal studies, reduction of various components of the IIS and JNK pathway led to decreased intestinal proliferation and extended lifespan in older female flies, with no significant effects on lifespan observed in male flies (Biteau et al. 2010). Rera et al. (2011) also demonstrated a similar trend following induced expression of dPGC-1- a *Drosophila* homologue of mammalian PGC-1, part of a group of fundamental regulators of various energy metabolism processes, such as glucose homeostasis and respiration. Magwire et al. (2010) stated that differences in genetic background can cause different phenotypes when the same gene is altered, but as both male and female flies for all genotypes used here were backcrossed onto the same w^{Dah} background, this was not the case. A possible explanation is derived from the finding by Jiang et al. (2009) that female flies were able to renew their midgut epithelium faster than males, suggesting that females may have higher basal proliferation rates. The flies used in those experiments were from a different background, but if the findings are to be generalised, then it can be hypothesised that increased intestinal Jak/Stat signalling (achieved here through knockdown of SOCS36E) may predispose female flies to premature mortality, as a result of intestinal dysplasia. Although no lifespan effects were observed in our EsgGAL/SOCS male flies, behavioural phenotypes, such as increased stress resistance (discussed in Chapter 6) were found when compared with control male flies, which indicates that the lack of a lifespan phenotype was not due to the absence of SOCS36E knockdown.

.

Following assessment of lifespan in unchallenged flies, whereby knockdown of SOCS36E resulted in decreased lifespan in female flies, we then aimed to investigate how this reduction in Jak/Stat regulation impacts upon survival following microbial-induced proliferation. Flies

were infected with the Gram-negative phytopathogen, *Ecc15*, at approximately 1 and 2 weeks of age. *Ecc15* itself is known to activate Jak/Stat signalling following damage induced to midgut cells caused by an oxidative burst targeted towards the pathogen, and subsequent epithelium repair due to release of Upds from damaged ECs (Buchon et al. 2009a, Jiang et al. 2009). In both male and female flies, infection with *Ecc15* had neither a positive, nor a negative effect on median or maximum lifespan. This was not entirely surprising as under normal circumstances, *Ecc15* will not kill *Drosophila*, although it does induce an immune response which ultimately leads to proliferation of ISCs and repair of the epithelium (Basset et al. 2000, Buchon et al. 2009a). It has been previously shown that infecting flies with *Ecc15* leads to an increase in ROS in the midgut (which is damaging to the cells) (Ha et al. 2005). In the experiments in this project, flies were only infected twice over the space of a week, early on in the flies' lifespan (at one and two weeks of age) and were in contact with the bacteria for two hours each time. Therefore, one reason *Ecc15* infection had little effect on lifespan may have been because the flies' contact with this bacteria was not long enough to produce the amount of ROS and subsequent cell damage that can lead to a reduction in lifespan. Also, it is not known how many flies in these experiments actually ingested the bacteria, and if they did, how much bacteria was ingested. To fully establish the impact SOCS36E and microbial-mediated midgut proliferation has on survival, flies could be: infected with *Ecc15* for longer periods of time and/or infected more frequently (e.g. once a week for at least 4 weeks), or infected with more pathogenic bacteria, such as *Pseudomonas aeruginosa* or *Pseudomonas entomophila*. Additionally, a feeding assay could be performed whereby a dye is incorporated into the bacterial suspension and the absorbance is measured in order to quantify the level of intake. Infection with *Ecc15* could also be confirmed through measurement of ROS, comparing levels (of superoxide, for example, Ha et al. 2005) in infected flies with uninfected flies, or expression levels of Duox and catalase, which are known to induce and remove ROS, respectively.

Proliferation in the midgut is known to increase following *Ecc15* infection (Buchon 2009a), and Buchon (personal communication) found that increased proliferation was sustained two days post-infection in SOCS36E knockdown flies, even after the bacteria had been cleared from the midgut. This will lead to an increase in cells in the midgut, which would inevitably affect the morphology of the gut, and could lead to dysplasia. However, SOCS36E knockdown alone may cause an increase in cellular proliferation due to dysregulation of the Jak/Stat pathway so it is speculated that this may have occurred in these flies, hence why the uninfected EsgGAL/SOCS females exhibited a reduced median lifespan. Additionally, there have been no published studies quantifying the difference in proliferation caused either by

SOCS36E knockdown alone, or with *Ecc15* infection. Buchon et al. (2009b) discovered that manipulation of midgut Jak/Stat signalling, either through depletion of Upd3 in ECs, or deletion of Stat92E, resulted in increased mortality, and therefore sensitivity to *Ecc15* following oral infection. However, we observed no difference in lifespan as a result of *Ecc15*-induced proliferation, either alone or combined with SOCS36E knockdown, indicating dysregulated Jak/Stat signalling in our flies did not affect their resistance to this pathogen, presumably because Jak/Stat activity was still present. Regarding EsgGAL/SOCS flies, it may be that knockdown of SOCS36E was actually beneficial and perhaps led to a faster clearance of bacteria from the midgut, due to faster epithelial turnover and renewal, although this cannot be confirmed without further experiments, such as visualisation of *Ecc15* in the midgut by using a GFP strain. Additional findings from Buchon et al. (2009a) show that the Jak/Stat pathway contributes to regulation of AMPs, as expression of Drosomycin-like 3 (Dro3, an antifungal peptide) was reduced following *Ecc15* infection in flies with decreased Jak/Stat activity, through the use of Stat and Upd3 RNAi. This is in spite of the fact that *Ecc15* is Gram-negative and activates the Imd pathway, and Dro3 is produced by the Toll pathway. Expression of Dro3 was also found to be weakly induced following the use of Hop loss-of-function mutant flies, but was strongly induced in Hop gain-of-function mutants in the absence of infection, indicating regulation of Jak/Stat prevents misexpression of this peptide. Although Dro3 (along with other AMPs, Buchon et al. 2009a, Gendrin et al. 2009) will be produced as a result of infection regardless (another potential explanation for the lack of lifespan effect by *Ecc15*), it could be hypothesised that based on the findings of Buchon et al. (2009a), increases in Jak/Stat signalling, due to knockdown of SOCS36E in this case, may also strongly induce Dro3, thus alleviating any negative effects that both *Ecc15* infection and SOCS36E knockdown combined may have had on lifespan, although again, this would need to be tested.

Following the observation that knockdown of SOCS36E in the midgut led to lifespan reduction in female flies, we performed quantitative PCR in order to confirm the effects of the RNAi. We assessed SOCS36E mRNA levels in dissected guts in male and female experimental flies, and our results indicated SOCS36E mRNA was not lower in either EsgGAL/SOCS males or females, compared to controls. One suggestion for this may have been due to the specificity of the knockdown- the parental genetic cross performed to generate the EsgGAL/SOCS line would lead to a reduction of SOCS36E mRNA in the ISCs only. Although *Drosophila* have a higher proportion of ISCs (around 800-1000 ISCs in a population of approximately 10,000 cells= 8-10%, Ohlstein and Spradling 2006) compared with humans (who are estimated to have 4-6 ISCs amongst a small intestinal crypt of 450 cells and a

colonic crypt of 2250 cells= ≤1%, Potten 1991, Bach et al. 2000), 8-10% of the overall midgut is still a small proportion, and for this experiment, RNA was extracted from whole midguts. Additionally, ISCs are not regularly dispersed through the fly midgut due to different demands between niches (Ohlstein and Spradling 2006). Furthermore, midguts were dissected from live, anaesthetised flies so both processes of CO_2 anaesthetisation and gut dissection would have induced stress and potentially damage to the flies, which are capable of activating JNK and Jak/Stat signalling, respectively (Biteau et al. 2008, Buchon et al. 2009b). JNK activity also leads to production of Upds (Jiang et al. 2009), which results in activation Jak/Stat signalling, which causes transcription of genes including SOCS36E as a result, potentially explaining the lack of significant differences in SOCS36E mRNA between knockdown and control flies. Upon dysregulation of cell signalling, there may be mechanisms in place to ensure homeostasis is preserved. For example, Xu et al. (2011) found that midgut Jak/Stat signalling is able to coordinate with the Wnt and EGFR pathways, as activation of one of these pathways is increased following dysregulation and diminishing activity in one of the other pathways, and this ensures efficient regulation of ISCs. Therefore, based on these findings, it could be speculated that midgut cells may upregulate SOCS36E expression in order to overcome knockdown of SOCS36E in ISCs, although to test this, a sensitive, cell-specific technique would be needed to distinguish between cell types and compare expression of SOCS36E, such as flow cytometry.

Immunofluorescence was also performed in order to confirm enhanced basal and microbial-induced midgut proliferation in knockdown flies (relative to controls), as first revealed by Buchon (personal communication). This would confirm that knockdown of SOCS36E did in fact result in increased Jak/Stat signalling through reduced regulation, and would also produce a midgut phenotype in conjunction with the lifespan phenotype (in females). Unfortunately, this was not confirmed, but was not completely unsuccessful as fluorescent PH3+ proliferating cells were found, although these were low in number, with one possible cause being low sample size. Using immunofluorescence with the same fly genotypes, Obasse (2012) confirmed increases in midgut proliferation following *Ecc15* infection, as shown by an increase in the number of nucleated cells, and this was regardless of genotype (as expected). However, infected knockdown flies also exhibited disorganised expression of the tight junction protein Dlg, as well as an increase in midgut diameter, possibly as a result of irregular cell arrangements and/or increased numbers of cells within the midgut. The altered Dlg expression could ultimately affect the barrier function of the midgut epithelium and result in increased permeability, which has shown to cause increased morbidity in mammalian systems (Song et al. 2009), as well as increased mortality in *Drosophila* (Rera et al. 2011).

This could be a possible explanation for the reduced lifespan in knockdown flies, but it does not explain why this phenotype was in female flies only.

The experimental method we used here also meant that the dissected midguts were prone to damage so it may have been the case that higher proliferating midgut regions were lost in the process. To overcome this, dissected midguts could be paraffin embedded and sectioned (as performed previously with mice ceca) before antibody staining. Although many sections may need to be visualised in order to gauge the proliferation over multiple planes of the midgut, the tissue will be adhered to microscope slides, minimising damage or loss. Additionally, in place of using immunofluorescence, flies could be used that have GFP associated with the EsgGAL4 driver, so that any proliferating Esg+ cells would fluoresce, and the fluorescent intensities could then be compared between genotypes. A further technique that could be used is *in situ* hybridisation, which would involve using an RNA probe complementary to a sequence in the SOCS36E mRNA. Using microscopy, this would allow visualisation of SOCS36E mRNA expression in the midguts of our experimental flies, with the expectation that more probe-mRNA binding, and thus SOCS36E mRNA expression, would be found in both control genotypes. As previously stated, in the experiments we conducted, it was not known how many flies ingested the bacterial suspension and in what quantity, especially as the infection period was only 2 hours. It is possible that very few flies ingested the *Ecc15*, hence why there were no obvious differences between genotypes. Results may be improved using a longer infection period, or more pathogenic bacteria, which would induce a stronger proliferative response in the midgut.

In conclusion, although we were unable to confirm SOCS36E knockdown through decreased midgut SOCS36E mRNA and increased midgut proliferation, we did obtain a phenotype and showed that this knockdown did lead to a gender-specific lifespan reduction in female flies; the cause of which will be explored in the next chapter. Our finding adds to, and is supported by the multitude of groups who have found dysregulation of midgut renewal pathways, and extensive damage to the midgut are detrimental to flies' survival (Amcheslavsky et al. 2009, Apidianakis and Rahme 2009, Apidianakis et al. 2009, Biteau et al. 2010, Buchon et al. 2009b, Chatterjee and Ip 2009, Jiang et al. 2009), and reiterates the importance of intestinal signalling pathway regulation in health.

Chapter 6:

The use of the fruit fly, *Drosophila melanogaster*, in establishing a model for the effects of regulation of intestinal cell turnover on healthspan

6.1 Rationale:

Since the start of the 20th century, there has been substantial progression in hygiene and diagnosis and treatment of diseases in the western world, leading to increased standards of living and ultimately, life expectancy (WWW, Centers for Disease Control and Prevention). For instance, in the UK, life expectancy in males increased from 75.7 years in 2000-2002, to 78.4 years in 2009-2011. Increases were also observed in females, although their life expectancies were higher than in males too, with 80.4 years in 2000-2002, to 82.4 in 2009-2011 (WWW, Office for National Statistics). However, in many individuals, an increase in age is associated with senescence and decreasing functional health (Grotewiel et al. 2005). One common feature that often accompanies an increase in age is a decline in motor function, which can also be known as locomotor, or functional (age-related) senescence and in humans, this may manifest as a decline in walking speed, or stiffness or pain in the joints, which could ultimately lead to decreased amounts of movement and walking. Functional senescence is often the first sign of a decline or degeneration of the nervous system (Camicioli et al. 1999), and is a common cause of increased morbidity and mortality (as well as possible increases in healthcare costs), due to the increase in falls and hospitalisations in the elderly (Jones and Grotewiel 2011). *Drosophila* have proven to be a good model for assessing functional senescence as many behaviours, including locomotor behaviours, are known to decline with increasing age in flies (as in humans) (Grotowiel et al. 2005), and with relatively short lifespans, behaviours can be assessed at different time points during the lifespan. The time point(s) at which different environmental or genetic interventions have their effects on locomotor senescence can also be established. One method to measure locomotor senescence is the negative geotaxis assay, which assesses the neuromuscular health of *Drosophila*. *Drosophila* naturally display a reflex response of upward walking following forced falling, and this assay utilises this behaviour to test climbing ability in a variety of ways: the time taken to climb a predetermined distance, the distance climbed within a certain amount of time, or a combination of the two- the number of flies to climb a predetermined distance within a certain amount of time. All flies, regardless of gender or genotype, exhibit a decline in climbing ability with age, although different genotypes and mutations can lead to a delay or acceleration in this decline (Gargano et al. 2005).

An increase in frequency of G.I disorders is also common in the elderly, with these including dysregulated homeostasis, in humans (Ciccocioppo et al. 2002) as well as rodents (Holt and Yeh 1988, 1989, Xiao et al. 2001), diminished regenerative potential following injury (Martin et al. 1998), and an increased incidence in cancer (James 1983, Geokas et al. 1985, Salles

2007). It is thought that ageing of intestinal cells, as well as the enteric nervous system, are major factors in the development of these conditions (Saffrey 2013). Additionally, a lot of research has been carried out in recent years into the effects that changes in the gut, and in the gut microbiota, have on CNS function and behaviour, and vice versa- a bidirectional relationship named the gut-brain axis. Examples of findings include stress-induced microbiota changes as a result of maternal separation in young rat (O'Mahony et al. 2009), altered feeding behaviour in mice following infection with *Helicobacter pylori*, even after the infection had been resolved (Bercik et al. 2002), as well as depression and mood disorders often reported in individuals with IBD, and vice versa (cited by Bercik et al. 2010). Therefore using our *Drosophila* model, we aimed to investigate how ISC knockdown of SOCS36E impacts on muscle and motor function and senescence (assessed first using the negative geotaxis assay), and whether the midgut Jak/Stat pathway (as well as changes to the microflora through *Ecc15* infection) is implicated in the gut-brain axis.

6.2 Assessment of SOCS36E knockdown on healthspan by measuring negative geotaxis

6.2.1 Neuromuscular function in female flies was not affected by SOCS36E knockdown and/or Ecc15 infection.

The negative geotaxis assay was performed on all three experimental genotypes in females once a week, both in uninfected flies and flies infected with *Ecc15* approximately at 1 and 2 weeks of age. Figure 6.1 shows that in both uninfected (a) and infected (b) females, there was a decline in performance index (P.I), and therefore neuromuscular health, with increasing age. A one-way ANOVA revealed that as expected, the reductions in P.I over time were found to be statistically significant with earlier performance in the assay, regardless of genotype. For instance, with all female flies, the P.Is at days 7 and 42 were significantly higher and lower than those at the other 5 time points, respectively ($p<0.05$). With regards to overall P.I, SOCS36E knockdown had neither a positive nor a negative significant effect, when compared to both control genotypes. Knockdown of SOCS36E did however have a positive significant effect on performance at day 7 in female flies ($p<0.05$), but at all remaining time points, all genotypes had similar P.I values, both in uninfected and infected cohorts, so this may have been due to inter-vial variation. Therefore, this indicates that disrupting intestinal Jak/Stat through ISC-specific knockdown of SOCS36E did not affect flies' performance in this assay, and therefore did not have a significant effect on the senescence of negative geotaxis behaviour.

Ecc15 infection was found to positively affect negative geotaxis in SOCS/+ and EsgGAL/SOCS females at days 7 and 42, respectively ($p<0.05$, data not shown, statistical analysis shown in table 6.1). However, these findings were obtained at individual, differing time points and not consistent across all three genotypes, and along with insignificant differences within genotypes upon infection, it can be concluded that microbial-induced proliferation through *Ecc15* infection (along with SOCS36E knockdown) neither accelerated nor delayed the age-associated decline in P.I, and therefore did not affect neuromuscular health in these flies.

a)

b)
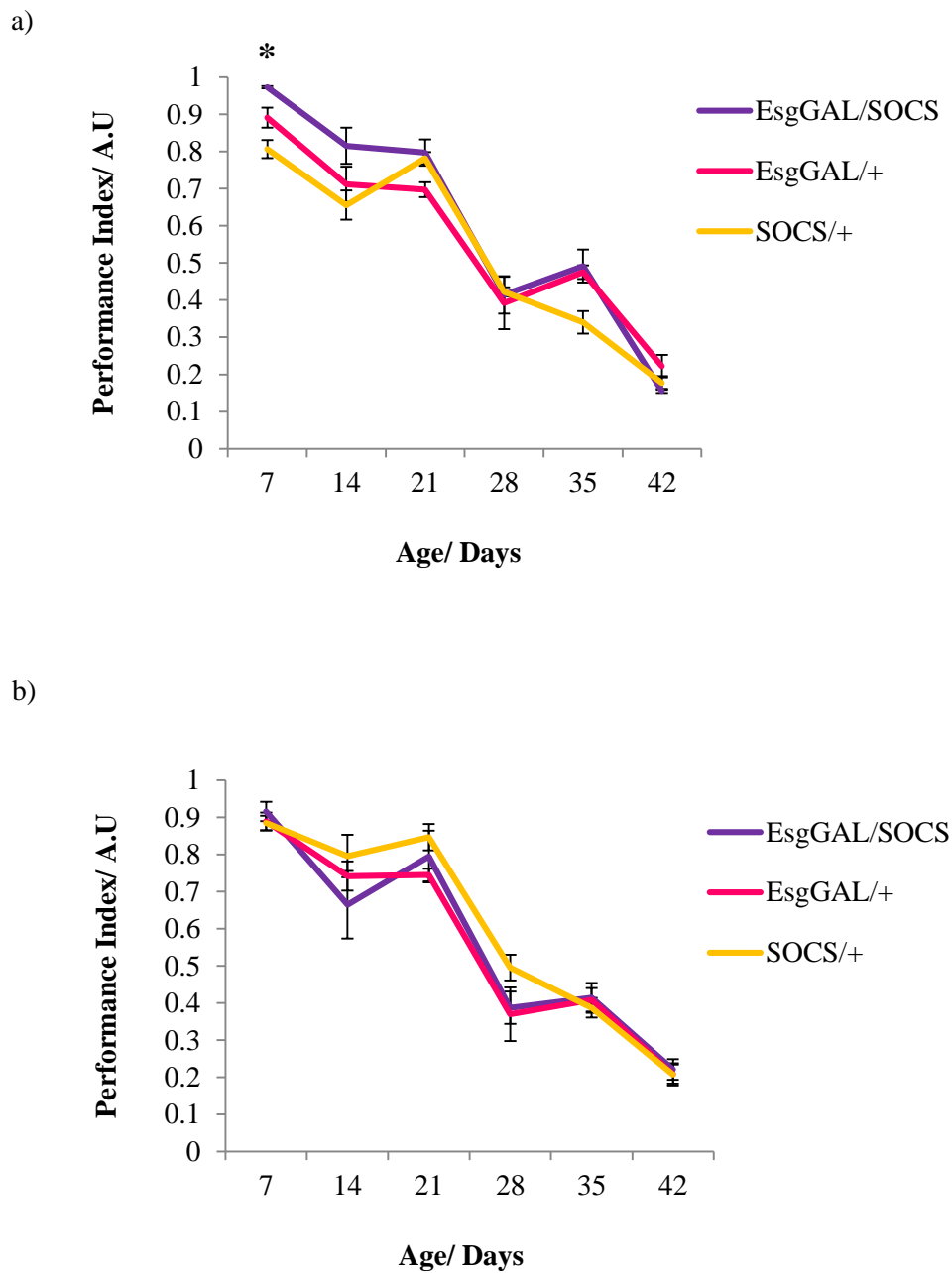
Figure 6.1: Assessment of neuromuscular health and functional senescence over time in uninfected and *Ecc15*-infected ISC SOCS36E knockdown female flies, plus controls.
Performance index (±SEM) with increasing age of (a) uninfected and (b) infected EsgGAL/SOCS females (purple) compared with EsgGAL/+ (pink) and SOCS/+ (orange) control genotypes. Negative geotaxis was carried out once a week, using a minimum of 21 flies and a maximum of 75 flies per genotype at each time point. (* = $p<0.05$, using a one-way ANOVA with Tukey's HSD).

Genotype	Age	7	14	21	28	35	42
EsgGAL/SOCS		**0.0578 (-)**	0.1809	0.9726	0.6953	0.2303	**0.0486 (+)**
EsgGAL/+		0.9526	0.6470	0.1151	0.8261	0.1051	0.7368
SOCS/+		**0.0386 (+)**	0.0776	0.1397	0.0843	0.2806	0.4117

Table 6.1: P-values calculated using JMP, showing statistical significance (and near significance, in bold) between performance indexes in uninfected female flies and their infected counterparts (using a Student's t-test). (+) indicates a positive effect of *Ecc15* infection, (-) indicates a negative effect of *Ecc15* infection.

When the assay was repeated in female flies, knockdown of SOCS36E had a significant positive effect on overall P.I when compared to EsgGAL/+ (p=0.036). However, as overall performances between EsgGAL/SOCS and SOCS/+ were similar and not significant, the differences observed cannot be mainly attributed to the knockdown. In infected females, ISC knockdown of SOCS36E also had neither a positive nor a negative effect at individual time points of the assay (shown in figure 6.2b). Within the uninfected cohort (figure 6.2a), EsgGAL/SOCS flies did have the highest average P.I between 19 and 40 days, although no statistical significance was found between both genotypes, only compared with EsgGAL/+ (p<0.01). Therefore, this difference in P.I cannot be just as a result of SOCS36E knockdown, or may possibly be due to a somewhat less than healthy group of EsgGAL/+ females (an observation also discovered during the exploratory walking assay, discussed further on in this chapter).

Figure 6.3 shows that performance in this assay was similar between all uninfected (a) and infected (b) flies, confirming *Ecc15*-induced midgut proliferation had no overall effect on P.I. As found in the first assay, infection had significant effects at individual time points, but not in all three genotypes at each time point (shown in figure 6.3a, b and c). For instance, *Ecc15* infection had a negative effect in EsgGAL/SOCS females at day 33 (figure 6.3a, p< 0.05), but positive effects on P.I in SOCS/+ at day 26, and EsgGAL/+ at day 33 (both p<0.01), suggesting infection may delay age-associated declines in this behaviour in control genotypes.

In summary, using negative geotaxis, we showed that disrupting the Jak/Stat pathway through SOCS36E knockdown had no effect on neuromuscular health in female flies. Midgut infection with *Ecc15* did not affect assay performance in these flies either, but may prolong further declines in senescence of this behaviour associated with increasing age. However, this can only be confirmed with a further repeat of this experiment.
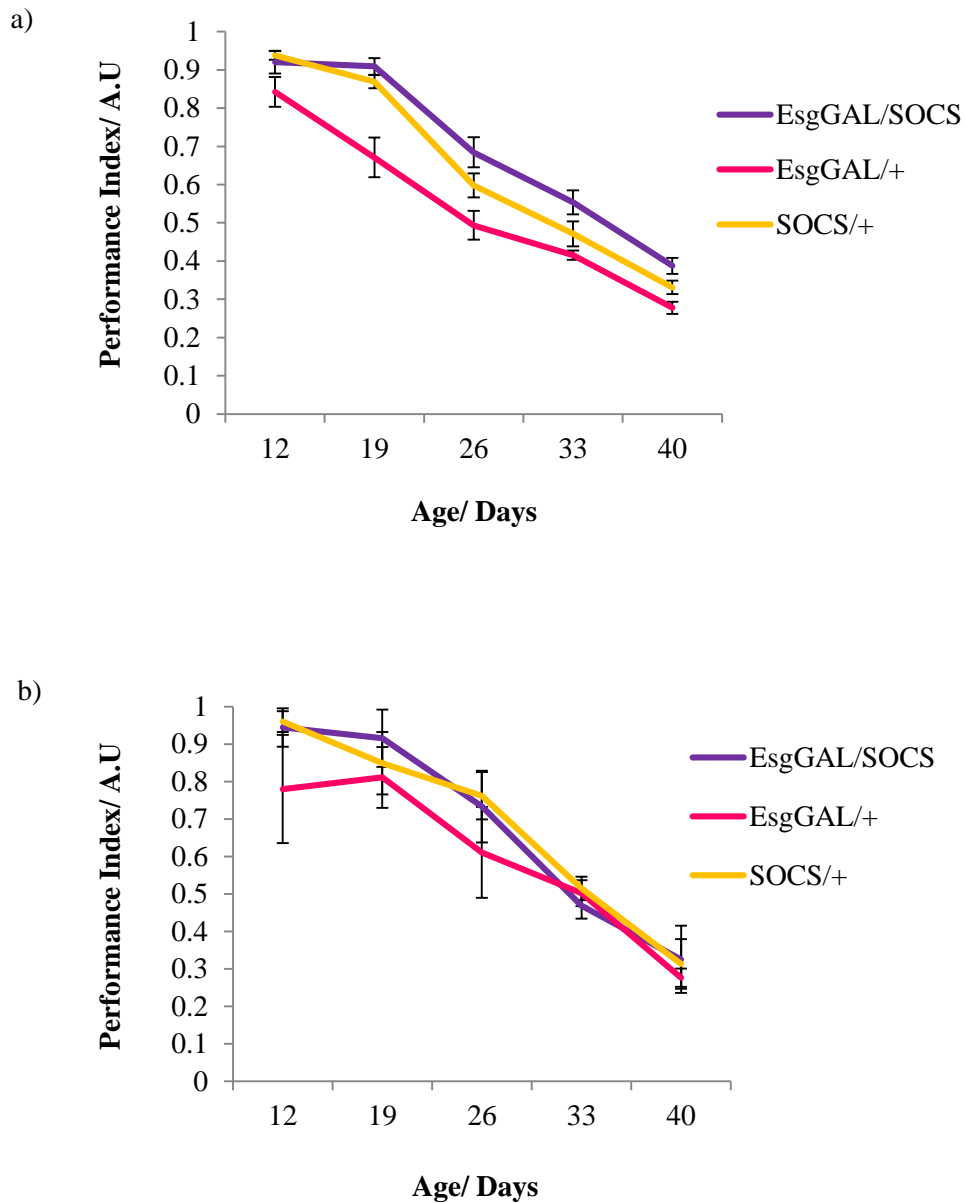
Figure 6.2: Assessment of neuromuscular health and functional senescence over time in uninfected and *Ecc15*-infected ISC SOCS36E knockdown female flies, plus controls.
Performance index (±SEM) with increasing age of (a) uninfected and (b) infected EsgGAL/SOCS females (purple) compared with EsgGAL/+ (pink) and SOCS/+ (orange) control genotypes. Negative geotaxis was carried out once a week, using a minimum of 21 flies and a maximum of 75 flies per genotype at each time point.
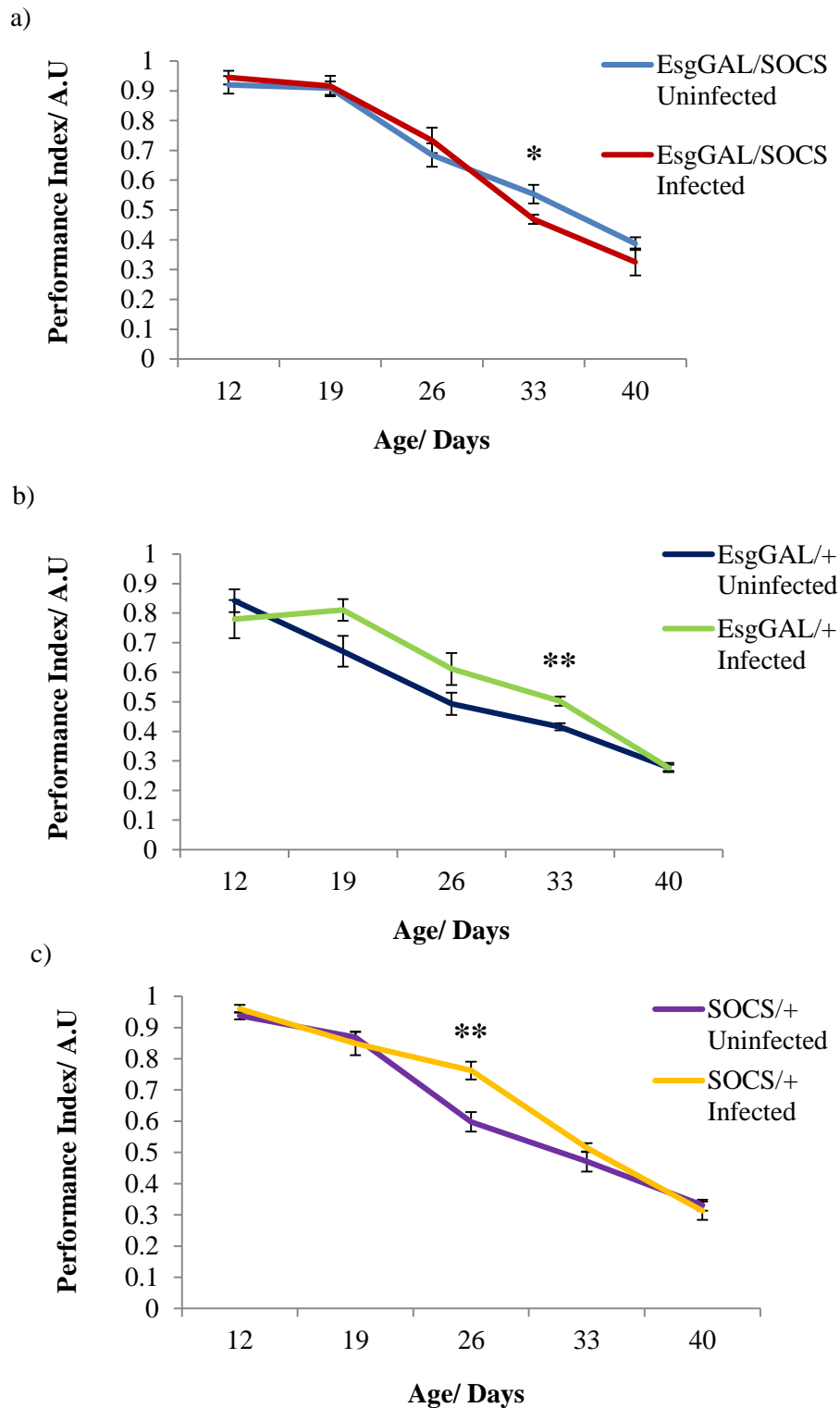
Figure 6.3: Assessment of *Ecc15* midgut infection on neuromuscular health and functional senescence over time using negative geotaxis in ISC SOCS36E knockdown female flies, plus relevant controls. Performance index (±SEM) with increasing age of (a) uninfected and infected EsgGAL/SOCS females, (b) uninfected and infected EsgGAL/+ females, and (c) uninfected and infected SOCS/+ females. (* = p<0.05, ** = p<0.01, using a Student's t-test).

The negative geotaxis assay was also carried out in male flies, and as found in the first assay conducted in female flies, there were no overall differences in P.I calculated between genotypes or infection groups (assessed using a one-way ANOVA). As expected, significant differences were found between P.Is at different time points within genotypes, and as in females flies, the trends observed were consistent across all three genotypes. However, statistical significance was only found between each of the first three time points, and the two final time points, suggesting a possible delay in the age-associated decline when compared to females. At day 7, SOCS36E knockdown in uninfected flies had a positive effect when performances were compared with EsgGAL/+ ($p < 0.05$) and SOCS/+ flies ($p < 0.0001$) (figure 6.4). This replicates the findings from the first assay in female flies (figure 6.1a).

Microbial-induced proliferation through *Ecc15* infection again had very little effect on assay performance, with inconsistent effects observed again across genotypes and individual time points (data not shown, statistical analysis in table 6.2). For instance, infection had a significant negative effect on assay performance in EsgGAL/SOCS and SOCS/+ males at days 7 and 14 respectively ($p < 0.05$), but also a positive effect in SOCS/+ males at day 35 ($p < 0.05$).

To summarise, neither SOCS36E knockdown, nor *Ecc15* infection-induced midgut proliferation had an overall effect on the performance index, and therefore locomotor senescence, of these male flies, replicating findings similar to those found in the first assay carried out in female flies.
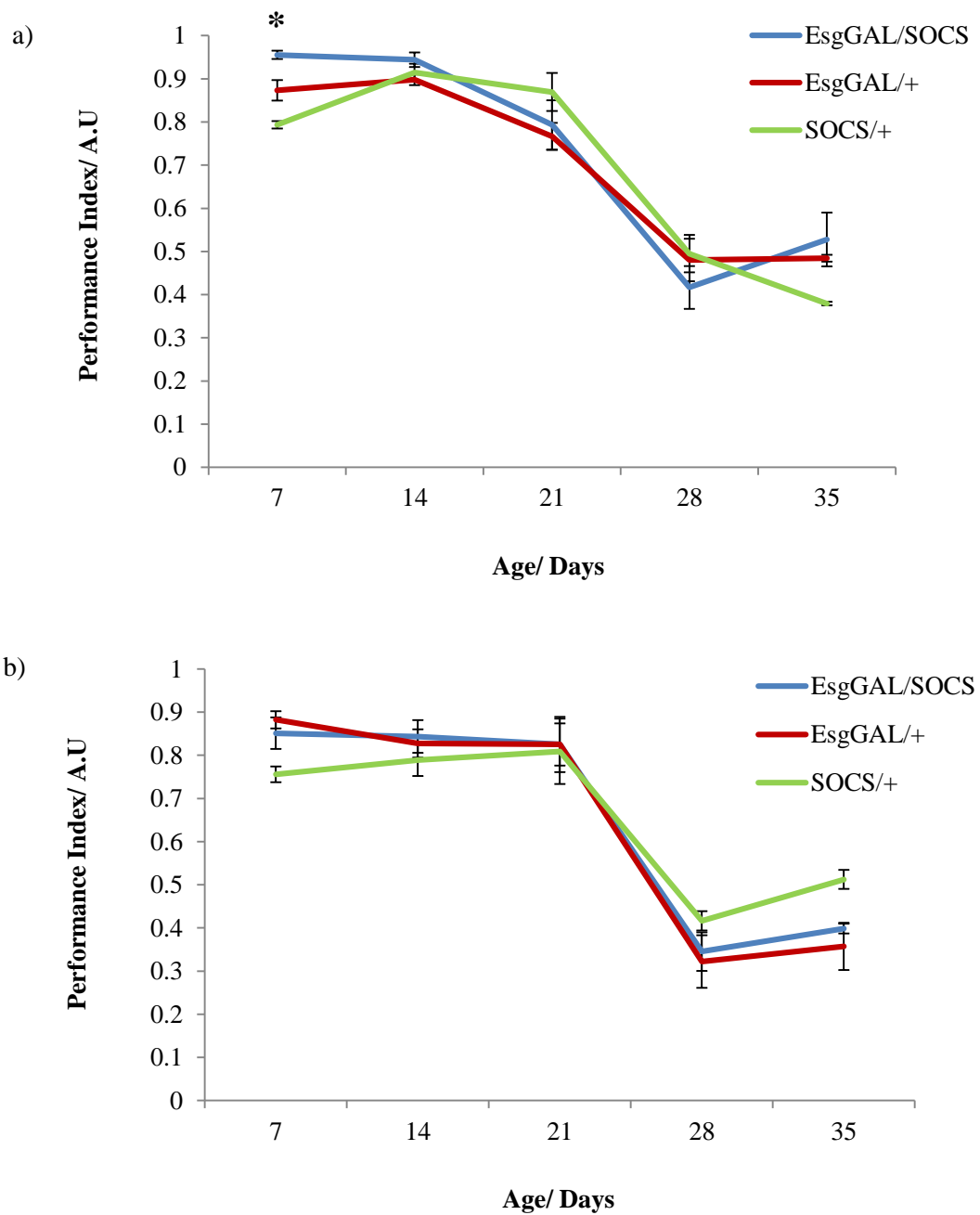
Figure 6.4: Assessment of neuromuscular health and functional senescence over time in uninfected and *Ecc15*-infected ISC SOCS36E knockdown male flies, plus controls.
Performance index (±SEM) with increasing age of (a) uninfected and (b) infected 139EsgGAL/SOCS males (blue) compared with EsgGAL/+ (red) and SOCS/+ (green) control genotypes. Negative geotaxis was carried out once a week, using a minimum of 21 flies and a maximum of 75 flies per genotype at each time point. (* = p<0.05, using a one-way ANOVA with Tukey's HSD).

Genotype	Age	7	14	21	28	35
EsgGAL/SOCS		**0.024 (-)**	**0.0411 (-)**	0.6842	0.3172	**0.0628 (-)**
EsgGAL/+		0.7834	0.0809	0.4348	0.0784	0.0843
SOCS/+		0.1421	**0.0181 (-)**	0.47	0.1479	**0.0002 (+)**

Table 6.2: P-values calculated using JMP, showing statistical significance (and near significance, in bold) between performance indexes in uninfected male flies and their infected counterparts (using a Student's t-test). (+) indicates a positive effect of *Ecc15* infection, (-) indicates a negative effect of *Ecc15* infection.

The negative geotaxis assay was repeated in uninfected and *Ecc15*-infected male flies, and as figure 6.5 (a) and (b) shows, knockdown of SOCS36E in ISCs had no significant effect, both on overall performance and at individual time points of the assay, regardless of infection status (both assessed using one-way ANOVAs). This confirmed that disrupting intestinal homeostasis via the Jak/Stat pathway did not accelerate nor delay the age-associated decline in neuromuscular health and functional senescence (in this assay) in male flies.

Similar to the previous results in both male and female flies, no overall significant effect of microbial-induced midgut proliferation on assay performance was calculated for any of the three genotypes ($p > 0.05$ using a one-way ANOVA). Additionally, with the exception of day 11 in EsgGAL/+ males, where infection negatively affected P.I ($p < 0.05$, data not shown, statistical analysis in table 6.3), assay performance was similar between all uninfected and infected males within each genotype. Together with results from figures 6.4 and 6.5, this reiterates that altering intestinal homeostasis in male flies by knocking down SOCS36E, as well as disrupting the microbiota through *Ecc15* infection, had no significant overall effects on P.I and therefore locomotor senescence, as determined by the negative geotaxis assay. These results however are in conjunction with the lack of extension/shortening of lifespan in SOCS36E knockdown males (reported in the previous chapter), suggesting this protein is not involved in the health of male flies (at least through methods used here). Although we were unable to confirm reduced SOCS36E mRNA levels in these flies, they did exhibit increased stress resistance (shown later in this chapter) along with female flies, who did have a reduced lifespan. Therefore, these findings suggest that the lack of effect on lifespan, and lack of phenotype in the negative geotaxis assay may not have been due to a lack of SOCS36E knockdown.
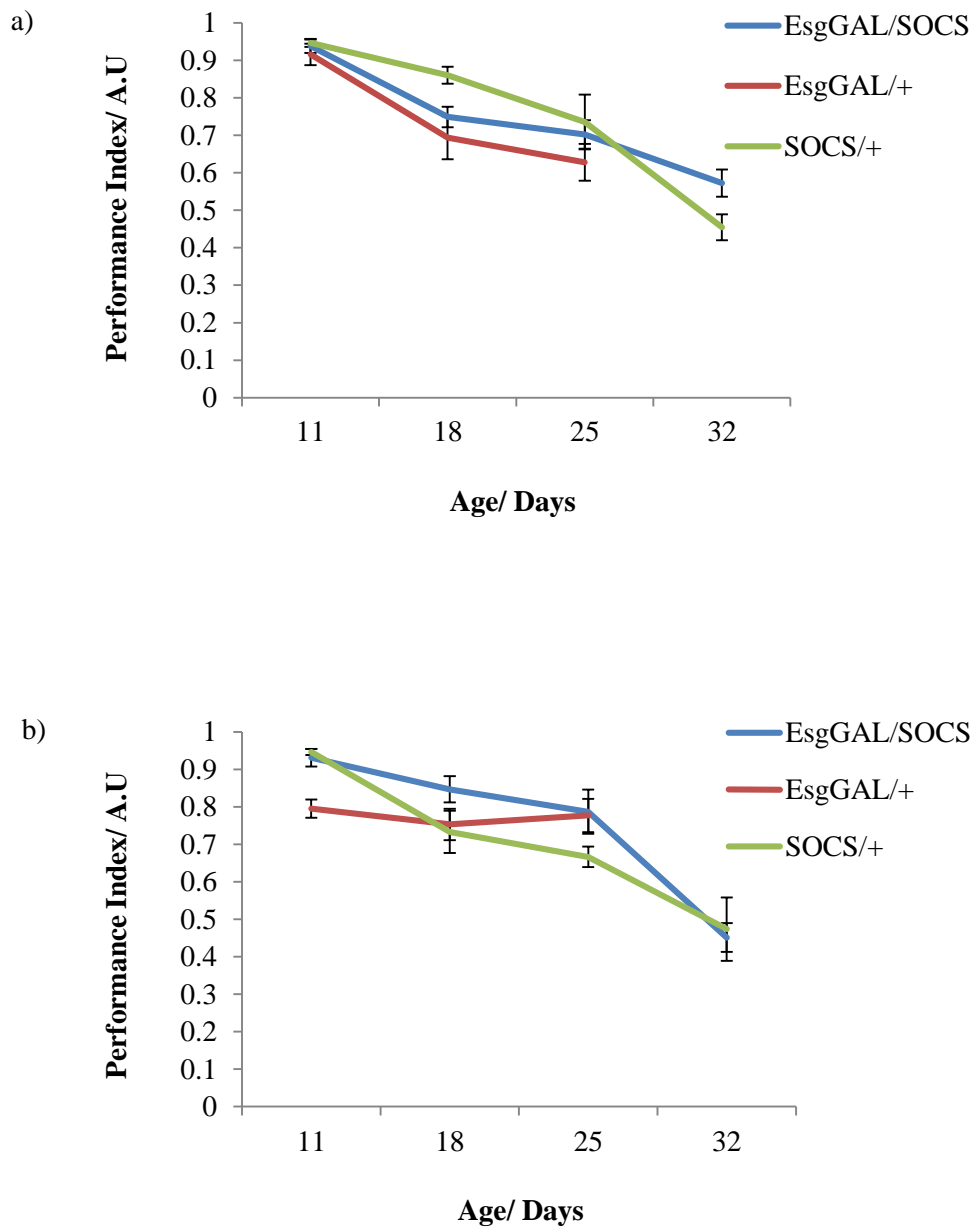
Figure 6.5: Assessment of *Ecc15* midgut infection on neuromuscular health and functional senescence over time using negative geotaxis in ISC SOCS36E knockdown male flies, plus relevant controls. Performance index (±SEM) with increasing age of (a) uninfected and (b) infected EsgGAL/SOCS males (blue) compared with EsgGAL/+ (red) and SOCS/+ (green) control genotypes. Negative geotaxis was carried out once a week, using a minimum of 21 flies and a maximum of 75 flies per genotype at each time point.

Genotype	Age	3	11	18	25	32
EsgGAL/SOCS		0.0806	0.8275	**0.0596** **(+)**	0.2592	0.0853
EsgGAL/+		0.248	**0.0124** **(-)**	0.4235	**0.0543** **(+)**	-
SOCS/+		**0.0192** **(+)**	0.9999	**0.0542** **(-)**	0.4009	0.8441

Table 6.3: P-values calculated using JMP, showing statistical significance (and near significance, in bold) between performance indexes in uninfected male flies and their infected counterparts (using a Student's t-test). (+) indicates a positive effect of *Ecc15* infection, (-) indicates a negative effect of *Ecc15* infection.

6.3 Assessment of exploratory walking senescence

Another assay used to measure motor function is the exploratory walking assay, as developed by Martin (2004). This assesses the spontaneous walking behaviour of fruit flies and involves filming flies inside a piece of apparatus containing four chambers, with each chamber occupying one fly. The dimensions of each chamber do not permit flight so only walking behaviours are observed. The assay is incredibly useful as it allows the dissection and analysis of many walking behaviours, such as: the total distance travelled, walking velocity, the number of times walking direction changed, as well as the time taken to change walking direction. The walking behaviours can also be divided further, as initiation and cessation of walking, and changes in walking speed and direction have decision making and neurological implications. Locomotion has shown to be controlled through the central complex and mushroom bodies located in the *Drosophila* brain. Strauss and Heisenberg (1993) found impaired walking activity (including walking speed, and straight line walking) in 15 mutant fly strains that affected the central complex structure. Martin et al. (1998) found that disruption of mushroom bodies, either chemically or genetically, led to an increase in walking activity, demonstrating their role in limiting excessive walking, through terminating periods of activity. The walking behaviours assessed using the assay developed by Martin (2004) naturally senesce with increasing age in *Drosophila*, as well as in humans (Grotewiel et al. 2005, Ismail et al. 2015). Therefore, this assay allows us to determine whether disrupting the homeostasis and microflora of flies, through knockdown of SOCS36E and infection with *Ecc15* respectively, will ultimately affect the natural senescence of multiple parameters of spontaneous walking, and the possible motor or neurological implications it could lead to. We used this assay to measure total walking distance, walking velocity, rotation frequency (the number of times walking direction changed), and also latency to the first rotation (the time taken to first change walking direction).

6.3.1 Both SOCS36E knockdown alone, and combined with Ecc15 infection had inconsistent effects on the age-associated decline in all walking parameters assessed in female flies

The exploratory walking assay was performed once a week in uninfected and *Ecc15*-infected experimental female flies (as well as males) and involved randomly sampling flies across each genotype, assessing various parameters of walking at multiple time points over the flies' lifespan. Figure 6.6 (a)-(d) compares all four parameters assessed in female flies, in both uninfected and infected cohorts. With the exception of rotation frequency at day 51 in uninfected flies, where SOCS36E knockdown had a positive effect (p<0.0001), no other significant differences (positive or negative) were observed between EsgGAL/SOCS flies and

both control genotypes, regardless of infection status. This indicates that the knockdown of SOCS36E in female flies did not affect any of the walking parameters assessed over the duration of their lifespan. Similar to the negative geotaxis results, infection with *Ecc15* had neither positive nor negative overall effects on walking senescence in any genotype. There were a few select time points across parameters where infection had significant effects on assay performance. However, these effects were not consistent within parameters, or within genotypes across parameters (statistics shown in table 6.4, figures shown in Appendices 1, 3, 5 and 7 for each parameter). Area under the curve analysis was also carried out to determine the total function in these female flies (Appendices 2, 4, 6 and 8), and in conjunction with the other results, there were no substantial differences observed, and any visible differences between genotypes or infection groups were not found to be statistically significant (tables A1-4 in Appendices).

In conclusion, ISC knockdown of SOCS36E, and interruption of microflora and induction of proliferation in the midgut through *Ecc15* infection did not alter the age-associated senescence of any of the walking parameters assessed in this assay, in female flies.

Uninfected   **Infected**

(a)

(b)

(c)

****

EsgGAL/SOCS

EsgGAL/+
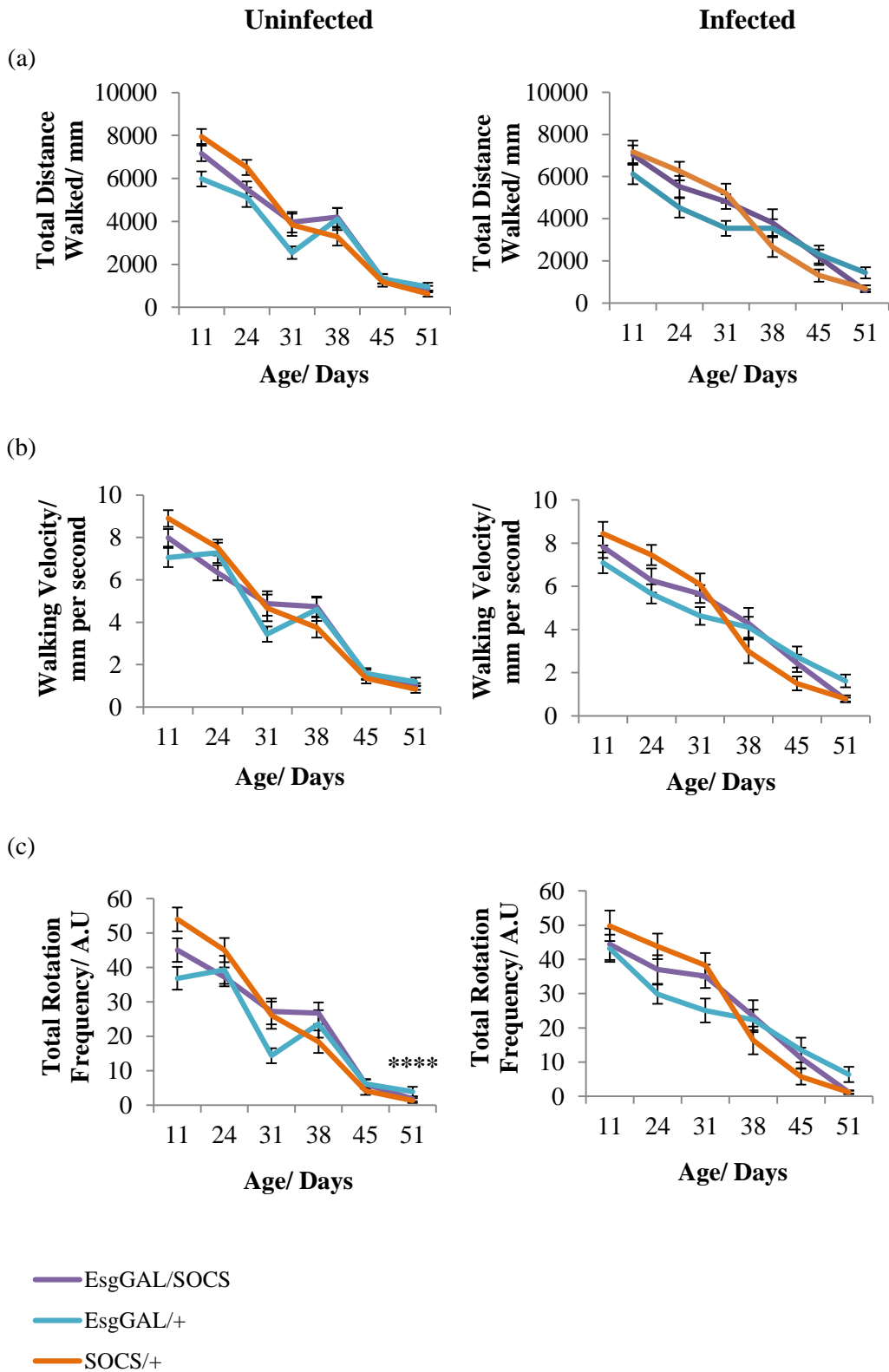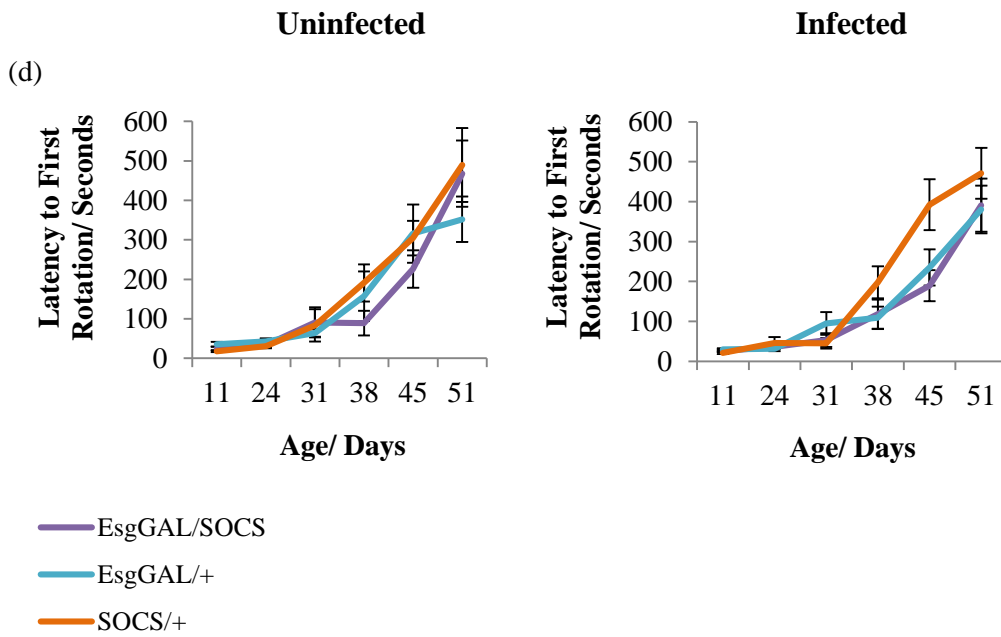
SOCS/+

Figure 6.6: Assessment of senescence of (a) walking distance, (b) walking velocity, (c) rotation frequency and (d) latency to the first rotation in uninfected and *Ecc15*-infected SOCS36E knockdown female flies, plus controls. Data are shown as a mean value (±SEM) for each time point for uninfected and infected EsgGAL/SOCS females (purple) compared with EsgGAL/+ (blue) and SOCS/+ (orange) control genotypes. Flies were recorded for 15 minutes each using a video camera, with a maximum of 15 flies used for each genotype at each time point. Videos were analysed using Ethovision XT software (Noldus). (**** = p<0.0001, using a one-way ANOVA with Tukey's HSD).

(a) **EsgGAL/SOCS**

Walking Behaviour	Age	11	24	31	38	45	51
Walking Distance		0.8134	0.9845	0.1597	0.6274	**0.0557** (+)	0.1146
Walking Velocity		0.8092	0.9181	0.2905	0.6015	**0.0634** (+)	0.2313
Rotation Frequency		0.9084	0.9578	0.1313	0.5565	0.1314	0.4634
Latency to First Rotation		0.9044	0.7471	0.3735	0.5618	0.5634	0.6195

(b) **EsgGAL/+**

Walking Behaviour	Age	11	24	31	38	45	51
Walking Distance		0.8183	0.3512	**0.0415** (+)	0.4082	**0.0502** (+)	0.1439
Walking Velocity		0.95	**0.02** (-)	**0.038** (+)	0.5023	**0.0465** (+)	0.2463
Rotation Frequency		0.2277	**0.0624** (-)	**0.0155** (+)	0.8008	**0.0674** (+)	0.3553
Latency to First Rotation		0.375	0.2357	0.3354	0.4898	0.3782	0.7609

(c) **SOCS/+**

Walking Behaviour	Age	11	24	31	38	45	51
Walking Distance		0.2235	0.6639	**0.0578** **(+)**	0.3447	0.7395	0.7799
Walking Velocity		0.5011	0.8947	0.0931	0.3008	0.7371	0.8117
Rotation Frequency		0.4578	0.8062	**0.0311** **(+)**	0.6855	0.5628	0.8781
Latency to First Rotation		0.3381	0.3262	0.3828	0.9156	0.3248	0.9134

Table 6.4: P-values calculated using JMP, showing significance (and near significance, in bold) between uninfected (a) EsgGAL/SOCS, (b) EsgGAL/+ and (c) SOCS/+ female flies and their infected counterparts (using a Student's t-test). (+) indicates a positive effect of *Ecc15* infection, (-) indicates a negative effect of *Ecc15* infection.

The walking assay was repeated in experimental female flies, and contrary to previous findings, there were overall negative effects of SOCS36E knockdown on walking distance, velocity and rotation frequency within *Ecc15*-infected females, when knockdown flies were compared with both control genotypes- EsgGAL/+ and SOCS/+ ($p<0.05$, using a one-way ANOVA with Tukey's HSD). In uninfected females however, there were significant positive effects of SOCS36E knockdown for all assessed parameters, but only when compared with EsgGAL/+ females (distance, velocity and rotation frequency- $p<0.0001$, latency to the first rotation- $p<0.05$). As figures 6.7-6.11 show, uninfected EsgGAL/+ females exhibited unusually diminished assay performance. As the sharp behavioural decreases were not observed in the first experiments, nor observed in the other control flies, SOCS/+, the results obtained in this repeat were considered anomalous, and were not included when analysing effects of SOCS36E knockdown. Therefore, within uninfected flies, assay performance of EsgGAL/SOCS females was compared to that of SOCS/+ flies only.

With the exception of latency to the first rotation, where no statistical differences were observed between uninfected EsgGAL/SOCS and SOCS/+ flies (figure 6.7d, left panel), knockdown of SOCS36E negatively affected the senescence of walking behaviours. These effects were observed at day 12 for walking distance and rotation frequency ($p=0.0099$), and day 16 for velocity ($p=0.0078$) (figure 6.7a-c, left panels), and therefore show that knockdown of ISC SOCS36E was disadvantageous at early time points of females' lifespan. Regarding latency to the first rotation, these results mirrored those from the first experiment (figure 6.6d, left panel), so therefore indicates that dysregulation of intestinal homeostasis through SOCS36E knockdown alone had no effect on this behaviour.

When determining the effect of ISC SOCS36E knockdown within female flies with induced midgut proliferation (through *Ecc15* infection), results contrasted those of both uninfected females, and infected females from the first experiment (figure 6.6a-d, right panels). Compared to both control genotypes, EsgGAL/SOCS had significant reductions in walking distance, velocity and rotation frequency; all at days 19 and 26 ($p<0.01$). SOCS36E knockdown in infected females also led to increased latency to the first rotation, thus demonstrating further negative effects, at day 26 ($p<0.0001$ and $p=0.0001$ compared to EsgGAL/+ and SOCS/+, respectively). Collectively, these observations indicate that knockdown of ISC SOCS36E coupled with infection-induced midgut proliferation was detrimental to multiple parameters of walking, and accelerated the age-associated declines in all four behaviours assessed.

Uninfected   **Infected**

(a)

(b)

(c)

EsgGAL/SOCS

EsgGAL/+
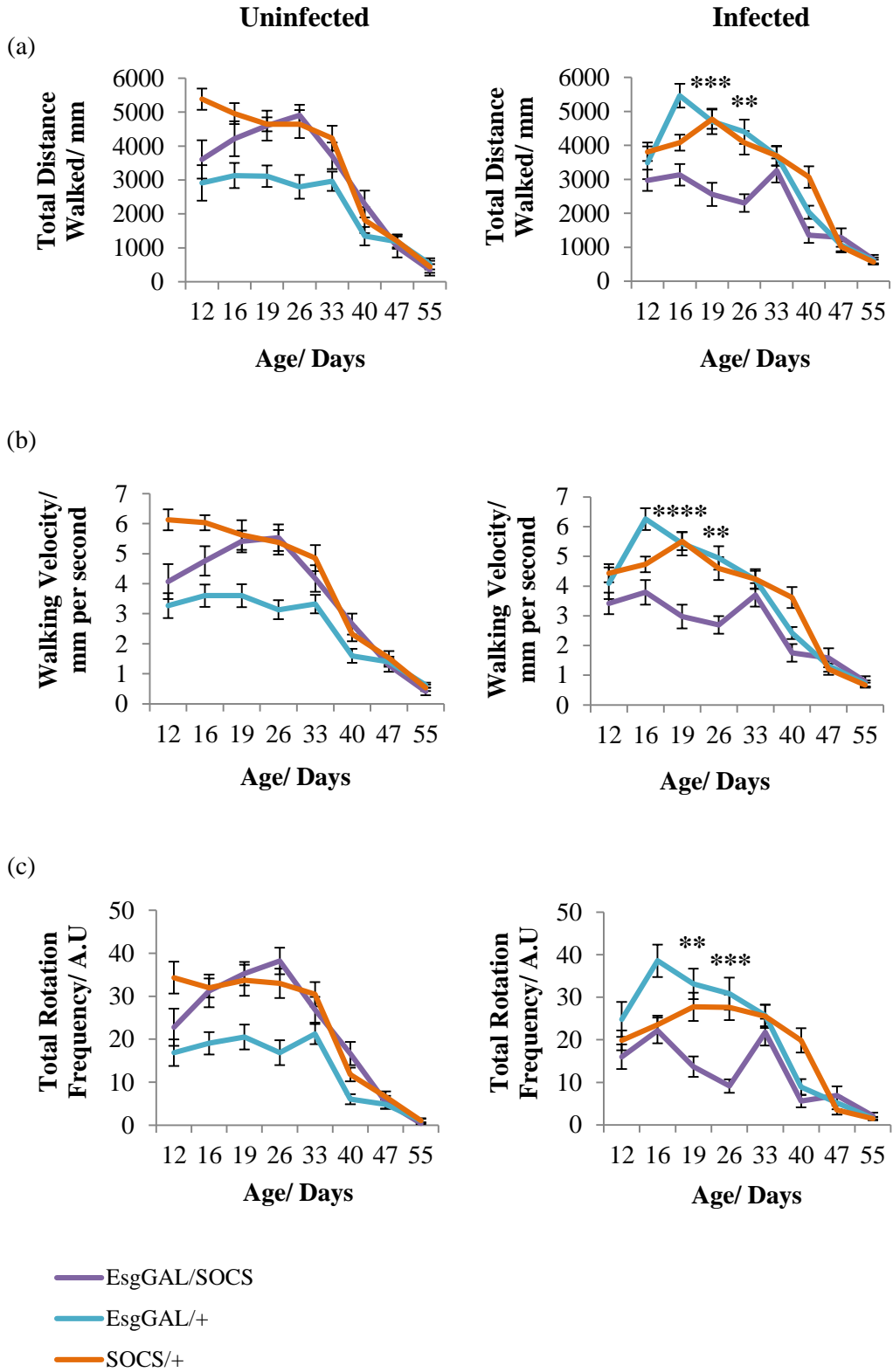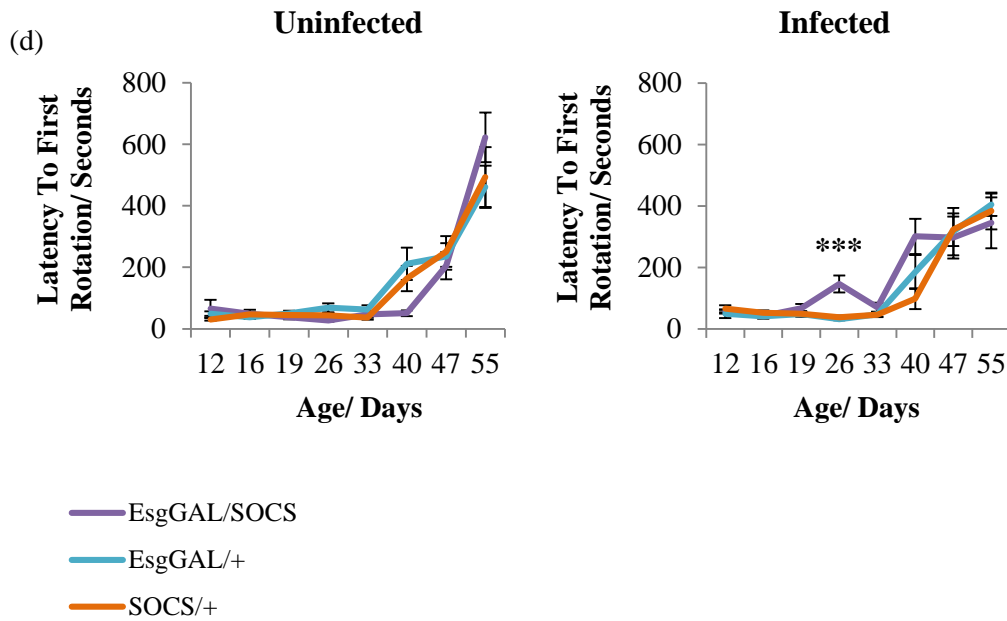
SOCS/+

Figure 6.7: Assessment of senescence of (a) walking distance, (b) walking velocity, (c) rotation frequency and (d) latency to the first rotation in uninfected and *Ecc15*-infected SOCS36E knockdown female flies, plus controls. Data are shown as a mean value (±SEM) for each time point for uninfected and infected EsgGAL/SOCS females (purple) compared with EsgGAL/+ (blue) and SOCS/+ (orange) control genotypes. Flies were recorded for 15 minutes each using a video camera, with a maximum of 15 flies used for each genotype at each time point. Videos were analysed using Ethovision XT software (Noldus). (** = p<0.01, *** = p<0.001, **** = p<0.0001, using a one-way ANOVA with Tukey's HSD).

We then assessed the effects of infection-induced midgut proliferation on exploratory walking within each genotype. *Ecc15* infection negatively affected overall assay performance of EsgGAL/SOCS females for all walking parameters ($p < 0.0001$ for distance, velocity, and rotation frequency, $p = 0.0019$ for rotation latency), and also with rotation frequency in SOCS/+ flies ($p = 0.0458$) (analysed using a Student's t-test). As observed in figure 6.7 (a-d, right panels), assay performance of infected EsgGAL/+ females was similar to that of SOCS/+ flies. Within the EsgGAL/+ cohort, uninfected females had greatly reduced walking speed, walking distances and rotation frequencies at several time points in comparison to infected females (figures 6.8b and e, and 6.9b, right panel). *Ecc15* infection was found to have overall significant positive effects on these three behaviours in EsgGAL/+ flies ($p < 0.0001$), indicating that infection rescued the diminished walking phenotypes in these flies. Assay performance of uninfected EsgGAL/+ was so negatively affected, that *Ecc15* infection had significant positive results at multiple time points within each walking parameter between days 16 and 40 ($p < 0.05$), often with overlapping time points between parameters.

Supporting results shown in figure 6.7 (a-c, right panels), infection with *Ecc15* had consistent negative effects in EsgGAL/SOCS females, reducing assay performance at days 19 and 26 for walking distance ($p = 0.0001$ and $p < 0.0001$, respectively, figure 6.8a), velocity ($p = 0.0001$ and $p < 0.0001$, respectively, figure 6.8d) and rotation frequency ($p < 0.0001$, figure 6.9a). Significant decreases were also observed in velocity at day 40 ($p = 0.0213$), and in rotation latency at days 26 and 40 ($p = 0.0002$, as shown in figure 6.9d). Therefore, results of figure 6.7-6.9 indicate that infection-induced midgut proliferation in EsgGAL/SOCS females accelerated the age-associated senescence of all assessed walking behaviours. Similarly, negative effects of infection-induced proliferation were observed in SOCS/+ flies at days 12 and 16 for walking distance ($p = 0.0007$ and $p = 0.0088$, respectively), velocity ($p = 0.0011$ and $p = 0.0014$, respectively) and rotation frequency ($p = 0.0025$ and $p = 0.0108$, respectively), as well as rotation latency at day 12 only ($p = 0.0067$). Interestingly, *Ecc15* infection also positively affected distance ($p = 0.0019$), velocity ($p = 0.0052$) and rotation frequency ($p = 0.0212$) at day 40 too. As these phenotypes occurred earlier than those in EsgGAL/SOCS, this demonstrates how infection during early life can have detrimental effects on host health.
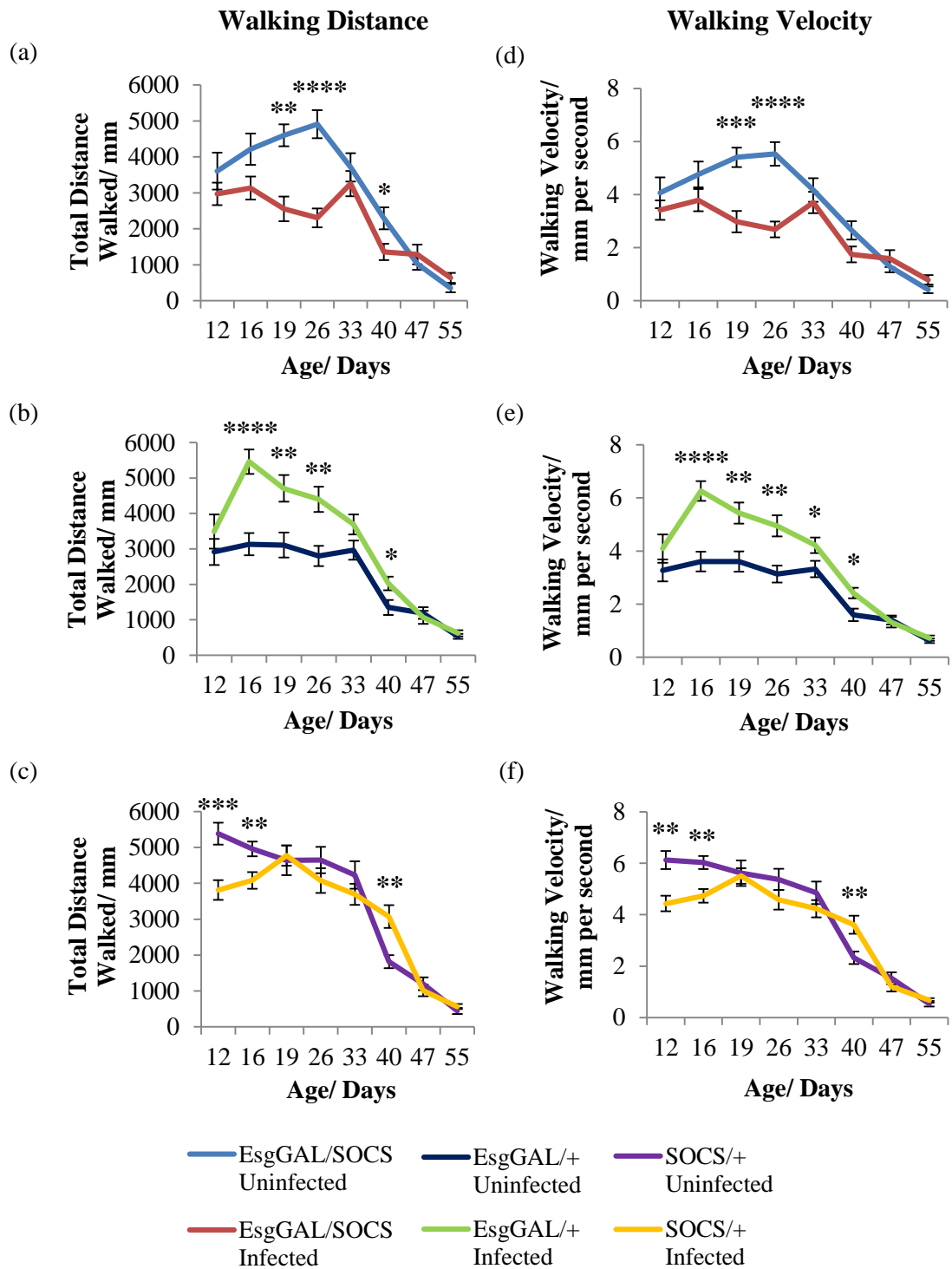
Figure 6.8: The effect of *Ecc15* infection on the age-associated decline of walking distance and velocity in SOCS36E knockdown and control female flies. Data are shown as a mean value (±SEM) for each time point for uninfected and infected (a) and (d) EsgGAL/SOCS, (b) and (e) EsgGAL/+ and (c) and (f) SOCS/+ female flies. (* = p<0.05, ** = p<0.01, *** = p<0.001, **** = p<0.0001, using a Student's t-test).
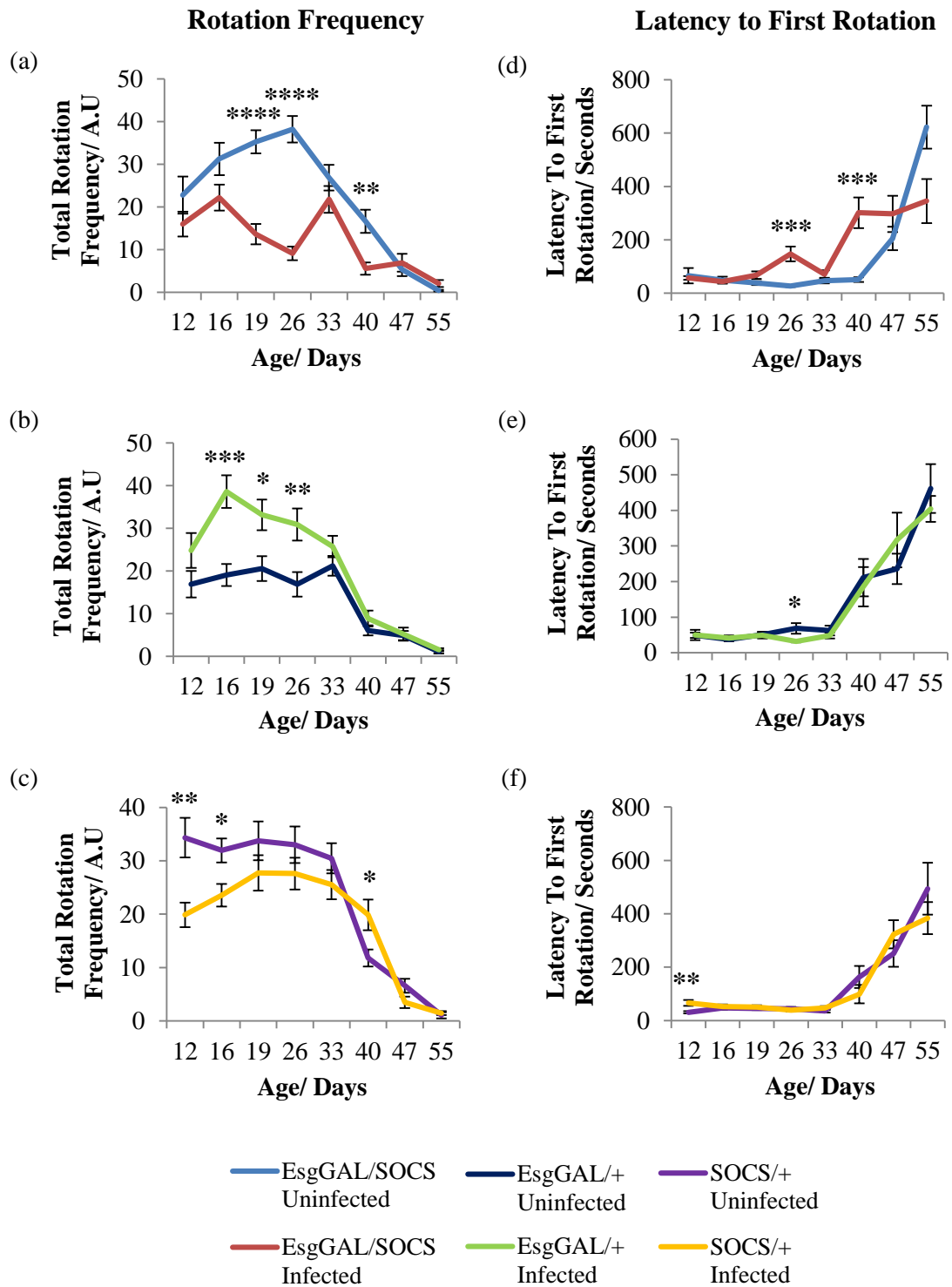
Figure 6.9: The effect of *Ecc15* infection on the age-associated decline of rotation frequency, and latency to the first rotation in SOCS36E knockdown and control female flies. Data are shown as a mean value (±SEM) for each time point for uninfected and infected (a) and (d) EsgGAL/SOCS, (b) and (e) EsgGAL/+ and (c) and (f) SOCS/+ female flies. (* = p<0.05, ** = p<0.01, *** = p<0.001, **** = p<0.0001, using a Student's t-test).

Area under the curve analysis was conducted to determine the total function of each parameter within genotypes, and assess potential effects of ISC SOCS36E knockdown and/or infection-induced midgut proliferation. Consistent with results in figures 6.7-6.9, knockdown of SOCS36E significantly decreased total function of distance walked ($p<0.0001$, figure 6.10a), walking velocity ($p<0.0001$, figure 6.10b) and rotation frequency ($p<0.001$, figure 6.11a) in *Ecc15*-infected females. SOCS36E knockdown also led to decreased total function of velocity within uninfected flies ($p=0.0188$, figure 6.10b), although within the EsgGAL/SOCS cohort, *Ecc15* infection significantly decreased the total function for all four walking parameters that were assessed ($p<0.01$, as shown in tables 6.5 and 6.6). Furthermore, EsgGAL/SOCS exhibited the lowest total function for rotation latency within the uninfected cohort of flies (figure 6.10b), demonstrating a positive outcome of dysregulated midgut Jak/Stat signalling, as this was the only behaviour where increases have negative connotations.

From the second set of results, it can be proposed that after discounting the data from uninfected EsgGAL/+ females, disrupting intestinal homeostasis through knockdown of SOCS36 in the ISCs of female flies led to decreases during early life in three of the four assessed parameters. Altering the midgut microbiota and inducing ISC proliferation through introduction of *Ecc15* also had a negative effect on exploratory walking- both over time and on total function- and exacerbated the age-associated declines in these behaviours. Therefore, these results give an indication that changes within the midgut environment were implicated in neurological-regulated behaviours. However, when coupled with the data from the first experiment, the observed effects seen in figures 6.7-6.11 can only be confirmed with a further repeat of this assay.
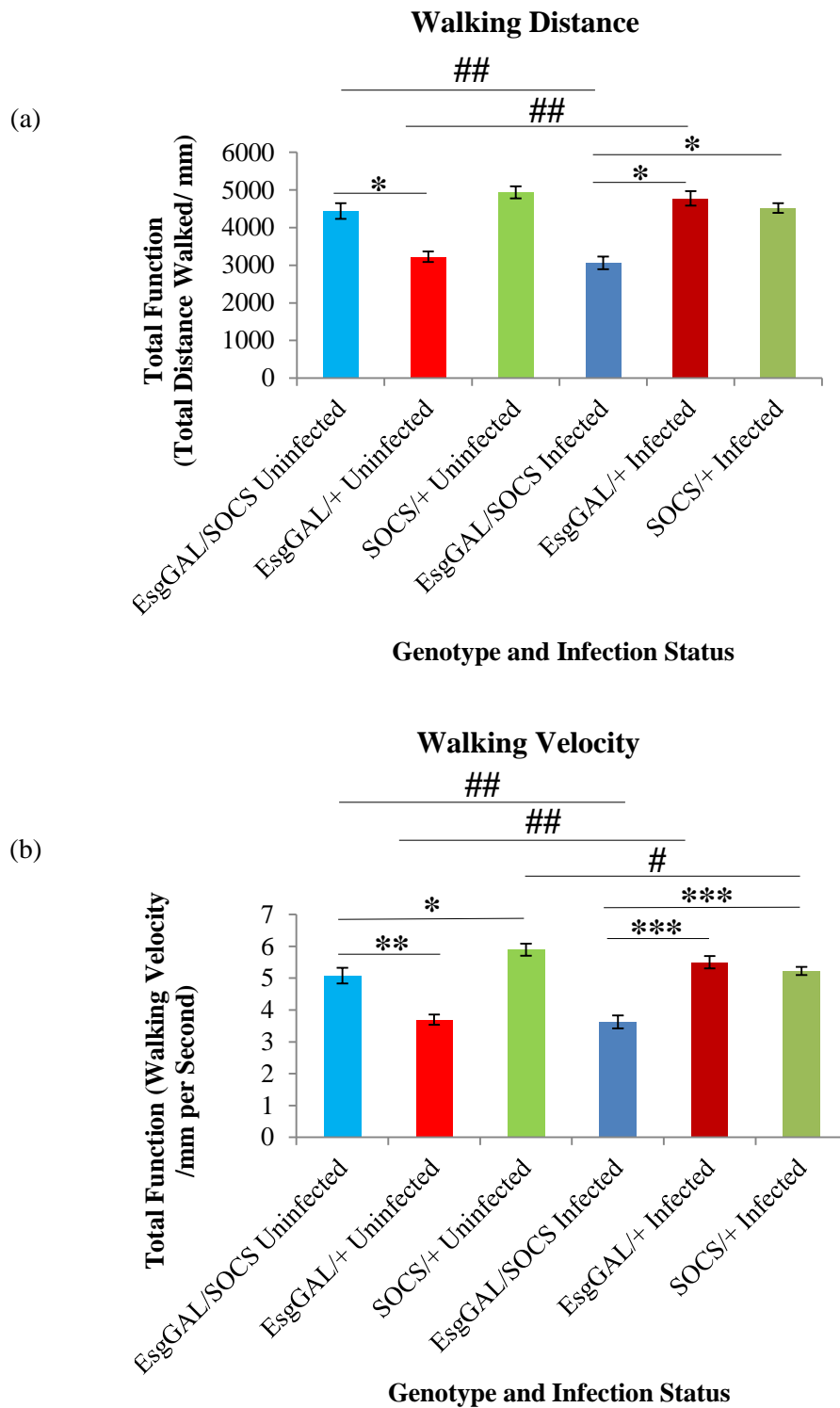
Figure 6.10: Total function of (a) distance walked, and (b) walking velocity (±SEM) in uninfected and *Ecc15*-infected SOCS36E knockdown female flies, plus controls. Total function was determined using the area under the curve at each time point of the assay, with a maximum of 15 flies used at each time point for each genotype and infection group. (* = p<0.05, ** = p<0.001, *** = p<0.0001, using a one-way ANOVA with Tukey's HSD. # = p<0.01, ## = p<0.0001, using a Student's t-test).

(a) **Walking Distance**

	EsgGAL/ SOCS Uninfected	EsgGAL/+ Uninfected	SOCS/+ Uninfected	EsgGAL/ SOCS Infected	EsgGAL/+ Infected	SOCS/+ Infected
EsgGAL/ SOCS Uninfected	x	**0.0001**	0.1184	**<0.0001**		
EsgGAL/+ Uninfected	**0.0001**	x			**<0.0001**	
SOCS/+ Uninfected	0.1184		x			0.0524
EsgGAL/ SOCS Infected	**<0.0001**			x	**<0.0001**	**<0.0001**
EsgGAL/+ Infected		**<0.0001**		**<0.0001**	x	
SOCS/+ Infected			0.0524	**<0.0001**		x

(b) **Walking Velocity**

	EsgGAL/ SOCS Uninfected	EsgGAL/+ Uninfected	SOCS/+ Uninfected	EsgGAL/ SOCS Infected	EsgGAL/+ Infected	SOCS/+ Infected
EsgGAL/ SOCS Uninfected	x	**<0.0001**	**0.0188**	**<0.0001**		
EsgGAL/+ Uninfected	**<0.0001**	x			**<0.0001**	
SOCS/+ Uninfected	**0.0188**		x			**0.0066**
EsgGAL/ SOCS Infected	**<0.0001**			x	**<0.0001**	**<0.0001**
EsgGAL/+ Infected		**<0.0001**		**<0.0001**	x	
SOCS/+ Infected			**0.0066**	**<0.0001**		x

Table 6.5: P-values calculated using JMP, showing significance (in bold) between uninfected and *Ecc15*-infected knockdown females and their relevant controls (using a one-way ANOVA with Tukey's HSD), as well as between uninfected female flies and their infected counterparts (using a Student's t-test), for total function of (a) walking distance, and (b) walking velocity.
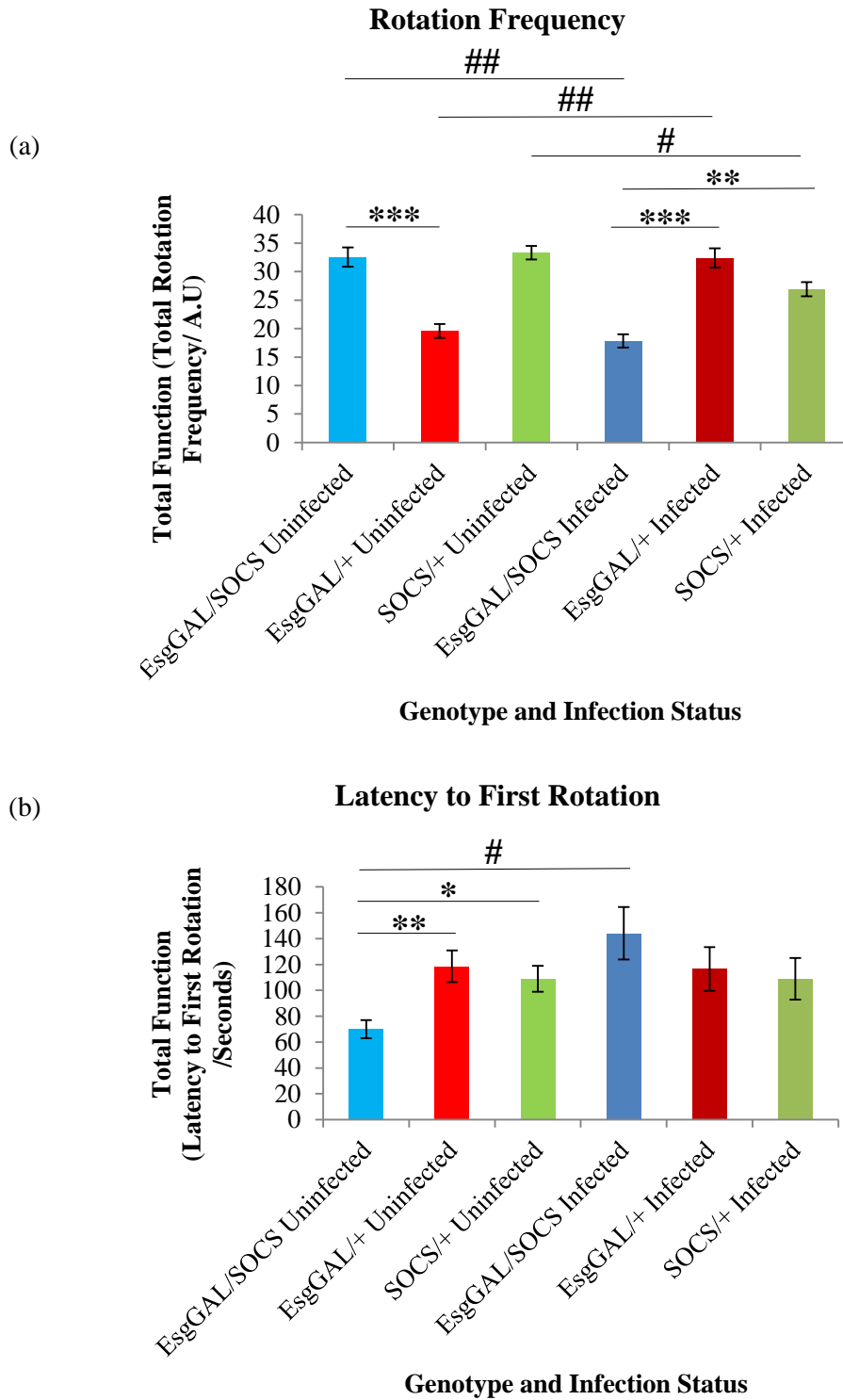
Figure 6.11: Total function of (a) rotation frequency, and (b) latency to the first rotation (±SEM) in uninfected and *Ecc15*-infected SOCS36E knockdown female flies, plus controls. Total function was determined using the area under the curve at each time point of the assay, with a maximum of 15 flies used at each time point for each genotype and infection group. (* = p<0.01, ** = p<0.001, *** = p<0.0001, using a one-way ANOVA with Tukey's HSD. # = p<0.001, ## = p<0.0001, using a Student's t-test).

(a) **Rotation Frequency**

	EsgGAL/ SOCS Uninfected	EsgGAL/+ Uninfected	SOCS/+ Uninfected	EsgGAL/ SOCS Infected	EsgGAL/+ Infected	SOCS/+ Infected
EsgGAL/ SOCS Uninfected	x	**<0.0001**	0.9143	**<0.0001**		
EsgGAL/+ Uninfected	**<0.0001**	x			**<0.0001**	
SOCS/+ Uninfected	0.9143		x			**0.0009**
EsgGAL/ SOCS Infected	**<0.0001**			X	**<0.0001**	**0.0001**
EsgGAL/+ Infected		**<0.0001**		**<0.0001**	x	
SOCS/+ Infected			**0.0009**	**0.0001**		x

(b) **Latency to the First Rotation**

	EsgGAL/ SOCS Uninfected	EsgGAL/+ Uninfected	SOCS/+ Uninfected	EsgGAL/ SOCS Infected	EsgGAL/+ Infected	SOCS/+ Infected
EsgGAL/ SOCS Uninfected	x	**0.0008**	**0.0091**	**0.0018**		
EsgGAL/+ Uninfected	**0.0008**	x			0.9261	
SOCS/+ Uninfected	**0.0091**		x			0.9967
EsgGAL/ SOCS Infected	**0.0018**			x	0.5232	0.3510
EsgGAL/+ Infected		0.9261		0.5232	x	
SOCS/+ Infected			0.9967	0.3510		x

Table 6.6: P-values calculated using JMP showing significance (in bold) between uninfected and *Ecc15*-infected knockdown females and their relevant controls (using a one-way ANOVA with Tukey's HSD), as well as between uninfected female flies and their infected counterparts (using a Student's t-test), for total function of (a) rotation frequency, and (b) latency to the first rotation.

The exploratory walking assay was performed in experimental male flies, alongside female flies, and also assessed the effect of dysregulated ISC proliferation (through knockdown of the *Drosophila* Jak/Stat pathway inhibitor, SOCS36E), with or without non-lethal midgut infection (using the Gram-negative phytopathogen, *Ecc15*) on the same parameters of walking. The first set of male results contrasted those of the first female set in that knockdown of SOCS36E in infected flies was found to have overall negative effects on walking distance and rotation frequency, when compared with both control genotypes ($p < 0.05$, and $p < 0.01$, respectively). For these parameters, SOCS36E knockdown in uninfected flies led to significant decreases in assay performance at day 31, in relation to both controls ($p < 0.05$, as shown in figure 6.12a and c). Upon infection with *Ecc15* however, these decreases were observed one week earlier, at day 24 ($p < 0.01$ and $p < 0.001$ for distance and rotation frequency, respectively), along with a significant reduction in distance walked relative to controls at day 31 as well ($p < 0.05$). Consistent with these results, assay performance was also negatively affected for velocity and rotation latency at day 24 ($p < 0.01$, shown in figure 6.12b and d). The results in figure 6.12 indicate that knockdown of ISC SOCS36E, either alone or coupled with *Ecc15*-infection induced midgut proliferation accelerated age-associated declines in several parameters of exploratory walking. However, where accelerations were observed in uninfected knockdown flies, introduction of *Ecc15* brought the declines forward by one week.

Uninfected   **Infected**

(a)

(b)

(c)

EsgGAL/SOCS

EsgGAL/+
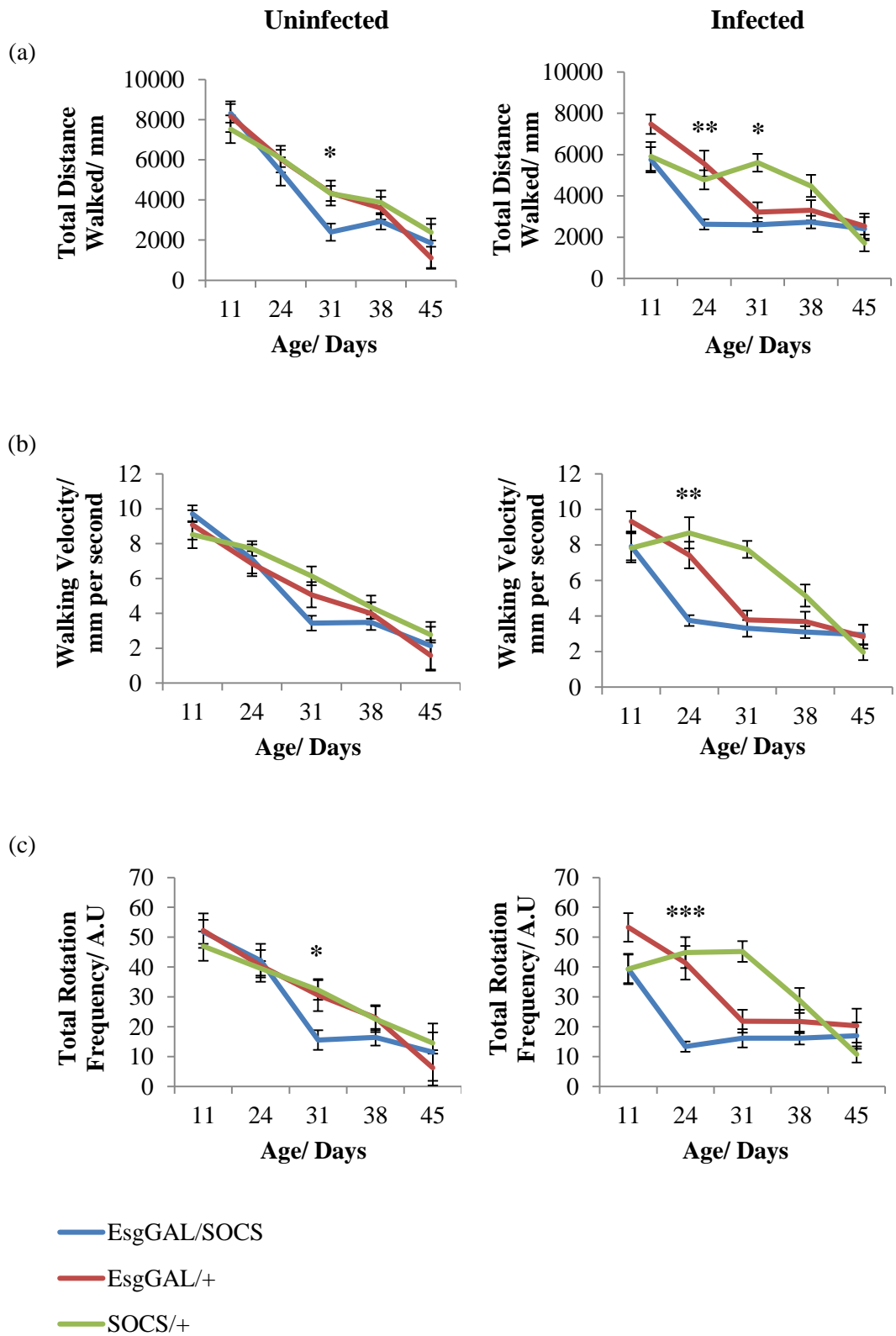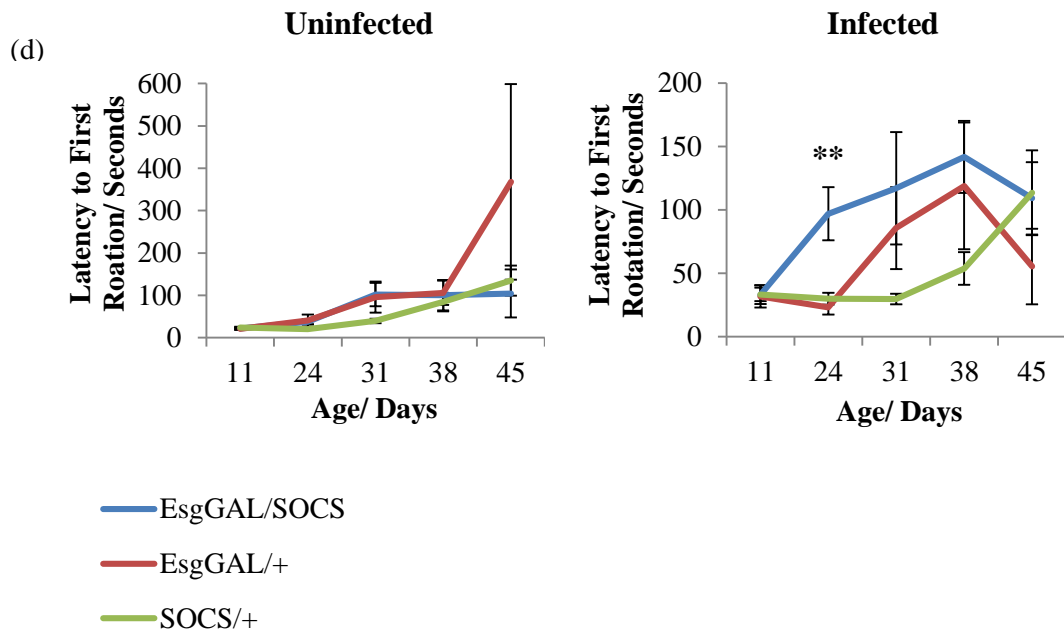
SOCS/+

Figure 6.12: Assessment of senescence of (a) walking distance, (b) walking velocity, (c) rotation frequency and (d) latency to the first rotation in uninfected and *Ecc15*-infected SOCS36E knockdown male flies, plus controls. Data are shown as a mean value (±SEM) for each time point for uninfected and infected EsgGAL/SOCS males (blue) compared with EsgGAL/+ (red) and SOCS/+ (green) control genotypes. Flies were recorded for 15 minutes each using a video camera, with a maximum of 15 flies used for each genotype at each time point. Videos were analysed using Ethovision XT software (Noldus). (* = p<0.05, ** = p<0.01, *** = p<0.001, using a one-way ANOVA with Tukey's HSD).

Consistent with findings from figure 6.12, *Ecc15* infection was found to exert significant negative effects on overall assay performance for all four parameters assessed within EsgGAL/SOCS flies (p<0.05). Also within this genotype, infection-induced proliferation led to significant declines at day 24 for distance walked (p=0.0009), walking velocity (p=0.0007) and rotation frequency (p<0.0001) (compared with uninfected EsgGAL/SOCS, shown in figure 6.13a and b, and figure 6.14a top panels, respectively). Rotation latency was also negatively affected at day 24 (p=0.0089, figure 6.14b, top panel), although this is a behaviour that displays age-associated increases. These results were exclusive to EsgGAL/SOCS males, as although infection negatively affected overall distance walked and rotation frequency in EsgGAL/+ flies (p=0.0138, and p=0.0358, respectively), no significant differences were observed at any of the five time points for all assessed parameters (figures 6.13 and 6.14, middle panels. The effects of infection in SOCS/+ were different again, both compared to EsgGAL/SOCS and EsgGAL/+ flies, and across parameters within the genotype, as *Ecc15*-induced midgut proliferation had an overall positive effect on rotation frequency (p=0.0351), significantly increasing the average number of rotations at day 31 (p=0.0111, figure 6.14c, bottom panel), and also positively affecting walking distance and velocity at day 31 too (p=0.0338, and p=0.035, respectively) (as shown in figure 6.13a and b, bottom panels).
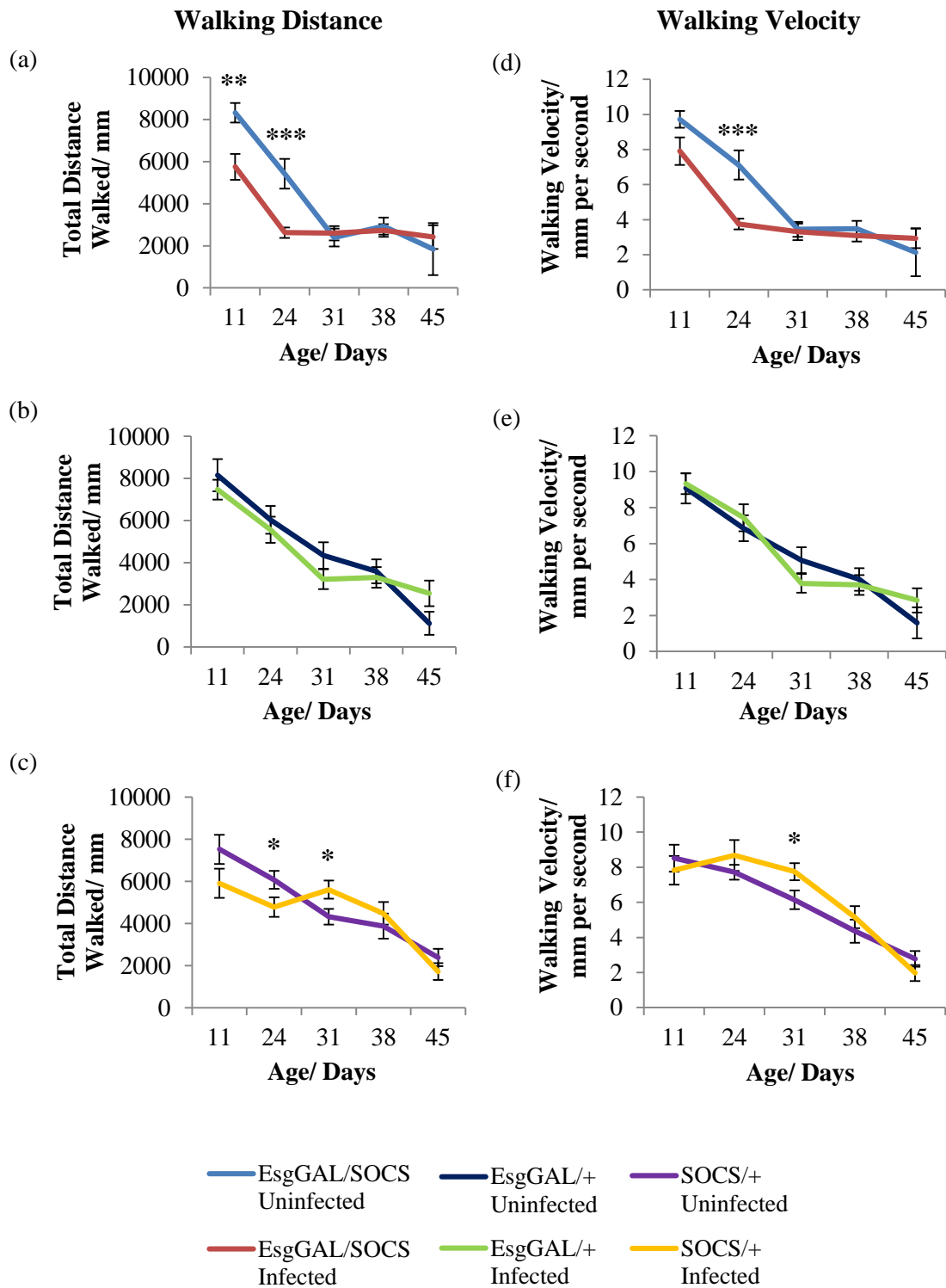
Figure 6.13: The effect of *Ecc15* infection on the age-associated decline on walking distance and velocity in SOCS36E knockdown and control male flies. Data are shown as a mean value (±SEM) for each time point for uninfected and infected (a) and (d) EsgGAL/SOCS, (b) and (e) EsgGAL/+ and (c) and (f) SOCS/+ male flies. (* = p<0.05, ** = p<0.01, *** = p<0.001, using a Student's t-test).
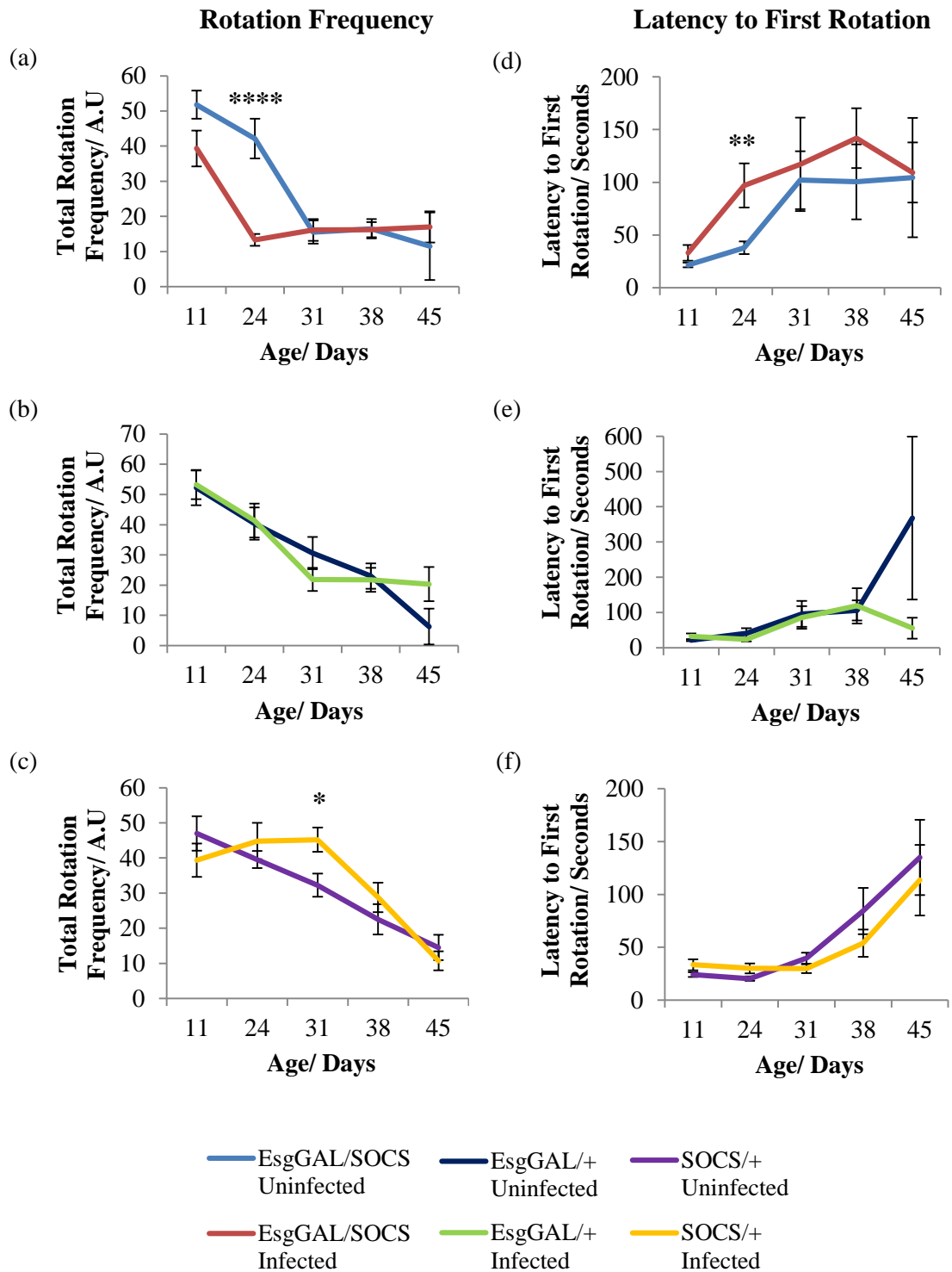
Figure 6.14: The effect of *Ecc15* infection on the age-associated decline on rotation frequency, and latency to the first rotation in SOCS36E knockdown and control male flies. Data are shown as a mean value (±SEM) for each time point for uninfected and infected (a) and (d) EsgGAL/SOCS, (b) and (e) EsgGAL/+ and (c) and (f) SOCS/+ male flies. (* = p<0.05, ** = p<0.01, **** = p<0.0001, using a Student's t-test).

In addition to effects of SOCS36E knockdown, and *Ecc15* infection on age-associated declines in walking behaviour, we also assessed the impact of these factors on total function, using area under the curve analysis. Consistent with figures 6.12-6.14, the total function of all four parameters were negatively affected following knockdown of ISC SOCS36E within infected flies (distance, velocity and rotation latency: $p<0.05$, rotation frequency: $p<0.01$, compared with both infected control genotypes) (shown in figures 6.15 and 6.16, a and b). Knockdown alone appeared to have visibly negative effects on total function too, although where significance was reached, it did not occur between EsgGAL/SOCS flies and both EsgGAL/+ and SOCS/+ controls (figure 6.15a and b, and figure 6.16a, with statistical values shown in tables 6.7 and 6.8). In agreement with findings in figures 6.13 and 6.14 demonstrating the effects of *Ecc15* within each genotype, infection led to significant decreases in total functions of distance walked ($p=0.0387$), velocity ($p=0.0172$) and rotation frequency ($p=0.0121$). Furthermore, although infection-induced proliferation had positive effects on three of the four walking behaviours at day 31 in SOCS/+ males, the increases must not have been that substantial as a whole as total function was only significantly increased with rotation frequency ($p=0.0336$, figure 6.16a). Similarly, *Ecc15* significantly decreased the overall distance walked and number of rotations exhibited by EsgGAL/+, although no differences in total function for all parameters were observed within this genotype.

In conclusion, the results from this experiment demonstrated that disrupting midgut homeostasis through knockdown of SOCS36E can be detrimental to some parameters of walking, although all four parameters were negatively affected following increased midgut proliferation in these flies, due to accelerations of age-associated behavioural declines and the overall performance and total function of each parameter. Therefore, due to changes in neurally-regulated behaviours as a result of disrupted homeostasis, our findings suggest a role of midgut Jak/Stat signalling in the gut-brain axis of male fruit flies.

Walking Distance

(a)

Walking Velocity

(b)
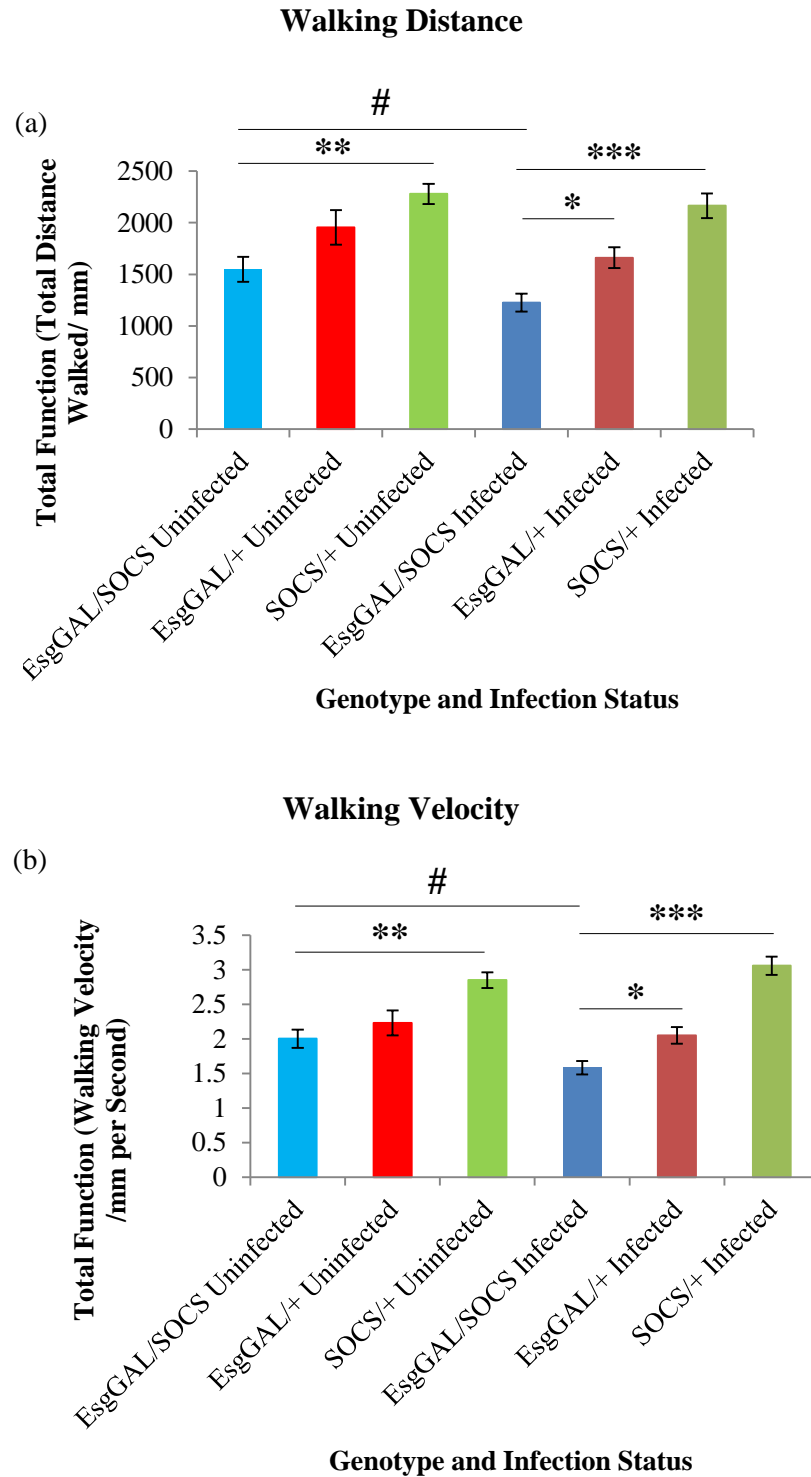
Figure 6.15: Total function of (a) distance walked and (b) walking velocity (±SEM) in uninfected and *Ecc15*-infected SOCS36E knockdown male flies, plus controls. Total function was determined using the area under the curve at each time point of the assay, with a maximum of 15 flies used at each time point for each genotype and infection group. (* = p<0.05, ** = p<0.001, *** = p<0.0001, using a one-way ANOVA with Tukey's HSD. # = p<0.05, using a Student's t-test).

(a) **Walking Distance**

	EsgGAL/SOCS Uninfected	EsgGAL/+ Uninfected	SOCS/+ Uninfected	EsgGAL/SOCS Infected	EsgGAL/+ Infected	SOCS/+ Infected
EsgGAL/SOCS Uninfected	x	0.0853	**0.0009**	**0.0387**		
EsgGAL/+ Uninfected	0.0853	x			0.1420	
SOCS/+ Uninfected	**0.0009**		x			0.4606
EsgGAL/SOCS Infected	**0.0387**			x	**0.0131**	**<0.0001**
EsgGAL/+ Infected		0.1420		**0.0131**	x	
SOCS/+ Infected			0.4606	**<0.0001**		x

(b) **Walking Velocity**

	EsgGAL/SOCS Uninfected	EsgGAL/+ Uninfected	SOCS/+ Uninfected	EsgGAL/SOCS Infected	EsgGAL/+ Infected	SOCS/+ Infected
EsgGAL/SOCS Uninfected	x	0.5138	**0.0005**	**0.0172**		
EsgGAL/+ Uninfected	0.5138	x			0.4190	
SOCS/+ Uninfected	**0.0005**		x			0.2378
EsgGAL/SOCS Infected	**0.0172**			x	**0.0205**	**<0.0001**
EsgGAL/+ Infected		0.4190		**0.0205**	x	
SOCS/+ Infected			0.2378	**<0.0001**		x

Table 6.7: P-values calculated using JMP showing significance (in bold) between uninfected and *Ecc15*-infected knockdown males and their relevant controls (using a one-way ANOVA with Tukey's HSD), as well as between uninfected and infected knockdown male flies (using a Student's t-test), for total function of (a) walking distance, and (b) walking velocity.
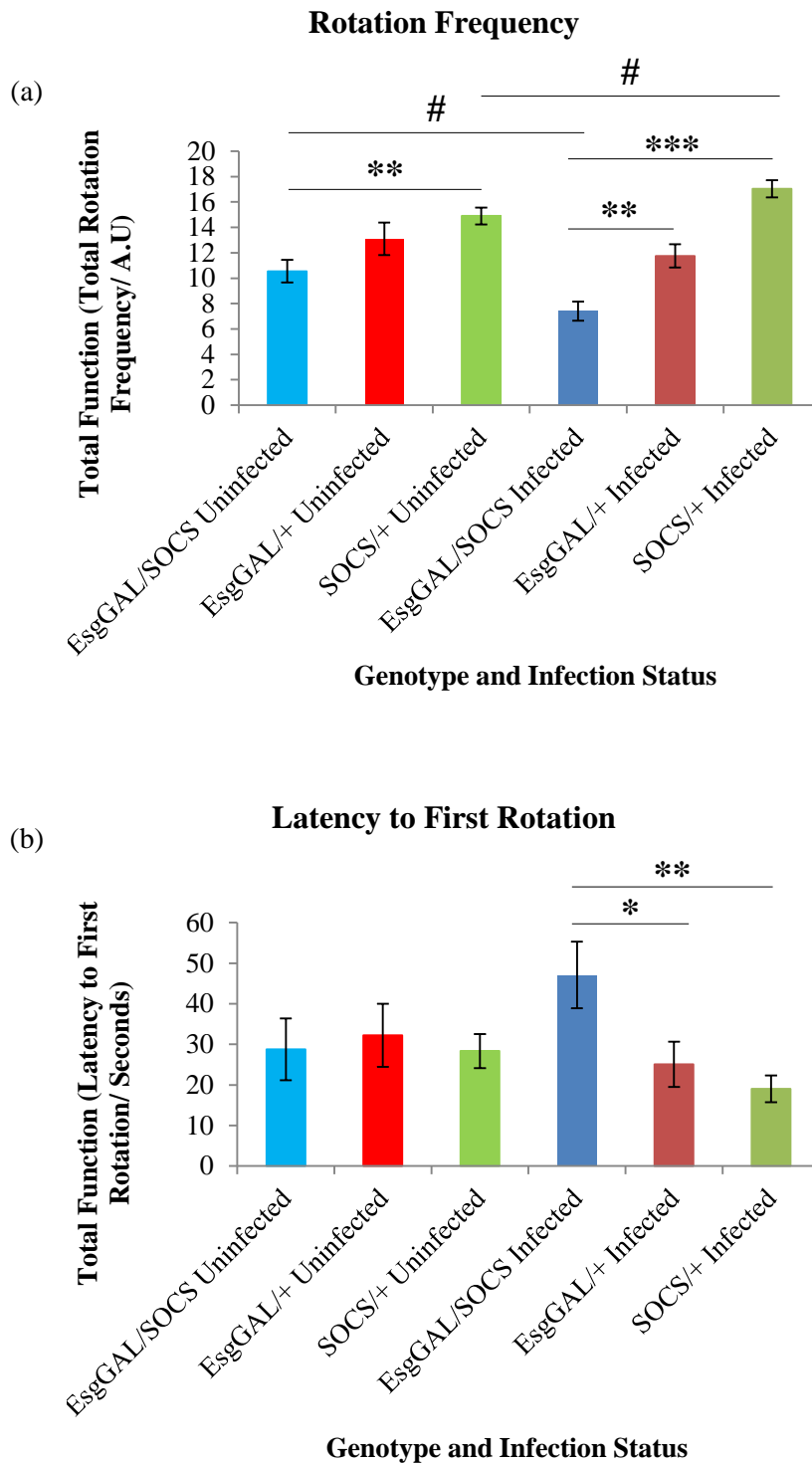
Figure 6.16: Total function of (a) rotation frequency, and (b) latency to the first rotation (±SEM) in uninfected and *Ecc15*-infected SOCS36E knockdown male flies, plus controls.
Total function was determined using the area under the curve at each time point of the assay, with a maximum of 15 flies used at each time point for each genotype and infection group. (* = $p<0.05$, ** = $p<0.001$, *** = $p<0.0001$, using a one-way ANOVA with Tukey's HSD. # = $p<0.05$, using a Student's t-test).

(a) **Rotation Frequency**

	EsgGAL/ SOCS Uninfected	EsgGAL/+ Uninfected	SOCS/+ Uninfected	EsgGAL/ SOCS Infected	EsgGAL/+ Infected	SOCS/+ Infected
EsgGAL/ SOCS Uninfected	x	0.1689	**0.0086**	**0.0121**		
EsgGAL/+ Uninfected	0.1689	x			0.4006	
SOCS/+ Uninfected	**0.0086**		x			**0.0336**
EsgGAL/ SOCS Infected	**0.0121**			x	**0.001**	**<0.0001**
EsgGAL/+ Infected		0.4006		**0.001**	x	
SOCS/+ Infected			**0.0336**	**<0.0001**		x

(b) **Latency to the First Rotation**

	EsgGAL/ SOCS Uninfected	EsgGAL/+ Uninfected	SOCS/+ Uninfected	EsgGAL/ SOCS Infected	EsgGAL/+ Infected	SOCS/+ Infected
EsgGAL/ SOCS Uninfected	x	0.9142	0.9988	0.1137		
EsgGAL/+ Uninfected	0.9142	x			0.4646	
SOCS/+ Uninfected	0.9988		x			0.0924
EsgGAL/ SOCS Infected	0.1137			x	**0.036**	**0.0058**
EsgGAL/+ Infected		0.4646		**0.036**	x	
SOCS/+ Infected			0.0924	**0.0058**		x

Table 6.8: P-values calculated using JMP showing significance (in bold) between uninfected and *Ecc15*-infected knockdown males and their relevant controls (using a one-way ANOVA with Tukey's HSD), as well as between uninfected and infected male flies (using a Student's t-test), for total function of (a) rotation frequency, and (b) latency to the first rotation.

When the exploratory walking assay was repeated in male flies, the findings mirrored those found in the repeat results for females, in that uninfected EsgGAL/+ males displayed greatly diminished assay performance for multiple parameters (as shown in figures 6.17-6.21). As a result, this led to overall positive effects of SOCS36E knockdown (compared to uninfected EsgGAL/+ males) and also overall positive effects of *Ecc15* infection (with infection appearing to rescue affected assay behaviour again, also seen in figures 6.8 and 6.9), for all four assessed walking behaviours ($p<0.05$). Although these findings indicate that the genotype in general was affected, rather than just EsgGAL/+ females, the cause is still unknown. Therefore, due to differences in assay performance between the two uninfected control genotypes in this set of experiments, and also between uninfected EsgGAL/+ males in both sets of experiments, we chose to regard this data as anomalous, and therefore were not included when considering effects of SOCS36E knockdown (with assay performance of uninfected EsgGAL/SOCS males compared to that of SOCS/+ flies only).

Within uninfected male flies, knockdown of ISC SOCS36E alone had more of a negative effect on walking behaviour in this second set of experiments as knockdown was found to decrease the overall distance walked ($p=0.0005$), walking velocity ($p=0.003$) and rotation frequency ($p<0.0001$), when compared to SOCS/+. Figure 6.17 (a)-(c) (left panels) show that SOCS36E knockdown significantly reduced walking distance and rotation frequency at both 19 and 26 days of age ($p<0.05$, and $p<0.001$, respectively), as well as walking speed at day 26 ($p=0.0004$). These results indicate that this ISC-specific knockdown led to acceleration in the age-associated declines in multiple walking behaviours. Interestingly, both walking distance and velocity were positively affected at day 47 in EsgGAL/SOCS flies, and this was in comparison to both SOCS/+ ($p=0.0392$, and $p=0.0279$, respectively) and EsgGAL/+ controls ($p=0.0168$, and $p=0.0184$, respectively). As figure 6.17 (d) (left panel) shows, all three experimental genotypes exhibited similar rotation latencies over the course of the walking assay, and mirrors the findings depicted in figure 6.12 (d), thus indicating ISC knockdown of SOCS36E alone did not affect age-associated changes in this particular walking behaviour.

Results of ISC SOCS36E knockdown in *Ecc15*-infected flies also differed from those in the first experiment in that the combined effects of these variables did not affect walking behaviours to the same extent, as no overall effects of SOCS36E knockdown (neither positive nor negative) on any parameter were found. Assay performance was negatively affected by SOCS36E knockdown in infected flies (figure 6.17a, b and c, right panels), although at different time points from those originally found; at 12 days of age, compared to day 24 (in

figure 6.12). However, these negative effects were observed in multiple parameters- distance ($p<0.05$), velocity ($p<0.01$) and rotation frequency ($p<0.05$) - therefore demonstrating SOCS36E knockdown and infection-induced midgut proliferation consistently diminished performance in this assay. These results are also in agreement with published findings that enteric infection early on in life can cause cognitive impairments, as well as increased morbidity (Bergstrom et al. 2012, Kolling et al. 2012). There were no significant effects observed of SOCS36E and *Ecc15* infection on latency to the first rotation (figure 6.17d), unlike in figure 6.12 (d), where age-associated increases were found to be accelerated at 24 days of age. However, this absence is consistent with results of uninfected males.

(a)

(b)

(c)

— EsgGAL/SOCS

— EsgGAL/+
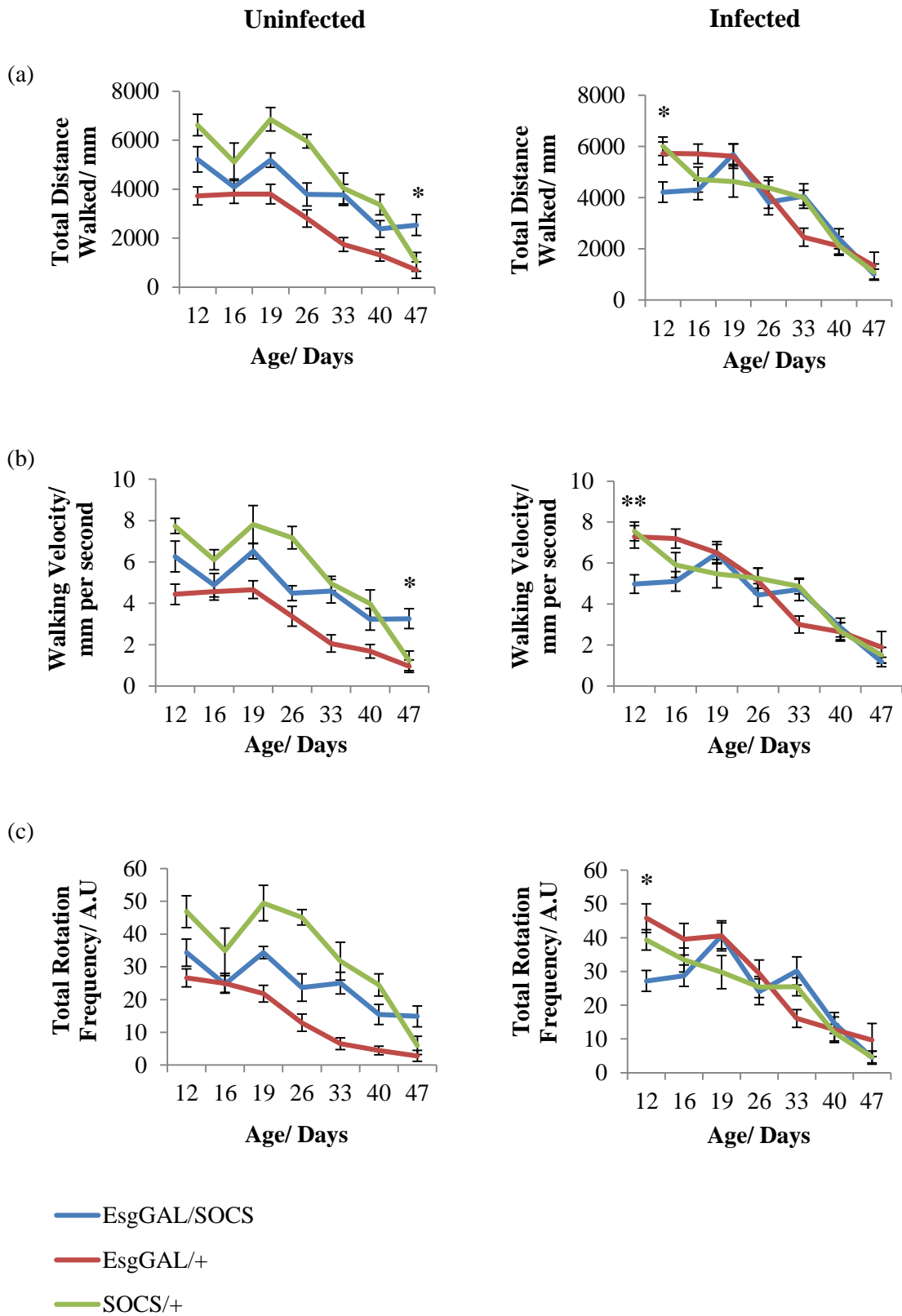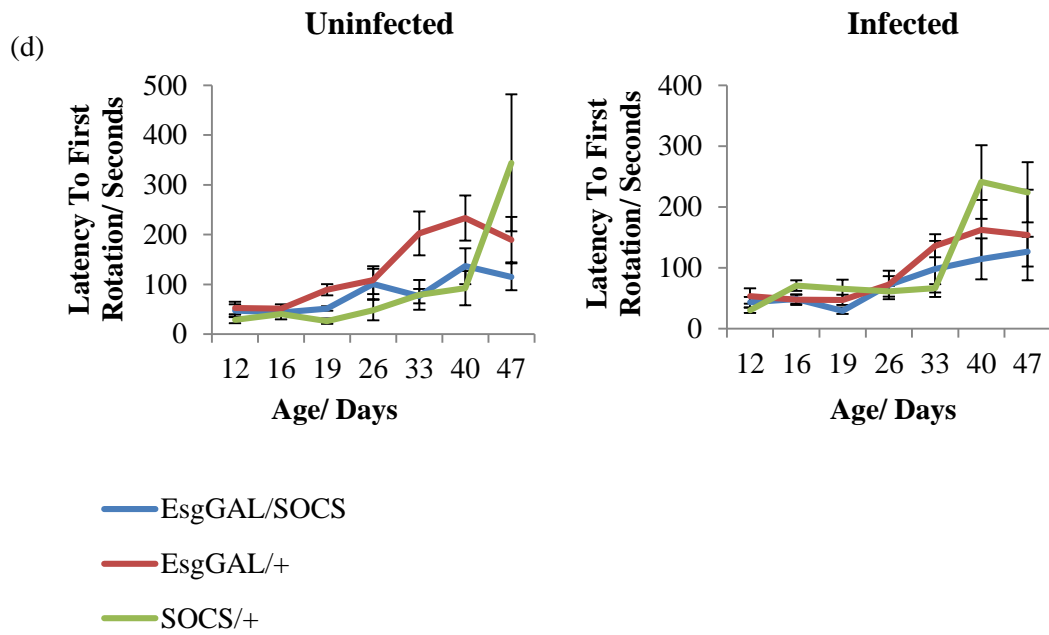
— SOCS/+

Figure 6.17: Assessment of senescence of (a) walking distance, (b) walking velocity, (c) rotation frequency and (d) latency to the first rotation in uninfected and *Ecc15*-infected SOCS36E knockdown male flies, plus controls. Data are shown as a mean value (±SEM) for each time point for uninfected and infected EsgGAL/SOCS males (blue) compared with EsgGAL/+ (red) and SOCS/+ (green) control genotypes. Flies were recorded for 15 minutes each using a video camera, with a maximum of 15 flies used for each genotype at each time point. Videos were analysed using Ethovision XT software (Noldus). (* = p<0.05, ** = p<0.01, *** = p<0.001, using a one-way ANOVA with Tukey's HSD).

Unlike our previous findings, *Ecc15* infection did not exert any overall significant positive or negative effects on any of the four parameters assessed in EsgGAL/SOCS flies. Consistent with figure 6.17 (a)-(c) though, where positive effects of SOCS36E knockdown alone were observed at day 47, *Ecc15* infection was also found to significantly reduce distance walked (p=0.0378), and velocity (p=0.0258) in EsgGAL/SOCS males at this time point, with effects on rotation frequency not quite reaching significance (p=0.0575). Unlike figure 6.14 (d), where *Ecc15* infection accelerated age-associated increases in first rotation latency at day 24, we found infection positively decreased rotation latency in EsgGAL/SOCS flies at day 19 (p=0.036).

Also contrasting previous results, infection-induced midgut proliferation elicited overall negative effects in SOCS/+ males for walking distance (p=0.0052), velocity (p=0.0182) and rotation frequency (p=0.0002), compared to positive effects found initially. The time points at which infection induced behavioural reductions were also consistent across these three parameters too, at 19, 26 and 40 days of age, along with rotation latency (shown in figure 6.18c and f, bottom panels, and figure 6.19c, bottom panel). Therefore, similar to findings in EsgGAL/SOCS males in the first set of experiments, *Ecc15* infection consistently accelerated age-associated declines in assay performance in SOCS/+ males, for all four assessed parameters of walking.
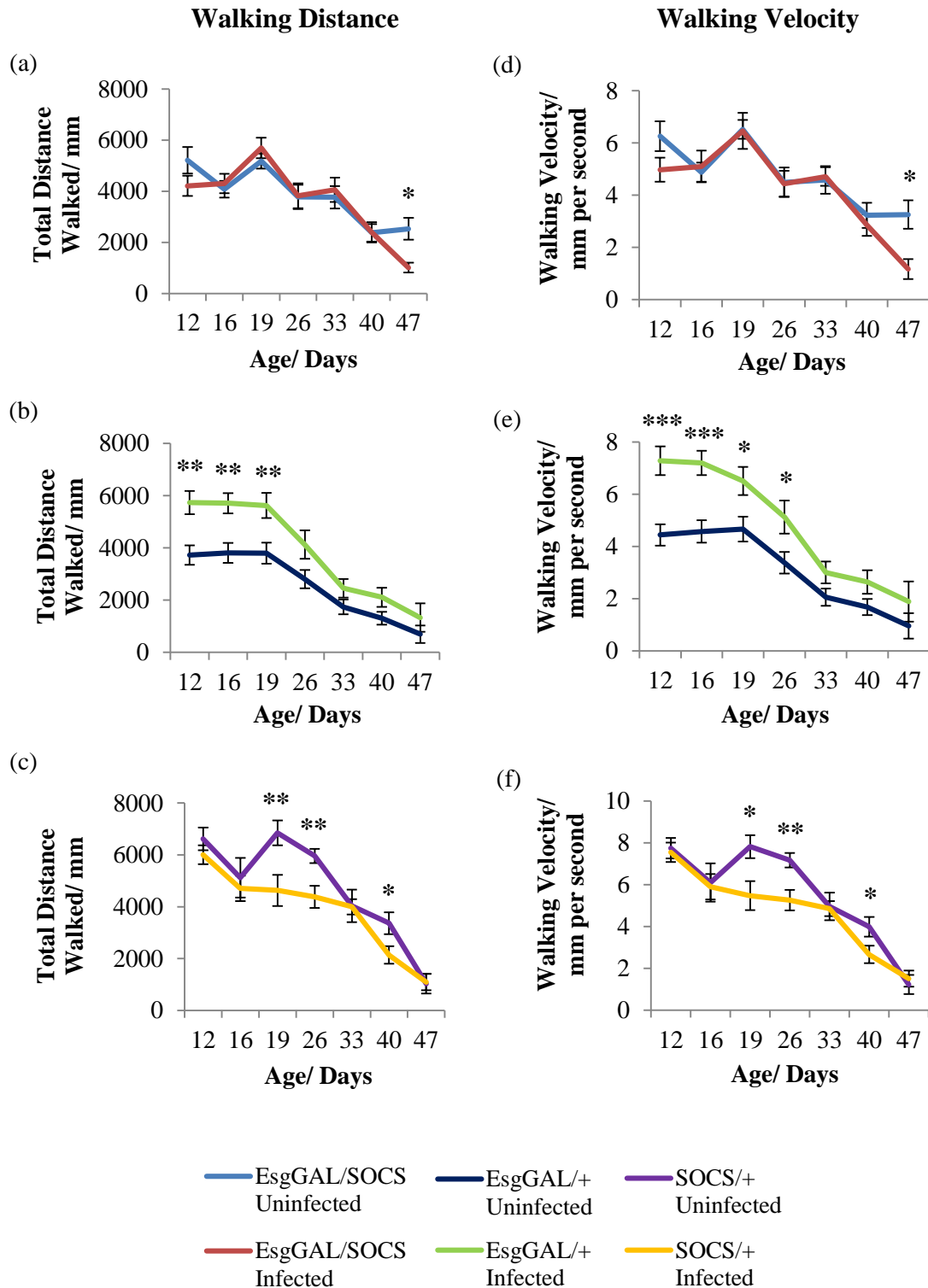
Figure 6.18: The effect of *Ecc15* infection on the age-associated decline on walking distance and velocity in SOCS36E knockdown and control male flies. Data are shown as a mean value (±SEM) for each time point for uninfected and infected (a) and (d) EsgGAL/SOCS, (b) and (e) EsgGAL/+ and (c) and (f) SOCS/+ male flies. (* = p<0.05, ** = p<0.01, *** = p<0.001, using a Student's t-test).
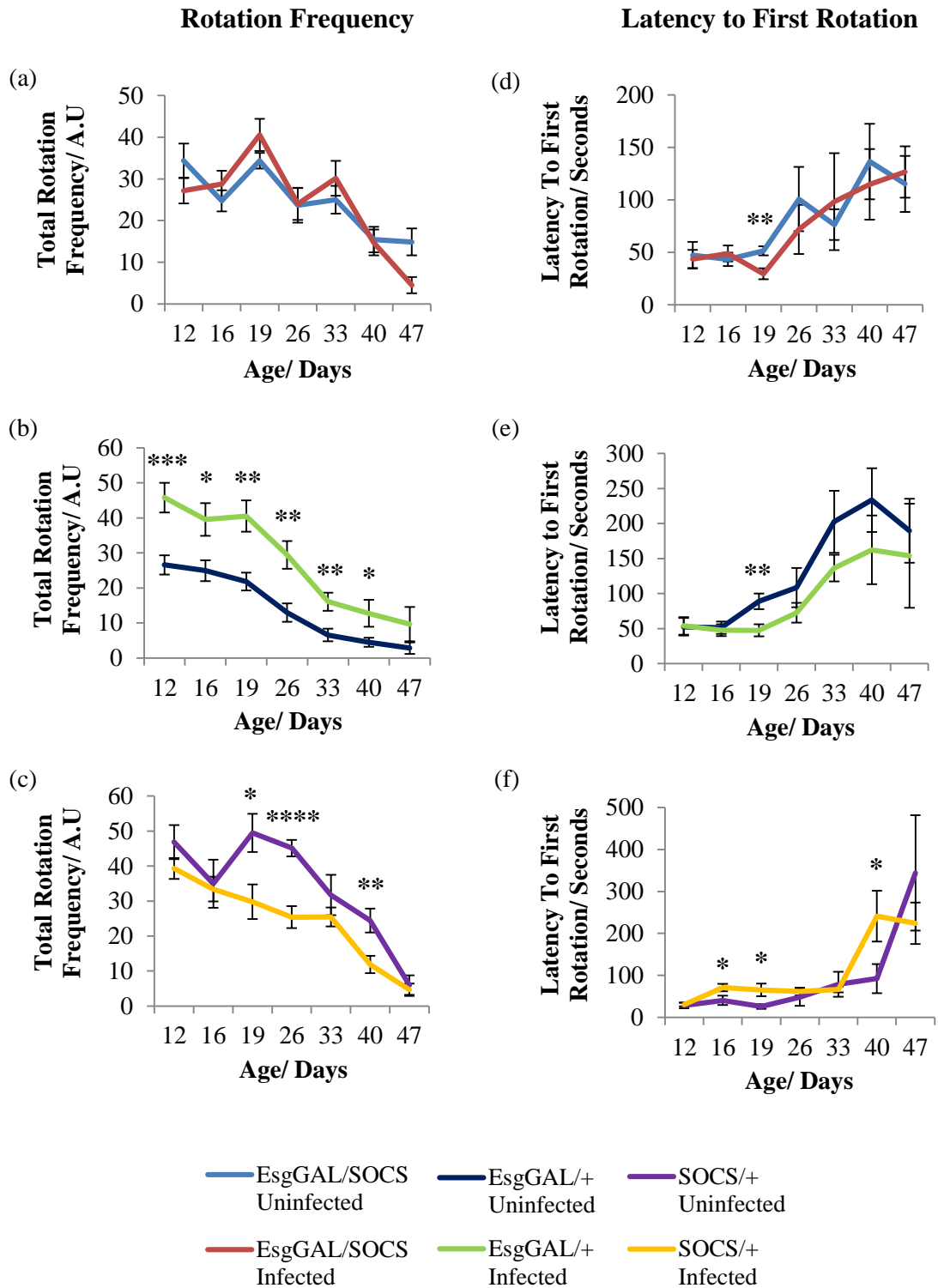
Figure 6.19: The effect of *Ecc15* infection on the age-associated decline on rotation frequency, and latency to the first rotation in SOCS36E knockdown and control male flies. Data are shown as a mean value (±SEM) for each time point for uninfected and infected (a) and (d) EsgGAL/SOCS, (b) and (e) EsgGAL/+ and (c) and (f) SOCS/+ male flies. (* = p<0.05, ** = p<0.01, **** = p<0.0001, using a Student's t-test).

The total function of each parameter in the experimental male flies was also assessed through area under the curve analysis, and in conjunction with our age-associated findings (figure 6.17), knockdown of SOCS36E significantly reduced the total function of walking distance (p=0.0004), velocity (p=0.0017) and rotation frequency (p<0.0001), relative to SOCS/+ within uninfected males (shown in figure 6.20a and b, and 6.21a). In this experiment, no significant (positive nor negative) effects were observed upon knockdown of SOCS36E in *Ecc15*-infected males, when compared with both infected controls (and also individually). Although this is supported by findings in figure 6.17 (right panels) where less dramatic effects of knockdown in infected flies were observed relative to figure 6.12, this largely contrasts findings from the initial analysis of total function (figures 6.15 and 6.16). Further to infection only negatively affecting performance of EsgGAL/SOCS males at select time points (rather than overall as found previously), there were no differences upon *Ecc15* infection within the EsgGAL/SOCS cohort. Infection-induced midgut proliferation consistently induced negative effects on total function in SOCS/+ males; for distance walked (p=0.0153), velocity (p=0.0326), rotation frequency (p<0.0001) and also latency to the first rotation (p=0.0225), supporting findings depicted in figures 6.18 and 6.19 (c) and (f) of infection effects during their lifespan.

In conclusion, these repeated set of results showed that disrupting Jak/Stat signalling through ISC-specific knockdown of SOCS36E accelerated the age-associated senescence in multiple parameters of exploratory walking, and negatively affected the total functions of these behaviours too. Unlike previous results in both males and females, midgut infection with *Ecc15* had very little effect on assay performance in EsgGAL/SOCS males, although negative effects were found at one time point in two of the four parameters (day 47). Due to the disparities between the two sets of results and the diminished assay performance of uninfected EsgGAL/+ males, a third set of data would ideally be needed to confirm any effects SOCS36E knockdown and/or *Ecc15* infection had on these walking behaviours. Although results differed between genders within experimental repeats, and also within genders across the two sets of results, it can be deduced that knockdown of SOCS36E alone, or coupled with *Ecc15* infection, did produce a negative phenotype in these experiments. As no effects were obtained in the negative geotaxis experiments, it can be concluded that SOCS36E knockdown, with or without infection, negatively affected the neurological aspect of walking, and not the muscular aspect.
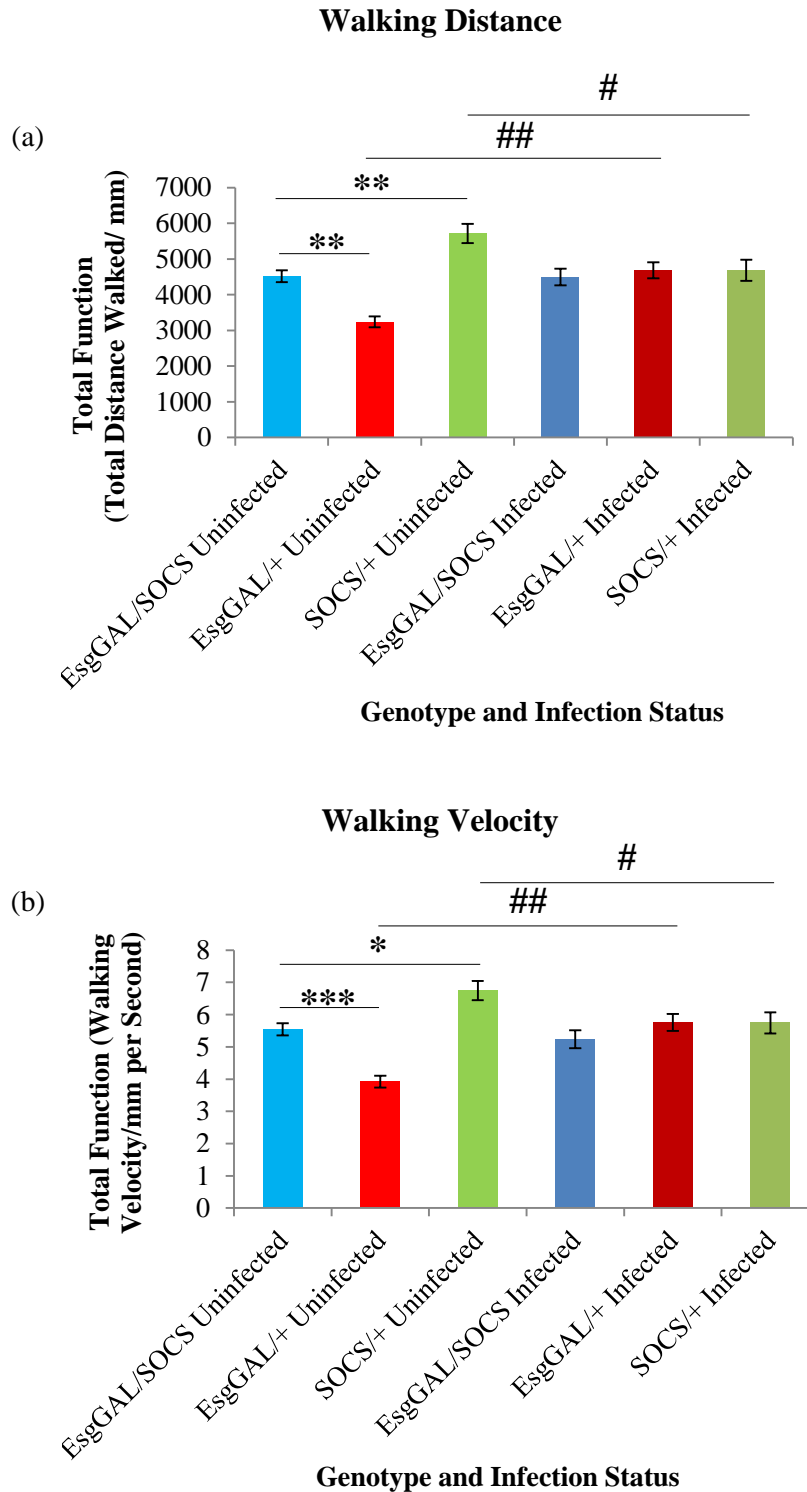
Figure 6.20: Total function of (a) distance walked, and (b) walking velocity (±SEM) in uninfected and *Ecc15*-infected SOCS36E knockdown male flies, plus controls. Total function was determined using the area under the curve at each time point of the assay, with a maximum of 15 flies used at each time point for each genotype and infection group. (* = $p < 0.01$, ** = $p < 0.001$, *** = $p < 0.0001$, using a one-way ANOVA with Tukey's HSD. # = $p < 0.05$, ## = $p < 0.0001$, using a Student's t-test).

(a) **Walking Distance**

	EsgGAL/ SOCS Uninfected	EsgGAL/+ Uninfected	SOCS/+ Uninfected	EsgGAL/ SOCS Infected	EsgGAL/+ Infected	SOCS/+ Infected
EsgGAL/ SOCS Uninfected	x	**0.0002**	**0.0004**	0.9433		
EsgGAL/+ Uninfected	**0.0002**	x			**<0.0001**	
SOCS/+ Uninfected	**0.0004**		x			**0.0153**
EsgGAL/ SOCS Infected	0.9433			x	0.8530	0.8594
EsgGAL/+ Infected		**<0.0001**		0.8530	x	
SOCS/+ Infected			**0.0153**	0.8594		x

(b) **Walking Velocity**

	EsgGAL/ SOCS Uninfected	EsgGAL/+ Uninfected	SOCS/+ Uninfected	EsgGAL/ SOCS Infected	EsgGAL/+ Infected	SOCS/+ Infected
EsgGAL/ SOCS Uninfected	x	**<0.0001**	**0.0017**	0.3658		
EsgGAL/+ Uninfected	**<0.0001**	x			**<0.0001**	
SOCS/+ Uninfected	**0.0017**		x			**0.0326**
EsgGAL/ SOCS Infected	0.3658			x	0.4168	0.4396
EsgGAL/+ Infected		**<0.0001**		0.4168	x	
SOCS/+ Infected			**0.0326**	0.4396		x

Table 6.9: P-values calculated using JMP showing significance (in bold) between uninfected knockdown males and their relevant controls (using a one-way ANOVA with Tukey's HSD), as well as between uninfected and *Ecc15*-infected control male flies (using a Student's t-test), for total function of (a) walking distance, and (b) walking velocity.

Rotation Frequency

(a)

Latency to First Rotation

(b)
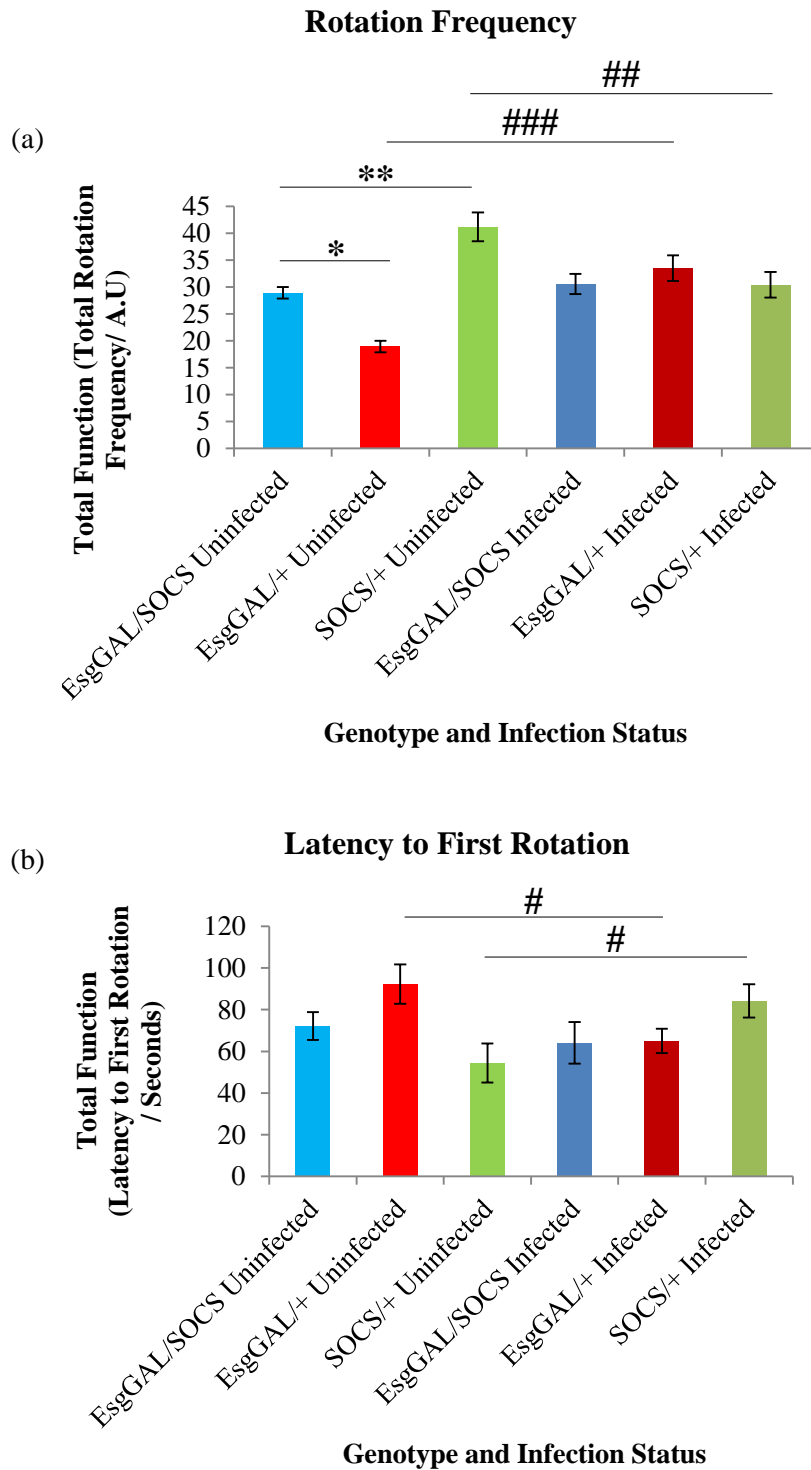
Figure 6.21: Total function of (a) rotation frequency, and (b) latency to the first rotation (±SEM) in uninfected and *Ecc15*-infected SOCS36E knockdown male flies, plus controls. Total function was determined using the area under the curve at each time point of the assay, with a maximum of 15 flies used at each time point for each genotype and infection group. (* = p<0.001, ** = p<0.0001, using a one-way ANOVA with Tukey's HSD. # = p<0.05, ## = p<0.01, ### = p<0.0001, using a Student's t-test).

(a) **Rotation Frequency**

	EsgGAL/ SOCS Uninfected	EsgGAL/+ Uninfected	SOCS/+ Uninfected	EsgGAL/ SOCS Infected	EsgGAL/+ Infected	SOCS/+ Infected
EsgGAL/ SOCS Uninfected	x	**0.0008**	**<0.0001**	0.4634		
EsgGAL/+ Uninfected	**0.0008**	x			**<0.0001**	
SOCS/+ Uninfected	**<0.0001**		x			**0.0056**
EsgGAL/ SOCS Infected	0.4634			x	0.6181	0.9991
EsgGAL/+ Infected		**<0.0001**		0.6181	x	
SOCS/+ Infected			**0.0056**	0.9991		x

(b) **Latency to the First Rotation**

	EsgGAL/ SOCS Uninfected	EsgGAL/+ Uninfected	SOCS/+ Uninfected	EsgGAL/ SOCS Infected	EsgGAL/+ Infected	SOCS/+ Infected
EsgGAL/ SOCS Uninfected	x	0.2359	0.3194	0.5043		
EsgGAL/+ Uninfected	0.2359	x			**0.0208**	
SOCS/+ Uninfected	0.3194		x			**0.0225**
EsgGAL/ SOCS Infected	0.5043			x	0.9961	0.1977
EsgGAL/+ Infected		**0.0208**		0.9961	x	
SOCS/+ Infected			**0.0225**	0.1977		x

Table 6.10: P-values calculated using JMP showing significance (in bold) between uninfected knockdown males and their relevant controls (using a one-way ANOVA with Tukey's HSD), as well as between uninfected and *Ecc15*-infected control male flies (using a Student's t-test), for total function of (a) rotation frequency, and (b) latency to the first rotation.

6.4 Assessment of ISC-specific knockdown of SOCS36E on stress resistance

Stress resistance studies have been performed on *Drosophila* for several decades, assessing such stressors as exposure to high and low temperatures, and resistance to starvation, dessication and oxidative stress. Such experiments can help determine the mechanisms and signalling pathways involved in increased sensitivity or tolerance of particular stressors. However, many results have revealed a common association of stress resistance with lifespan, in that an increase is often found with extended lifespan, as well as the reciprocal of decreased resistance coupled with shortened lifespan (Arking et al. 1991, Luckinbill 1998, Mockett et al. 2001). Functional senescence has also been implicated in this relationship, with senescence of locomotor behaviours coupled with decreased lifespan and decreased oxidative stress resistance, and vice versa. However, this is not always the case, as gain of function in Superoxide dismutase 1 (Sod1, an antioxidant enzyme) led to extended lifespan and increased oxidative stress resistance, but had no effect on functional senescence (reviewed by Jones and Grotewiel 2011). Results obtained here showed that ISC-specific knockdown on SOCS36E neither delayed nor accelerated functional senescence (as assessed using negative geotaxis), and led to a decrease in median lifespan, although this was exclusive to female flies. Knockdown of SOCS36E (either alone or coupled with midgut infection) also produced a negative phenotype regarding spontaneous locomotor behaviour although these results were not as distinct. Therefore, we used our ISC-SOCS36E knockdown *Drosophila* model to determine whether intestinal Jak/Stat signalling is implicated in stress resistance, especially as regulated midgut homeostasis has already been shown to be essential for survival of fruit flies. Also, we aimed to investigate whether our model follows previous findings, and determine whether the shortening of lifespan (in female flies at least) would result in increased stress sensitivity.

6.4.1 ISC-specific knockdown of SOCS36E was beneficial to male and female flies under starvation conditions.

The first stressor investigated in experimental flies was resistance to starvation. From 4 days following eclosion, all flies were maintained in vials consisting of 1.5% agar, rather than standard food, with survival analysis then carried out daily for both genders as previously described. Figure 6.22 shows the survival analysis under starvation conditions for (a) female and (b) male experimental flies, with table 6.11 showing the median, maximum, and mean lifespans for all six groups of flies. Despite figure 6.22 (a) showing slight differences in the median lifespans of all three female genotypes, all three were calculated to have median lifespans of 2.5 days (shown in table 6.11). EsgGAL/SOCS females however, were found to

have a higher maximum lifespan of 4.5 days, compared with 3.5 for both control genotypes, and a slightly higher mean lifespan of 3.4 days, compared with 3.1 and 2.8 days for EsgGAL/+ and SOCS/+ females, respectively. Using the chi-squared p-value log-rank test, the differences in survival between EsgGAL/SOCS and SOCS/+ females were found to be statistically significant (p<0.0001). Unfortunately, differences between EsgGAL/SOCS and EsgGAL/+ females did not quite reach significance (p=0.055), perhaps due to the similarities in both median and mean lifespans, although these results could indicate that knockdown of SOCS36E could be slightly advantageous for female flies under starvation conditions.

Figure 6.22 (b) shows a more clear-cut difference in median lifespans between EsgGAL/SOCS males and the two control genotypes (which were 3.5 and 2.5 days respectively). However, in spite of how survival results are depicted for EsgGAL/SOCS males, the median, maximum and mean lifespans for these flies were all calculated to be 3.5 days (shown in table 6.11). The maximum lifespans of the control genotypes were also 3.5 days (in contrast to the trend seen in females), with mean lifespans both found to be 3.0- half a day less than EsgGAL/SOCS. The increases in both median and mean lifespans in EsgGAL/SOCS were found to be highly significant when compared with both EsgGAL/+ and SOCS/+ males (p<0.0001, assessed using the chi-squared p-value log-rank test), showing that knockdown of SOCS36E was beneficial during starvation in both male and female flies.

Genotype and Gender	Median Lifespan/ Days	Maximum Lifespan/ Days	Mean Lifespan/ Days
EsgGAL/SOCS Female	2.5	4.5	3.4
EsgGAL/+ Female	2.5	3.5	3.1
SOCS/+ Female	2.5	3.5	2.8
EsgGAL/SOCS Male	3.5	3.5	3.5
EsgGAL/+ Male	2.5	3.5	3.0
SOCS/+ Male	2.5	3.5	3.0

Table 6.11: Median, maximum and mean lifespans of both female and male SOCS36E knockdown flies and relevant controls, following starvation.

a)

b)
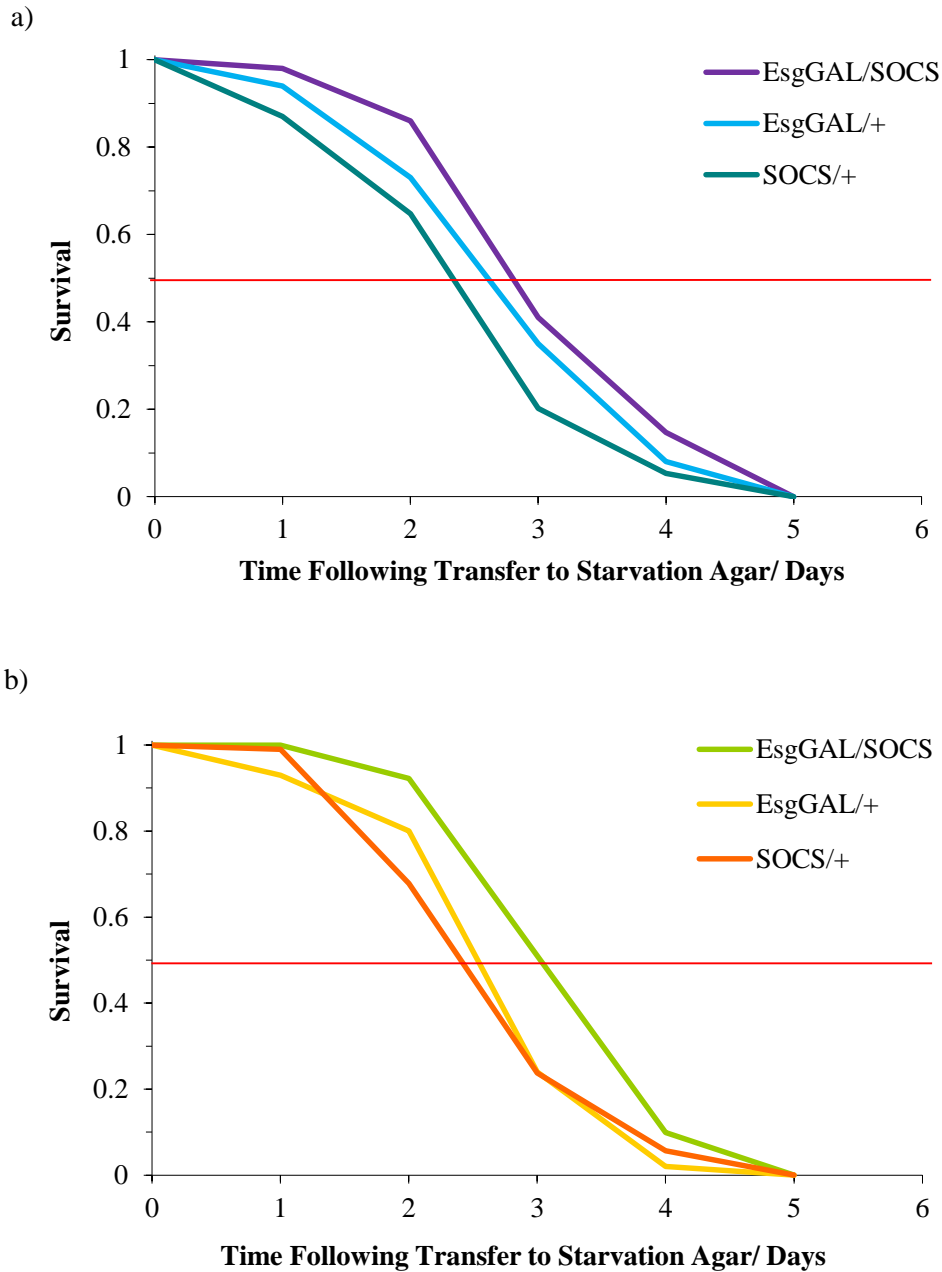
Figure 6.22: Survival analysis of (a) female and (b) male SOCS36E knockdown flies during starvation, compared with control genotypes, EsgGAL/+ and SOCS/+. Survival of (a) EsgGAL/SOCS female flies (purple), compared with EsgGAL/+ (blue) and SOCS/+ (turquoise) control genotypes, along with (b) EsgGAL/SOCS male flies (green), compared with EsgGAL/+ (yellow) and SOCS/+ (orange) control genotypes. (Red line indicates median lifespan). (n=100). Differences in lifespans between EsgGAL/SOCS, and SOCS/+ in females, and between EsgGAL/SOCS, and EsgGAL/+ and SOCS/+ within males were calculated using a chi-squared p-value log-rank test- $p < 0.0001$.

In this experiment, after 4 days post-eclosion on standard food, male and female experimental flies were transferred to vials containing 1.5% agar, with 5% sugar and 5% H_2O_2, with survival analysis then carried out daily. Figure 6.23 shows survival curves of all three experimental genotypes in (a) female and (b) male flies following exposure to H_2O_2, and as shown in figure 6.22 (a), the median lifespan of EsgGAL/SOCS females appears to be slightly higher than those of the control genotypes. However, as table 6.12 shows, all female flies had median lifespans of 2.5 days. All three female genotypes also exhibited maximum lifespans of 3.5 days following exposure to H_2O_2, although mean lifespans differed in that EsgGAL/SOCS females had a mean lifespan of 3.4 days, with both control genotypes exhibiting mean lifespans of 3.1 days. Despite similarities in all three lifespan values for the knockdown and control females, a chi-squared p-value log-rank test found significant differences between the lifespans of EsgGAL/SOCS and both EsgGAL/+ ($p<0.01$) and SOCS/+ ($p<0.001$) females. This suggests that knockdown of SOCS36E led to an increase in average lifespan following an increase in oxidative stress through exposure to H_2O_2.

Although figure 6.23 (b) does not to appear to show differences in median lifespan as distinct as those in 6.22 (b) between knockdown and control males, the median lifespan of EsgGAL/SOCS males was calculated to be one day higher than both controls, at 3.5 days (table 6.12). This echoes the results of table 6.11, along with all three cohorts of male flies having maximum lifespans of 3.5 days. When mean lifespans were compared, EsgGAL/SOCS males had the longest again with 3.7 days, compared with 3.2 and 3.5 days found in EsgGAL/+ and SOCS/+ males, respectively- a trend also seen in the female flies following H_2O_2 exposure. A chi-squared p-value log-rank test found statistical significance when EsgGAL/SOCS flies were compared with both EsgGAL/+ ($p<0.0001$) and SOCS/+ ($p<0.05$) males. These results confirm the ability that SOCS36E knockdown is able to prolong mean lifespan after exposure to H_2O_2 is not gender specific, although an increase in median lifespan was limited to male flies only- a finding also seen with starvation resistance.

Genotype and Gender	Median Lifespan/ Days	Maximum Lifespan/ Days	Mean Lifespan/ Days
EsgGAL/SOCS Female	2.5	3.5	3.4
EsgGAL/+ Female	2.5	3.5	3.1
SOCS/+ Female	2.5	3.5	3.1
EsgGAL/SOCS Male	3.5	3.5	3.7
EsgGAL/+ Male	2.5	3.5	3.2
SOCS/+ Male	2.5	3.5	3.5

Table 6.12: Median, maximum and mean lifespans of female and male SOCS36E knockdown flies and relevant controls, following exposure to hydrogen peroxide.

a)

b)
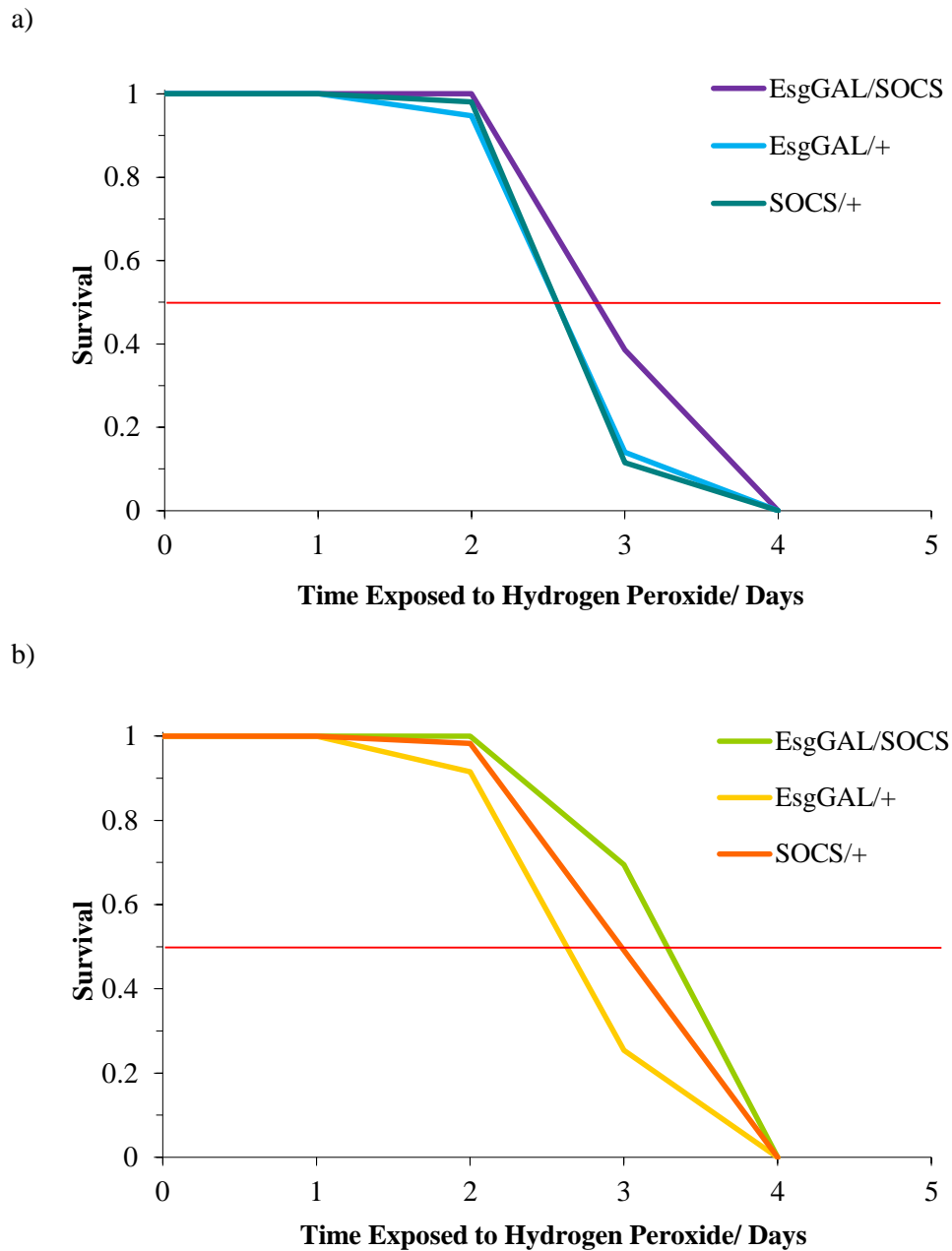
Figure 6.23: Survival analysis of (a) female and (b) male SOCS36E knockdown flies following H$_2$O$_2$ exposure, compared with control genotypes, EsgGAL/+ and SOCS/+. Survival of (a) EsgGAL/SOCS female flies (purple), compared with EsgGAL/+ (blue) and SOCS/+ (turquoise) control genotypes, along with (b) EsgGAL/SOCS male flies (green), compared with EsgGAL/+ (yellow) and SOCS/+ (orange) control genotypes. (Red line indicates median lifespan). (n=60). Differences in lifespans between EsgGAL/SOCS, and EsgGAL/+ and SOCS/+ were calculated using a chi-squared p-value log-rank test- $p < 0.05$.

One approach to assessing flies' resistance to cold stress is to measure the time it takes flies to recover following exposure to lower temperatures for a certain period of time, and was the chosen method here. Flies at 10 days of age were kept at 4°C for 4 hours, before transferral to 25°C, where the time taken to recover and fully stand was recorded. Any flies that failed to recover after sixty minutes and were unresponsive to physical stimulation were counted as dead. Figure 6.24 shows the average chill coma recovery time for all three experimental female genotypes and shows that while knockdown of SOCS36E positively reduced recovery time compared to EsgGAL/+ (p=0.036), there was very little difference between EsgGAL/SOCS and SOCS/+ - 22.3±2 and 23.5±2 seconds, respectively (p=0.936). This suggests that the results obtained are not primarily due to ISC knockdown of SOCS36E.
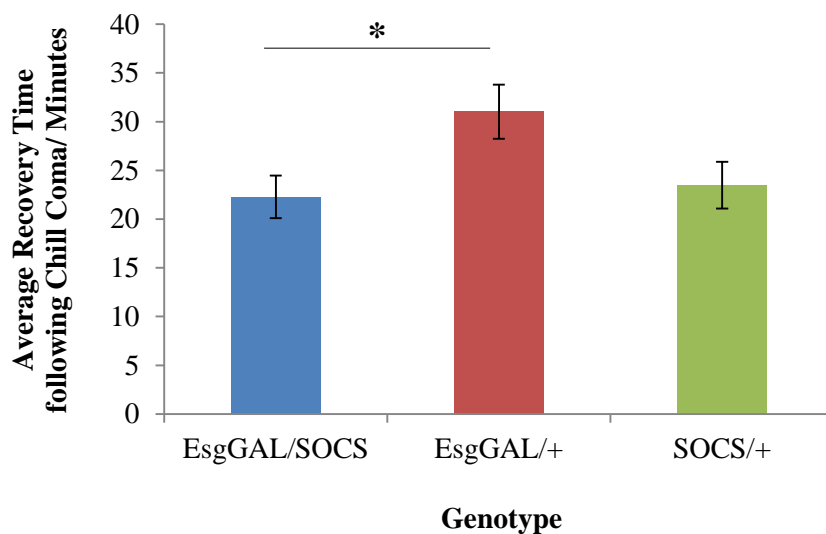
Figure 6.24: Average recovery times of SOCS36E knockdown females, plus relevant controls, following chill coma. Flies were kept at 4°C for 4 hours before recovery at 25°C, with the time taken to fully stand recorded for each fly, in all three genotypes. (EsgGAL/SOCS- blue, n=46, EsgGAL/+ - red, n=43, and SOCS/+ - green, n=46). (* = p<0.05, using a one-way ANOVA with Tukey's HSD).

Figure 6.25 shows the chill coma recovery times for the male experimental flies and as seen in figure 6.24, EsgGAL/+ had the highest recovery time with 30±3 seconds, although the difference in recovery time between EsgGAL/+, and EsgGAL/SOCS and SOCS/+ was smaller in males. This resulted in a lack of statistical significance between EsgGAL/+ and EsgGAL/SOCS males (p>0.05). Also similar to results obtained in female flies, chill coma recovery times for EsgGAL/SOCS and SOCS/+ were almost identical, with average times calculated as 27.8±3 and 27.1±3 seconds, respectively. Overall, results from figures 6.24 and 6.25 indicate that ISC-knockdown of SOCS36E had neither a positive nor a negative effect on chill coma resistance. Collectively, these stress resistance experiments showed that whilst a shortening of lifespan was observed in female flies only following SOCS36E knockdown, this alteration of the Jak/Stat pathway was beneficial under conditions of starvation and oxidative stress, both in males and females.
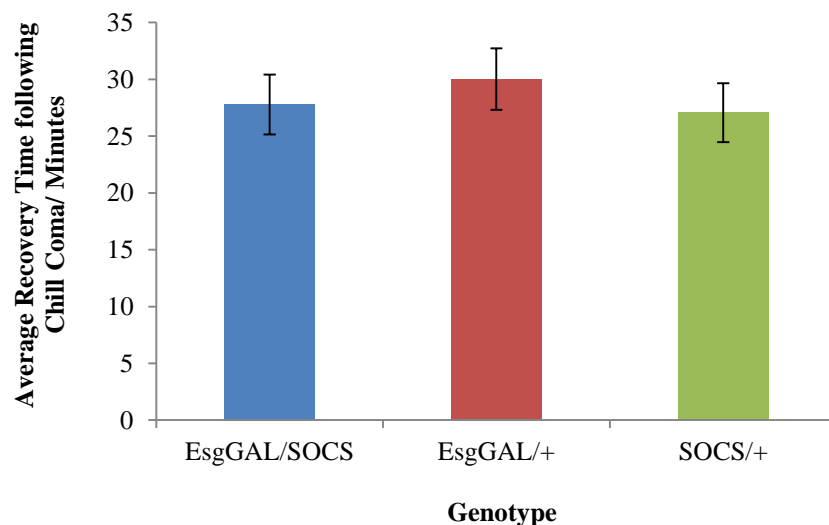
Figure 6.25: Average recovery times of SOCS36E knockdown males, plus relevant controls, following chill coma. Flies were kept at 4°C for 4 hours before recovery at 25°C, with the time taken to fully stand recorded for each fly, in all three genotypes. (EsgGAL/SOCS- blue, n=48, EsgGAL/+ - red, n=49, and SOCS/+ - green, n=44).

6.5 Assessment of female fecundity as a potential mechanism for decreased lifespan in SOCS36E knockdown flies

In contrast to stress resistance, fecundity has been found to have an inverse relationship with longevity, in that an extension in lifespan is associated with decreased fecundity, and vice versa (Chapman and Partridge 1996, Slack et al. 2010). As fecundity (in both males and females) is very energy-costly, it is thought that a decrease in fecundity (for example, through reduced egg laying in females), leads to increased energy availability which can be utilised for homeostatic processes and maintaining healthy tissues, thus lengthening the lifespan of the organism (Kirkwood 1977, Kirkwood and Holliday 1979, Kirkwood and Cremer 1982). Increased fecundity would require more energy than usual, which may be transferred away from other organ systems, potentially leaving the organism more susceptible to injury and infection in which they may not be able to sufficiently resolve, thus shortening lifespan (Kirkwood 1977, Kirkwood and Holliday 1979, Kirkwood and Cremer 1982). Additionally, increases in reproduction either early or late on in the flies' lifespan, has shown to result in shortening and extension of flies' lifespans, respectively (Clare and Luckinbill 1985). As the reduction in lifespan observed here was confined to female EsgGAL/SOCS, we measured fecundity in knockdown and control females by determining the number of eggs laid per female with increasing age, and per female on average, in order to determine whether an increase in fecundity could be a possible mechanism behind the lifespan phenotype in females.

6.5.1 ISC-knockdown of SOCS36E had no effect on female fecundity

Figure 6.26 shows the average number of eggs laid by each female (per genotype) (a) per day over the duration of the experiment, and (b) in total during their lifespan, with (a) showing at each of the five time points of the experiment, EsgGAL/SOCS females, on average, laid less eggs per day. Using a one-way ANOVA (with Tukey's HSD), this observed reduction was statistically significant at 5 days of age, but only when compared with EsgGAL/+ ($p=0.0083$, SOCS/+ $p=0.7582$). Collectively, this continuous reduction led to EsgGAL/SOCS females laying less eggs overall, with 13 ± 1 per female, compared with 20 ± 3 and 17 ± 2 for EsgGAL/+ and SOCS/+, respectively (as shown in figure 6.26b), although these differences were not statistically significant. In summary, although ISC-knockdown of SOCS36E in females appeared to negatively affect egg laying, both over time and for number of eggs laid per female, these observations were not found to be significant. Therefore, it can be concluded that the reduction of lifespan in knockdown females was not as a result of changes in fecundity.

a)

b)
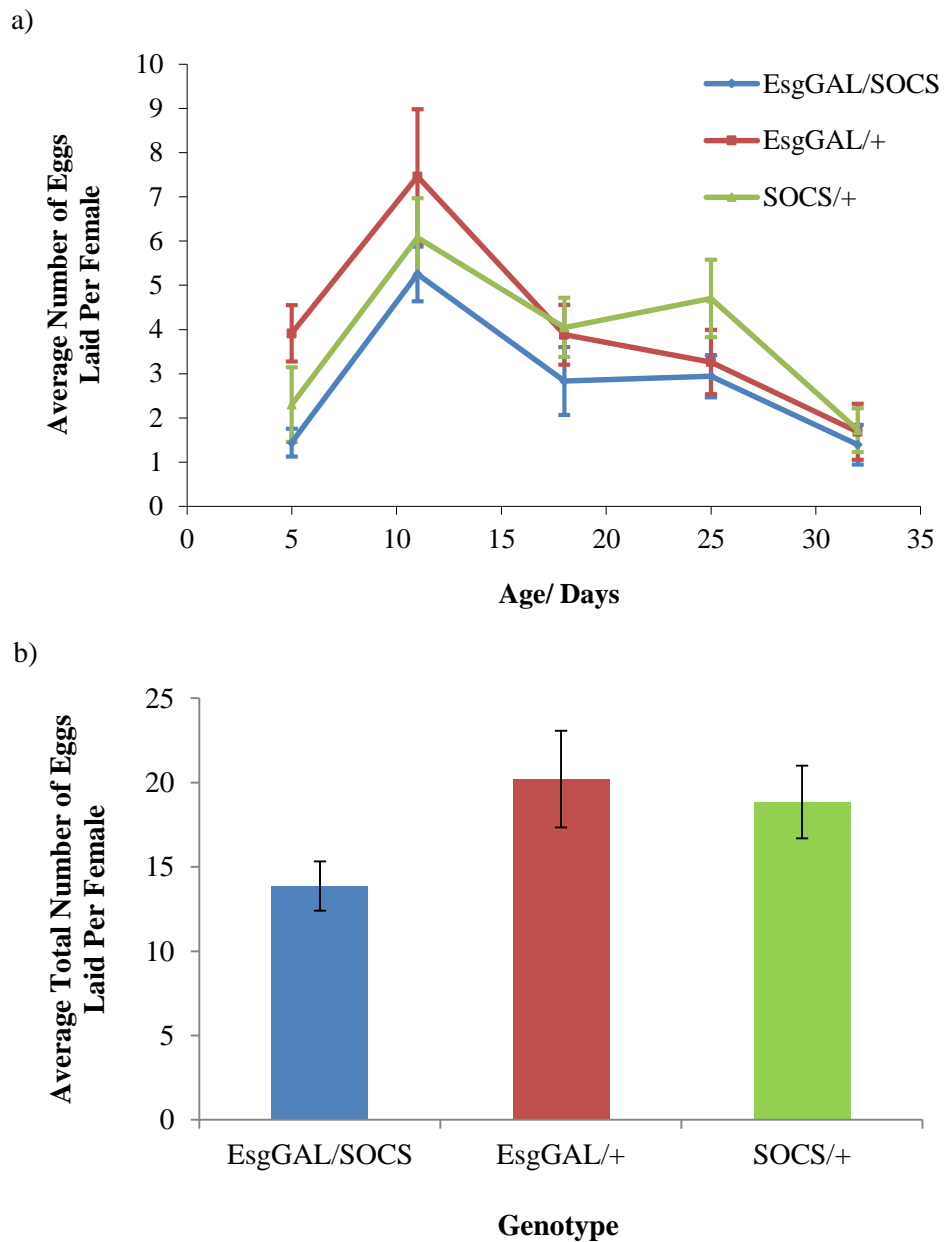
Figure 6.26: Assessment of fecundity, as measured by egg laying, in SOCS36E knockdown female flies, compared with controls. The average number of eggs (±SEM) laid per female (a) per day, and (b) in total in EsgGAL/SOCS female flies (blue), compared with EsgGAL/+ (red) and SOCS/+ (green) control genotypes. 100 flies were used for each genotype at the start of the experiment, with analysis of fecundity carried out in conjunction with survival analysis.

6.6 Assessment of barrier function using the Smurf assay

It was presumed that due to the ISC-specific knockdown of SOCS36E, there would be an increase in proliferation of midgut cells in these flies and this could lead to an increase in total midgut cell number. This could ultimately affect the architecture of the midgut and could be detrimental to the health of the fly if food or pathogens normally confined to, and dealt with by the midgut enter the surrounding tissues due to a reduction or loss of midgut integrity. We aimed to assess barrier integrity through the Smurf assay, as developed by Rera et al. (2011), whereby blue food dye in incorporated into the food. Once ingested, this dye is confined to and is visible in the proboscis and crop (the equivalent of the mammalian stomach) in flies with intact midguts. However, in flies where midgut integrity is compromised, the dye enters surrounding tissues, causing the entire fly to become blue, and is thus termed a "Smurf" fly.

w^{Dah} flies of varying ages were used initially to optimise the assay and determine whether there was a time point at which integrity was lost and "Smurf" flies became visible. Figure 6.27 shows images taken of flies following time spent on standard food containing blue dye, and shows that at each of the three ages used (11, 24 and 68 days old), dye was confined to the proboscis and crop, with no differences observed between the two genders. Figure 6.27 (b) shows a "Smurf" fly that was observed at 11 days of age. However, this was considered to be anomalous as this was the only "Smurf" fly detected out of all flies tested, and was deemed to be unhealthy due to the somewhat shrivelled appearance of the fly shown in the image, and also because this fly died not long after the assay was performed.

6.6.1 SOCS36E knockdown flies did not exhibit compromised barrier integrity

Following results from w^{Dah} flies, experimental flies were first tested at 53 days of age, approximately 4 and 6 days after the median lifespans for SOCS/+ and EsgGAL/+, and 3 days after the maximum lifespan of EsgGAL/SOCS (table 5.1). As seen in figure 6.27, no "Smurf" flies were obtained in these old flies (figure 6.28a-c). The assay was repeated a final time at a later time point (62 days of age), however only using EsgGAL/+ flies, as there were no surviving flies for EsgGAL/SOCS and SOCS/+. Even at this later time point (2 days after the maximum lifespan), no "Smurf" flies were obtained (figure 6.28d and e). The fly in figure 6.28 (d) still had dye confined to the proboscis and crop, whereas the fly imaged in figure 6.28 (e) had dye incorporated further into the abdomen, although this still had not infiltrated completely into surrounding tissues (as seen in figure 6.27b). These results suggest that ISC-

knockdown of SOCS36E did not affect integrity of the midgut, as assessed using the Smurf assay.
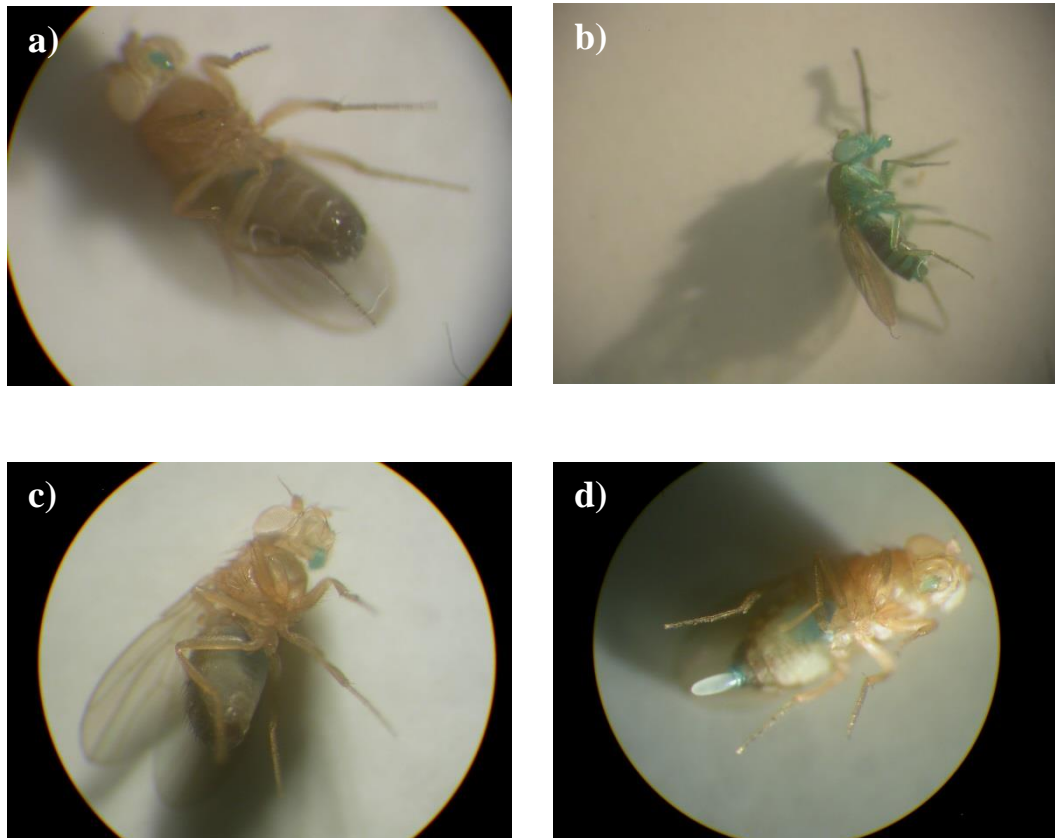
Figure 6.27: Assessment of midgut integrity in w$^{\text{Dah}}$ flies at different ages, using the Smurf assay. Images of flies at 11 (a and b- male and female, respectively), 24 (c-male) and 68 (d- female) days of age. Flies spent 9 hours on standard food including 2.5% w/v blue food dye before brief anaesthetisation and imaging, using a Nikon Coolpix 990 digital camera. (n≥10 per gender, per time point).
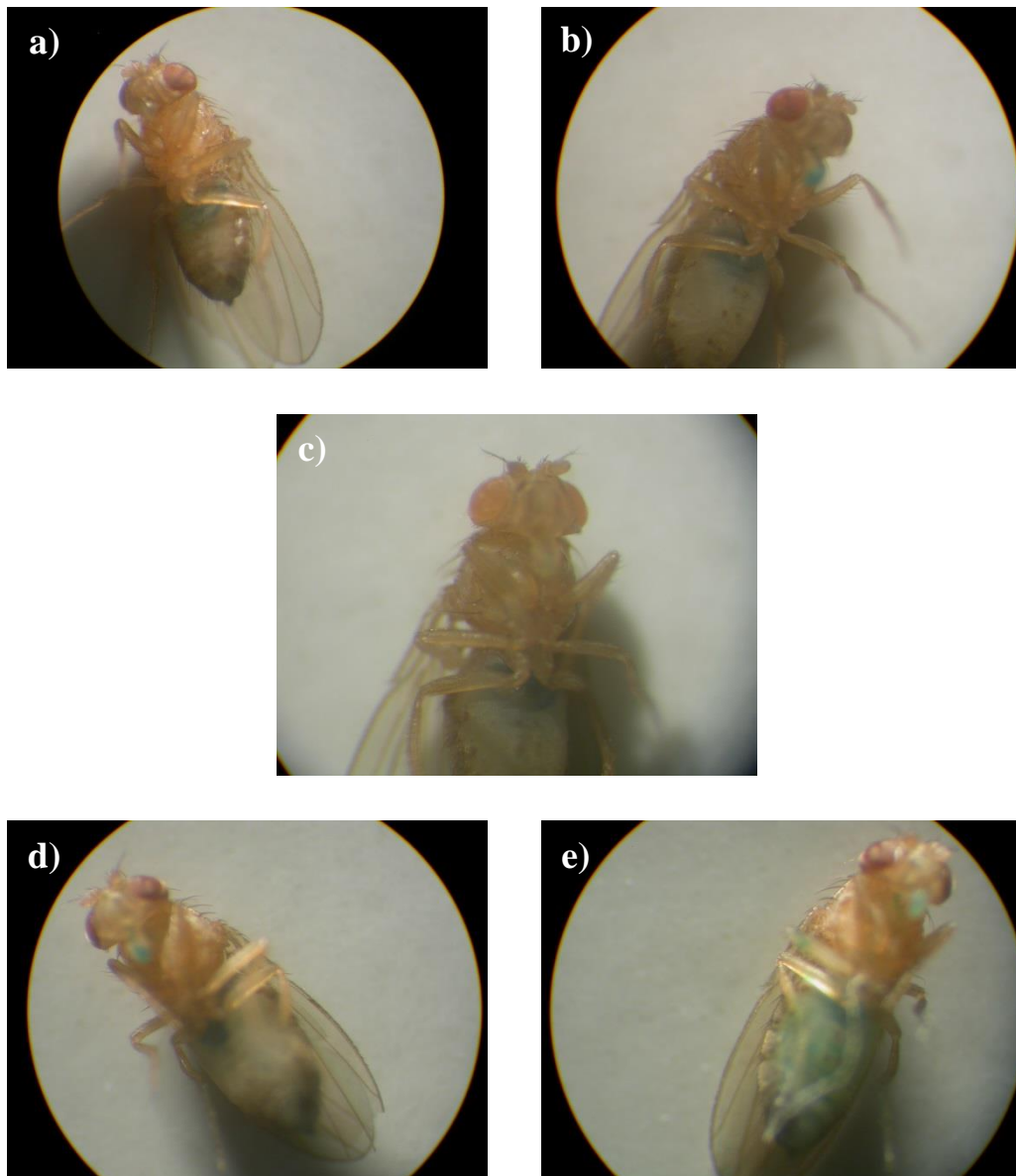
Figure 6.28: Assessment of midgut integrity in SOCS36E knockdown flies, plus controls, using the Smurf assay. Images of (a) EsgGAL/SOCS, (b) EsgGAL/+ and (c) SOCS/+ female flies at 53 days of age, along with (d) and (e) EsgGAL/+ females at 62 days. Flies spent 9 hours on standard food including 2.5% w/v blue food dye before brief anaesthetisation and imaging, using a Nikon Coolpix 990 digital camera. (n≥10 per genotype, per time point).

6.7 Discussion

In the human population, particularly in western societies, people are generally living longer, and this is due to improved nutrition, hygiene, housing conditions, for instance, as well as vast advances in the field of medicine in the last century (WWW, Centers for Disease Control and Prevention). Despite this, conditions common in elderly populations, such as cancer and neurodegenerative diseases are still prevalent. Therefore, living longer may not be beneficial if there is also an increase in morbidity. Functional senescence is an even more common feature that accompanies increasing age, that in itself, can lead to increased morbidity or mortality (Jones and Grotewiel 2011), and is often the first indication of a decline of the nervous system (Camicioli et al. 1999). *Drosophila* also exhibit age-associated functional senescence (Grotowiel et al. 2005), and due to their relatively short lifespans, locomotor behaviours in particular can be assessed at multiple time points over the duration of the lifespan. Additionally, due to the genetic tools available in the fly, it is easy to determine which organ systems are involved in locomotor functioning, and its age-associated decline. There are also a multitude of assays that can be used to dissect and analyse several behaviours that senesce with increasing age, such as negative geotaxis and assessment of spontaneous walking for locomotion, as well as other behaviours, such as olfaction and memory, for example.

We first used the negative geotaxis assay to assess neuromuscular health of knockdown males and females (plus controls), both uninfected and following midgut infection, using a non-lethal phytopathogen, *Ecc15*. From two sets of experiments, we found that ISC-knockdown of SOCS36E had little effect on the expected decline in assay performance with increasing age, in both males and females. There have been studies that have found proportional links between lifespan and negative geotaxis, for instance extended lifespan delays functional senescence, and vice versa (reviewed by Jones and Grotewiel 2011). However, there are also cases where flies exhibited increased oxidative stress and in some instances, an extension in lifespan, but neither an acceleration nor delay of functional senescence. Martin et al. (2009 a and b) found that whilst a loss of function of Sod1 and 2 (antioxidant enzymes) shortened lifespan and accelerated functional senescence, gain of function mutations in these enzymes led to an extension of lifespan (at least in the case of Sod1), but had no effect on senescence. In the flies used here, it may the case that although ISC-knockdown of SOCS36E reduced lifespan (in females only), the reduction was not as large as those often reported (Martin et al. 2009 a, and b). The negative impact of the knockdown may have been confined to one particular organ/tissue/cell type, and therefore did not extend to the musculature or neurons

involved in this reflex behaviour. Additionally, it be may that there is little to no crosstalk between the midgut and both the motor neurons and somatic muscles in *Drosophila*, so the proposed increase in midgut Jak/Stat signalling due to SOCS36E knockdown did not lead to increased or a compensatory decrease in Jak/Stat signalling in either of these locations, resulting in normal muscle ageing and negative geotaxis performance. Negative geotaxis experiments using an array of genotypes have also found that rates of functional senescence is dependent on the genetic background of the fly. For instance, using several wildtype flies, all on different backgrounds, Gargano et al. (2005) found that Lausanne-S flies had the best performance in a negative geotaxis assay, followed by Samarkand, Oregon-R and Canton-S. Miquel et al. (1976) reported that age-related declines in negative geotaxis performance occurs between 14-21 days of age, whereas males used here did not show substantial performance declines until after 21 days. Multiple studies have also found that negative geotaxis declined to a minimum approximately at 35 days of age (reviewed by Grotowiel et al. 2005), while the P.I of all flies used here at 35 days was between 0.3 and 0.7. Unfortunately, there were not enough flies to perform the assay past 6-7 weeks of age, but even at this point, a P.I of 0 was never achieved, indicating that the neuromuscular health of these flies did not fully deteriorate. Therefore, results indicate that locomotor behaviour (as well as other behaviours assessed in biological models) can vary between experiments and that genotype is a strong influence on assay performance. Additionally, we came to the conclusion that the RNAi and infection we introduced were unable to noticeably improve or delay functional decline any further.

Along with knockdown of SOCS36E, we also found that midgut infection with *Ecc15* did not substantially affect functional senescence using this particular assay. There were individual time points where infection had an effect, although these were not consistent across experimental repeats in terms of the genotype affected, whether infection had a positive or negative effect (or none at all) and when in the flies' lifespan this effect took place. Very few studies have been conducted investigating infection in *Drosophila* and how performance in the negative geotaxis assay is affected. Linderman et al. (2012) did find that infection with the Gram-positive bacteria, *Listeria monocytogenes*, reduced the climbing distance 4 seconds post-startle in Oregon-R flies, but not w[1118]. There are several reasons explaining the differences in phenotypes obtained. First, flies used by Linderman et al. (2012) were injected with *L. monocytogenes*, inducing a systemic infection, whereas flies we used were orally infected, thus confining *Ecc15* to the midgut so it may well not be expected to affect motor neurons and musculature, especially when the midgut integrity of all genotypes was not compromised during their lifespan (as shown by the Smurf assay). Secondly, as discussed

previously, performance in the negative geotaxis assay is heavily dependent on the genetic background of the flies, and both sets of flies (Oregon-R flies and w^{1118}) used by Linderman et al. (2012) were of a different background to flies used in this project (w^{Dah}). Thirdly, unless repair of the midgut epithelium is impaired, *Ecc15* is not lethal to fruit flies, whereas *Drosophila* strains will succumb to *L. monocytogenes* within a week of infection (Jensen et al. 2006, Ayres et al. 2008- although systemic infection was also used in both cases here) so it is assumed that this bacteria may affect more systems within the fly than *Ecc15*. Also, as discussed in the previous chapter, in our experiments, flies were only infected at one and two weeks of ages, and were in contact with the bacteria for two hours each time. It may be that this contact was not long enough, and did not generate as much of an immune response, or a sufficient amount of ROS to elicit an effect in the musculature of the flies used here, especially as it is not known how many flies in these experiments actually ingested the bacteria, and if they did, how much bacteria was ingested.

Although there were very few differences between all three genotypes in assay performance, in both uninfected and infected cohorts, this may have been due to the way in which negative geotaxis was assessed. We quantified the number of flies that climbed a certain distance in a tube within a certain time frame, as well as the number that remained at the bottom, and used an equation to change these into an indicator of performance and therefore, locomotor function. Rhodenizer et al. (2008) determined that the age-associated decline in negative geotaxis was due to an increased latency to initiate climbing, but predominantly a decrease in climbing speed, therefore if we assessed both of those factors, we may observe differences in variables that affect climbing ability as a whole between genotypes/infection groups, and perhaps determine effects on functional senescence more definitively.

In addition to escape responses, locomotion is a crucial part of many other behaviours in flies, including foraging for food, responses to stimuli and stress, and courtship and reproduction, for instance. As in innate escape responses (assessed here through the negative geotaxis assay), spontaneous locomotor behaviours will rely on musculature for movement towards or away from something, as well as the brain for speed and duration of walking. Locomotion has shown to be controlled through the central complex and mushroom bodies located in the *Drosophila* brain. Strauss and Heisenberg (1993) found impaired walking activity (including walking speed and straight line walking) in 15 mutant fly strains that affected the central complex structure. Regarding mushroom bodies, Martin et al. (1998) found that disruption, either chemically or genetically, led to an increase in walking activity, demonstrating that

mushroom bodies are responsible for limiting excessive walking, through terminating periods of activity. This finding is also conserved in crickets and grasshoppers (cited by Martin et al. 1998). Therefore, we used the exploratory walking assay, as developed by Martin (2004), to assess the effects of both ISC-knockdown of SOCS36E, and midgut infection with *Ecc15*, on multiple parameters of (spontaneous) walking, in particular on the declines associated with increasing age, and ultimately on the CNS, and central complex and mushroom bodies within the fly brain.

Considering the overall results from the assay as a whole, all flies exhibited age-associated declines in all walking behaviours, regardless of gender, genotype or infection status, strengthening the use of this particular assay in assessing functional senescence and consistent with results obtained in the w^{Dah} background (Ismail et al. 2015). In accordance with previous findings, flies did exhibit a decrease in total distance walked as age increased (Le Bourg and Minois 1999, cited in Grotewiel et al. 2005). This correlates with an age-associated reduction in walking speed, which also mirrors our results and those of Rhodenizer et al. (2008) obtained using negative geotaxis. However, Le Bourg (1987) (cited in Grotewiel et al. 2005) also found that activity consistently decreased with age in females, whereas in males, there were increases until 5 weeks of age, followed by decreases. Results obtained here showed that in the first set of experiments in females, function did decline from the first time point, but, there was much more variability in assay performance in the second set, in that declines were first observed at time points between 16 and 40 days of age, across all parameters and genotypes. In the first set of experiments in male flies, several genotypes demonstrated a decline in function from the first time point until 24 or 31 days of age, where plateaus in assay performance were seen (also across multiple genotypes and parameters of walking). Conversely, in the second set, declines were observed from the first time point for all parameters. There was a substantial amount of functional variability, within genotypes, infection groups and genders, even before cross-comparison, so it is not completely possible to make generalisations regarding functional senescence, particularly as locomotor behaviour is heavily influenced by genetic backgrounds (Fernández et al. 1999, Gargano et al. 2005) and from the results of both of locomotor assays, appears to be inherently variable.

Considering *Ecc15* midgut infection alone first, overall, results were not wholly consistent. In females, any effects on assay performance (whether positive or negative) in the first set of experiments were irregular in that they were not replicated across parameters within the same genotype, or in all three experimental genotypes for one or more parameters. In the second set

however, infection was found to have overall negative effects and reduce total function across all four parameters assessed in EsgGAL/SOCS, as well as have a negative effect during ageing, accelerating the age-associated decline of each behaviour (with this taking place at 19 and 26 days of age, as well as at 40 days). *Ecc15* infection also negatively affected exploratory activity in SOCS/+ females, both at ages coinciding with infection time points (12 and 16 days) and overall total function. Similar to these results, from the first set of experiments in males, *Ecc15* infection had an overall negative effect on exploratory activity and total function in EsgGAL/SOCS males, and also accelerated age-associated declines in each parameter (occurring at a similar time point, at 24 days of age). In contrast, results from the second experiments revealed infection affected locomotor activity in EsgGAL/SOCS males early on in their lifespan, at 12 days of age, and this was found for walking distance, velocity, and rotation frequency. In SOCS/+ however, results mirrored those of EsgGAL/SOCS females, with infection negatively affecting total function as well as bringing forward the time point of age-associated decline to 19 and 26 days. In EsgGAL/+ females and males, midgut infection actually rescued the diminished assay performance, so the negative effects observed were still in 2 out of the 3 genotypes, and therefore occurred irrespective of genotype, despite variety in the affected time points. Over the last few decades, a lot of research has been carried out into the effects that changes in the gut, and in the gut microbiota, have on CNS function and behaviour, and vice versa- a bidirectional relationship named the gut-brain axis. Many studies, using rodents in particular, have shown neural-related implications as a result of changes in the G.I tract. Examples include induction of anxiety-like behaviour (as well as colonic inflammation and an increase in circulating pro-inflammatory cytokines) following *T. muris* infection (Bercik et al. 2010). Bercik et al. (2009) also found that infection with *Helicobacter pylori* resulted in changes in feeding behaviour in mice, and altered mRNA expression in areas of the brain responsible for regulating feeding, and this was still evident two months following bacterial clearance. Regarding locomotor behaviours, experiments in rodents characterise decreased activity and increased hesitation as indicators of anxiety. Nonetheless, Lyte et al. (2006) found that *Citrobacter rodentium* infection led to decreases in walking distance and exploration in mice within 8 hours of infection. This was in conjunction with a lack of histological inflammation and production of inflammatory cytokines, indicating the observations arose from effects of *C. rodentium* on the brain, rather than as a result of morbidity. The same group found infection with a different intestinal pathogen, *Campylobacter jejuni* (a pathogen known to cause gastroenteritis in humans) also reduced exploratory behaviours in mice (Goehler et al. 2008), thus supporting results obtained here. Further support comes from similar studies that found stress early on in life can lead to mood, behavioural and microbiota changes. Rat pups that encountered maternal separation daily between 2 and 12 days old, demonstrated decreases in movement, an absence of

exploratory behaviours as well as increased colonic motility when assessed at 7-8 weeks of age (O'Mahony et al. 2009). Increased colonic motility is a common symptom of IBS- a disorder strongly linked with stress and mood disorders (cited by Whitehead et al. 1980). Additionally, Bailey and Coe (1999) found that the stress induced as a result of 3 days of maternal separation resulted in a decrease in Lactobacilli in rhesus macaque monkeys. In monkeys that were also colonised with pathogenic species (such as *Shigella* and *Campylobacter*), higher titres of these bacteria were observed where decreases of Lactobacilli also occurred. These results demonstrate the importance of a balanced, stable microflora and how in addition to dysbiosis, instability may also leave individuals more susceptible to intestinal infections (and the associated consequences/symptoms of those) due to less competition from beneficial bacteria and their advantages (reviewed by Scholtens et al. 2012). For instance, Lactobacilli can act as antibacterials, due to their ability to produce bacteriocins (cited by Bailey and Coe, 1999). In this project, flies were infected at two time points early on in their lifespans (7 and 14 days of age), and will have endured stress from multiple sources-brief anaesthetisation, starvation and exposure to bacteria during the infection process, production of ROS by the Duox enzyme during the immune response (Ha et al. 2005), and increases in midgut proliferation in order to replace damaged cells and aid in bacterial clearance (Buchon et al. 2009a). Therefore, our walking experiments allowed us to discover the gut-brain axis had been affected in our flies, as we observed significant negative effects on CNS-regulated walking behaviours following *Ecc15* midgut infection.

In addition to the negative effects of *Ecc15* infection, we found that regarding SOCS36E, knockdown also led to accelerations in the age-associated decline of multiple walking parameters assessed and a reduction in total function of these behaviours, with *Ecc15* infection found to exacerbate these declines and cause them to occur earlier in the flies' lifespan. These results suggest that *Drosophila* Jak/Stat signalling (in the midgut in particular) may be implicated in the gut-brain axis. There has been little research on midgut changes and locomotor behaviour in *Drosophila*, and very little direct research into the Jak/Stat pathway and the gut-brain axis, in any biological model, which led us to speculate during the interpretation of our results, based on similar findings in various studies (discussed in the remainder of this chapter). However, Rajan and Perrimon (2012) discovered that upon feeding, Upd2 (one of the *Drosophila* Jak/Stat ligands) was released from the fat body (the equivalent of the mammalian liver) and was able to activate Jak/Stat in neurons within the brain. This led to release of *Drosophila* insulin-like peptides (Dilps) from insulin-producing cells (IPCs, also located in the brain). Dilps are responsible for the promotion of growth and also fat storage, with these processes perturbed following reduction of Upd2 in the fat body

(through RNAi) (Rajan and Perrimon 2012). Although these functional changes arose as a result of altered nutritional status (from a more starved state to a fed state) rather than midgut infection as performed here, these findings demonstrate that a component of the Jak/Stat pathway originating outside of the brain, is able to influence CNS-regulated processes (i.e. growth and energy storage, Rajan and Perrimon 2012).

We hypothesised that knockdown of SOCS36E in Esg+ midgut cells would lead to dysregulated Jak/Stat signalling due to a reduction in feedback inhibition, potentially leading to an increase in proliferation in these cells. This may have altered the architecture of the midgut due to an increase in the number of cells, and this was actually demonstrated by Obasse (2012) who found SOCS36E knockdown (particularly in *Ecc15*- infected flies) resulted in increased midgut diameter, and disruption of Dlg (a protein found in septate junctions of epithelial cells responsible for cell polarity, Woods et al. 1997). Using wildtype larvae (Oregon-R), Basset et al. (2000) reported there were some cases of *Ecc15* translocation from the gut, with bacteria detected in the haemolymph and also in the respiratory tract. We attempted to assess midgut integrity of our experimental flies using the "Smurf" assay (Rera et al. 2011). Although we observed no differences between knockdown and control flies, the phenotype of increased permeability and the appearance of "Smurf" flies are closely associated with mortality. Therefore, as no "Smurf" flies were observed, and an associated increase in mortality was not observed at the time points assessed, it is to be assumed that the flies were healthy in that respect. Expression levels of additional midgut cell junctions, such as E-cadherin, could therefore be assessed in order to fully determine whether SOCS36E affected midgut integrity. Additionally, if an *Ecc15*-GFP strain was to be used, microscopy could be used to determine whether the bacterial had indeed entered the periphery in these flies, and also the brain in particular.

The observation that early-life infection with *Ecc15* in knockdown flies resulted in accelerations in the decline of all assessed walking parameters correlates with findings that early enteric infections and diseases can lead to impairments of cognitive development (reviewed by Kolling et al. 2012), and that enteric infections are known to cause morbidity and mortality (cited by Bergstrom et al. 2012). In addition to effects of enteric infection, SOCS36E in flies has also been found to be associated with cognition and brain function. Copf et al. (2011) found that overexpression of SOCS36E in the mushroom bodies of the brain impaired long-term memory. Although in this study the overexpression was directly targeted to the brain, our discovery that ISC-knockdown of SOCS36E negatively affected

walking behaviours that have been shown to be regulated by the mushroom bodies (Strauss and Heisenberg 1993, Martin et al. 1998), suggests that appropriately regulated Jak/Stat signalling may be essential for efficient functioning of the brain. In order to test this, the exploratory walking assay could be repeated using flies with knockdown of SOCS36E specifically targeted to the mushroom bodies to determine whether this would further exacerbate the declines in walking behaviours we observed here.

We previously showed here that reductions in intestinal SOCS3 led to increases in the enzyme, IDO, both *in vitro* and *in vivo* (chapters 3 and 4, respectively). In addition to its role in catabolising the essential amino acid, tryptophan (Higuchi and Hayaishi 1967) and inducing tolerance (Munn et al. 1998, 1999, Fallarino et al. 2002), increases in IDO have been reported in many neurological disorders and is thought to be implicated in the gut-brain axis. For instance, increased IDO expression has been found in IBD sufferers (Wolf et al. 2004, Ferdinande et al. 2008), with depression also a common ailment in IBD too (cited by Bercik et al. 2010). Effects detrimental to neurological health often occur following IDO activation due to the depletion of tryptophan and production of neurotoxic metabolites downstream in the kynurenine pathway, which are capable of causing neuronal death (Grohmann et al. 2003). Conversion of tryptophan to kynurenine by IDO (and subsequent enzymes) reduces the amount of serotonin that can be produced from tryptophan, with decreases in serotonin also common in neurological disorders (such as depression, Myint and Kim 2003). Immune activation, for instance through bacterial infection, induces IDO (both in humans and mice, Wirleitner et al. 2003, Bell and Else 2011), and this can occur in the circulation (as well as in the brain) leading to an increase in peripheral tryptophan and tryptophan catabolites, which are capable of crossing the blood brain barrier.

The enzyme tryptophan 2,3-dioxygenase ,TDO, like IDO, is responsible for catabolism of tryptophan and also converts tryptophan into kynurenine. *Drosophila* possess their own TDO, encoded by the gene vermilion (cited by Baglioni 1959), and this is a functional ortholog of both mammalian TDO and IDO (Green et al 2012), as shown by the inability of vermilion mutants to form formylkynurenine (the precursor of kynurenine) from tryptophan (Baglioni 1960). Tryptophan depletion in flies can also be damaging, as prevention of this process through the use of two different inhibitors (α-methyl tryptophan, and 5-methyl tryptophan), and vermilion mutants, has been reported to extend both mean and maximum lifespan (Oxenkrug 2010, Oxenkrug et al. 2011). More specifically, ingestion of berberine (a compound also able to inhibit the conversion of tryptophan to kynurenine) also led to

extensions in mean, median and maximum lifespans, and increased locomotor activity, as assessed by vertical climbing (a method similar to negative geotaxis) (Navrotskaya et al. 2012).

Previous studies in mice have reported increases in IDO following SOCS3 silencing using siRNA, and increased proteasomal degradation of IDO following overexpression of SOCS3 (Orabona et al. 2005, 2008), thus potentially producing a negative correlational relationship. Combined with our *in vitro* and *in vivo* findings (in chapters 3 and 4), and the described neurological implications of IDO, we propose that knockdown of SOCS36E in Esg+ cells may lead to increased levels of TDO in the midgut (potentially due to a reduction in degradation processes). This in turn may result in increased amounts of tryptophan catabolites, which upon crossing of the blood brain barrier, can have neurotoxic effects (and ultimately lead to neurodegeneration). However, to test this hypothesis, we would assess whether midgut and/or brain expression of TDO increased following knockdown of SOCS36E, both in uninfected flies, and *Ecc15*-infected flies (as several different pathogens have reported to induce IDO in mammals, Wirleitner et al. 2003, Bell and Else 2011), and if so, whether this would impact on CNS-regulated behaviours.

Another proposed mechanism for our SOCS36E knockdown-mediated behavioural phenotypes involves neuropeptides, and these are peptide molecules produced either in the CNS and/or in the intestines or midgut (in mammals and *Drosophila*, respectively). Following recognition of changes in the local environment by neural or midgut cells, these peptides will carry out their own respective functions once converted from the prepropeptide form to a propeptide and coordinate systemic communication between cells. Each individual peptide can exhibit a multitude of functions, which all collectively involve regulation of development, fecundity, feeding and digestion, locomotor activity and cognitive function, which all ultimately impact on flies' behaviour and/or lifespan (cited by Nässel and Winther 2010). As in mammals, the source of neuropeptides in the *Drosophila* gut is the EECs, which are exclusively found in the midgut (not in either the foregut or hindgut, Veenstra et al. 2008), and these make up one of the two midgut epithelium cell types in *Drosophila*, generated as a result of EB differentiation. The Jak/Stat pathway has been found to be involved in the differentiation of midgut cells, with many studies reporting active Jak/Stat signalling in ISCs and EBs only, not the differentiated ECs and EECs, with a reduction or loss of signalling leading to an accumulation of Esg+ cells, with no differentiation cell markers expressed (Buchon et al. 2009b, Jiang et al. 2009, Beebe et al. 2010, Lin et al. 2010). Other results,

however, are conflicting. For instance, Jiang et al. (2009) found that a reduction in Jak/Stat signalling, achieved through either the use of Stat92E or Dome (receptor) RNAi, or Stat92E mutant flies, resulted in an inability of midgut cells to differentiate into ECs. Although Lin et al. (2010) observed a reduction in the number of ECs in mutant flies for Dome, and Hop (Jak), the number of EECs were reduced as well. However, using Stat92E mutant flies, they were able to detect ECs in the midgut, but there were lower numbers of EECs present, thus concluding that low levels of Jak/Stat signalling resulted in EBs differentiating into EECs, with high levels favouring differentiation into ECs. In contrast to both Jiang et al. (2009) and Lin et al. (2010), Beebe et al. (2010) reported that Jak/Stat activity, in particular Stat92E, was required for the differentiation of EBs into both ECs and EECs. Due to the inconsistency of these findings, we cannot speculate whether or how differentiation would be affected as a result of SOCS36E knockdown in ISCs. If the amount of EECs were affected (due to increased numbers of progenitor cells, or ECs, for instance), this may ultimately impact on neuropeptide production and/or recognition, and thus, communication with the CNS, although this can only be speculated without performing cell lineage studies.

There are studies however, that have reported altered locomotor activity as a result of altered neuropeptide expression. For example, although the flies used were of a different genetic background to our experimental flies, Song et al. (2014) reported an increase in locomotor activity following *Drosophila* tachykinin (DTK) RNAi in the brain and midgut combined- with DTKs comprising of a family of peptides expression in both the CNS and midgut, named for their function in gut muscle contraction (Siviter et al. 2000). The majority of studies have investigated neuropeptide expression in the CNS exclusively due to their roles in regulating locomotor behaviours, with DTK depletion in central complex neurons leading to increases in the number of activity-rest bouts, for example (Kahsai et al. 2010). This emphasises an area in locomotor research that could be explored further, particularly with regards to our interests of Jak/Stat signalling and the gut-brain axis.

In addition to the locomotor experiments, experimental flies were exposed to several stressors in order to explore whether knockdown of SOCS36E in Esg+ cells affected their resistance, and whether the reduced lifespan in female EsgGAL/SOCS flies correlated to changes in stress resistance. A considerable amount of research has been conducted into associations between lifespan and stress resistance, and the ability to select for these phenotypes for several generations. Many studies have reported direct correlations between lifespan and resistance to different stressors, in that extended lifespan can be associated with increased

resistance to one or more stressors, and vice versa. For example, long-lived methuselah (a gene encoding a G protein-coupled receptor, Lin et al. 1998) mutant flies were found to have increased resistance to starvation, high temperatures and paraquat (an inducer of oxidative stress) (Lin et al. 1998, Cook-Wiens and Grotewiel 2002). Broughton et al. (2005) found that in addition to an extension of median and maximum lifespans, ablation of IPCs in the brain resulted in increased resistance to both starvation and oxidative stress. Conversely, knockdown of Sod1 and 2 reduced lifespan whilst leaving flies more sensitive and susceptible to oxidative stress (Martin et al. 2009a and b). Based on these findings, and those similar from other studies, it was to be assumed that for female EsgGAL/SOCS flies at least, that the reduced lifespan would result in decreased resistance to one or more of the stressors assessed. However, we discovered that SOCS36E knockdown proved to be advantageous following starvation and induced oxidative stress (through exposure to hydrogen peroxide) in both female and male flies, whilst no differences in chill coma recovery times were found between knockdown and control flies for both genders. These results indicate that the mechanism involved in starvation and/or oxidative stress resistance, and tolerance of cold/reduced temperatures may be independently regulated, and this has been demonstrated by Broughton et al. (2005). As stated above, ablation of IPCs in the *Drosophila* brain increased resistance to oxidative stress and starvation, but also increased susceptibility to heat and cold stress. There are additional studies where an inverse or lack of relationship between longevity and stress resistance was found. For instance, Force et al. (1995) discovered there were no changes in starvation resistance in flies with increased longevity. Conversely, Harshman et al. (1999) found that in *Drosophila* lines selected for female starvation resistance, males also exhibited increased resistance to starvation, with both genders also displaying increased resistance to dessication, oxidative stress and exposure to solvent fumes. However, these increases were not associated with extensions in lifespan. Similarly, Martin et al. (2009b) found that whilst overexpression of Sod2 in the muscles of flies would have been beneficial against oxidative damage, it did not lead to an extension of lifespan (nor a delay in functional senescence). Further experiments could be performed to deduce whether midgut Jak/Stat signalling is implicated in resistance to other stressors, such as heat and dessication.

With respect to starvation resistance, many studies have reported increased resistance to be associated with an increase in body weight and/or increased lipid and carbohydrate content/storage in flies (Hoffmann and Harshman 1999). This may be one possible explanation for increased starvation resistance in SOCS36E knockdown flies, although could not be confirmed without performing additional experiments, comparing body weights between knockdown and control male and female flies, and also assays to determine

differences in stored lipids, trehalose and glycogen in these flies, as it is not known how the proposed increase in proliferating midgut cells would affect nutrient digestion and storage. Alternatively, another possible mechanism for increased starvation resistance may not be increased energy stores at all, but perhaps the rate at which this stored energy is consumed (reviewed by Rion and Kawecki 2007). If reserves are depleted at a slower rate in knockdown flies compared to controls, this will prolong the time in which these flies can survive without access to a food source.

In the disposable soma theory of ageing, Salmon et al. (2001) discussed that decreases in lifespan can be due to lipid reserves shifting energy towards reproduction, leading to an increase in egg production, which suggests the converse may be true too. Therefore, we proposed that increased fecundity may be a factor implicated in the shortening of lifespan in SOCS36E knockdown female flies. We discovered that although no statistical significance was achieved, there was a tendency of EsgGAL/SOCS females to produce lower average numbers of eggs at each time point (with counts started from 5 days of age). In order to fully determine if this lack of fecundity phenotype is accurate, larger numbers of females could be used (≥300), and more frequent counts could be performed; every time females are transferred into fresh vials (every 2-3 days) rather than once a week as carried out here. Conversely, as fecundity and lifespan are often inversely correlated, and ISC knockdown of SOCS36E had negative effects on both of those parameters here (along with multiple walking behaviours), it may be that the tendency for EsgGAL/SOCS females to lay fewer eggs could just be the result of poor health and function, rather than associated with lifespan and/or stress resistance. However, before this theory can be confirmed, assessment of egg viability should be considered as reductions in eggs laid at each assessed time point, and in eggs laid per female by EsgGAL/SOCS flies may be insignificant if egg viability is similar between EsgGAL/SOCS females and the two control genotypes, or perhaps higher.

Additionally, as resistance to both starvation and oxidative stress involved the midgut in this case (through reduced intake and digestion of food, and ingestion of hydrogen peroxide, respectively), the increased resistance to these two stressors exhibited by EsgGAL/SOCS flies may have been due to the proposed increase in turnover of midgut cells induced through knockdown of SOCS36E. Starvation has shown to cause atrophy of intestinal crypts and villi in mammals, due to increased cell death, and reduced cell proliferation as a result of increased cell cycle duration (Michael and Hodges 1973, Aldewachi et al. 1975). This can ultimately lead to a decrease in the weight of the intestinal tissue. Ortega et al. (1996) found that at a

cellular level, starvation diminished enzyme activity in the small intestine as well as impaired synthesis of both DNA and proteins, and also cell differentiation (as measured by the decreased expression of differentiation markers, Shaw et al. 2012). Collectively, these can impair intestinal function and lead to increased intestinal permeability and translocation of luminal contents, potentially resulting in increased morbidity and mortality (cited by Song et al. 2009). It was proposed that there would be increased midgut proliferation in EsgGAL/SOCS flies due to reduced regulation of Jak/Stat signalling, and this may have replenished cells damaged as a result of decreased nutrition (and the associated effects) sooner than in control flies. This could have helped to maintain the midgut epithelium and barrier function, until energy reserves became depleted and/or the rate of SOCS36E knockdown-induced renewal became insufficient to overcome the rate of cell damage and death.

In conclusion, we performed various behavioural assays in order to determine the effects of ISC-specific SOCS36E knockdown (and thus midgut homeostasis) on health and function using the model organism, *Drosophila melanogaster*. To summarise, we found that SOCS36E knockdown accelerated age-associated declines in spontaneous walking, although reflex-induced locomotion was not affected, which suggested midgut Jak/Stat signalling was capable of influencing CNS- and not muscle-regulated behaviours, and that midgut Jak/Stat signalling may be implicated in the *Drosophila* gut-brain axis. Furthermore, this ISC-specific knockdown was found to be beneficial during conditions of starvation and oxidative stress, but these effects were not sustained when chill coma recovery times and fecundity in female flies were assessed. Collectively, these results suggest that, as with the homologues in mammalian systems, SOCS36E is a complex multi-functional protein that is capable of influencing multiple pathways and tissues, and therefore, more investigation is needed to fully elucidate its complete role in biological organisms.

Chapter 7:

Discussion and

Future Work

One fundamental purpose of performing biomedical research is to try and uncover what is not known in human health and disease. However, due to many constraints, such as time, money ethics, and genetic and environmental variability, it is not always possible to carry out studies using human samples, or within humans themselves. There are a multitude of biological models available, ranging from culturing cells in plates and flasks to mammals such as rodents, dogs and monkeys, and these are used as alternatives to humans and have proven successful in a number of research fields (such as immunology). In relation to this project, our area of interest concerned suppressor of cytokine signalling proteins (SOCS3 specifically), which is implicated in many cellular functions such as negative regulation of the Jak/Stat pathway, cell proliferation, proteasomal degradation and apoptosis to name a few (Krebs and Hilton 2001).

There has been a range of research investigating the role of SOCS3 and the regulation of Jak/Stat in particular, in the mammalian G.I tract, although the majority of studies relate to dysregulated homeostasis and disease processes. We chose to perform experiments in three different biological models: an *in vitro* model involving the use of an untransformed human intestinal epithelial cell line (HIECs), and two *in vivo* models using mice and *Drosophila melanogaster*. The use of multiple models allowed us to investigate the role of intestinal SOCS3 in different contexts. For instance, using HIEC cells, we were able to investigate the impact of intestinal SOCS3 on proliferation and cytokine production, both in the basal state and following microbial stimulation, whereas our *in vivo* models allowed us to investigate the impact of intestinal SOCS proteins on normal and microbial-induced proliferation at a tissue level and in the organism as a whole, in mice and *Drosophila* respectively.

7.1 SOCS3 and Intestinal Homeostasis

With regards to *in vitro* and mouse intestinal models, much research has been conducted into regulation of Jak/Stat signalling and proliferation by SOCS3. However, the vast majority of these findings are obtained either using cancer cell lines, or using disease models to induce dysregulation of homeostasis, such as the AOM/DSS colitis-associated carcinogenesis murine model. For instance, proliferation of IECs *in vitro* was reduced following overexpression of SOCS3 in the normal rat IEC cell line, and in the adenocarcinoma Caco-2 cell line (Rigby et al. 2007). Inflammation-mediated IEC repair using DSS in mice resulted in enhanced crypt proliferation and hyperplasia following IEC-specific SOCS3 deletion (Rigby et al. 2007).

Conversely, increased levels of SOCS3 have been found in IBD clinical studies, or IBD models, and SOCS3 is induced due to increased levels of IL-6, and consequently Stat3 activity (Suzuki et al. 2001). However, due to SOCS3's role in limiting proliferation, it is thought that the IBD-associated increases in its expression could be detrimental during IEC repair processes. Thagia et al. (2015) found that overexpression of SOCS3 led to reductions in microbial-mediated wound healing, as well as increases in flagellin-induced TNF-α production which would drive inflammation in an *in vivo* setting. Although such studies have been insightful, their results cannot be completely generalised to regulation of intestinal homeostasis in a non-pathological setting. Therefore, we aimed to use our three models to investigate the role of SOCS3 in normal intestinal homeostasis.

In our *in vitro* model, we conducted experiments using the recently developed, untransformed HIEC cell line (Perreault and Beaulieu 1996), and found that there were very few differences in cell number following treatment with multiple TLR ligands. However, microbe-mediated proliferation was significantly increased following knockdown of SOCS3, suggesting that SOCS3 is able to maintain intestinal homeostasis through limiting TLR-induced proliferation, and this is supported by findings that SOCS3 can either limit TLR signalling directly through inhibition of MyD88, TRAF6 or TAK1 signal transduction proteins, or, inhibit pathways that are activated as a result of TLR signalling (such as IL-6) (Frobøse et al. 2006, Yoshimura et al. 2007). Despite these findings, knockdown of SOCS3 in unstimulated HIEC cells did not significantly increase cell number and thus proliferation either. These findings were also observed in unstimulated IEC SOCS3 knockout mice, in our experiments and also by Rigby et al. (2007), suggesting that in absence of proliferation-inducing agents, dysregulation of Jak/Stat signalling does not affect cell number, or that other mechanisms are in place to ensure homeostasis is maintained. For instance, in the *Drosophila* midgut, the Jak/Stat pathway operates in cooperation with the EGFR and Wnt, as activation is increased following dysregulation and diminishing activity in one of the other pathways, ensuring efficient regulation of ISCs (Xu et al. 2011).

Both pro- and anti-inflammatory cytokines are produced as a result of microbe recognition, and their regulation is not only important for immune activation and microbe clearance, but also with respect to IEC homeostasis. For instance, increases in pro-inflammatory cytokines, particularly if coupled with decreased production of anti-inflammatory cytokines, can cause damage to cells, as well drive proliferation which can be detrimental if sustained. However, overexpression of anti-inflammatory cytokines can also be unfavourable as pathogens may

induce IEC damage if they remain undetected due to increased immune tolerance. From our results, it can be suggested that SOCS3 is implicated in mediating tolerance as TLR-mediated TNF-α and IL-10 expression was not significantly different from that of untreated SOCS3-sufficient HIECs. Upon knockdown of SOCS3 however, expression of both TNF-α and IL-10 was altered both in unstimulated and microbial-stimulated cells, indicating SOCS3 may limit increases in both proliferation and cytokine production that occur as a result of TLR signalling, and with respect to IECs in particular, help contribute to their hyporesponsive state. We also investigated the regulation of IDO expression by SOCS3, with IDO also implicated in immune tolerance. This is due to its enzymatic ability to catabolise tryptophan, which leads to suppression of T-cell proliferation, and induction of Tregs. Similar to previous results, microbial ligands did not induce significant fold-changes in IDO (with the exception of IFN-γ, which is a potent inducer of IDO, Yoshida et al. 1981, Yasui et al. 1986). IDO expression was significantly increased regardless of cell treatment, following SOCS3 knockdown, in agreement with findings of Orabona et al. (2005), who discovered increases in IDO following reductions in SOCS3 using siRNA (although this was in DCs). Therefore, these findings suggest SOCS3 is able regulate immune tolerance at multiple levels, which ultimately also aims to protect the integrity of IECs.

A number of studies have been conducted in *Drosophila* demonstrating the importance of regulated midgut homeostasis on host health, due to induction of dysregulation having negative effects, reducing the lifespan of the fly (Buchon et al. 2009b, Biteau et al. 2010, for example). In relation to mammalian systems, the *Drosophila* Jak/Stat pathway is considered to be "simplified" due to the presence of fewer components, and this can facilitate its investigation and manipulation. For instance, mammals have 8 SOCS proteins, whereas *Drosophila* have 3 (Greenhalgh et al. 2002, Hou et al. 2002). Within the midgut, the Jak/Stat pathway has been studied considerably due to its large involvement in differentiation as well as proliferation. Studies have revealed that Jak/Stat signalling is required for regulation of both basal and injury- or infection-induced proliferation (Buchon et al. 2009a, Jiang et al. 2009), and that regulation of the Jak/Stat pathway is essential as flies lacking either the Jak/Stat activating ligand, Upd, or Stat92E exhibit increased mortality following infection with a (usually) non-lethal bacteria (*Ecc15*) (Buchon et al. 2009b). In addition to its regulation of ISC proliferation, the *Drosophila* Jak/Stat pathway is itself regulated by the gut microbiota, with increased bacterial loads found to result in increased turnover, and this process is further promoted during ageing (Buchon et al. 2009b). Therefore, these findings demonstrate the key role the *Drosophila* Jak/Stat pathway plays in not only maintaining gut homeostasis, but also the health and survival of the fly. Although SOCS36E (a functional homologue of mammalian

SOCS3, Callus and Mathey-Prevot 2002) is known to be induced following activation of midgut Jak/Stat signalling, research is often focused on other components of the pathway, such as Upd, Hop and Stat92E (Buchon et al. 2009b, Jiang et al. 2009, Beebe et al. 2010, Lin et al. 2010, for example), so we utilised the short lifespan of *Drosophila* and investigated the impact of SOCS36E on midgut homeostasis and how survival and ageing were affected. We discovered that knockdown of SOCS36E in ISCs led to significant reductions in the lifespan of female flies only, although work carried out here was unable to determine the mechanism behind this sexual dimorphism. However, this result further demonstrates the importance of regulated Jak/Stat signalling on midgut health, and thus, is in agreement with previous findings, contributing to this particular area of research. It also may translate to the effects that prolonged dysregulated Jak/Stat signalling has on the wellbeing of the host.

Despite the negative implications of our behavioural and lifespan results, ISC knockdown of SOCS36E was beneficial to flies under conditions of starvation and oxidative stress (using H_2O_2), demonstrating that this dysregulated Jak/Stat signalling can have positive functional effects, and this was also observed in our *T.muris* mouse model. However, combined with the *T. muris* results, this could indicate that positive functional outcomes of reduced SOCS-mediated dysregulation are possibly restricted to younger animals as they have a more sufficient capacity to adapt to changes in cell signalling, before repercussions manifest or accumulate.

7.2 SOCS3 and Cancer

The role of SOCS proteins as tumour suppressors is well-established due to increased proliferation, hyperplasia and tumour development that can arise from its reduced expression or loss as a whole (for instance, through promoter hypermethylation-induced silencing, or through genetic tools such as RNAi or Cre-Lox recombinase techniques). Decreased SOCS3 expression has been found in a range of tumour types, including those in the G.I tract, which is relevant to our area of interest (He et al. 2003, Weber et al. 2005, Ogata et al. 2006, Rigby et al. 2007, Li et al. 2009). Our initial experiments revealed certain differences between the normal HIEC cell line, and the commonly used, adenocarcinoma cell line, Caco-2, which were in agreement with studies in the literature. Specifically, we established the presumed low SOCS3 (mRNA) expression and increased proliferative nature (both basally and following microbial stimulation) of Caco-2 cells, and also discovered that similar SOCS3 mRNA levels

in the normal, untransformed HIEC cell line (achieved through siRNA knockdown) also induced increased TLR-mediated proliferative responses, indicating in these normal intestinal cells, a reduction in SOCS3 was sufficient to induce cancer-like phenotypes. As stated previously, we also assessed the SOCS3-mediated regulation of TLR-induced cytokines, and discovered that in both unstimulated and microbial-stimulated HIECs, SOCS3 reduction altered the cytokine profiles of these cells, as we observed decreases in IL-10 and increases in TNF-α and IDO- all phenotypes that have been observed in cancer (Uyttenhove et al. 2003, Mocellin et al. 2005, Zhang and Schluesener 2006, Oft 2014), thus indicating that these molecular changes associated with reductions or loss of SOCS3 may promote or enhance tumourigenesis. These results also open the door for investigation into SOCS3-mediated expression of additional cytokines (for example, other inflammatory cytokines, such as IFN-γ or IL-1), or potential mechanisms from the results we have shown here. For instance, in our SOCS3 knockdown HIECs (SOCS3^{Low}), there were increases in TNF-α and IDO, as well as decreases in IL-10 mRNA expression. As these cytokines are able to counteract the activity of one another (e.g. TNF-α and IL-10), it would be interesting to see if our observations were related. To test this, we could repeat our TLR stimulation experiments, and inhibit TNF-α/ IL-10/ IDO, and see if this would lead to subsequent changes in expression of the remaining two molecules.

Treatment with AOM and DSS in mice is known to induce colonic tumours in a model of CAC regardless of genotype, and IEC-specific deletion of SOCS3 is known to enhance tumourigenesis in this model, therefore suggesting that upon promotion of intestinal turnover, proliferative responses were enhanced following dysregulation of Jak/Stat through loss of inhibitor, SOCS3. This was demonstrated in our *in vitro* HIEC model, but also in our *T. muris* mouse model. This was demonstrated by *T. muris*-induced alterations of crypt dynamics that are indicative of increased intestinal turnover, regardless of genotype (in agreement with other studies, Artis et al. 1999, Cliffe et al. 2005). Within our infected mice, enhanced IEC turnover in our SOCS3-deleted mice (HO-VC) was demonstrated by an increase in the number of proliferating cells in higher crypt positions (compared to SOCS3-sufficient mice, HO-WT). IDO is known to be induced during *T. muris* infection (in multiple genotypes, shown here and by Datta et al. 2005 and, Bell and Else 2011), and as demonstrated by our *in vitro* findings, and those *in vivo* in DCs (Orabona et al. 2005, Orabona et al. 2008), an indirectly proportional relationship exists between IDO and SOCS3. Although our methods used were not sensitive enough to detect changes in IDO expression between infected HO-WT and HO-VC mice, based on other findings, we could perhaps speculate that *T. muris*-induced IDO expression may be higher in the HO-VC mice (possibly as a result of decreased proteasomal degradation,

Orabona et al. 2005). Shaw et al. (under revision in Immunology and Cell Biology) obtained a positive functional phenotype in HO-VC by means of more efficient expulsion of *T. muris* worms. However, as IDO is known to limit cell proliferation (particularly T-cells) and promote immune tolerance (Munn et al. 1998, Bell and Else 2011), it is to be assumed that increased IDO as a result of infection and reduced IEC SOCS3, also coupled with enhanced turnover, may be unfavourable and potentially promote tumourigenesis if sustained (particularly in low dose, chronic *T. muris* infections). Research into helminth infection is expanding, in inflammatory and autoimmune disorders especially (such as IBD), due to its ability to shift immune dominance from Th1-mediated responses to Th2-mediated responses (Finlay et al. 2014). However, there have been reports of helminth-induced carcinogenesis, due to their capability to induce lesions in tissue, thus potentially perpetuating inflammation-driven tumour development, for example (Kojima et al. 1981, Oikonomopoulou et al. 2014). Although in a different model system, infection with the Gram-negative bacteria, *Ecc15*, in *Drosophila* operates in similar ways to *T. muris*; increasing gut proliferation, inducing immune responses, with clearance/susceptibility also dependent on genotype. Using the *Drosophila* model ours is based on, Buchon (personal communication) found that *Ecc15*-induced midgut proliferation was increased following knockdown of SOCS36E in ISCs, and this proliferative response was sustained in these flies even 2 days post-infection, whereas proliferation decreased and returned to more basal levels in wildtype flies. Collectively, these results could extend the role of SOCS3 in inflammation/colitis-associated carcinogenesis to include bacterial and helminth infection too. In order to test this, both HO-WT and HO-VC could be infected with *T. muris* for a longer period of time, with intestinal tissue then assessed for tumourigenesis, for instance through number and size of tumours if present.

In addition to conservation of signalling pathways in the regulation of intestinal homeostasis, *Drosophila* are also able to develop midgut tumours following dysregulation of said pathways. For instance, Lee et al. (2009) discovered that loss of APC was also able to result in hyperplasia and multilayering of cells, distorting the midgut as a result. Interestingly, Salomon and Jackson (2008) proposed that ageing pre-disposed flies to tumourigenesis, as they reported the development of midgut tumours in unstimulated/ uninfected, wildtype flies by 4 weeks of age, with the number of flies developing tumours increasing with increasing age. The presence of these tumours resulted in obstruction of the gut lumen, with tissue changes resembling those seen in dysplastic mammalian guts. These findings, coupled with those of mammalian studies reporting a reduction of loss of SOCS3 in tumours, and that female flies may exhibit higher rates of turnover in the midgut (Jiang et al. 2009), could suggest that our SOCS36E knockdown female flies could have been pre-disposed to hyperplasia and possibly

dysplasia, particularly as our female flies lived longer than flies studied by Salomon and Jackson (2008). Although this would require further investigation, it could potentially lead to expansion of Jak/Stat-mediated cancer research in an additional biological model.

7.3 SOCS3 and the Gut-Brain Axis

The gut microbiota has often been described as the "forgotten organ" due to the sheer number of bacterial cells and genes in relation to those of the host (Tancrède 1992, DuPont and DuPont 2011), and also due to the roles they are able to carry out in addition to those of the host cells within the intestine. These include the ability to regulate IEC homeostasis in model organisms (Rakoff-Nahoum et al. 2004, Buchon et al. 2009b), aiding in metabolism and digestion, that can lead to beneficial byproducts such as SCFAs (Nguyen et al. 2015) as well as production of antimicrobials (Yurist-Doutsch et al. 2014) and intestinal and immune development (Abrams et al. 1962, Rakoff-Nahoum et al. 2004, Natividad and Verdu 2013, Yurist-Doutsch et al. 2014). However, the effects of the microbiota are not exclusive to the G.I tract, with several studies demonstrating both positive and negative effects on CNS function and behaviour as a result of changes in the gut and gut microbiota, and vice versa. This bi-directional relationship that has been uncovered is termed the gut-brain axis, and results from communication between the gut and the brain, for example through neural pathways and signalling molecules such as cytokines, hormones and neuropeptides (Collins et al. 2012).

We observed in our *Drosophila* model that knockdown of SOCS36E in ISCs, either with or without midgut infection-induced proliferation, resulted in exacerbation of age-associated declines in multiple walking behaviours that have been reported to be regulated in the *Drosophila* brain (Strauss and Heisenberg 1993, Martin et al. 1998), thus suggesting that midgut Jak/Stat signalling may be implicated in the gut-brain axis in flies. Additionally, Jak/Stat has been found to be present in human, mouse and *Drosophila* brains (Copf et al. 2011, Hime and Abud 2013, Nicolas et al. 2013), which raises the possibility of signalling crosstalk between the gut and the brain. Dysregulated SOCS3 expression is also implicated in IBD (Suzuki et al. 2001, Li et al. 2010)- a disorder associated with the gut-brain axis, although very few direct or correlational studies have actually been conducted regarding SOCS proteins and the mammalian gut-brain axis. In *Drosophila*, there are select studies that could suggest a relationship involving Jak/Stat signalling does exist. For instance, the

nutritional status (i.e. fed or starved) of fruit flies is detected by the fat body (the equivalent of the mammalian liver), and following feeding, the Jak/Stat ligand, Upd2, is produced in the fat body, which then activates certain neurons in the brain, resulting in the production of *Drosophila* insulin-like peptides (Dilps) by insulin-producing cells (IPCs), also located in the brain (Rajan and Perrimon 2012). Dilps are responsible for the promotion of growth and also fat storage, with these processes perturbed following reduction of Upd2 in the fat body (through RNAi) (Rajan and Perrimon 2012). Positive changes in nutritional status produce Upd2 in the fat body, which presumably arise from the detection of food within the midgut. Upds are also produced in the midgut by ECs during injury and infection (Buchon et al. 2009a, Jiang et al. 2009), so it would be interesting to determine whether the findings of Rajan and Perrimon (2012) would be observed, or perhaps altered as a result of *Ecc15-* and/or SOCS36E knockdown-induced midgut changes, which would be indicative of Jak/Stat signalling crosstalk and potentially more involvement in the Jak/Stat pathway. Furthermore, there are additional behaviours that are neuronally-regulated that we could assess in *Drosophila* (such as learning and memory) to further elucidate the role of midgut SOCS36E in the gut-brain axis.

Mice have been studied extensively with regards to the gut-brain axis, particularly in terms of modification of the microbiota either through probiotic administration or enteric infection, and the subsequent behaviour and/or brain biochemical changes, aided by the number of behavioural and molecular experiments available to test this phenomenon. In relation to our mouse model, Bercik et al. (2010) found that in addition to the induction of intestinal inflammation, *T. muris* infection increased anxiety-like behaviours in mice as well as induced molecular changes in the brain. In our model, we showed *T. muris* infection resulted in alterations in crypt dynamics, in HO-WT mice; some of which were enhanced in HO-VC mice. Therefore, knowing that *T. muris* induces neural changes along with our observations of diminished walking behaviour following ISC knockdown of SOCS36E and midgut infection in flies, it would be interesting to determine whether the genotypic and phenotypic changes induced in our mouse model would impact on the functioning of the CNS.

Finally, together with its role in cancer and immune tolerance, there are several studies implicating IDO in the gut-brain axis due to its ability to promote production of kynurenine from tryptophan, as opposed to serotonin, with decreased serotonin common in mood disorders, and increases in both IDO and depression reported in IBD too (Wolf et al. 2004, Ferdinande et al. 2008, Bercik et al. 2010). Our findings from our HIEC and mouse models,

along with those by Orabona et al. (2005) and (2008), demonstrated an indirectly proportional relationship between IDO. IDO expression in the circulation and brain can also be found following infection elsewhere (Stone and Darlington, 2013), so it could be proposed that gut infection (in either of our *in vivo* models) could result in increased systemic and/or neural IDO expression, which may be enhanced following knockdown of SOCS proteins, although this cannot be confirmed without further testing.

In conclusion, there are numerous models that are used in biomedical research, each associated with several advantages and disadvantages. When translating findings to human health and disease, it can be beneficial to conduct experiments in multiple models, as identical or similar results may not be obtained, even under the same conditions (such as reducing intestinal SOCS, as carried out here). Due to the dominance of research on SOCS proteins in dysregulated gut homeostasis in disease, we investigated its role in normal homeostasis. We consistently found unfavourable effects following reduction of IEC SOCS, subsequently impacting on proliferation and cytokine profiles, tumour tolerance and, survival and the gut-brain axis, in our HIEC, mouse and *Drosophila* models, respectively. Functional outcomes of IEC SOCS knockdown were revealed through enhanced *T. muris*-induced crypt cell turnover (and subsequent promotion of worm expulsion, Shaw et al., under revision in Immunology and Cell Biology), and increased stress resistance in *Drosophila*, which potentially suggests there may be short-term positive effects of reduced IEC SOCS when animals are relatively young, due to an increased capability to adapt to homeostatic and environmental changes, in comparison with older animals. Collectively, our results indicate that SOCS (SOCS3 and SOCS36E specifically) are complex, multi-faceted proteins whose roles are still yet to be fully elucidated. Overall, they demonstrate the importance of efficiently regulated IEC Jak/Stat signalling, and consequently homeostasis, not only within the G.I tract, but also in different tissues, and these are ultimately capable of negatively impacting on host health.

References

Abraham C. and Cho J.H. (2009) Inflammatory Bowel Disease. *N Engl J Med.* 361(21): 2066-2078

Abrams G.D., Bauer H. and Sprinz H. (1963) Influence of the Normal Flora on Mucosal Morphology and Cellular Renewal in the Ileum. A Comparison of Germ-Free and Conventional Mice. *Lab Invest.* **12**: 355-364

Abreu M.T., Arnold E.T., Thomas L.S., Gonsky R., Zhou Y., Hu B. and Arditi M. (2002) TLR4 and MD-2 Expression is Regulated by Immune-Mediated Signals in Human Intestinal Epithelial Cells. *J Biol Chem.* **277**(23): 20431-20437

Abreu M.T., Thomas L.S., Arnold E.T., Lukasek K., Michelsen K.S. and Arditi M. (2003) TLR Signaling at the Intestinal Epithelial Interface. *J Endotoxin Res.* **9**(5): 322-330

Abreu M.T. (2010) Toll-Like Receptor Signalling in the Intestinal Epithelium: How Bacterial Recognition Shapes Intestinal Function. *Nat Rev Immunol.* **10**(2): 131-144

Agaisse H., Petersen U.M., Boutros M., Mathey-Prevot B. and Perrimon N. (2003) Signaling Role of Hemocytes in *Drosophila* JAK/STAT-Dependent Response to Septic Injury. *Dev Cell.* **5**(3): 441-450

Agoston D.V. (2013) Of Timescales, Animal Models, and Human Disease: The 50th Anniversary of *C. elegans* as a Biological Model. *Front Neurol.* **4**: 129

Akhtar L.N. and Benveniste E.N. (2011) Viral Exploitation of Host SOCS Protein Functions. *J Virol.* **85**(5): 1912-1921

Alberts B., Johnson A., Lewis J., Raff M., Roberts K. and Walter P. (2002) *Isolating cells and growing them in culture. Molecular Biology of the Cell, 4th Edition.* Garland Science. New York.

Aldewachi H.S., Wright N.A., Appleton D.R. and Watson A.J. (1975) The Effect of Starvation and Refeeding on Cell Population Kinetics in the Rat Small Bowel Mucosa. *J Anat.* **119**(Pt 1): 105-121

Allen A., Hutton D.A. and Pearson J.P. (1998) The MUC2 Gene Product: A Human Intestinal Mucin. *Int J Biochem Cell Biol.* **30**(7): 797-801

Ambros V. (2004) The Functions of Animal MicroRNAs. *Nature.* **431**(7006): 350-355

Amcheslavsky A., Jiang J. and Ip Y.T. (2009) Tissue Damage-Induced Intestinal Stem Cell Division in *Drosophila*. *Cell Stem Cell.* **4**(1): 49-61

Apidianakis Y. and Rahme L.G. (2009) *Drosophila melanogaster* as a Model Host for Studying *Pseudomonas aeruginosa* Infection. *Nature Protocols.* **4**(9): 1285

Apidianakis Y., Pitsouli C., Perrimon N. and Rahme L. (2009) Synergy Between Bacterial Infection and Genetic Predisposition in Intestinal Dysplasia. *Proceedings of the National Academy of Sciences.* **106**(49): 20883-20888

Apidianakis Y. and Rahme L.G. (2011) *Drosophila melanogaster* as a Model for Human Intestinal Infection and Pathology. *Dis Model Mech.* **4**(1): 21-30

Arbouzova N.I. and Zeidler M.P. (2006) JAK/STAT Signalling in *Drosophila*: Insights into Conserved Regulatory and Cellular Functions. *Development.* **133**(14): 2605-2616

Arking R., Buck S., Berrios A., Dwyer S. and Baker G.T. 3rd. (1991) Elevated Paraquat Resistance can be used as a Bioassay for Longevity in a Genetically Based Long-Lived Strain of *Drosophila*. *Dev Genet.* **12**(5): 362-370

Artis D., Potten C.S., Else K.J., Finkelman F.D. and Grencis R.K. (1999) *Trichuris muris*: Host Intestinal Epithelial Cell Hyperproliferation during Chronic Infection is Regulated by Interferon-Gamma. *Exp Parasitol.* **92**(2):144-153

Artursson P. (1990) Epithelial Transport of Drugs in Cell Culture. I: A Model for Studying the Passive Diffusion of Drugs over Intestinal Absorbtive (Caco-2) Cells. *Journal of Pharmaceutical Sciences.* **79**(6): 476-482

Augeron C. and Laboisse C.L. (1984) Emergence of Permanently Differentiated Cell Clones in a Human Colonic Cancer Cell Line in Culture after Treatment with Sodium Butyrate. *Cancer Res.* **44**(9): 3961-3969

Autschbach F., Braunstein J., Helmke B., Zuna I., Schürmann G., Niemir Z.I., Wallich R., Otto H.F. and Meuer S.C. (1998) *In situ* Expression of Interleukin-10 in Noninflamed Human Gut and in Inflammatory Bowel Disease. *Am J Pathol.* **153**(1): 121-130

Ayres J.S., Freitag N. and Schneider D.S. (2008) Identification of *Drosophila* Mutants Altering Defense of and Endurance to *Listeria monocytogenes* Infection. *Genetics.* **178**(3): 1807-1815

Babon J.J., Yao S., DeSouza D.P., Harrison C.F., Fabri L.J., Liepinsh E., Scrofani S.D., Baca M. and Norton R.S. (2005) Secondary Structure Assignment of Mouse SOCS3 by NMR Defines the Domain Boundaries and Identifies an Unstructured Insertion in the SH2 Domain. *Febs Journal.* **272**(23): 6120-6130

Babon J.J., McManus E.J., Yao S., DeSouza D.P., Mielke L.A., Sprigg N.S., Willson T.A., Hilton D.J., Nicola N.A., Baca M., Nicholson S.E. and Norton R.S. (2006) The Structure of SOCS3 Reveals the Basis of the Extended SH2 Domain Function and Identifies an Unstructured Insertion that Regulates Stability. *Mol Cell.* **22**(2): 205-216

Babon J.J. and Nicola N.A. (2012) The Biology and Mechanism of Action of Suppressor of Cytokine Signaling 3. *Growth Factors.* **30**(4): 207-219

Bach S.P., Renehan A.G. and Potten C.S. (2000) Stem Cells: The Intestinal Stem Cell as a Paradigm. *Carcinogenesis.* **21**(3): 469-476

Baetz A., Frey M., Heeg K. and Dalpke A.H. (2004) Suppressor of Cytokine Signaling (SOCS) Proteins Indirectly Regulate Toll-Like Receptor Signaling in Innate Immune Cells. *J Biol Chem.* **279**(52): 54708-54715

Baglioni C. (1959) Genetic Control of Tryptophan Peroxidaseoxidase in *Drosophila melanogaster. Nature.* **184**(Suppl 14): 1084-1085

Baglioni C. (1960) Genetic Control of Tryptophan Pyrrolase in *Drosophila melanogaster* and *Drosophila uirilis. Heredity.* **15**: 87-96

Bailey M.T. and Coe C.L. (1999) Maternal Separation Disrupts the Integrity of the Intestinal Microflora in Infant Rhesus Monkeys. *Dev Psychobiol.* **35**(2): 146-155

Balkwill F. and Mantovani A. (2001) Inflammation and Cancer: Back to Virchow? *Lancet.* **357**(9255): 539-545

Bancroft A.J., Else K.J. and Grencis R.K. (1994) Low-level Infection with *Trichuris muris* Significantly Affects the Polarization of the CD4 Response. *Eur J Immunol.* **24**(12): 3113-3118

Bancroft A.J., Else K.J., Sypek J.P. and Grencis R.K. (1997) Interleukin-12 Promotes a Chronic Intestinal Nematode Infection. *Eur J Immunol.* **27**(4): 866-870

Barker N., van Es J.H., Kuipers J., Kujala P., van den Born M., Cozijnsen M., Haegebarth A., Korving J., Begthel H., Peters P.J. and Clevers H. (2007) Identification of Stem Cells in Small Intestine and Colon by Marker Gene Lgr5. *Nature.* **449**(7165): 1003-1007

Barreau F. and Hugot J.P. (2014) Intestinal Barrier Dysfunction Triggered by Invasive Bacteria. *Curr Opin Microbiol.* **17**: 91-98

Basset A., Khush R.S., Braun A., Gardan L., Boccard F., Hoffmann J.A. and Lemaitre B. (2000) The Phytopathogenic Bacteria *Erwinia carotovora* Infects *Drosophila* and Activates an Immune Response. *Proc Natl Acad Sci U.S.A* **97**(7): 3376-3381.

Becker G.H., Meyer J. and Necheles H. (1950) Fat Absorption in Young and Old Age. *Gastroenterology.* **14**(1): 80-92

Beebe K., Lee W.C. and Micchelli C.A. (2010) JAK/STAT Signaling Coordinates Stem Cell Proliferation and Multilineage Differentiation in the *Drosophila* Intestinal Stem Cell Lineage. *Dev Biol.* **338**(1): 28-37

Bell L.V. and Else K. J. (2011) Regulation of Colonic Epithelial Cell Turnover by IDO Contributes to the Innate Susceptibility of SCID Mice to *Trichuris muris* Infection. *Parasite Immunology.* **33**: 244–249

Benoit Y.D., Paré F., Francoeur C., Jean D., Tremblay E., Boudreau F., Escaffit F. and Beaulieu J.F. (2010) Cooperation between HNF-1α, Cdx2, and GATA-4 in Initiating an Enterocytic Differentiation Program in a Normal Human Intestinal Epithelial Progenitor Cell Line. *Am J Physiol Gastrointest Liver Physiol.* **298**(4): G504-517

Bercik P., De Giorgio R., Blennerhassett P., Verdu E.F., Barbara G. and Collins S.M. (2002) Immune-Mediated Neural Dysfunction in a Murine Model of Chronic *Helicobacter pylori* Infection. *Gastroenterology.* **123**: 1205–1215

Bercik P., Verdú E.F., Foster J.A., Lu J., Scharringa A., Kean I., Wang L., Blennerhassett P. and Collins S.M. (2009) Role of Gut-Brain Axis in Persistent Abnormal Feeding Behavior in Mice following Eradication of *Helicobacter pylori* Infection. *Am J Physiol Regul Integr Comp Physiol.* **296**(3): R587-594

Bercik P., Verdu E.F., Foster J.A., Macri J., Potter M., Huang X., Malinowski P., Jackson W., Blennerhassett P., Neufeld K.A., Lu J., Khan W.I., Corthesy-Theulaz I., Cherbut C., Bergonzelli G.E. and Collins S.M. (2010) Chronic Gastrointestinal Inflammation Induces Anxiety-Like Behavior and Alters Central Nervous System Biochemistry in Mice. *Gastroenterology.* **139**(6): 2102-2112

Berg D.J., Davidson N., Kühn R., Müller W., Menon S., Holland G., Thompson-Snipes L., Leach M.W. and Rennick D. (1996) Enterocolitis and Colon Cancer in Interleukin-10-Deficient Mice are Associated with Aberrant Cytokine Production and CD4(+) TH1-Like Responses. *J Clin Invest.* **98**(4): 1010-1020

Bergstrom K.S., Sham H.P., Zarepour M. and Vallance B.A. (2012) Innate Host Responses to Enteric Bacterial Pathogens: A Balancing Act between Resistance and Tolerance. *Cell Microbiol.* **14**(4): 475-484

Berlato C., Cassatella M.A., Kinjyo I., Gatto L., Yoshimura A. and Bazzoni F. (2002) Involvement of Suppressor of Cytokine Signaling-3 as a Mediator of the Inhibitory Effects of IL-10 on Lipopolysaccharide-Induced Macrophage Activation. *J Immunol.* **168**(12): 6404-6411

Besson M. and Martin J.R. (2005) Centrophobism/Thigmotaxis, a New Role for the Mushroom Bodies in *Drosophila*. *J Neurobiol.* **62**(3): 386-396

Bina S., Wright V.M., Fisher K.H., Milo M. and Zeidler M.P. (2010) Transcriptional Targets of *Drosophila* JAK/STAT Pathway Signalling as Effectors of Haematopoietic Tumour Formation. *EMBO Rep.* **11**(3): 201-207

Binari R. and Perrimon N. (1994) Stripe-Specific Regulation of Pair-Rule Genes by Hopscotch, a Putative Jak Family Tyrosine Kinase in *Drosophila*. *Genes Dev.* **8**(3): 300-312

Biteau B., Hochmuth C.E. and Jasper H. (2008) JNK Activity in Somatic Stem Cells Causes Loss of Tissue Homeostasis in the Aging *Drosophila* Gut. *Cell Stem Cell.* **3**(4): 442-455

Biteau B., Karpac J., Supoyo S., DeGennaro M., Lehmann R. and Jasper H. (2010) Lifespan Extension by Preserving Proliferative Homeostasis in *Drosophila*. *PLoS Genetics.* **6**(10): e1001159

Biteau B., Karpac J., Hwangbo D. and Jasper H. (2011) Regulation of *Drosophila* Lifespan by JNK Signaling. *Exp Gerontol.* **46**(5): 349-354

Bjerknes M. and Cheng H. (1981) The Stem-Cell Zone of the Small Intestinal Epithelium. I. Evidence from Paneth Cells in the Adult Mouse. *Am J Anat.* **160**(1): 51-6

Blum J.E., Fischer C.N., Miles J. and Handelsman J. (2013) Frequent Replenishment Sustains the Beneficial Microbiome of *Drosophila melanogaster*. *MBio.* **4**(6): e00860-13

Bonfini A., Liu X. and Buchon N. (2016) From Pathogens to Microbiota: How *Drosophila* Intestinal Stem Cells React to Gut Microbes. *Dev Comp Immunol.* pii: S0145-305X(16)30032-5

Boosani C.S. and Agrawal D.K. (2015) Methylation and MicroRNA-Mediated Epigenetic Regulation of SOCS3. *Mol Biol Rep.* **42**(4): 853-872

Booth C. and Potten C.S. (2000) Gut Instincts: Thoughts on Intestinal Epithelial Stem Cells. *J Clin Invest.* **105**(11): 1493-1499

Bowie A. and O'Neill L.A. (2000) The Interleukin-1 Receptor/Toll-Like Receptor Superfamily: Signal Generators for Pro-Inflammatory Interleukins and Microbial Products. *J Leukoc Biol.* **67**(4): 508-514

Brand A.H. and Perrimon N. (1993) Targeted Gene Expression as a Means of Altering Cell Fates and Generating Dominant Phenotypes. *Development.* **118**(2): 401-415

Brandacher G., Perathoner A., Ladurner R., Schneeberger S., Obrist P., Winkler C., Werner E.R., Werner-Felmayer G., Weiss H.G., Göbel G., Margreiter R., Königsrainer A.,

Fuchs D. and Amberger A. (2006) Prognostic Value of Indoleamine 2,3-Dioxygenase Expression in Colorectal Cancer: Effect on Tumor-Infiltrating T Cells. *Clin. Cancer Res.* **12**(4):1144-1151

Broderick N.A., Buchon N. and Lemaitre B. (2014) Microbiota-Induced Changes in *Drosophila melanogaster* Host Gene Expression and Gut Morphology. *MBio.* **5**(3): e01117-14

Broughton S.J., Piper M.D., Ikeya T., Bass T.M., Jacobson J., Driege Y., Martinez P., Hafen E., Withers D.J., Leevers S.J. and Partridge L. (2005) Longer Lifespan, Altered Metabolism, and Stress Resistance in *Drosophila* from Ablation of Cells Making Insulin-Like Ligands. *Proc Natl Acad Sci USA.* **102**(8): 3105-3110

Brown S., Hu N. and Hombría J.C. (2001) Identification of the First Invertebrate Interleukin JAK/STAT Receptor, the *Drosophila* Gene domeless. *Curr Biol.* **11**(21): 1700-1705

Buchon N., Broderick N.A., Poidevin M., Pradervand S. and Lemaitre B. (2009a) *Drosophila* Intestinal Response to Bacterial Infection: Activation of Host Defense and Stem Cell Proliferation. *Cell Host Microbe.* **5**(2): 200-211

Buchon N., Broderick N.A., Chakrabarti S. and Lemaitre B. (2009b) Invasive and Indigenous Microbiota Impact Intestinal Stem Cell Activity Through Multiple Pathways in *Drosophila*. *Genes & Development.* **23**: 2333-2344

Buchon N., Broderick N.A., Kuraishi T. and Lemaitre B. (2010) *Drosophila* EGFR pathway coordinates stem cell proliferation and gut remodeling following infection. *BMC Biol.* **8**:152

Buchon N., Osman D., David F.P., Fang H.Y., Boquete J.P., Deplancke B. and Lemaitre B. (2013a) Morphological and molecular characterization of adult midgut compartmentalization in *Drosophila*. *Cell Rep.* **3**(5): 1725-1738

Buchon N., Broderick N.A. and Lemaitre B. (2013b) Gut Homeostasis in a Microbial World: Insights from *Drosophila melanogaster*. *Nat Rev Microbiol.* **11**(9): 615-626

Cady S.G. and Sono M. (1991(1-Methyl-DL-Tryptophan, Beta-(3-Benzofuranyl)-DL-Alanine (the oxygen analog of tryptophan), and Beta-[3-Benzo(b)thienyl]-DL-Alanine (the sulfur analog of tryptophan) are Competitive Inhibitors for Indoleamine 2,3-Dioxygenase. *Arch Biochem Biophys.* **291**(2): 326-333

Callus B.A. and Mathey-Prevot B. (2002) SOCS36E, A Novel *Drosophila* SOCS Protein, Suppresses JAK/STAT and EGF-R Signalling in the Imaginal Wing Disc. *Oncogene.* **21**(31): 4812-4821

Camicioli R., Moore M.M., Sexton G., Howieson D.B. and Kaye J.A. (1999) Age-Related Changes Associated with Motor Function in Healthy Older People. *J Am Geriatr Soc* **47**: 330-334

Capo F., Charroux B. and Royet J. (2016) Bacteria Sensing Mechanisms in *Drosophila* Gut: Local and Systemic Consequences. *Dev Comp Immunol.* pii: S0145-305X(16)30001-5

Carballo M., Conde M., El Bekay R., Martín-Nieto J., Camacho M.J., Monteseirín J., Conde J., Bedoya F.J. and Sobrino F. (1999) Oxidative Stress Triggers STAT3 Tyrosine Phosphorylation and Nuclear Translocation in Human Lymphocytes. *J Biol Chem.* **274**(25): 17580-17586

Cario E. and Podolsky D.K. (2000) Differential Alteration in Intestinal Epithelial Cell Expression of Toll-Like Receptor 3 (TLR3) and TLR4 in Inflammatory Bowel Disease. *Infect Immun.* **68**(12): 7010-7017

Cario E., Gerken G. and Podolsky D.K. (2004) Toll-Like Receptor 2 Enhances ZO-1-Associated Intestinal Epithelial Barrier Integrity via Protein Kinase C. *Gastroenterology.* **127**(1): 224-238

Cario E. (2005) Bacterial Interactions with Cells of the Intestinal Mucosa: Toll-Like Receptors and NOD2. *Gut.* **54**(8): 1182-1193

Cassatella M.A., Gasperini S., Bovolenta C., Calzetti F., Vollebregt M., Scapini P., Marchi M., Suzuki R., Suzuki A. and Yoshimura A. (1999) Interleukin-10 (IL-10) Selectively Enhances CIS3/SOCS3 mRNA Expression in Human Neutrophils: Evidence for an IL-10-Induced Pathway that is Independent of STAT Protein Activation. *Blood.* **94**(8): 2880-2889

Chandler J.A., Lang J.M., Bhatnagar S., Eisen J.A. and Kopp A. (2011) Bacterial Communities of Diverse *Drosophila* Species: Ecological Context of a Host-Microbe Model System. *PLoS Genet.* **7**(9):e1002272

Chapman T., Liddle L.F., Kalb J.M., Wolfner M.F. and Partridge L. (1995) Cost of Mating in *Drosophila melanogaster* Females is Mediated by Male Accessory Gland Products. *Nature.* **373**(6511): 241-244

Chapman T. and Partridge L. (1996) Female Fitness in *Drosophila melanogaster*: An Interaction between the Effect of Nutrition and of Encounter Rate with Males. *Proc Biol Sci.* **263**(1371): 755-759

Charroux B. and Royet J. (2012) Gut-Microbiota Interactions in Non-Mammals: What can we learn from *Drosophila*? *Semin Immunol.* **24**(1): 17-24

Chatterjee M. and Ip Y.T. (2009) Pathogenic Stimulation of Intestinal Stem Cell Response in *Drosophila*. *J. Cell. Physiol.* **220**: 664–671

Cheng H. and Leblond C.P. (1974) Origin, Differentiation, and Renewal of the Four Main Epithelial Cell Types in the Mouse Small Intestine. V. Unitarian Theory of the Origin of the Four Epithelial Cell Types. *Am J Anat.* 141: 537-562

Chippindale A.K., Gibbs A.G., Sheik M., Yee K.J., Djawdan M., Bradley T.J. and Rose M.R. (1998) Resource Acquisition and the Evolution of Stress Resistance in *Drosophila melanogaster*. *Evolution.* 1342-1352

Choi N.H., Kim J.G., Yang D.J., Kim Y.S. and Yoo M.A. (2008) Age-Related Changes in *Drosophila* Midgut are Associated with PVF2, a PDGF/VEGF-Like Growth Factor. *Aging Cell.* **7**(3): 318-334

Ciacci-Woolwine F., Blomfield I.C., Richardson S.H. and Mizel S.B. (1998) *Salmonella* Flagellin Induces Tumor Necrosis Factor Alpha in a Human Promonocytic Cell Line. *Infect Immun.* **66**(3): 1127-1134

Ciccocioppo R., Di Sabatino A., Luinetti O., Rossi M., Cifone M.G. and Corazza G.R. (2002) Small Bowel Enterocyte Apoptosis and Proliferation are Increased in the Elderly. *Gerontology.* **48**(4): 204-208

Clare M.J. and Luckinbill L.S. (1985) The Effects of Gene-Environment Interaction on the Expression of Longevity. *Heredity.* **55**(Pt 1): 19-26

Cliffe L.J. and Grencis R.K. (2004) The *Trichuris muris* System: A Paradigm of Resistance and Susceptibility to Intestinal Nematode Infection. *Adv. Parasitol.* **57**: 255-307

Cliffe L.J., Humphreys N.E., Lane T.E., Potten C.S., Booth C. and Grencis R.K. (2005) Accelerated Intestinal Epithelial Cell Turnover: A New Mechanism of Parasite Expulsion. *Science.* **308**(5727):1463-1465

Collins S.M. and Bercik P. (2009) The Relationship between Intestinal Microbiota and the Central Nervous System in Normal Gastrointestinal Function and Disease. *Gastroenterology.* **136**(6): 2003-2014

Collins S.M., Surette M. and Bercik P. (2012) The Interplay between the Intestinal Microbiota and the Brain. *Nat Rev Microbiol.* **10**(11): 735-742

Cook-Wiens E. and Grotewiel M.S. (2002) Dissociation between Functional Senescence and Oxidative Stress Resistance in *Drosophila*. *Exp Gerontol.* **37**(12): 1347-1357

Copf T., Goguel V., Lampin-Saint-Amaux A., Scaplehorn N. and Preat T. (2011) Cytokine Signaling Through the JAK/STAT Pathway is Required for Long-Term Memory in *Drosophila*. *Proc Natl Acad Sci USA.* **108**(19): 8059-8064

Corvinus F.M., Orth C., Moriggl R., Tsareva S.A., Wagner S., Pfitzner E.B., Baus D., Kaufmann R., Huber L.A., Zatloukal K., Beug H., Ohlschläger P., Schütz A., Halbhuber K.J. and Friedrich K. (2005) Persistent STAT3 Activation in Colon Cancer is Associated with Enhanced Cell Proliferation and Tumor Growth. *Neoplasia.* **7**(6): 545-555

Croker B.A., Krebs D.L., Zhang J.G., Wormald S., Willson T.A., Stanley E.G., Robb L., Greenhalgh C.J., Förster I., Clausen B.E., Nicola N.A., Metcalf D., Hilton D.J., Roberts A.W. and Alexander W.S. (2003) SOCS3 Negatively Regulates IL-6 Signaling *in vivo*. *Nat Immunol.* **4**(6): 540-545

Croker B.A., Kiu H. and Nicholson S.E. (2008) SOCS Regulation of the JAK/STAT Signalling Pathway. *Semin Cell Dev Biol.* **19**(4): 414-422

Daig R., Rogler G., Aschenbrenner E., Vogl D., Falk W., Gross V., Schölmerich J. and Andus T. (2000) Human Intestinal Epithelial Cells Secrete Interleukin-1 Receptor Antagonist and Interleukin-8 but not Interleukin-1 or Interleukin-6. *Gut.* **46**(3): 350-358

Datta R., deSchoolmeester M.L., Hedeler C., Paton N.W., Brass A.M. and Else K.J. (2005) Identification of Novel Genes in Intestinal Tissue that are Regulated after Infection with an Intestinal Nematode Parasite. *Infect Immun.* **73**(7):4025-4033

Davies D.H. (2013) Immune System. *eLS.*

De Robertis M., Massi E., Poeta M.L., Carotti S., Morini S., Cecchetelli L., Signori E. and Fazio V.M. (2011) The AOM/DSS Murine Model for the Study of Colon Carcinogenesis: From Pathways to Diagnosis and Therapy Studies. *J. Carcinog.* **10**:9

DeGruttola A.K., Low D., Mizoguchi A. and Mizoguchi E. (2016) Current Understanding of Dysbiosis in Disease in Human and Animal Models. *Inflamm Bowel Dis.* **22**(5): 1137-1150

Devineni A.V. and Heberlein U. (2012) Acute Ethanol Responses in *Drosophila* are Sexually Dimorphic. *Proc Natl Acad Sci U S A.* **109**(51): 21087-21092

Dionne M.S. and Schneider D.S. (2008) Models of Infectious Diseases in the Fruit Fly *Drosophila melanogaster. Dis Model Mech.* **1**(1): 43-49

Dominguez-Bello M.G., Costello E.K., Contreras M., Magris M., Hidalgo G., Fierer N. and Knight R. (2010) Delivery Mode Shapes the Acquisition and Structure of the Initial Microbiota across Multiple Body Habitats in Newborns. *Proc Natl Acad Sci U S A.* **107**(26): 11971-11975

Dostert C., Jouanguy E., Irving P., Troxler L., Galiana-Arnoux D., Hetru C., Hoffmann J.A. and Imler J.L. (2005) The Jak-STAT Signaling Pathway is required but not sufficient for the Antiviral Response of *Drosophila. Nat Immunol.* **6**(9): 946-953

Duchmann R., Kaiser I., Hermann E., Mayet W., Ewe K. and Meyer zum Büschenfelde K.H. (1995) Tolerance Exists Towards Resident Intestinal Flora but is Broken in Active Inflammatory Bowel Disease (IBD). *Clin Exp Immunol.* 102(3): 448-455

DuPont A.W. and DuPont H.L. (2011) The Iintestinal Microbiota and Chronic Disorders of the Gut. *Nat Rev Gastroenterol Hepatol.* **8**(9): 523-531

Duval D., Reinhardt B., Kedinger C. and Boeuf H. (2000) Role of Suppressors of Cytokine Signaling (Socs) in Leukemia Inhibitory Factor (LIF) -Dependent Embryonic Stem Cell Survival. *FASEB J.* **14**(11): 1577-1584

el Marjou F., Janssen K.P., Chang B.H., Li M., Hindie V., Chan L., Louvard D., Chambon P., Metzger D. and Robine S. (2004) Tissue-Specific and Inducible Cre-Mediated Recombination in the Gut Epithelium. *Genesis.* **39**(3): 186-193

Else K. and Wakelin D. (1989) Genetic Variation in the Humoral Immune Responses of Mice to the Nematode *Trichuris muris*. *Parasite Immunol.* **11**(1): 77-90

Else K.J. and Grencis R.K. (1991) Helper T-Cell Subsets in Mouse Trichuriasis. *Parasitol Today.* **7**(11): 313-316

Fahmy M.A.M. (1954). An Investigation on the Life Cycle of *Trichuris muris*. *Parasitology.* **44**(1-2): 50-57

Fallarino F., Grohmann U., Vacca C., Bianchi R., Orabona C., Spreca A., Fioretti M.C. and Puccetti P. (2002) T Cell Apoptosis by Tryptophan Catabolism. *Cell Death Differ.* **9**(10): 1069-1077

Fallarino F., Grohmann U., You S., McGrath B.C., Cavener D.R., Vacca C., Orabona C., Bianchi R., Belladonna M.L., Volpi C., Santamaria P., Fioretti M.C. and Puccetti P. (2006) The Combined Effects of Tryptophan Starvation and Tryptophan Catabolites Down-Regulate T Cell Receptor Zeta-Chain and Induce a Regulatory Phenotype in Naive T Cells. *J Immunol.* **176**(11): 6752-6761

Fallingborg J. (1999) Intraluminal pH of the Human Gastrointestinal Tract. *Dan Med Bull.* **46**(3): 183-196

Ferdinande L., Demetter P., Perez-Novo C., Waeytens A., Taildeman J., Rottiers I., Rottiers P., De Vos M. and Cuvelier C.A. (2008) Inflamed Intestinal Mucosa Features a Specific Epithelial Expression Pattern of Indoleamine 2,3-Dioxygenase. *Int. J. Immunopathol. Pharmacol.* **21**(2): 289-295

Fernández J.R., Grant M.D., Tulli N.M., Karkowski L.M. and McClearn G.E. (1999) Differences in Locomotor Activity across the Lifespan of *Drosophila melanogaster*. *Exp Gerontol.* **34**(5): 621-631

Finlay C.M., Walsh K.P. and Mills K.H. (2014) Induction of Regulatory Cells by Helminth Parasites: Exploitation for the Treatment of Inflammatory Diseases. *Immunol Rev.* **259**(1): 206-230

Fire A., Xu S., Montgomery M.K., Kostas S.A., Driver S.E. and Mello C.C. (1998) Potent and Specific Genetic Interference by Double-Stranded RNA in *Caenorhabditis elegans*. *Nature.* **391**(6669): 806-811

Fogh J. and Trempe G. (1975) New Human Tumor Cell Lines. *In Human tumor cells in vitro*, pp. 115-159. Springer US.

Force A.G., Staples T., Soliman S. and Arking R. (1995) Comparative Biochemical and Stress Analysis of Genetically Selected *Drosophila* Strains with Different Longevities. *Dev. Genet.* **17**: 340–351

Fowler K. and Partridge L. (1989) A Cost of Mating in Female Fruitflies. *Nature.* **338**: 760–761

Friberg M., Jennings R., Alsarraj M., Dessureault S., Cantor A., Extermann M., Mellor A.L., Munn D.H. and Antonia S.J. (2002) Indoleamine 2,3-Dioxygenase Contributes to Tumor Cell Evasion of T Cell-Mediated Rejection. *Int J Cancer.* **101**(2): 151-155.

Fritz J.V., Desai M.S., Shah P., Schneider J.G. and Wilmes P. (2013) From Meta-omics to Causality: Experimental Models for Human Microbiome Research. *Microbiome.* **1**(1): 14

Frobøse H., Rønn S.G., Heding P.E., Mendoza H., Cohen P., Mandrup-Poulsen T. and Billestrup N. (2006) Suppressor of Cytokine Signaling-3 Inhibits Interleukin-1 Signaling by Targeting the TRAF-6/TAK1 Complex. *Mol Endocrinol.* **20**(7):1587-1596

Frosali S., Pagliari D., Gambassi G., Landolfi R., Pandolfi F. and Cianci R. (2015) How the Intricate Interaction among Toll-Like Receptors, Microbiota, and Intestinal Immunity Can Influence Gastrointestinal Pathology. *J Immunol Res.* **2015**: 489821

Frumento G., Rotondo R., Tonetti M., Damonte G., Benatti U. and Ferrara G.B. (2002) Tryptophan-Derived Catabolites are Responsible for Inhibition of T and Natural Killer Cell Proliferation Induced by Indoleamine 2,3-Dioxygenase. *J Exp Med.* **196**(4): 459-468

Furness J.B., Rivera L.R., Cho H.J., Bravo D.M. and Callaghan B. (2013) The Gut as a Sensory Organ. *Nat Rev Gastroenterol Hepatol.* **10**(12): 729-740

Gargano J.W., Martin I., Bhandari P. and Grotewiel M.S. (2005) Rapid Iterative Negative Geotaxis (RING): A New Method for Assessing Age-Related Locomotor Decline in *Drosophila*. *Exp Gerontol.* **40**(5):386-395

Gendrin M., Welchman D.P., Poidevin M., Hervé M. and Lemaitre B. (2009) Long-Range Activation of Systemic Immunity Through Peptidoglycan Diffusion in *Drosophila*. *PLoS Pathog.* **5**(12): e1000694

Geokas M., Conteas C.N. and Majumdar A.P.N. (1985) The Aging Gastrointestinal Tract, Liver and Pancreas. *Clin. Geriat. Med.* **1**: 177-205

Gerbe F., Legraverend C. and Jay P. (2012) The Intestinal Epithelium Tuft Cells: Specification and Function. *Cell Mol Life Sci.* **69**(17): 2907-2917

Glittenberg M.T., Kounatidis I., Christensen D., Kostov M., Kimber S., Roberts I. and Ligoxygakis P. (2011) Pathogen and Host Factors are needed to provoke a Systemic Host Response to Gastrointestinal Infection of *Drosophila* Larvae by *Candida albicans*. *Dis Model Mech.* **4**(4): 515-25

Goehler L.E., Park S.M., Opitz N., Lyte M. Gaykema R.P. (2008) *Campylobacter jejuni* Infection Increases Anxiety-Like Behavior in the Holeboard: Possible Anatomical Substrates for Viscerosensory Modulation of Exploratory Behavior. *Brain Behav Immun.* **22**(3): 354-366

Green E.W., Campesan S., Breda C., Sathyasaikumar K.V., Muchowski P.J., Schwarcz R., Kyriacou C.P. and Giorgini F. (2012) *Drosophila* Eye Color Mutants as Therapeutic Tools for Huntington Disease. *Fly (Austin).* **6**(2): 117-120

Greenhalgh C.J., Miller M.E., Hilton D.J. and Lund P.K. (2002) Suppressors of Cytokine Signaling: Relevance to Gastrointestinal Function and Disease. *Gastroenterology.* **123**(6): 2064-2081

Grivennikov S., Karin E., Terzic J., Mucida D., Yu G.Y., Vallabhapurapu S., Scheller J., Rose-John S., Cheroutre H., Eckmann L. and Karin M. (2009) IL-6 and Stat3 are Required for Survival of Intestinal Epithelial Cells and Development of Colitis-Associated Cancer. *Cancer Cell.* **15**(2):103-13

Grohmann U., Fallarino F. and Puccetti P. (2003) Tolerance, DCs and Tryptophan: Much Ado about IDO. *Trends Immunol.* **24**(5): 242-248

Grotewiel M.S., Martin I., Bhandari P. and Cook-Wiens E. (2005) Functional Senescence in *Drosophila melanogaster*. *Ageing Research Reviews* **4**: 372–397

Guarner F. and Malagelada J.R. (2003) Gut Flora in Health and Disease. *Lancet.* **361**(9356): 512-519

Guezguez A., Paré F., Benoit Y.D., Basora N. and Beaulieu J.F. (2014) Modulation of Stemness in a Human Normal Intestinal Epithelial Crypt Cell Line by Activation of the WNT Signaling Pathway. *Exp Cell Res.* **322**(2): 355-364

Guo L., Karpac J., Tran S.L. and Jasper H. (2014) PGRP-SC2 Promotes Gut Immune Homeostasis to Limit Commensal Dysbiosis and Extend Lifespan. *Cell.* **156**(1-2): 109-122

Ha E.M., Oh C.T., Bae Y.S. and Lee W.J. (2005) A Direct Role for Dual Oxidase in *Drosophila* Gut Immunity. *Science.* **310**(5749): 847-850

Haan S., Ferguson P., Sommer U., Hiremath M., McVicar D.W., Heinrich P.C., Johnston J.A. and Cacalano N.A. (2003) Tyrosine Phosphorylation Disrupts Elongin Interaction and Accelerates SOCS3 Degradation. *J Biol Chem.* **278**(34): 31972-31979

Hamilton K.E., Simmons J.G., Ding S., Van Landeghem L. and Lund P.K. (2011) Cytokine Induction of Tumor Necrosis Factor Receptor 2 is Mediated by STAT3 in Colon Cancer Cells. *Mol Cancer Res.* **9**(12): 1718-1731

Hanahan D. and Weinberg R.A. (2000) The Hallmarks of Cancer. *Cell.* **100**(1): 57-70

Hanauer S.B. (2006) Inflammatory Bowel Disease: Epidemiology, Pathogenesis, and Therapeutic Opportunities. *Inflamm Bowel Dis.* 12(5): S3-9

Harshman L.G., Moore K.M., Sty M.A. and Magwire M.M. (1999) Stress Resistance and Longevity in Selected Lines of *Drosophila melanogaster*. *Neurobiol Aging.* **20**(5): 521-529

He B., You L., Uematsu K., Zang K., Xu Z., Lee A.Y., Costello J.F., McCormick F. and Jablons D.M. (2003) SOCS-3 is Frequently Silenced by Hypermethylation and Suppresses Cell Growth in Human Lung Cancer. *Proc Natl Acad Sci U S A.* **100**(24): 14133-14138

Hedrich H. ed. (2004) *The Laboratory Mouse.* Academic Press.

Helfand S.L. and Rogina B. (2003) Genetics of Aging in the Fruit Fly, *Drosophila melanogaster*. *Annu. Rev. Genet.* **37**: 329-348

Helmby H., Takeda K., Akira S. and Grencis R.K. (2001) Interleukin (IL)-18 Promotes the Development of Chronic Gastrointestinal Helminth Infection by Downregulating IL-13. *J Exp Med.* **194**(3): 355-364

Hermiston M.L. and Gordon J.I. (1995) Inflammatory Bowel Disease and Adenomas in Mice Expressing a Dominant Negative N-Cadherin. *Science.* **270**(5239): 1203-1207

Herranz H., Hong X., Hung N.T., Voorhoeve P.M. and Cohen S.M. (2012) Oncogenic Cooperation between SOCS Family Proteins and EGFR Identified using a *Drosophila* Epithelial Transformation Model. *Genes Dev.* **26**(14): 1602-1611

Hidalgo I.J., Raub T.J. and Borchardt R.T. (1989) Characterization of the Human Colon Carcinoma Cell Line (Caco-2) as a Model System for Intestinal Epithelial Permeability. *Gastroenterology.* **96**(3): 736-749

Higuchi K. and Hayaishi O. (1967) Enzymic Formation of D-Kynurenine from D-Tryptophan. *Arch Biochem Biophys.* **120**(2): 397-403

Hime G. and Abud H. eds. (2013) *Transcriptional and Translational Regulation of Stem Cells.* Springer.

Hoffmann A. and Harshman L. (1999) Desiccation and Starvation Resistance in *Drosophila*: Patterns of Variation at the Species, Population and Intrapopulation Levels. *Heredity.* **83**(6): 637-643

Hold G.L. and El-Omar E.M. (2008) Genetic Aspects of Inflammation and Cancer. *Biochem J.* **410**(2): 225-235

Holt P.R. and Yeh K.Y. (1988) Colonic Proliferation is Increased in Senescent Rats. *Gastroenterology.* **95**(6): 1556-1563

Holt P.R. and Yeh K.Y. (1989) Small Intestinal Crypt Cell Proliferation Rates are Increased in Senescent Rats. *J Gerontol.* **44**(1): B9-14

Hooper L.V. and Gordon J.I. (2001) Commensal Host-Bacterial Relationships in the Gut. *Science.* **292**(5519): 1115-1118

Hooper L.V. and Macpherson A.J. (2010) Immune Adaptations that Maintain Homeostasis with the Intestinal Microbiota. *Nat Rev Immunol.* **10**(3): 159-169

Hou S.X., Zheng Z., Chen X. and Perrimon N. (2002) The Jak/STAT Pathway in Model Organisms: Emerging Roles in Cell Movement. *Dev Cell.* **3**(6): 765-778

Hwu P., Du M.X., Lapointe R., Do M., Taylor M.W. and Young H.A. (2000) Indoleamine 2,3-Dioxygenase Production by Human Dendritic Cells Results in the Inhibition of T Cell Proliferation. *J Immunol.* **164**(7): 3596-3599

Iliadi K.G., Knight D. and Boulianne G.L. (2012) Healthy Aging - Insights from *Drosophila*. *Front Physiol.* **3**:106

Ino K., Yoshida N., Kajiyama H., Shibata K., Yamamoto E., Kidokoro K., Takahashi N., Terauchi M., Nawa A., Nomura S., Nagasaka T., Takikawa O. and Kikkawa F. (2006) Indoleamine 2,3-Dioxygenase is a Novel Prognostic Indicator for Endometrial Cancer. *Br J Cancer.* **95**(11):1555-1561

Ismail M.Z., Hodges M.D., Boylan M., Achall R., Shirras A. and Broughton S.J. (2015) The *Drosophila* Insulin Receptor Independently Modulates Lifespan and Locomotor Senescence. *PLoS One.* **10**(5): e0125312

Itakura E., Huang R.R., Wen D.R., Paul E., Wünsch P.H. Cochran A.J. (2011) IL-10 Expression by Primary Tumor Cells Correlates with Melanoma Progression from Radial to Vertical Growth Phase and Development of Metastatic Competence. *Mod Pathol.* **24**(6): 801-809

Ito S., Ansari P., Sakatsume M., Dickensheets H., Vazquez N., Donnelly R.P., Larner A.C. and Finbloom D.S. (1999) Interleukin-10 Inhibits Expression of both Interferon Alpha- and Interferon Gamma-Induced Genes by Suppressing Tyrosine Phosphorylation of STAT1. *Blood.* **93**(5):1456-1463

James O.F.W. (1983) Gastrointestinal and Liver Function in Old Age. *Clin. Gastroenterol.* **12**: 671- 691

Jensen R.L., Pedersen K.S., Loeschcke V., Ingmer H. and Leisner J.J. (2007) Limitations in the use of *Drosophila melanogaster* as a Model Host for Gram-Positive Bacterial Infection. *Lett Appl Microbiol.* **44**(2): 218-223

Jiang H., Patel P.H., Kohlmaier A., Grenley M.O., McEwen D.G. and Edgar B.A. (2009) Cytokine/Jak/Stat Signaling Mediates Regeneration and Homeostasis in the *Drosophila* Midgut. *Cell* **137**(7): 1343-1355

Jiang H. and Edgar B.A. (2011) Intestinal Stem Cells in the Adult *Drosophila* Midgut. *Exp Cell Res.* **317**(19): 2780-2788

Johansson M.E., Phillipson M., Petersson J., Velcich A., Holm L. and Hansson G.C. (2008) The Inner of the Two Muc2 Mucin-Dependent Mucus Layers in Colon is Devoid of Bacteria. *Proc Natl Acad Sci U S A.* **105**(39): 15064-15069

Jones M.A. and Grotewiel M. (2011) *Drosophila* as a Model for Age-Related Impairment in Locomotor and Other Behaviors. *Exp Gerontol.* **46**(5): 320-325

Kabeya Y., Mizushima N., Ueno T., Yamamoto A., Kirisako T., Noda T., Kominami E., Ohsumi Y. and Yoshimori T. (2000) LC3, a Mammalian Homologue of Yeast Apg8p, is localized in Autophagosome Membranes after processing. *EMBO J.* **19**(21): 5720-5728

Kahsai L., Martin J.R. and Winther A.M. (2010) Neuropeptides in the *Drosophila* Central Complex in Modulation of Locomotor Behavior. *J Exp Biol.* **213**(Pt 13): 2256-2265

Kararli T.T. (1995) Comparison of the Gastrointestinal Anatomy, Physiology, and Biochemistry of Humans and Commonly Used Laboratory Animals. *Biopharm Drug Dispos.* **16**(5): 351-380

Kaur N., Chen C.C., Luther J. and Kao J.Y. (2011) Intestinal Dysbiosis in Inflammatory Bowel Disease. *Gut Microbes.* **2**(4): 211-216

Khush R.S., Leulier F. and Lemaitre B. (2001) *Drosophila* Immunity: Two Paths to NF-Kappa B. *Trends Immunol.* **22**(5): 260-264

Kierszenbaum A.L. and Tres L. (2015) *Histology and Cell Biology: An Introduction to Pathology.* Elsevier Health Sciences.

Kiger A.A., Jones D.L., Schulz C., Rogers M.B. and Fuller M.T. (2001) Stem Cell Self-Renewal Specified by JAK-STAT Activation in Response to a Support Cell Cue. *Science.* **294**(5551): 2542-2545

Kim T.H., Li F., Ferreiro-Neira I., Ho L.L., Luyten A., Nalapareddy K., Long H., Verzi M. and Shivdasani R.A. (2014) Broadly Permissive Intestinal Chromatin Underlies Lateral Inhibition and Cell Plasticity. *Nature.* **506**(7489): 511-515

Kirkwood T.B. (1977) Evolution of Ageing. *Nature.* **270**(5635): 301-304

Kirkwood T.B. and Holliday R. (1979) The Evolution of Ageing and Longevity. *Proc R Soc Lond B Biol Sci.* **205**(1161): 531-546

Kirkwood T.B. and Cremer T. (1982) Cytogerontology since 1881: A Reappraisal of August Weismann and a Review of Modern Progress. *Hum Genet.* **60**(2): 101-121

Kirkwood T.B.L. (2004) Intrinsic Ageing of Gut Epithelial Stem Cells. *Mechanisms of Ageing and Development.* **125**: 911-915

Kitajima S., Morimoto M., Sagara E., Shimizu C. and Ikeda Y. (2001) Dextran Sodium Sulfate-Induced Colitis in Germ-Free IQI/Jic Mice. *Exp Anim.* **50**(5): 387-395

Kleinzeller A., Douglas F.M., Benos D.J. and Peracchia C. (1999) *Gap Junctions: Molecular Basis of Cell Communication in Health and Disease: Molecular Basis of Cell Communication in Health and Disease* (Vol. 49). Academic Press.

Kobayashi M., Kweon M.N., Kuwata H., Schreiber R.D., Kiyono H., Takeda K. and Akira S. (2003) Toll-Like Receptor-Dependent Production of IL-12p40 causes Chronic Enterocolitis in Myeloid Cell-Specific Stat3-Deficient Mice. *J Clin Invest.* **111**(9): 1297-1308

Kolling G., Wu M. and Guerrant R.L. (2012) Enteric Pathogens Through Life Stages. *Front Cell Infect Microbiol.* **2**: 114

Kojima Y., Sakuma H., Izumi R., Nakagawara G., Miyazaki I. and Yoshimura H. (1981) A Case of Granuloma of the Ascending Colon due to Penetration of *Trichuris trichiura*. *Gastroenterol Jpn.* **16**(2): 193-196

Kostic A.D., Howitt M.R. and Garrett W.S. (2013) Exploring Host-Microbiota Interactions in Animal Models and Humans. *Genes Dev.* **27**(7): 701-718

Krebs D.L. and Hilton D.J. (2001) SOCS Proteins: Negative Regulators of Cytokine Signaling. *Stem Cells.* **19**(5): 378-387

Kucharzik T., Stoll R., Lügering N. and Domschke W. (1995) Circulating Antiinflammatory Cytokine IL-10 in Patients with Inflammatory Bowel Disease (IBD). *Clin Exp Immunol.* **100**(3): 452-456

Kühn R., Löhler J., Rennick D., Rajewsky K. and Müller W. (1993) Interleukin-10-Deficient Mice Develop Chronic Enterocolitis. *Cell.* **75**(2): 263-274

Larsen L. and Röpke C. (2002) Suppressors of Cytokine Signalling: SOCS. *APMIS.* **110**(12): 833-844

Lee K.A., Kim S.H., Kim E.K., Ha E.M., You H., Kim B., Kim M.J., Kwon Y. and Ryu J.H. (2013) Bacterial-Derived Uracil as a Modulator of Mucosal Immunity and Gut-Microbe Homeostasis in *Drosophila*. *Cell.* **153**(4): 797–811

Lee K.H., Moon K.J., Kim H.S., Yoo B.C., Park S., Lee H., Kwon S., Lee E.S. and Yoon S. (2008) Increased Cytoplasmic Levels of CIS, SOCS1, SOCS2, or SOCS3 are Required for Nuclear Translocation. *FEBS Lett.* **582**(15): 2319-2324

Lee W.C., Beebe K., Sudmeier L. and Micchelli C.A. (2009) Adenomatous Polyposis Coli Regulates *Drosophila* Intestinal Stem Cell Proliferation. *Development.* **136**(13): 2255-2264

Lehane M.J. (1997) Peritrophic Matrix Structure and Function. *Annu Rev Entomol.* **42**: 525-550

Lemaitre B. and Hoffmann J. (2007) The Host Defense of *Drosophila melanogaster*. *Annu Rev Immunol.* **25**: 697-743

Levine B., Mizushima N. and Virgin H.W. (2011) Autophagy in Immunity and Inflammation. *Nature.* **469**(7330): 323-335

Li W., Dowd S.E., Scurlock B., Acosta-Martinez V. and Lyte M. (2009) Memory and Learning Behavior in mice is Temporally Associated with Diet-Induced Alterations in Gut Bacteria. *Physiol Behav.* **96**(4-5): 557-567

Li Y., de Haar C., Chen M., Deuring J., Gerrits M.M., Smits R., Xia B., Kuipers E.J. and van der Woude C.J. (2010) Disease-Related Expression of the IL6/STAT3/SOCS3 Signalling Pathway in Ulcerative Colitis and Ulcerative Colitis-Related Carcinogenesis. *Gut.* **59**(2):227-235

Licato L.L., Keku T.O., Wurzelmann J.I., Murray S.C., Woosley J.T., Sandler R.S. and Brenner D.A. (1997) *In vivo* Activation of Mitogen-Activated Protein Kinases in Rat Intestinal Neoplasia. *Gastroenterology.* **113**(5): 1589-1598

Liehl P., Blight M., Vodovar N., Boccard F. and Lemaitre B. (2006) Prevalence of Local Immune Response against Oral Infection in a *Drosophila*/Pseudomonas Infection Model. *PLoS Pathog.* **2**(6): e56

Lin G., Xu N. and Xi R. (2010) Paracrine Unpaired Signaling Through the JAK/STAT Pathway Controls Self-Renewal and Lineage Differentiation of *Drosophila* Intestinal Stem Cells. *J Mol Cell Biol.* **2**(1):37-49

Lin J. and Hackam D.J. (2011) Worms, Flies and Four-Legged Friends: The Applicability of Biological Models to the Understanding of Intestinal Inflammatory Diseases. *Dis Model Mech.* **4**(4): 447-456

Lin Q., Lai R., Chirieac L.R., Li C., Thomazy V.A., Grammatikakis I., Rassidakis G.Z., Zhang W., Fujio Y., Kunisada K., Hamilton S.R. and Amin H.M. (2005) Constitutive Activation of JAK3/STAT3 in Colon Carcinoma Tumors and Cell Lines: Inhibition of JAK3/STAT3 Signaling Induces Apoptosis and Cell Cycle Arrest of Colon Carcinoma Cells. *Am J Pathol.* **167**(4): 969-980

Lin Y.J., Seroude L. and Benzer S. (1998) Extended Life-Span and Stress Resistance in the *Drosophila* Mutant *methuselah*. *Science.* **282**(5390): 943-946

Linderman J.A., Chambers M.C., Gupta A.S. and Schneider D.S. (2012) Infection-Related Declines in Chill Coma Recovery and Negative Geotaxis in *Drosophila melanogaster. PLoS One.* **7**(9): e41907

Liu C., Haynes P.R., Donelson N.C., Aharon S. and Griffith L.C. (2015) Sleep in Populations of *Drosophila melanogaster. eneuro.* **2**(4): ENEURO-0071

Liu Z., Gan L., Zhou Z., Jin W. and Sun C. (2015) SOCS3 Promotes Inflammation and Apoptosis via Inhibiting JAK2/STAT3 Signaling Pathway in 3T3-L1 Adipocyte. *Immunobiology.* **220**(8): 947-953

Loeffler M. and Potten C.S. (1997). Stem Cells and Cellular Pedigrees- A Conceptual Introduction. Stem Cells. *San Diego: Academic Press.* 1-27

Lucchetta E.M. and Ohlstein B. (2012) The *Drosophila* Midgut: A Model for Stem Cell Driven Tissue Regeneration. *Wiley Interdiscip Rev Dev Biol.* **1**(5): 781-788

Luckinbill L.S. (1998) Selection for Longevity Confers Resistance to Low-Temperature Stress in *Drosophila melanogaster. J. Gerontol. A Biol. Sci. Med. Sci.* **53**: B147–B153

Lyte M., Li W., Opitz N., Gaykema R.P. and Goehler L.E. (2006) Induction of Anxiety-Like Behavior in Mice during the Initial Stages of Infection with the agent of Murine Colonic Hyperplasia *Citrobacter rodentium. Physiol Behav.* **89**(3): 350-357

Madara J.L. (1982) Cup Cells: Structure and Distribution of a Unique Class of Epithelial Cells in Guinea Pig, Rabbit, and Monkey Small Intestine. *Gastroenterology.* **83**(5): 981-994

Magwere T., Chapman T. and Partridge L. (2004) Sex Differences in the Effect of Dietary Restriction on Life Span and Mortality Rates in Female and Male *Drosophila melanogaster. J Gerontol A Biol Sci Med Sci.* **59**(1): 3-9

Magwire M.M., Yamamoto A., Carbone M.A., Roshina N.V., Symonenko A.V., Pasyukova E.G., Morozova T.V. and Mackay T.F. (2010) Quantitative and Molecular Genetic Analyses of Mutations Increasing *Drosophila* Life Span. *PLoS Genet.* **6**(7): e1001037

Majumdar A.P. (2003) Regulation of Gastrointestinal Mucosal Growth During Aging. *J Physiol Pharmacol.* **54**(Suppl 4): 143-154

Marianes A. and Spradling A.C. (2013) Physiological and Stem Cell Compartmentalization within the *Drosophila* Midgut. *Elife.* 2: e00886

Marshman E., Booth C. and Potten C.S. (2002) The Intestinal Epithelial Stem Cell. *BioEssays.* **24**: 91-98

Martin I., Jones M.A. and Grotewiel M. (2009a) Manipulation of Sod1 Expression Ubiquitously, but not in the Nervous System or Muscle, Impacts Age-Related Parameters in *Drosophila. FEBS Lett.* **583**(13): 2308-2314

Martin, I., Jones, M.A., Rhodenizer, D., Zheng, J., Warrick, J.M., Seroude, L. and Grotewiel, M. (2009b) Sod2 Knockdown in the Musculature has Whole-Organism Consequences in *Drosophila. Free Radic. Biol. Med.* **47**: 803–813

Martin J.R., Ernst R. and Heisenberg M. (1998) Mushroom Bodies Suppress Locomotor Activity in *Drosophila melanogaster. Learn Mem.* **5**(1-2): 179-191

Martin J.R., Ernst R. and Heisenberg M. (1999) Temporal Pattern of Locomotor Activity in *Drosophila melanogaster. J Comp Physiol A.* **184**(1): 73-84

Martin J.R. (2004) A Portrait of Locomotor Behaviour in *Drosophila* Determined by a Video-Tracking Paradigm. *Behav Processes.* **67**(2): 207-219

Martin K., Potten C.S., Roberts S.A. and Kirkwood T.B. (1998) Altered Stem Cell Regeneration in Irradiated Intestinal Crypts of Senescent Mice. *J Cell Sci.* **111**(16): 2297-2303

Martinez-Medina M., Aldeguer X., Gonzalez-Huix F., Acero D. and Garcia-Gil L.J. (2006) Abnormal Microbiota Composition in the Ileocolonic Mucosa of Crohn's Disease Patients as Revealed by Polymerase Chain Reaction-Denaturing Gradient Gel Electrophoresis. *Inflamm Bowel Dis.* **12**(12): 1136-1145

Mayer E.A., Tillisch K. and Gupta A. (2015) Gut/Brain Axis and the Microbiota. *J Clin Invest.* **125**(3): 926-938

McGuire S.E., Le P.T., Osborn A.J., Matsumoto K. and Davis R.L. (2003) Spatiotemporal Rescue of Memory Dysfunction in *Drosophila. Science.* **302**(5651): 1765-1768

Meager A. and Wadhwa M. (2013) Interleukins. *eLS.*

Medzhitov R., Preston-Hurlburt P., Kopp E., Stadlen A., Chen C., Ghosh S. and Janeway C.A. Jr. (1998) MyD88 is an Adaptor Protein in the hToll/IL-1 Receptor Family Signaling Pathways. *Mol Cell.* **2**(2): 253-258

Mestas J. and Hughes C.C. (2004) Of Mice and not Men: Differences between Mouse and Human Immunology. *J Immunol.* **172**(5): 2731-2738

Metghalchi S., Ponnuswamy P., Simon T., Haddad Y., Laurans L., Clément M., Dalloz M., Romain M., Esposito B., Koropoulis V., Lamas B., Paul J.L., Cottin Y., Kotti S., Bruneval P., Callebert J., den Ruijter H., Launay J.M., Danchin N., Sokol H., Tedgui A., Taleb S. and Mallat Z. (2015) Indoleamine 2,3-Dioxygenase Fine-Tunes Immune Homeostasis in Atherosclerosis and Colitis through Repression of Interleukin-10 Production. *Cell Metab.* **22**(3): 460-471

Micchelli C.A. and Perrimon N. (2006) Evidence that Stem Cells Reside in the Adult *Drosophila* Midgut Epithelium. *Nature.* **439**(7075): 475-479

Michael E. and Hodges R.D. (1973) Histochemical Changes in the Fowl Small Intestine Associated with Enhanced Absorption after Feed Restriction. *Histochemie.* **36**(1): 39-49

Michaylira C.Z., Simmons J.G., Ramocki N.M., Scull B.P., McNaughton K.K., Fuller C.R. and Lund P.K. (2006) Suppressor of Cytokine Signaling-2 Limits Intestinal Growth and Enterotrophic Actions of IGF-I *in vivo*. *Am J Physiol Gastrointest Liver Physiol.* **291**(3): G472-481

Miller M.E., Michaylira C.Z., Simmons J.G., Ney D.M., Dahly E.M., Heath J.K. and Lund P.K. (2004) Suppressor of Cytokine Signaling-2: A Growth Hormone-Inducible Inhibitor of Intestinal Epithelial Cell Proliferation. *Gastroenterology.* **127**(2): 570-581

Miquel J., Lundgren P.R., Bensch K.G. and Atlan H. (1976) Effects of Temperature on the Life Span, Vitality and Fine Structure of *Drosophila melanogaster. Mech Ageing Dev.* **5**(5): 347-370

Mitsuyama K., Matsumoto S., Rose-John S., Suzuki A., Hara T., Tomiyasu N., Handa K., Tsuruta O., Funabashi H., Scheller J., Toyonaga A. and Sata M. (2006) STAT3 Activation via Interleukin 6 Trans-Signalling contributes to Ileitis in SAMP1/Yit mice. *Gut.* **55**(9): 1263-1269

Mocellin S., Marincola F.M. and Young H.A. (2005) Interleukin-10 and the Immune Response Against Cancer: A Counterpoint. *J Leukoc Biol.* **78**(5): 1043-1051

Mockett R.J., Orr W.C., Rahmandar J.J., Sohal B.H. and Sohal R.S. (2001) Antioxidant Status and Stress Resistance in Long- and Short-Lived Lines of *Drosophila melanogaster. Exp. Gerontol.* **36**: 441–463

Montgomery R.D., Haeney M.R., Ross I.N., Sammons H.G., Barford A.V., Balakrishnan S., Mayer P.P., Culank L.S., Field J. and Gosling P. (1978) The Ageing Gut: A Study of Intestinal Absorption in Relation to Nutrition in the Elderly. *Q J Med.* **47**(186): 197-24

Moore R.J., Owens D.M., Stamp G., Arnott C., Burke F., East N., Holdsworth H., Turner L., Rollins B., Pasparakis M., Kollias G. and Balkwill F. (1999) Mice Deficient in Tumor Necrosis Factor-Alpha are Resistant to Skin Carcinogenesis. *Nat Med.* **5**(7): 828-831

Morgan N.S., Heintzelman M.B. and Mooseker M.S. (1995) Characterization of Myosin-IA and Myosin-IB, Two Unconventional Myosins Associated with the *Drosophila* Brush Border Cytoskeleton. *Dev Biol.* **172**(1): 51-71

Morris K.V. and Mattick J.S. (2014) The Rise of Regulatory RNA. *Nat Rev Genet.* **15**(6): 423-437

Mosmann T.R., Cherwinski H., Bond M.W., Giedlin M.A. and Coffman R.L. (1986) Two Types of Murine Helper T Cell Clone. I. Definition According to Profiles of Lymphokine Activities and Secreted Proteins. *J Immunol.* **136**(7): 2348-2357

Mouse Genome Sequencing Consortium, Waterston R.H., Lindblad-Toh K., Birney E., Rogers J., Abril J.F., Agarwal P., …et al. (2002) Initial Sequencing and Comparative Analysis of the Mouse Genome. *Nature.* **420**(6915): 520-562

Mow W.S., Vasiliauskas E.A., Lin Y.C., Fleshner P.R., Papadakis K.A., Taylor K.D., Landers C.J., Abreu-Martin M.T., Rotter J.I., Yang H. and Targan S.R. (2004) Association of Antibody Responses to Microbial Antigens and Complications of Small Bowel Crohn's Disease. *Gastroenterology.* **126**(2): 414-424

Muller A.J., DuHadaway J.B., Donover P.S., Sutanto-Ward E. and Prendergast G.C. (2005) Inhibition of Indoleamine 2,3-Dioxygenase, an Immunoregulatory Target of the Cancer Suppression Gene Bin1, Potentiates Cancer Chemotherapy. *Nat Med. 11*(3): 312-319

Munn D.H., Zhou M., Attwood J.T., Bondarev I., Conway S.J., Marshall B., Brown C. and Mellor A.L. (1998) Prevention of Allogeneic Fetal Rejection by Tryptophan Catabolism. *Science.* **281**(5380): 1191-1193

Munn D.H., Shafizadeh E., Attwood J.T., Bondarev I., Pashine A. and Mellor A.L. (1999) Inhibition of T Cell Proliferation by Macrophage Tryptophan Catabolism. *J Exp Med.* **189**(9): 1363-1372

Murray P.J. (2006) Understanding and Exploiting the Endogenous Interleukin-10/STAT3-Mediated Anti-Inflammatory Response. *Curr Opin Pharmacol.* **6**(4): 379-386

Myint A.M. and Kim Y.K. (2003) Cytokine-Serotonin Interaction through IDO: A Neurodegeneration Hypothesis of Depression. *Med Hypotheses.* **61**(5-6): 519-525

Nakagawa R., Naka T., Tsutsui H., Fujimoto M., Kimura A., Abe T., Seki E., Sato S., Takeuchi O., Takeda K., Akira S., Yamanishi K., Kawase I., Nakanishi K. and Kishimoto T. (2002) SOCS-1 Participates in Negative Regulation of LPS Responses. *Immunity.* **17**(5): 677-687

Nässel D.R. and Winther A.M. (2010) *Drosophila* Neuropeptides in Regulation of Physiology and Behavior. *Prog Neurobiol.* **92**(1): 42-104

Natividad J.M. and Verdu E.F. (2013) Modulation of Intestinal Barrier by Intestinal Microbiota: Pathological and Therapeutic Implications. *Pharmacol Res.* **69**(1): 42-51

Navrotskaya V.V., Oxenkrug G., Vorobyova L.I. and Summergrad P. (2012) Berberine Prolongs Life Span and Stimulates Locomotor Activity of *Drosophila melanogaster. Am J Plant Sci.* **3**(7A): 1037-1040

Nehme N.T., Liégeois S., Kele B., Giammarinaro P., Pradel E., Hoffmann J.A., Ewbank J.J. and Ferrandon D. (2007) A Model of Bacterial Intestinal Infections in *Drosophila melanogaster. PLoS Pathog.* **3**(11): e173

Neutra M.R. (1998) Current Concepts in Mucosal Immunity. V Role of M Cells in Transepithelial Transport of Antigens and Pathogens to the Mucosal Immune System. *Am J Physiol.* **274**(5 Pt 1): G785-791

Nguyen T.L., Vieira-Silva S., Liston A. and Raes J. (2015) How Informative is the Mouse for Human Gut Microbiota Research? *Dis Model Mech.* **8**(1): 1-16

Nicolas C.S., Amici M., Bortolotto Z.A., Doherty A., Csaba Z., Fafouri A., Dournaud P., Gressens P., Collingridge G.L. and Peineau S. (2013) The Role of JAK-STAT Signaling within the CNS. *JAKSTAT.* **2**(1): e22925

Nicholson S.E., Willson T.A., Farley A., Starr R., Zhang J.G., Baca M., Alexander W.S., Metcalf D., Hilton D.J. and Nicola N.A. (1999) Mutational Analyses of the SOCS Proteins Suggest a Dual Domain Requirement but Distinct Mechanisms for Inhibition of LIF and IL-6 Signal Transduction. *EMBO J.* **18**(2): 375-385

Niemand C., Nimmesgern A., Haan S., Fischer P., Schaper F., Rossaint R., Heinrich P.C. and Müller-Newen G. (2003) Activation of STAT3 by IL-6 and IL-10 in Primary Human Macrophages is Differentially Modulated by Suppressor of Cytokine Signaling 3. *J Immunol.* **170**(6): 3263-3272

O'Mahony S.M., Marchesi J.R., Scully P., Codling C., Ceolho A.M., Quigley E.M., Cryan J.F. and Dinan T.G. (2009) Early Life Stress Alters Behavior, Immunity, and Microbiota in Rats: Implications for Irritable Bowel Syndrome and Psychiatric Illnesses. *Biol. Psychiatry.* **65**(3): 263-267

Oba T., Yasukawa H., Sasaki K.I., Futamata N., Mawatari K., Kyougoku S., Nagata T., Hoshijima M., Knowlton K. and Imaizumi T. (2009) Cardiac-Specific Deletion of SOCS3 Prevented Myocardial Apoptosis after Acute Myocardial Infarction Through Inhibiting Mitochondrial Damage. *Journal of Cardiac Failure.* **15**(7): S151

Obasse I.C. (2012) Disruption of Intestinal Stem Cell Turnover and Consequences on the Intestinal Epithelial Barrier. *Masters Project Dissertation.* 1-54

Oft M. (2014) IL-10: Master Switch from Tumor-Promoting Inflammation to Antitumor Immunity. *Cancer Immunol Res.* **2**(3): 194-199

Ogata H., Kobayashi T., Chinen T., Takaki H., Sanada T., Minoda Y., Koga K., Takaesu G., Maehara Y., Iida M. and Yoshimura A. (2006) Deletion of the SOCS3 Gene in Liver Parenchymal Cells Promotes Hepatitis-Induced Hepatocarcinogenesis. *Gastroenterology.* **131**(1): 179-193

Ogawa K., Hara T., Shimizu M., Ninomiya S., Nagano J., Sakai H., Hoshi M., Ito H., Tsurumi H., Saito K., Seishima M., Tanaka T. and Moriwaki H. (2012) Suppression of Azoxymethane-Induced Colonic Preneoplastic Lesions in Rats by 1-Methyltryptophan, an Inhibitor of Indoleamine 2,3-Dioxygenase. *Cancer Sci.* **103**(5): 951-958

Ohlstein B. and Spradling A. (2006) The Adult *Drosophila* Posterior Midgut is Maintained by Pluripotent Stem Cells. *Nature* **439**(7075): 470-474

Ohlstein B. and Spradling A. (2007) Multipotent *Drosophila* Intestinal Stem Cells Specify Daughter Cell Fates By Differential Notch Signaling. *Science.* **315**(5814): 988-992

Oikonomopoulou K., Brinc D., Hadjisavvas A., Christofi G., Kyriacou K. and Diamandis E.P. (2014) The Bifacial Role of Helminths in Cancer: Involvement of Immune and Non-Immune Mechanisms. *Crit Rev Clin Lab Sci.* **51**(3): 138-148

Okamoto A., Nikaido T., Ochiai K., Takakura S., Saito M., Aoki Y., Ishii N., Yanaihara N., Yamada K., Takikawa O., Kawaguchi R., Isonishi S., Tanaka T. and Urashima M. (2005) Indoleamine 2,3-Dioxygenase Serves as a Marker of Poor Prognosis in Gene Expression Profiles of Serous Ovarian Cancer Cells. *Clin Cancer Res.* **11**(16):6030-6039

Orabona C., Belladonna M.L., Vacca C., Bianchi R., Fallarino F., Volpi C., Gizzi S., Fioretti M.C., Grohmann U. and Puccetti P. (2005) Cutting Edge: Silencing Suppressor of Cytokine Signaling 3 Expression in Dendritic Cells turns CD28-Ig from Immune Adjuvant to Suppressant. *J Immunol.* **174**(11): 6582-6586

Orabona C., Pallotta M.T., Volpi C., Fallarino F., Vacca C., Bianchi R., Belladonna M.L., Fioretti M.C., Grohmann U. and Puccetti P. (2008) SOCS3 Drives Proteasomal Degradation of Indoleamine 2,3-Dioxygenase (IDO) and Antagonizes IDO-Dependent Tolerogenesis. *Proc. Natl. Acad. Sci. USA.* **105**(52): 20828-20833

Orban P.C., Chui D. and Marth J.D. (1992) Tissue- and Site-Specific DNA Recombination in Transgenic Mice. *Proc Natl Acad Sci U S A.* **89**(15): 6861-6865

Ortega M.A., Nunez M.C., Suarez M.D., Gil A. Sanchez-Pozo A. (1996) Age-Related Response of the Small Intestine to Severe Starvation and Refeeding in Rats. *Ann Nutr Metab.* **40**: 351-358

Otte J.M., Cario E. and Podolsky D.K. (2004) Mechanisms of Cross Hyporesponsiveness to Toll-Like Receptor Bacterial Ligands in Intestinal Epithelial Cells. *Gastroenterology.* **126**(4): 1054-1070

Oxenkrug G.F. (2010) The Extended Life Span of *Drosophila melanogaster* Eye-Color (White and Vermilion) Mutants with Impaired Formation of Kynurenine. *J Neural Transm.* **117**: 23-26

Oxenkrug G.F., Navrotskaya V., Voroboyva L. Summergrad P. (2011) Extension of Life Span of *Drosophila melanogaster* by the Inhibitors of Tryptophan-Kynurenine Metabolism. *Fly (Austin).* **5**(4): 307-309

Ozaki Y., Edelstein M.P. and Duch D.S. (1987) The Actions of Interferon and Antiinflammatory Agents on Induction of Indoleamine 2, 3-Dioxygenase in Human Peripheral Blood Monocytes. *Biochemical and Biophysical Research Communications.* **144**(3): 1147-1153

Pageot L.P., Perreault N., Basora N., Francoeur C., Magny P. and Beaulieu J.F. (2000) Human Cell Models to Study Small Intestinal Functions: Recapitulation of the Crypt-Villus Axis. *Microsc Res Tech.* **49**(4): 394-406

Paredes J.C., Welchman D.P., Poidevin M. and Lemaitre B. (2011) Negative Regulation by Amidase PGRPs Shapes the *Drosophila* Antibacterial Response and Protects the Fly from Innocuous Infection. *Immunity.* **35**(5): 770-779

Partridge L., Green A. and Fowler K. (1987) Effects of Egg-Production and of Exposure to Males on Female Survival in *Drosophila melanogaster*. *J. Insect Physiol.* **33**: 745–749

Patel P.H. and Edgar B.A. (2014) Tissue Design: How *Drosophila* Tumors Remodel Their Neighborhood. *Semin Cell Dev Biol.* **28**: 86-95

Perreault N. and Beaulieu J.F. (1996) Use of the Dissociating Enzyme Thermolysin to Generate Viable Human Normal Intestinal Epithelial Cell Cultures. *Exp Cell Res.* **224**(2): 354-364

Piessevaux J., Lavens D., Peelman F. and Tavernier J. (2008) The Many Faces of the SOCS Box. *Cytokine Growth Factor Rev.* **19**(5-6): 371-381

Pinto M., Appay M.D., Simonassmann P., Chevalier G., Dracopoli N., Fogh J. and Zweibaum A. (1982) Enterocytic Differentiation of Cultured Human-Colon Cancer-Cells by Replacement of Glucose by Galactose in the Medium. *Biology of the Cell.* **44**(2): 193-196

Pinto M. (1983) Enterocyte-Like Differentiation and Polarization of the Human Colon Carcinoma Cell Line Caco-2 in Culture. *Biol. Cell.* **47**: 323-330

Potten C.S. and Loeffler M. (1990) Stem Cells: Attributes, Cycles, Spirals, Pitfalls and Uncertainties. Lessons for and from the Crypt. *Development.* **110**(4): 1001-1020

Potten C.S. (1991) Regeneration in Epithelial Proliferative Units as Exemplified by Small Intestinal Crypts. *Ciba Found Symp.* **160**: 54-71

Potten C.S. (1998) Stem Cells in Gastrointestinal Epithelium: Numbers, Characteristics and Death. *Philos Trans R Soc Lond B Biol Sci.* **353**(1370): 821-830

Potten C.S., Gandara R., Mahida Y.R., Loeffler M. and Wright N.A. (2009) The Stem Cells of Small Intestinal Crypts: Where are they? *Cell Prolif.* **42**(6): 731-750

Prideaux L., Kang S., Wagner J., Buckley M., Mahar J.E., De Cruz P., Wen Z., Chen L., Xia B., van Langenberg D.R., Lockett T., Ng S.C., Sung J.J., Desmond P., McSweeney C., Morrison M., Kirkwood C.D. and Kamm M.A. (2013) Impact of Ethnicity, Geography, and Disease on the Microbiota in Health and Inflammatory Bowel Disease. *Inflamm Bowel Dis.* **19**(13): 2906-2918

Prowse N. and Partridge L. (1997) The Effects of Reproduction on Longevity and Fertility in Male *Drosophila melanogaster*. *Journal of Insect Physiology.* **43**(6): 501-512

Quante M. and Wang T.C. (2008) Inflammation and Stem Cells in Gastrointestinal Carcinogenesis. *Physiology.* **23**: 350-359

Quaroni A., Wands J., Trelstad R.L. and Isselbacher K.J. (1979) Epithelioid Cell Cultures from Rat Small Intestine. Characterization by Morphologic and Immunologic Criteria. *The Journal of Cell Biology.* **80**(2): 248-265

Radtke F. and Clevers H. (2005) Self-Renewal and Cancer of the Gut: Two Sides of a Coin. *Science.* **307**(5717): 1904-1909

Rajan A. and Perrimon N. (2012) *Drosophila* Cytokine Unpaired 2 Regulates Physiological Homeostasis by Remotely Controlling Insulin Secretion. *Cell.* **151**(1): 123-137

Rajasekaran A.K., Hojo M., Huima T. and Rodriguez-Boulan E. (1996) Catenins and Zonula Occludens-1 Form a Complex During Early Stages in the Assembly of Tight Junctions. *J Cell Biol.* **132**(3): 451-463

Rakoff-Nahoum S., Paglino J., Eslami-Varzaneh F., Edberg S. and Medzhitov R. (2004) Recognition of Commensal Microflora by Toll-Like Receptors is Required for Intestinal Homeostasis. *Cell.* **118**(2): 229-241

Rakoff-Nahoum S. (2006) Why Cancer and Inflammation? *Yale J Biol Med.* **79**: 123-130

Rakoff-Nahoum S. and Medzhitov R. (2007) Regulation of Spontaneous Intestinal Tumorigenesis Through the Adaptor Protein MyD88. *Science.* **317**(5834): 124-127

Rakoff-Nahoum S. and Medzhitov R. (2009) Toll-Like Receptors and Cancer. *Nat Rev Cancer.* **9**(1): 57-63

Rawlings J.S., Rennebeck G., Harrison S.M., Xi R. and Harrison D.A. (2004) Two *Drosophila* Suppressors of Cytokine Signaling (SOCS) Differentially Regulate JAK and EGFR Pathway Activities. *BMC Cell Biol.* **5**(1): 38

Rera M., Bahadorani S., Cho J., Koehler C.L., Ulgherait M., Hur J.H., Ansari W.S., Lo T. Jr., Jones D.L. and Walker D.W. (2011) Modulation of Longevity and Tissue Homeostasis by the *Drosophila* PGC-1 Homolog. *Cell Metab.* **14**(5):623-634

Rhodenizer D., Martin I., Bhandari P., Pletcher S.D. and Grotewiel M. (2008) Genetic and Environmental Factors Impact Age-Related Impairment of Negative Geotaxis in *Drosophila* by Altering Age-Dependent Climbing Speed. *Exp Gerontol.* **43**(8): 739-748

Richard M., Grencis R.K., Humphreys N.E., Renauld J.C. and Van Snick J. (2000) Anti-IL-9 Vaccination Prevents Worm Expulsion and Blood Eosinophilia in *Trichuris muris*-Infected Mice. *Proc Natl Acad Sci U S A.* **97**(2): 767-772

Rigby R.J., Simmons J.G., Greenhalgh C.J., Alexander W.S. and Lund P.K. (2007) Suppressor of Cytokine Signaling 3 (SOCS3) Limits Damage-Induced Crypt Hyper-Proliferation and Inflammation-Associated Tumorigenesis in the Colon. *Oncogene* **26**: 4833-4841

Rion S. and Kawecki T.J. (2007) Evolutionary Biology of Starvation Resistance: What we have learned from *Drosophila*. *J Evol Biol.* **20**(5): 1655-1664

Roberts A.W., Robb L., Rakar S., Hartley L., Cluse L., Nicola N.A., Metcalf D., Hilton D.J. and Alexander W.S. (2001) Placental Defects and Embryonic Lethality in Mice Lacking Suppressor of Cytokine Signaling 3. *Proc Natl Acad Sci U S A.* **98**(16): 9324-9329

Rogler G. and Andus T. (1998) Cytokines in Inflammatory Bowel Disease. *World J Surg.* **22**(4): 382-389

Royet J. (2011) Epithelial Homeostasis and the Underlying Molecular Mechanisms in the Gut of the Insect Model *Drosophila melanogaster*. *Cell Mol Life Sci.* **68**(22): 3651-3660

Rousset M., Dussaulx E., Chevalier G. and Zweibaum A. (1978) Expression Phénotypique des Antigènes Coliques Polymorphes (WZ) dans les Adénocarcinomes du Côlon Humain. *CR Acad. Sci.(Paris).* **286**: 659-662

Rudolph K.L. ed. (2010) *Molecular Mechanisms of Adult Stem Cell Aging* (Vol. 1). Karger Medical and Scientific Publishers

Ryu J.H., Kim S.H., Lee H.Y., Bai J.Y., Nam Y.D., Bae J.W., Lee D.G., Shin S.C., Ha E.M. and Lee W.J. (2008) Innate Immune Homeostasis by the Homeobox Gene Caudal and Commensal-Gut Mutualism in *Drosophila*. *Science.* **319**(5864): 777-782

Ryu J.H., Ha E.M. and Lee W.J. (2010) Innate Immunity and Gut-Microbe Mutualism in *Drosophila*. *Dev Comp Immunol.* **34**(4): 369-376

Saffrey M.J. (2013) Cellular Changes in the Enteric Nervous System during Ageing. *Dev. Biol.* **382**(1): 344-355

Salles N. (2007) Basic Mechanisms of the Aging Gastrointestinal Tract. *Dig Dis.* **25**(2): 112-117

Salmon A.B., Marx D.B. and Harshman L.G. (2001) A Cost of Reproduction in *Drosophila melanogaster*: Stress Susceptibility. *Evolution.* **55**: 1600–1608

Salomon R.N. and Jackson F.R. (2008) Tumors of Testis and Midgut in Aging Flies. *Fly* **2**(6): 265-268

Sarafian T.A., Montes C., Imura T., Qi J., Coppola G., Geschwind D.H. and Sofroniew M.V. (2010) Disruption of Astrocyte STAT3 Signaling Decreases Mitochondrial Function and Increases Oxidative Stress *in vitro*. *PLoS One.* **5**(3):e9532

Sasaki A., Yasukawa H., Suzuki A., Kamizono S., Syoda T., Kinjyo I., Sasaki M., Johnston J.A. and Yoshimura A. (1999) Cytokine-Inducible SH2 Protein-3 (CIS3/SOCS3) Inhibits Janus Tyrosine Kinase by Binding through the N-Terminal Kinase Inhibitory Region as well as SH2 Domain. *Genes Cells.* **4**(6): 339-351

Schmidt G.H., Winton D.J. and Ponder B.A. (1988) Development of the Pattern of Cell Renewal in the Crypt-Villus Unit of Chimaeric Mouse Small Intestine. *Development* **103**(4): 785-790

Scholtens P.A., Oozeer R., Martin R., Amor K.B. and Knol J. (2012) The Early Settlers: Intestinal Microbiology in Early Life. *Annu Rev Food Sci Technol.* **3**: 425-447

Sekirov I., Russell S.L., Antunes L.C. and Finlay B.B. (2010) Gut Microbiota in Health and Disease. *Physiol Rev.* **90**(3): 859-904

Sellon R.K., Tonkonogy S., Schultz M., Dieleman L.A., Grenther W., Balish E., Rennick D.M. and Sartor R.B. (1998) Resident Enteric Bacteria are Necessary for Development of Spontaneous Colitis and Immune System Activation in Interleukin-10-Deficient Mice. *Infect Immun.* **66**(11): 5224-5231

Seya T. and Miyake K. (2009) Toll-Like Receptors. *eLS.*

Shanbhag S. and Tripathi S. (2009) Epithelial Ultrastructure and Cellular Mechanisms of Acid and Base Transport in the *Drosophila* Midgut. *J Exp Biol.* **212**: 1731-1744

Sharon G., Segal D., Ringo J.M., Hefetz A., Zilber-Rosenberg I. and Rosenberg E. (2010) Commensal Bacteria play a role in Mating Preference of *Drosophila melanogaster. Proc Natl Acad Sci U S A.* **107**(46): 20051-20056

Shaw D., Gohil K. and Basson M.D. (2012) Intestinal Mucosal Atrophy and Adaptation. *World J Gastroenterol.* **18**(44): 6357-6375

Shaw R.L., Kohlmaier A., Polesello C., Veelken C., Edgar B.A. and Tapon N. (2010) The Hippo Pathway Regulates Intestinal Stem Cell Proliferation During *Drosophila* Adult Midgut Regeneration. *Development.* **137**(24): 4147-4158

Simon A.R., Rai U., Fanburg B.L. and Cochran B.H. (1998) Activation of the JAK-STAT Pathway by Reactive Oxygen Species. *Am J Physiol.* **275**(6 Pt 1): C1640-1652

Sitko J.C., Yeh B., Kim M., Zhou H., Takaesu G., Yoshimura A., McBride W.H., Jewett A., Jamieson C.A. and Cacalano N.A. (2008) SOCS3 Regulates p21 Expression and Cell Cycle Arrest in response to DNA Damage. Cell Signal. 20(12): 2221-2230

Siviter R.J., Coast G.M., Winther A.M., Nachman R.J., Taylor C.A., Shirras A.D., Coates D., Isaac R.E. and Nässel D.R. (2000) Expression and Functional Characterization of a *Drosophila* Neuropeptide Precursor with Homology to Mammalian Preprotachykinin A. *J Biol Chem.* **275**(30): 23273-23280

Slack C., Werz C., Wieser D., Alic N., Foley A., Stocker H., Withers D.J., Thornton J.M., Hafen E. and Partridge L. (2010) Regulation of Lifespan, Metabolism, and Stress Responses by the *Drosophila* SH2B Protein, Lnk. *PLoS Genet.* **6**(3): e1000881

Song J., Wolf S.E., Wu X.W., Finnerty C.C., Gauglitz G.G., Herndon D.N. and Jeschke M.G. (2009) Starvation-Induced Proximal Gut Mucosal Atrophy Diminished with Aging. *JPEN J Parenter Enteral Nutr.* **33**(4): 411-416

Song W., Veenstra J.A. and Perrimon N. (2014) Control of Lipid Metabolism by Tachykinin in *Drosophila. Cell Rep.* **9**(1): 40-47

Souba W.W. and Wilmore D.W. eds. (2001) Surgical Research. *Academic Press.* p.605

Spencer C.C., Howell C.E., Wright A.R. and Promislow D.E. (2003) Testing an 'Aging Gene' in Long-Lived *Drosophila* Strains: Increased Longevity Depends on Sex and Genetic Background. *Aging Cell.* **2**(2): 123-130

Staley B.K. and Irvine K.D. (2010) Warts and Yorkie Mediate Intestinal Regeneration by Influencing Stem Cell Proliferation. *Curr Biol.* **20**(17): 1580-1587

Starr R., Willson T.A., Viney E.M., Murray L.J., Rayner J.R., Jenkins B.J., Gonda T.J., Alexander W.S., Metcalf D., Nicola N.A. and Hilton D.J. (1997) A Family of Cytokine-Inducible Inhibitors of Signalling. *Nature.* **387**(6636): 917-921

Stec W.J. and Zeidler M.P. (2011) *Drosophila* SOCS Proteins. *J Signal Transduct.* **2011**: 894510

Stec W., Vidal O. and Zeidler M.P. (2013) *Drosophila* SOCS36E Negatively Regulates JAK/STAT Pathway Signaling Via Two Separable Mechanisms. *Mol Biol Cell.* **24**(18): 3000-3009

Stilling R.M., Dinan T.G. and Cryan J.F. (2014) Microbial Genes, Brain & Behaviour - Epigenetic Regulation of the Gut-Brain Axis. *Genes Brain Behav.* **13**(1): 69-86

Stone T.W. and Darlington L.G. The Kynurenine Pathway as a Therapeutic Target in Cognitive and Neurodegenerative Disorders. *Br J Pharmacol.* **169**(6): 1211-1227

Strauss R. and Heisenberg M. (1993) A Higher Control Center of Locomotor Behavior in the *Drosophila* Brain. *J Neurosci.* **13**(5): 1852-1861

Sun L., Nava G.M. and Stappenbeck T.S. (2011) Host Genetic Susceptibility, Dysbiosis, and Viral Triggers in Inflammatory Bowel Disease. *Curr Opin Gastroenterol.* **27**(4): 321-327

Suzuki A., Hanada T., Mitsuyama K., Yoshida T., Kamizono S., Hoshino T., Kubo M., Yamashita A., Okabe M., Takeda K., Akira S., Matsumoto S., Toyonaga A., Sata M. and Yoshimura A. (2001) CIS3/SOCS3/SSI3 Plays a Negative Regulatory Role in STAT3 Activation and Intestinal Inflammation. *J Exp Med.* **193**(4): 471-481

Suzuki T. (2013) Regulation of Intestinal Epithelial Permeability by Tight Junctions. *Cell Mol Life Sci.* **70**(4): 631-659

Takeda K., Clausen B.E., Kaisho T., Tsujimura T., Terada N., Förster I. and Akira S. (1999) Enhanced Th1 Activity and Development of Chronic Enterocolitis in Mice Devoid of Stat3 in Macrophages and Neutrophils. *Immunity.* **10**(1): 39-49

Takeda K., Kaisho T. and Akira S. (2003) Toll-Like Receptors. *Annu Rev Immunol.* **21**: 335-376

Tancrède C. (1992) Role of Human Microflora in Health and Disease. *Eur J Clin Microbiol Infect Dis.* **11**(11): 1012-1015

Taupin D. and Podolsky D.K. (2003) Trefoil Factors: Initiators of Mucosal Healing. *Nat Rev Mol Cell Biol.* **4**(9): 721-732

Thagia I., Shaw E.J., Smith E., Else K.J. and Rigby R.J. (2015) Intestinal Epithelial Suppressor of Cytokine Signaling 3 Enhances Microbial-Induced Inflammatory Tumor Necrosis Factor-α, Contributing to Epithelial Barrier Dysfunction. *Am J Physiol Gastrointest Liver Physiol.* **308**(1): G25-31

Thomas S.R. and Stocker R. (1999) Redox Reactions related to Indoleamine 2,3-Dioxygenase and Tryptophan Metabolism along the Kynurenine Pathway. *Redox Rep.* **4**(5): 199-220

Todd I. (2010) Cells of the Immune System. *eLS.*

Treit D. and Fundytus M. (1988) Thigmotaxis as a Test for Anxiolytic Activity in Rats. *Pharmacol Biochem Beha.* **31**(4): 959-962

Treuting, P.M. and Dintzis, S.M. (2011) *Comparative Anatomy and Histology: A Mouse and Human Atlas* (Expert Consult). Academic Press.

Uematsu S. and Akira S. (2008) Toll-Like Receptors (TLRs) and their Ligands. *Handb Exp Pharmacol.* (183): 1-20

Uyttenhove C., Pilotte L., Théate I., Stroobant V., Colau D., Parmentier N., Boon T. and Van den Eynde B.J. (2003) Evidence for a Tumoral Immune Resistance Mechanism Based on Tryptophan Degradation by Indoleamine 2,3-Dioxygenase. *Nat. Med.* **9**(10):1269-1274

van der Flier L.G. and Clevers H. (2009) Stem Cells, Self-Renewal, and Differentiation in the Intestinal Epithelium. *Annu Rev Physiol.* **71**: 241-260

Van der Sluis M., De Koning B.A., De Bruijn A.C., Velcich A., Meijerink J.P., Van Goudoever J.B., Büller H.A., Dekker J., Van Seuningen I., Renes I.B. and Einerhand A.W. (2006) Muc2-Deficient Mice Spontaneously Develop Colitis, Indicating that MUC2 is Critical for Colonic Protection. *Gastroenterology.* **131**(1): 117-129

Veenstra J.A., Agricola H.J. and Sellami A. (2008) Regulatory Peptides in Fruit Fly Midgut. *Cell Tissue Res.* **334**(3): 499-516

Vijay-Kumar M., Sanders C.J., Taylor R.T., Kumar A., Aitken J.D., Sitaraman S.V., Neish A.S., Uematsu S., Akira S., Williams I.R. and Gewirtz A.T. (2007) Deletion of TLR5 results in Spontaneous Colitis in Mice. *J Clin Invest.* **117**(12): 3909-3921

Wakelin D. (1973) The Stimulation of Immunity to *Trichuris muris* in Mice Exposed to Low-Level Infections. *Parasitology*. **66**(1): 181-189

Walker A.W., Sanderson J.D., Churcher C., Parkes G.C., Hudspith B.N., Rayment N., Brostoff J., Parkhill J., Dougan G. and Petrovska L. (2011) High-Throughput Clone Library Analysis of the Mucosa-Associated Microbiota Reveals Dysbiosis and Differences Between Inflamed and Non-Inflamed Regions of the Intestine in Inflammatory Bowel Disease. *BMC Microbiology.* **11**(1): 7

Wang M.C., Bohmann D. and Jasper H. (2003) JNK Signaling Confers Tolerance to Oxidative Stress and Extends Lifespan in *Drosophila*. *Dev Cell.* **5**(5): 811-816

Wang Y., Srinivasan K., Siddiqui M.R., George S.P., Tomar A. and Khurana S. (2008) A Novel Role for Villin in Intestinal Epithelial Cell Survival and Homeostasis. *J Biol Chem.* **283**(14): 9454-9464

Wang R., Lu M., Zhang J., Chen S., Luo X., Qin Y. and Chen H. (2011) Increased IL-10 mRNA Expression in Tumor-Associated Macrophage Correlated with Late Stage of Lung Cancer. *J Exp Clin Cancer Res.* **30**: 62

Ward J. M., Yamamoto R. S. and Brown C.A. (1973) Pathology of Intestinal Neoplasms and Other Lesions in Rats Exposed to Azoxymethane. *Journal of the National Cancer Institute* **51**(3): 1029-1039

Weber A., Hengge U.R., Bardenheuer W., Tischoff I., Sommerer F., Markwarth A., Dietz A., Wittekind C. and Tannapfel A. (2005) SOCS-3 is Frequently Methylated in Head and Neck Squamous Cell Carcinoma and its Precursor Lesions and Causes Growth Inhibition. *Oncogene.* **24**(44): 6699-6708

Wei X., Wang G., Li W., Hu X., Huang Q., Xu K., Lou W., Wu J., Liang C., Lou Q., Qian C. and Liu L. (2014) Activation of the JAK-STAT3 Pathway is Associated with the Growth of Colorectal Carcinoma Cells. *Oncol Rep.* **31**(1): 335-341

Whitehead W.E., Engel B.T. and Schuster M.M. (1980) Irritable Bowel Syndrome: Physiological and Psychological Differences between Diarrhea-Predominant and Constipation-Predominant Patients. *Dig Dis Sci.* **25**(6): 404-413

Wirleitner B., Neurauter G., Schröcksnadel K., Frick B. and Fuchs D. (2003) Interferon-Gamma-Induced Conversion of Tryptophan: Immunologic and Neuropsychiatric Aspects. *Curr Med Chem.* **10**(16): 1581-1591

Wolf A.M., Wolf D., Rumpold H., Moschen A.R., Kaser A., Obrist P., Fuchs D., Brandacher G., Winkler C., Geboes K., Rutgeerts P. and Tilg H. (2004) Overexpression of Indoleamine 2,3-Dioxygenase in Human Inflammatory Bowel Disease. *Clin Immunol.* **113**(1): 47-55

Wong A.C., Vanhove A.S. and Watnick P.I. (2016) The Interplay Between Intestinal Bacteria and Host Metabolism in Health and Disease: Lessons from *Drosophila melanogaster. Dis Model Mech.* **9**(3): 271-281

Woods D.F., Wu J.W. and Bryant P.J. (1997) Localization of Proteins to the Apico-Lateral Junctions of *Drosophila* Epithelia. *Dev Genet.* **20**(2): 111-118

Wright N.A. (2000) Epithelial Stem Cell Repertoire in the Gut: Clues to the Origin of Cell Lineages, Proliferative Units and Cancer. *Int J Exp Pathol.* **81**(2): 117-143

Xiao Z.Q., Moragoda L., Jaszewski R., Hatfield J.A., Fligiel S.E. and Majumdar A.P. (2001) Aging is associated with Increased Proliferation and Decreased Apoptosis in the Colonic Mucosa. *Mech Ageing Dev.* **122**(15): 1849-1864

Xiong H., Zhang Z.G., Tian X.Q., Sun D.F., Liang Q.C., Zhang Y.J., Lu R., Chen Y.X. Fang J.Y. (2008) Inhibition of JAK1, 2/STAT3 Signaling Induces Apoptosis, Cell Cycle Arrest, and Reduces Tumor Cell Invasion in Colorectal Cancer Cells. *Neoplasia.* **10**(3): 287-297

Xu N., Wang S.Q., Tan D., Gao Y., Lin G. and Xi R. (2011) EGFR, Wingless and JAK/STAT Signaling Cooperatively Maintain *Drosophila* Intestinal Stem Cells. *Dev Biol.* **354**(1): 31-43

Yan R., Small S., Desplan C., Dearolf C.R. and Darnell J.E. Jr. (1996) Identification of a Stat Gene that Functions in *Drosophila* Development. *Cell.* **84**(3): 421-430

Yasui H., Takai K., Yoshida R. and Hayaishi O. (1986) Interferon Enhances Tryptophan Metabolism by Inducing Pulmonary Indoleamine 2, 3-Dioxygenase: Its Possible Occurrence in Cancer Patients. *Proceedings of the National Academy of Sciences.* **83**(17): 6622-6626

Yoshida R., Imanishi J., Oku T., Kishida T. and Hayaishi O. (1981) Induction of Pulmonary Indoleamine 2, 3-Dioxygenase by Interferon. *Proceedings of the National Academy of Sciences.* **78**(1): 129-132

Yoshimura A., Naka T. and Kubo M. (2007) SOCS Proteins, Cytokine Signalling and Immune Regulation. *Nat Rev Immunol.* **7**(6):454-465

Yoshiura S., Ohtsuka T., Takenaka Y., Nagahara H., Yoshikawa K. and Kageyama R. (2007) Ultradian Oscillations of Stat, Smad, and Hes1 Expression in Response to Serum. *Proc Natl Acad Sci USA.* **104**(27): 11292-11297

Yurist-Doutsch S., Arrieta M.C., Vogt S.L. and Finlay B.B. (2014) Gastrointestinal Microbiota-Mediated Control of Enteric Pathogens. *Annu Rev Genet.* **48**: 361-382

Zackular J.P., Baxter N.T., Iverson K.D., Sadler W.D., Petrosino J.F., Chen G.Y. and Schloss P.D. (2013) The Gut Microbiome Modulates Colon Tumorigenesis. *MBio.* **4**(6): e00692-13

Zhang J.G., Farley A., Nicholson S.E., Willson T.A., Zugaro L.M., Simpson R.J., Moritz R.L., Cary D., Richardson R., Hausmann G., Kile B.T., Kent S.B., Alexander W.S., Metcalf D., Hilton D.J., Nicola N.A. and Baca M. (1999) The Conserved SOCS Box Motif in Suppressors of Cytokine Signaling Binds to Elongins B and C and may couple Bound Proteins to Proteasomal Degradation. *Proc Natl Acad Sci U S A.* **96**(5): 2071-2076

Zhang Z. and Schluesener H.J. (2006) Mammalian Toll-Like Receptors: From Endogenous Ligands to Tissue Regeneration. *Cell Mol Life Sci.* **63**(24): 2901-2907

Zhao X., Qi R., Sun C. and Xie Y. (2012) Silencing SOCS3 could Inhibit TNF-α Induced Apoptosis in 3T3-L1 and Mouse Preadipocytes. *Mol Biol Rep.* **39**(9): 8853-8860

Zouein F.A., Kurdi M. and Booz G.W. (2013) Dancing Rhinos in Stilettos: The Amazing Saga of the Genomic and Nongenomic Actions of STAT3 in the Heart. *JAKSTAT.* **2**(3):e24352

Websites

Cell Signalling Biology (Accessed 19th April 2016)

http://www.cellsignallingbiology.org/csb/007/csb007.pdf

Centers for Disease Control and Prevention (Accessed 27th April 2016)

http://www.cdc.gov/mmwr/preview/mmwrhtml/mm4829a1.htm

Cold Springs Harbor Protocols (Accessed 17th May 2016)

http://cshprotocols.cshlp.org/content/2008/7/pdb.top49/F2.large.jpg

FlyBase (Short Neuropeptide F) (Accessed 13th April 2016)

http://flybase.org/reports/FBgn0032840.html

FlyBase (Ion Transfer Peptide) (Accessed 13th April 2016)

http://flybase.org/reports/FBgn0035023.html

Human Ageing Genomic Resources (Accessed 21st April 2016)

http://genomics.senescence.info/species/entry.php?species=Mus_musculus

Johns Hopkins School of Public Health (Accessed 25th May 2016)- Russell W.M.S., Burch R.L. and Hume C.W. (1959) The Principles of Humane Experimental Technique.

http://altweb.jhsph.edu/pubs/books/humane_exp/het-toc

Manchester University Fly Facility (Accessed 28th May 2016)

https://droso4schools.wordpress.com/organs/

Mutagenetix South Western Medical Centre (Accessed 28th May 2016)

http://mutagenetix.utsouthwestern.edu/phenotypic/phenotypic_rec.cfm?pk=234

Office for National Statistics (Accessed 27th April 2016)

https://www.ons.gov.uk/peoplepopulationandcommunity/healthandsocialcare/healthandlifeexpectancies/datasets/changesinhealthylifeexpectancyhle
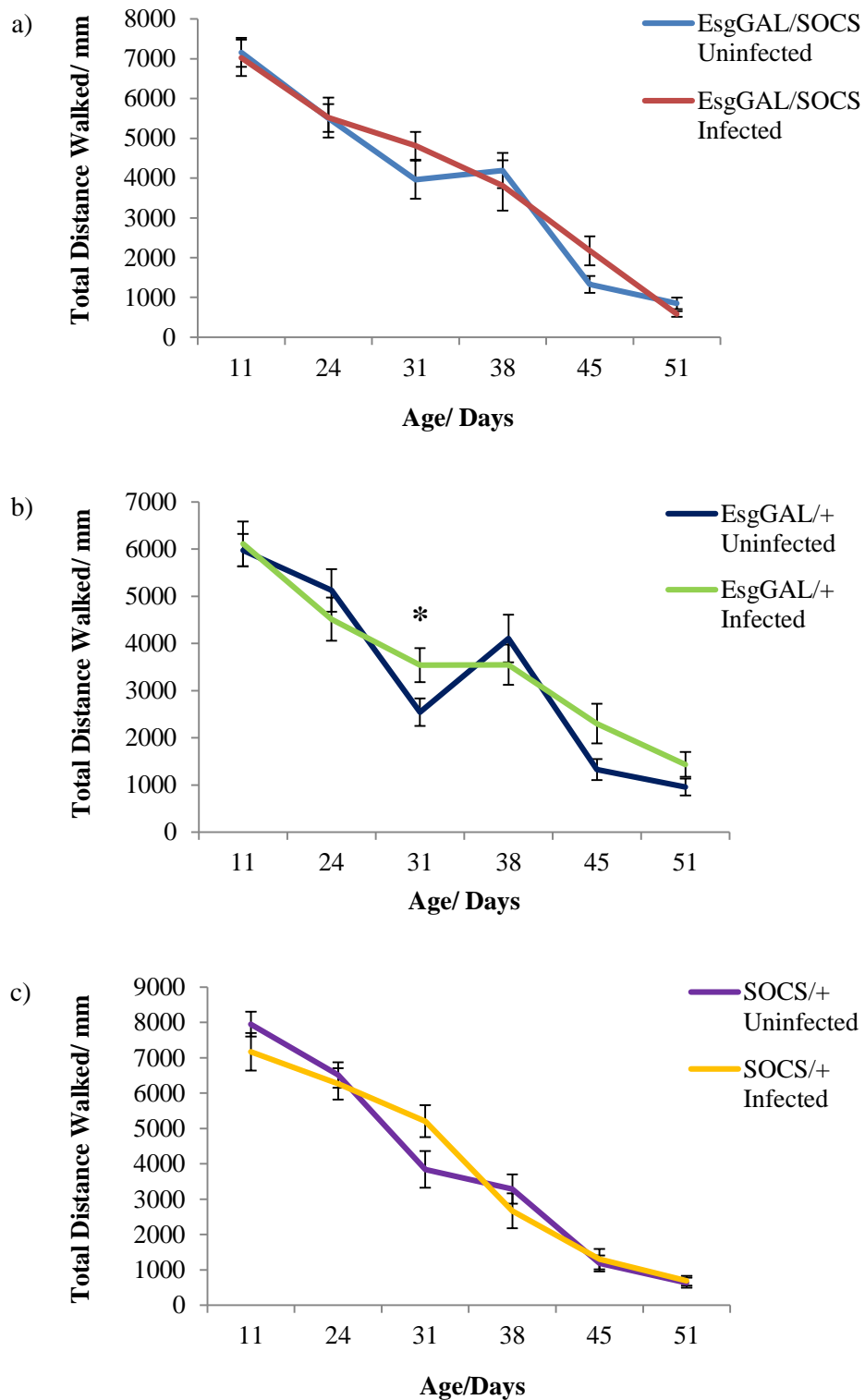
The Immune System in Health and Disease (Accessed 28th May 2016)

http://what-when-how.com/rheumatology/introduction-to-the-immune-system-the-immune-system-in-health-and-disease-rheumatology-part-2/

Transgenic Animal Web (Accessed 21st April 2016)
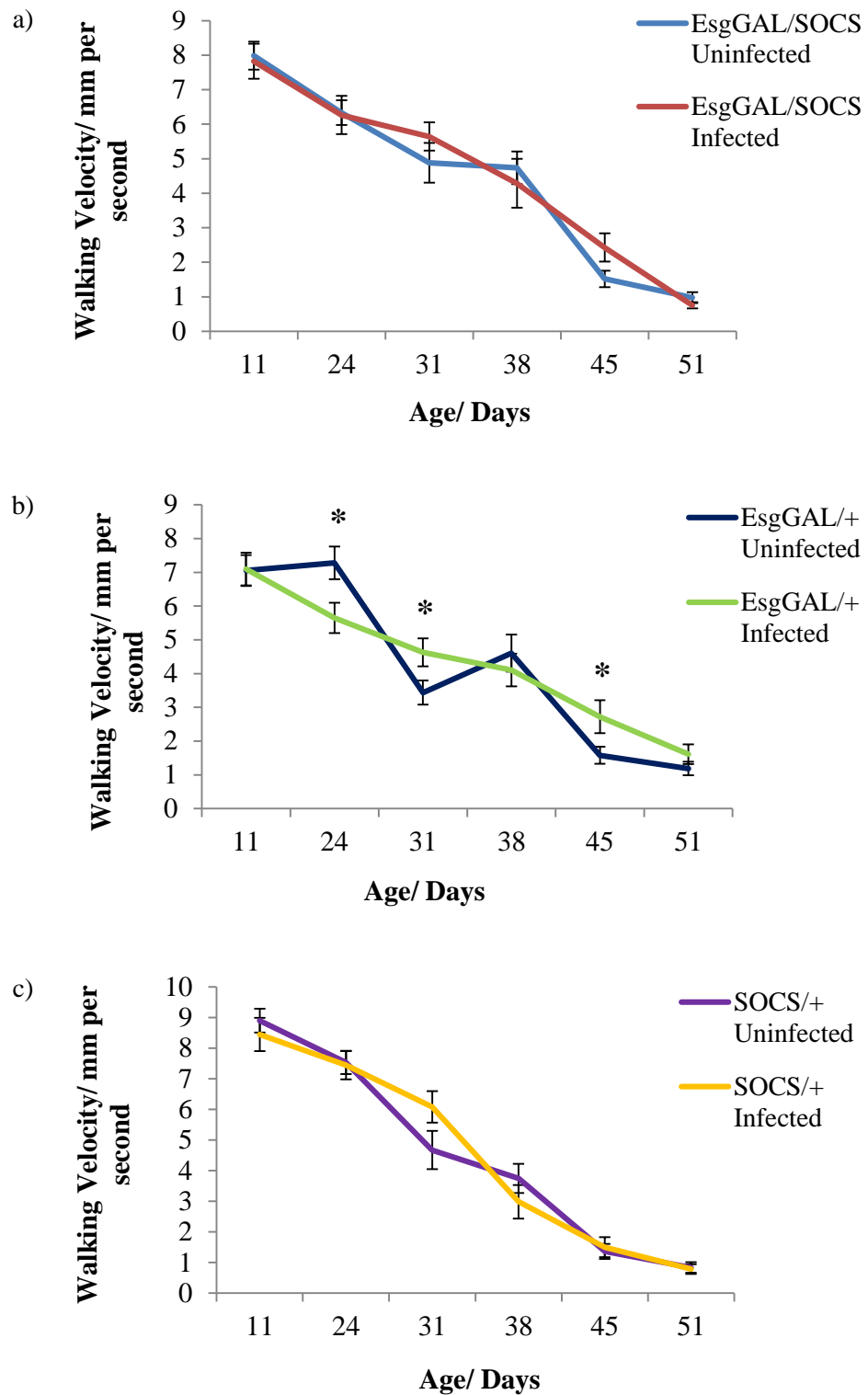
https://www.med.umich.edu/tamc/breed.html

Appendix 1: The effect of *Ecc15* infection on the age-associated decline on walking distance in SOCS36E knockdown and control female flies. Data are shown as a mean value (±SEM) for each time point for uninfected and infected (a) EsgGAL/SOCS, (b) EsgGAL/+ and (c) SOCS/+ female flies. (* = p<0.05, using a Student's t-test).
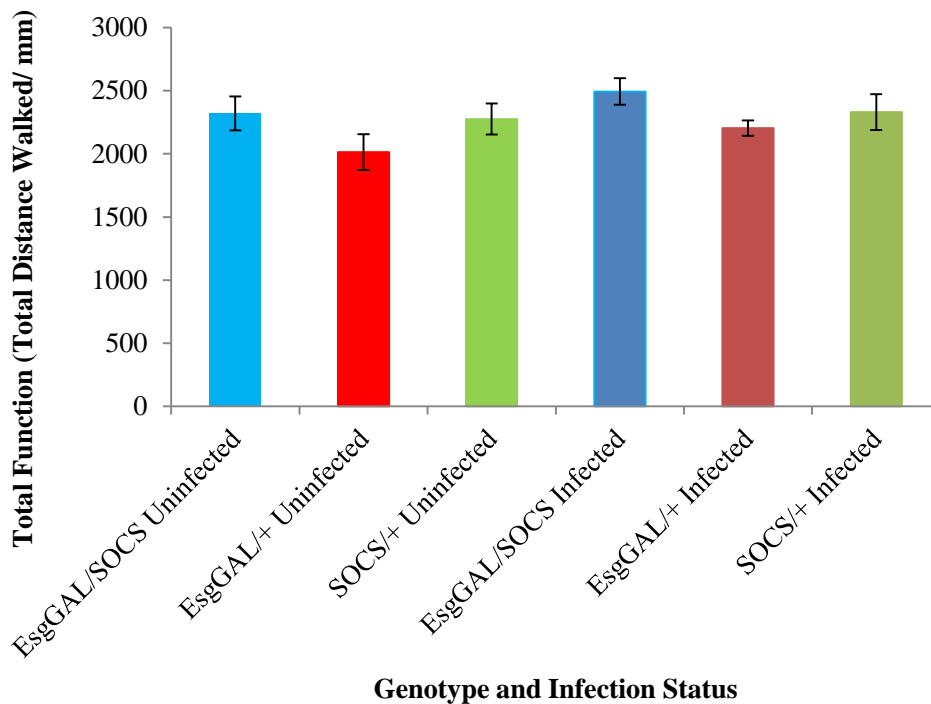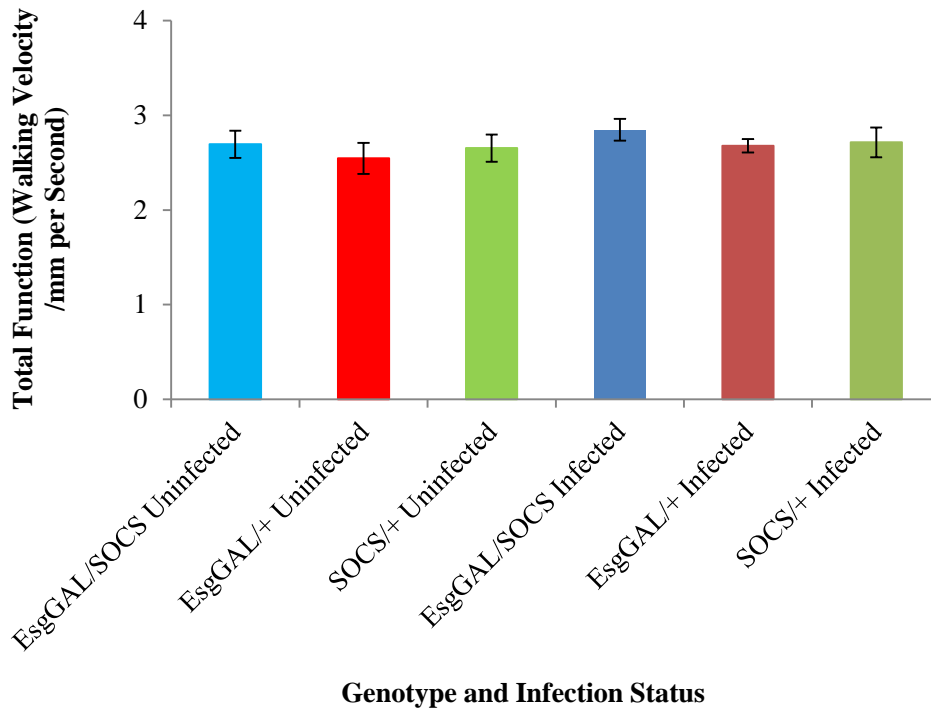
Appendix 2: Total function of distance walked (±SEM) in uninfected and *Ecc15*-infected SOCS36E knockdown flies, plus controls. Total function was determined using the area under the curve at each time point of the assay, with a maximum of 15 flies used at each time point for each genotype and infection group.

	EsgGAL/ SOCS Uninfected	EsgGAL/+ Uninfected	SOCS/+ Uninfected	EsgGAL/ SOCS Infected	EsgGAL/+ Infected	SOCS/+ Infected
EsgGAL/ SOCS Uninfected	x	0.2412	0.9681	0.3211		
EsgGAL/+ Uninfected	0.2412	x			0.2248	
SOCS/+ Uninfected	0.9681		x			0.7722
EsgGAL/ SOCS Infected	0.3211			x	0.1534	0.5385
EsgGAL/+ Infected		0.2248		0.1534	x	
SOCS/+ Infected			0.7722	0.5385		x

Table A1: P-values calculated using JMP, for differences in total function between uninfected and *Ecc15*-infected knockdown female flies and their relevant controls (using a one-way ANOVA with Tukey's HSD), as well as between uninfected female flies and their infected counterparts (using a Student's t-test).
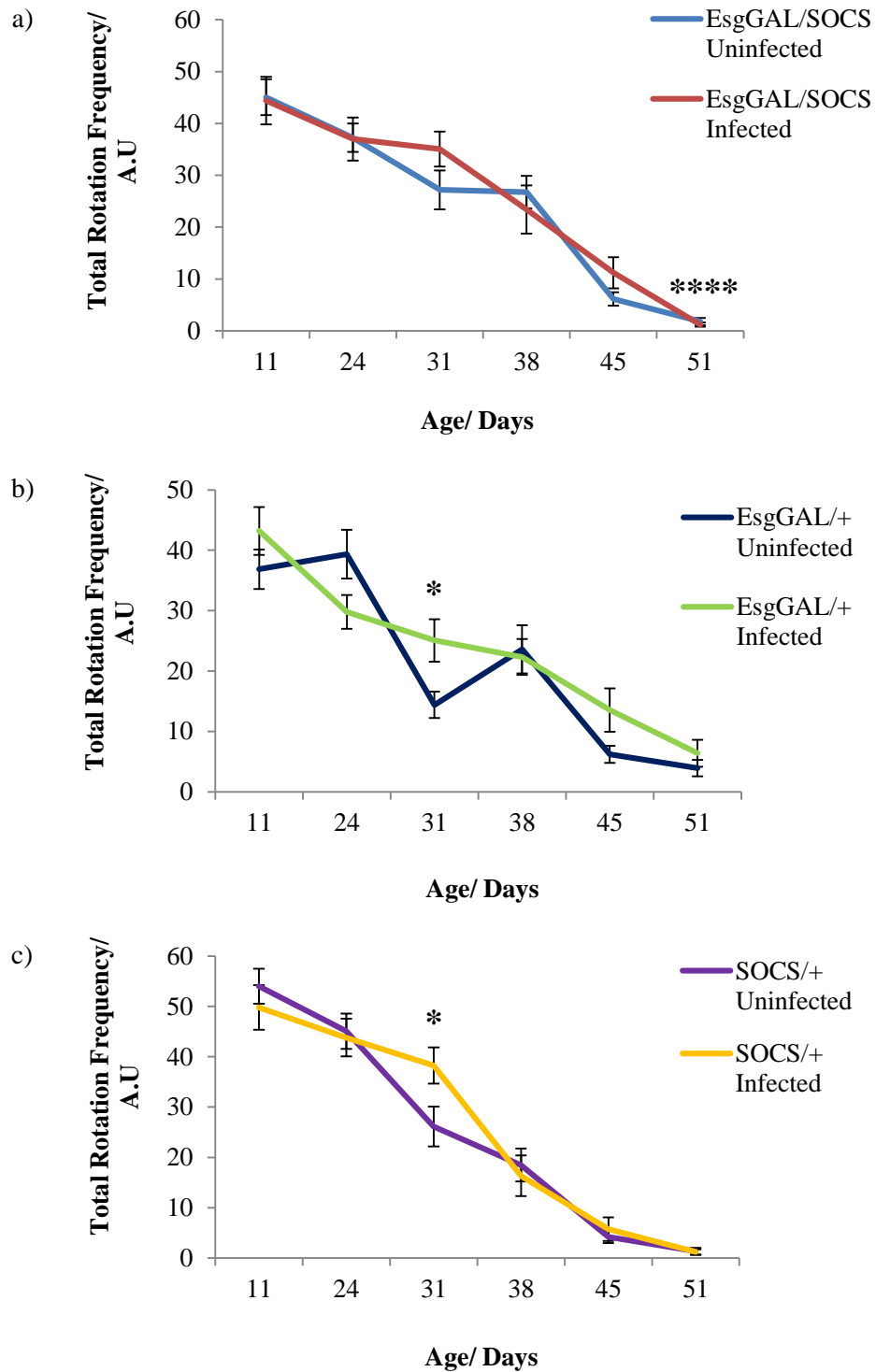
319

Appendix 3: The effect of *Ecc15* infection on the age-associated decline on walking velocity in SOCS36E knockdown and control female flies. Data are shown as a mean value (±SEM) for each time point for uninfected and infected (a) EsgGAL/SOCS, (b) EsgGAL/+ and (c) SOCS/+ female flies. (* = p<0.05, using a Student's t-test).
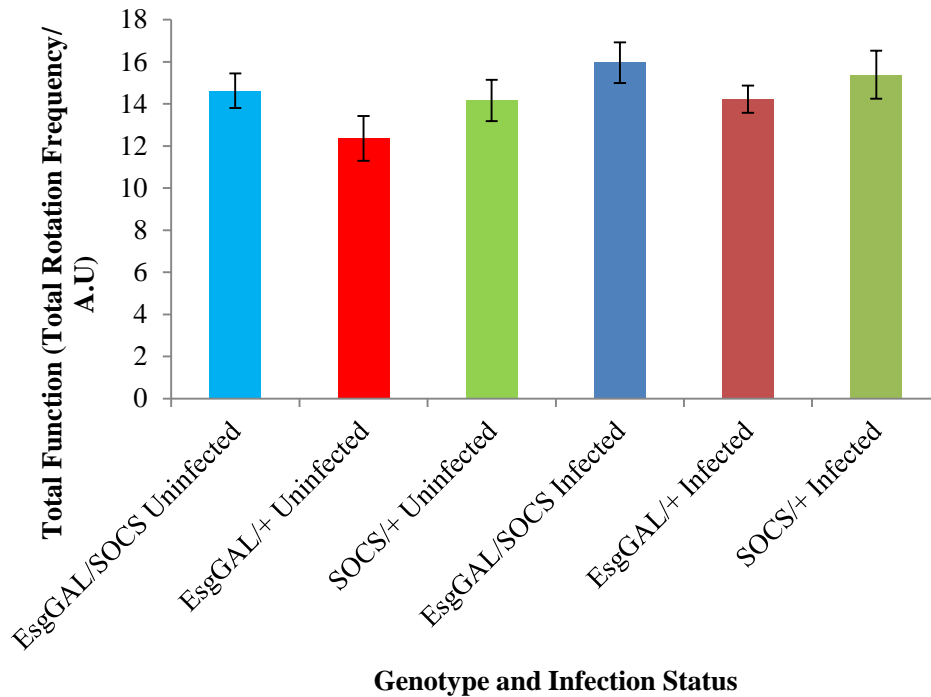
Genotype and Infection Status

Appendix 4: Total function of walking velocity (±SEM) in uninfected and *Ecc15*-infected SOCS36E knockdown flies, plus controls. Total function was determined using the area under the curve at each time point of the assay, with a maximum of 15 flies used at each time point for each genotype and infection group.

	EsgGAL/ SOCS Uninfected	EsgGAL/+ Uninfected	SOCS/+ Uninfected	EsgGAL/ SOCS Infected	EsgGAL/+ Infected	SOCS/+ Infected
EsgGAL/ SOCS Uninfected	x	0.7689	0.9807	0.4137		
EsgGAL/+ Uninfected	0.7689	x			0.4603	
SOCS/+ Uninfected	0.9807		x			0.7766
EsgGAL/ SOCS Infected	0.4137			x	0.5860	0.7140
EsgGAL/+ Infected		0.4603		0.5860	x	
SOCS/+ Infected			0.7766	0.7140		x

Table A2: P-values calculated using JMP, for differences in total function between uninfected and *Ecc15*-infected knockdown female flies and their relevant controls (using a one-way ANOVA with Tukey's HSD), as well as between uninfected female flies and their infected counterparts (using a Student's t-test).
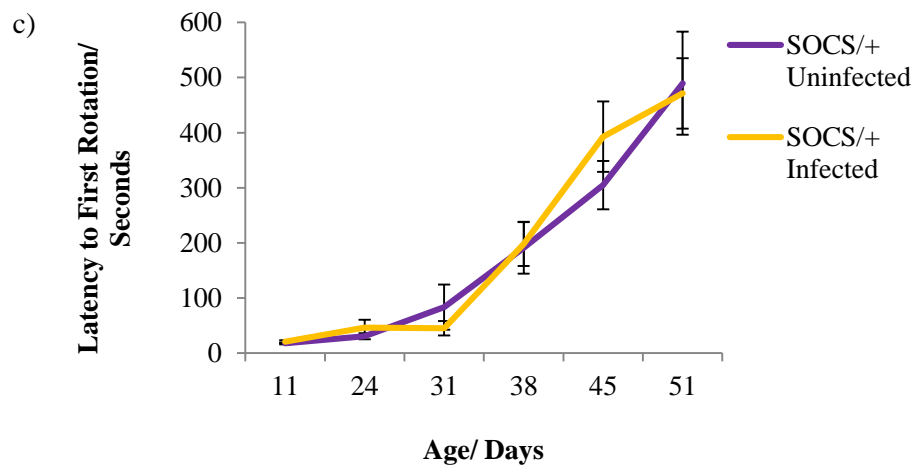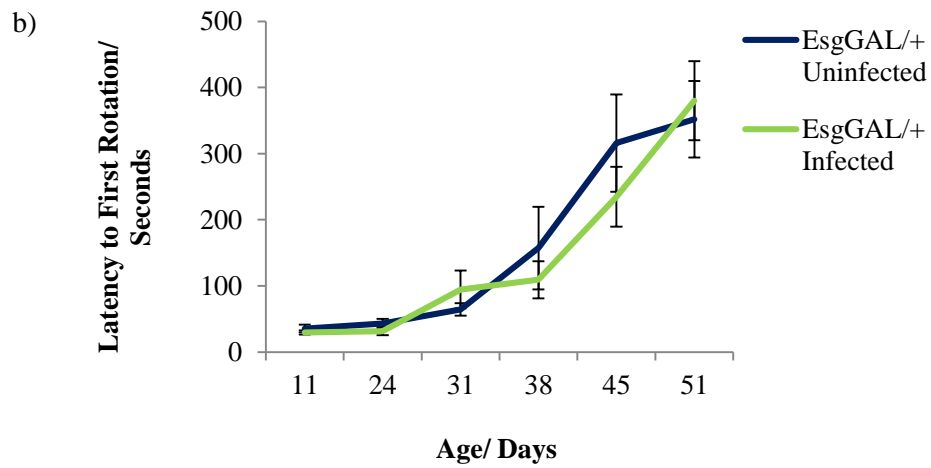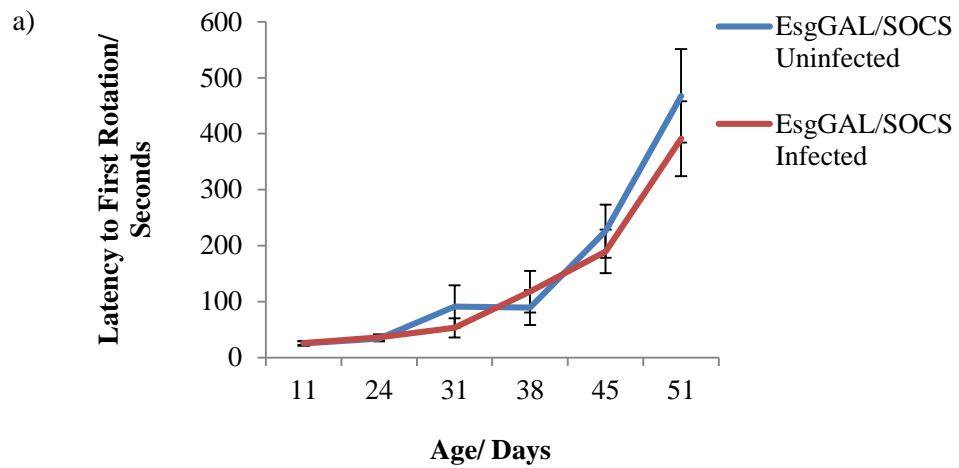
Appendix 5: The effect of *Ecc15* infection on the age-associated decline on rotation frequency in SOCS36E knockdown and control female flies. Data are shown as a mean value (±SEM) for each time point for uninfected and infected (a) EsgGAL/SOCS, (b) EsgGAL/+ and (c) SOCS/+ female flies. (* = p<0.05, **** = p<0.0001, using a Student's t-test).
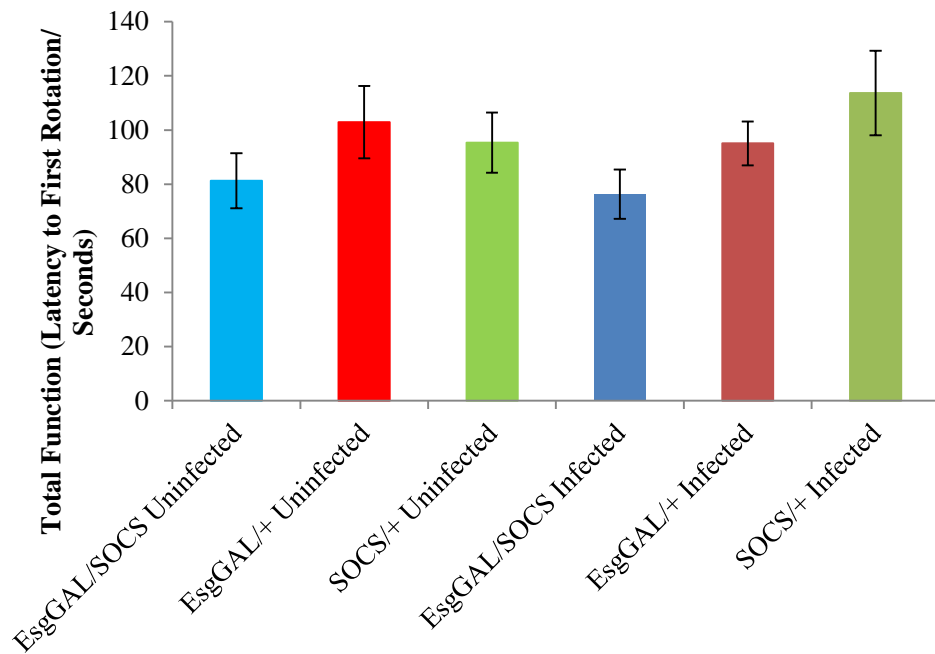
Appendix 6: Total function of rotation frequency (±SEM) in uninfected and *Ecc15*-infected SOCS36E knockdown female flies, plus controls. Total function was determined using the area under the curve at each time point of the assay, with a maximum of 15 flies used at each time point for each genotype and infection group.

	EsgGAL/ SOCS Uninfected	EsgGAL/+ Uninfected	SOCS/+ Uninfected	EsgGAL/ SOCS Infected	EsgGAL/+ Infected	SOCS/+ Infected
EsgGAL/ SOCS Uninfected	x	0.2283	0.9362	0.3026		
EsgGAL/+ Uninfected	0.2283	x			0.1459	
SOCS/+ Uninfected	0.9362		x			0.4233
EsgGAL/ SOCS Infected	0.3026			x	0.4007	0.9033
EsgGAL/+ Infected		0.1459		0.4007	x	
SOCS/+ Infected			0.4233	0.9033		x

Table A3: P-values calculated using JMP, for differences in total function of rotation frequency between uninfected and *Ecc15*-infected knockdown female flies and their relevant controls (using a one-way ANOVA with Tukey's HSD), as well as between uninfected female flies and their infected counterparts (using a Student's t-test).

Appendix 7: The effect of *Ecc15* infection on the age-associated increase on latency to the first rotation in SOCS36E knockdown and control female flies. Data are shown as a mean value (±SEM) for each time point for uninfected and infected (a) EsgGAL/SOCS, (b) EsgGAL/+ and (c) SOCS/+ female flies.

Genotype and Infection Status

Appendix 8: Total function of rotation latency (±SEM) in uninfected and *Ecc15*-infected SOCS36E knockdown female flies, plus controls. Total function was determined using the area under the curve at each time point of the assay, with a maximum of 15 flies used at each time point for each genotype and infection group.

	EsgGAL/ SOCS Uninfected	EsgGAL/+ Uninfected	SOCS/+ Uninfected	EsgGAL/ SOCS Infected	EsgGAL/+ Infected	SOCS/+ Infected
EsgGAL/ SOCS Uninfected	x	0.3959	0.6722	0.7194		
EsgGAL/+ Uninfected	0.3959	x			0.6197	
SOCS/+ Uninfected	0.6722		x			0.3452
EsgGAL/ SOCS Infected	0.7194			x	0.4831	0.0645
EsgGAL/+ Infected		0.6197		0.4831	x	
SOCS/+ Infected			0.3452	0.0645		x

Table A4: P-values calculated using JMP, for differences in total function between uninfected and *Ecc15*-infected knockdown female flies and their relevant controls (using a one-way ANOVA with Tukey's HSD), as well as between uninfected female flies and their infected counterparts (using a Student's t-test).

Final Volume (L)	0.5	1	1.5	2	3	4	4.5	5
Water (ml)	350	700	1050	1400	2100	2800	3150	3500
Agar (g)	7.5	15	22.5	30	45	60	67.5	75
Sugar (g)	25	50	75	100	150	200	225	250
Yeast (g)	50	100	150	200	300	400	450	500
Water to add at end (ml)	76	170	265	359	548	737	832	926
Nipagen (ml)	15	30	45	60	90	120	135	150
Propionic Acid (ml)	1.5	3	4.5	6	9	12	13.5	15

- Heat the water and stir in the agar, then bring to the boil.

- Once boiled, add the sugar and yeast.

- Stir until the mixture has a smooth consistency and bring to the boil again.

- Remove from heat and once settled, add the extra water as indicated.

- Allow the mixture to cool to 60°C.

- Add nipagen and propionic acid, then dispense as required.

Appendix 9: The recipe for standard 0.5 Sugar/ 1.0 Yeast *Drosophila* media, used for maintenance of both stock and experimental flies.